



HAL
open science

Design of targeted photosensitizer-conjugates towards Neuropilin-1 and folate receptors for improving the selectivity of anti-cancer photodynamic therapy

Amirah Mohd Gazzali

► **To cite this version:**

Amirah Mohd Gazzali. Design of targeted photosensitizer-conjugates towards Neuropilin-1 and folate receptors for improving the selectivity of anti-cancer photodynamic therapy. Human health and pathology. Université de Lorraine, 2016. English. NNT : 2016LORR0122 . tel-01470491

HAL Id: tel-01470491

<https://theses.hal.science/tel-01470491>

Submitted on 17 Feb 2017

HAL is a multi-disciplinary open access archive for the deposit and dissemination of scientific research documents, whether they are published or not. The documents may come from teaching and research institutions in France or abroad, or from public or private research centers.

L'archive ouverte pluridisciplinaire **HAL**, est destinée au dépôt et à la diffusion de documents scientifiques de niveau recherche, publiés ou non, émanant des établissements d'enseignement et de recherche français ou étrangers, des laboratoires publics ou privés.



AVERTISSEMENT

Ce document est le fruit d'un long travail approuvé par le jury de soutenance et mis à disposition de l'ensemble de la communauté universitaire élargie.

Il est soumis à la propriété intellectuelle de l'auteur. Ceci implique une obligation de citation et de référencement lors de l'utilisation de ce document.

D'autre part, toute contrefaçon, plagiat, reproduction illicite encourt une poursuite pénale.

Contact : ddoc-theses-contact@univ-lorraine.fr

LIENS

Code de la Propriété Intellectuelle. articles L 122. 4

Code de la Propriété Intellectuelle. articles L 335.2- L 335.10

http://www.cfcopies.com/V2/leg/leg_droi.php

<http://www.culture.gouv.fr/culture/infos-pratiques/droits/protection.htm>



UNIVERSITÉ
DE LORRAINE



Thèse

Ecole Doctoral RP2E n°410 :
Science et Ingénierie, Ressources, Procédés, Produits et Environnement

Pour l'obtention du titre de
Docteur de l'Université de Lorraine

Présentée et soutenue publiquement le 19 Septembre 2016 par :

Amirah MOHD GAZZALI

Intitulée :

Conception de photosensibilisateurs conjugués ciblant le récepteur
Neuropiline-1 ou le récepteur à l'acide folique pour l'amélioration de la
sélectivité de la thérapie photodynamique anti-cancéreuse

Devant le jury composé de :

Jean-Olivier DURAND	<i>Dr-CNRS, Université de Montpellier 2</i>	Rapporteur
Claude TAILLEFUMIER	<i>Pr, Université Clermont-Ferrand</i>	Rapporteur
Habibah A. WAHAB	<i>Pr, Universiti Sains Malaysia</i>	Examineur
Jérôme DEVY	<i>MC, Université de Reims Champagne Ardenne</i>	Examineur
Régis VANDERESSE	<i>CR-CNRS, LCPM, Nancy</i>	Directeur
Céline FROCHOT	<i>DR-CNRS, LRGP, Nancy</i>	Co-Directrice
Samir ACHERAR	<i>MC, LCPM, Nancy</i>	Co-Encadrant

Laboratoire de Chimie Physique Macromoléculaire (LCPM), UMR 7375, CNRS-UL
Laboratoire des Réactions et Génie des Procédés (LRGP), UMR 7274, CNRS-UL
1, Rue Grandville, 54001 Nancy, France

2016

Acknowledgement

I would like to express my utmost sincere gratitude to several important people who were and have always been there for me especially throughout the past three and a half years. My thesis advisor Dr Régis Vanderesse, who always encourages, guides and believes in me even during the toughest time, like a father to his daughter. I would also like to thank my co-advisor, Dr Céline Frochot for all the advices that she had offered to me on multiple things, science and life affairs alike. For all the fruitful discussion and guidance, for all the encouragement that was given to me during the course of the PhD, I could not thank you enough.

A big appreciation is also dedicated to Dr Samir Acherar, who was always there, entertaining all my questions and is always open for discussion on the project. The expert in click chemistry field, the critical mind and detailed characteristic of Dr Acherar has helped me in many ways. Thank you very much for all the guidance that was given to me, surely they will be useful in the future.

My gratitude is also dedicated to the evaluators of this thesis: Dr Jean-Olivier Durand, Prof. Claude Taillefumier, Prof. Habibah A. Wahab and Dr Jérôme Devy, for their constructive feedback on improving the thesis. It is indeed an honour to have them in the jury of the thesis. I truly appreciate the effort of all juries to fulfil the task, and especially to Prof. Habibah A. Wahab who took the trouble flying all the way from Malaysia.

My deepest gratitude will also be for my sponsors; the Ministry of Higher Education Malaysia, Universiti Sains Malaysia and School of Pharmaceutical Sciences USM for giving me the opportunity to further my education to the doctorate level. I am very grateful for all the financial help that was given to me and my little family to be in France for the whole three and a half years.

I would also want to express my appreciation to the people from LCPM who have made the PhD journey more interesting and full of colours: Prof Alain Durand (Director of LCPM), Prof Brigitte Jamart (Director of GSOB), Dr Marie-Christine Averlant-Petit (Co-director of LCPM), Dr Axelle Arault (MC), Dr Guillaume Pickaert (MC) and Dr Jacques Bodriguel (MC). Not forgetting Dr Olivier Fabre who had relentlessly entertained my needs for NMR analysis. Also many thank you also to LRGP for providing me multiple resources in completing my research works.

The marvellous people in the PDTeam of Nancy; Dr Philippe Arnoux who helped me multiple times in photophysical analysis, Dr Ludovic Colombeau who was the saviour, always there when I needed help with laboratory works, Mme Mathilde Achard who helped me especially in mass analysis, Dr Francis Baros with his advices, Dr Khalil Zaghdoudi, Dr Rima Chouikrat and Dr Aurélie Stallivieri who helped me during my initial years and remains as friends through-out this PhD journey. Not forgetting my dear Zahraa Youseff who is like a little sister to me, going through the difficult phases together, crying and laughing. To Mathilde Lobry, Eugenia Longarela del Hoyo and Pierre Althuser, thank you for your helping hands that you had given me. Also to Florent Le Guern, thank you for sharing works and laboratory management.

Another special thank you is also for Mohamad Ibrahim Abdel Moneim, for all the tea and biscuits that we have had together. Thank you for the friendship that you have extended to my family, and all the helping hands that were given to us. We could never repay you.

To my family: my mother and father who have always been supporting me from the beginning, my brother and sisters, my niece and nephews, thank you for everything. My in-law family, thank you very much for all the help and for allowing your son and brother to be with me, 13,000 km away from you.

The last and most thoughtful thank you would be for my husband, Zikrullah Ismail, who has endured the hardship and difficulties with me, but nevertheless stayed by my side until the end, who had to quit his job just to be with me and who has always been supporting me and giving me strength when I feel like quitting. I do not think that I have enough words to say thank you. But, dear husband, thank you very much. To my children, Anas Zuhayli and Anisse Zulfa, maybe you will not even remember these years that we have spent in Nancy, but just so both of you know that your presence was one of the pillars of strength that has kept me going. We love you so much.

To everyone that has contributed in one way or another, either directly or indirectly in the completion of this manuscript, I offer you my greatest gratitude and thank you from the bottom of my heart. I will always remember all of you and this PhD journey as one of the most interesting and memorable episodes of my life.

Thank you. *Merci beaucoup. Terima kasih.*

*Specially dedicated to
My husband, my son and my daughter
My dear mother and father*

Résumé

La thérapie photodynamique (PDT) est une modalité de traitement du cancer qui offre de nombreux avantages. Cette technique repose sur une accumulation plus ou moins sélective d'un photosensibilisateur (PS) dans les cellules tumorales ou les néovaisseaux alimentant les tumeurs, suivie d'une irradiation lumineuse pour activer le PS. Lorsqu'il est irradié, ce PS interagit avec l'oxygène moléculaire pour conduire à la production d'espèces réactives de l'oxygène cytotoxiques, en particulier l'oxygène singlet. La PDT engendre des réactions apoptotiques et nécrotiques au sein de tumeurs traitées et produit des effets microvasculaires menant à l'inflammation et à l'hypoxie.

Une stratégie pour améliorer l'efficacité de la PDT est l'élaboration de photosensibilisateurs de troisième génération (PSS), composés d'un PS couplé à un agent de ciblage qui peuvent être des peptides, des anticorps monoclonaux, des LDL ou des hydrates de carbone. Il est également possible d'utiliser des systèmes d'administration avancés tels que des liposomes ou des nanoparticules. Ces stratégies permettent de délivrer directement le PS aux sites tumoraux.

Ces travaux de thèse ont porté sur l'amélioration de la localisation du PS à travers le design de constructions moléculaires composées d'un PS couplé à une unité d'adressage. La première partie de la thèse porte sur l'étude d'un acide PS couplé à l'acide folique (PS-FA). L'acide folique est une unité de ciblage qui se lie efficacement au récepteur de l'acide folique sur-exprimé dans de nombreuses tumeurs. Nous avons particulièrement vérifié la stabilité de l'acide folique sous l'influence des facteurs environnementaux tels que la lumière, l'oxygène, le milieu, le temps et de température. Les expériences ont été réalisées en utilisant un plan d'expériences et les résultats ont été analysés statistiquement. D'une manière générale, on constate que le conjugué PS-acide folique présente un profil de stabilité amélioré par rapport à la molécule d'acide folique seule.

La deuxième partie est consacrée à l'étude du peptide KDKPPR ciblant la neuropiline-1 (NRP-1), un récepteur surexprimé dans les néo-vaisseaux. Plusieurs modifications ont été faites sur ce peptide d'avoir des informations sur l'importance de chaque acide aminé quant à l'affinité du peptide pour NRP-1. Les acides aminés ont été remplacés l'un après l'autre par une alanine (alanine-scanning). Tous les analogues ont été testés grâce à des tests ELISA et il a été constaté que les quatre derniers acides aminés (-KPPR) sont essentiels pour l'affinité pour NRP-1 et le remplacement de ces acides aminés par l'alanine provoque une importante perte d'affinité dans l'ordre de KDKPPA > KDKPAR = KDKAPR > KDAPPR. Les deux premiers acides aminés (KD-) sont moins cruciaux pour la liaison au récepteur et pourraient être remplacés par l'alanine.

La troisième partie de la thèse a consisté en la synthèse de porphyrines couplées à des blocs porteurs de 1, 2 ou 3 peptides par la technique de chimie click pour former différentes plate-formes avec des nombres variables de porphyrines et de peptides. L'intérêt de cette approche est de pouvoir étudier la possibilité d'avoir plus d'une porphyrine pour améliorer l'activité photodynamique et, en parallèle plus d'un peptide pour améliorer la capacité de ciblage. Différents facteurs influençant le rendement de synthèse des blocs les porphyrines ont été étudiés. En ce qui concerne les blocs porteurs de peptides, deux approches différentes de synthèse ont été réalisées: en phase solide et en phase liquide. Tous les produits obtenus ont été caractérisés par spectroscopie de masse et par RMN. Les rendements de synthèse de ces blocs varient de 13 à 97%. Les caractéristiques photophysiques des différents blocs porteurs de

porphyrine ont également été mesurées et aucune différence notable n'a été détectée entre ces plateformes et la porphyrine pure.

Abstract

Photodynamic therapy (PDT) is a cancer therapy modality that could offer many advantages. It relies on some selective uptake of a photosensitizing molecule in a tumour followed by exposure to the appropriate wavelength of light to activate the photosensitizer. When activated by light irradiation, the photosensitizer (PS) interacts with molecular oxygen to produce cytotoxic reactive oxygen species, especially a short-lived species known as singlet oxygen. PDT elicits both apoptotic and necrotic responses within treated tumors and produces microvascular injury leading to inflammation and hypoxia.

One possible way to improve the effectiveness of PDT is the elaboration of third generation photosensitizers (PSs) which consisted of PSs with targeting agents. The targeting agent could be peptides, monoclonal antibodies, LDL or carbohydrates, or it is also possible to use advanced delivery systems such as liposomes or nanoparticles.

This thesis is hence focusing on the improvement of PS delivery through studying conjugates of PS-targeting agent. The first part of the thesis deals with the study of a PS-folic acid (PS-FA). FA is a well-know targeting unit which bonds with high efficiency to folic acid receptor over-expressed in many cancer cells. We particularly checked the stability of folic acid under the influence of environmental factors such as light, oxygen, medium, time length and temperature. The experiments were conducted through Design of Experiment approach and the results were analyzed statistically. In general, it was found that the PS-FA conjugate has improved stability profile as compared to free folic acid molecule.

The second part is devoted to the study of KDKPPR peptide designed to target neuropilin-1, a receptor over-expressed in neo-vessels. Several modifications were made on this peptide to have information on the importance of each amino acid on the receptor binding of the peptide. The modifications conducted include a technique called alanine-scanning, besides modifying the peptide into *retro* and *retro-inverso* peptides. All the analogues were tested through ELISA assays to investigate the effect of the modifications on the NRP-1 binding efficiency. It was found that the last four amino acids (-KPPR) are essential for the affinity for NRP-1 and the replacement of these amino acids with alanine causes a significant lost of affinity in the order of KDKPPA>KDKPAR=KDKAPR>KDAPPR. The first two amino acids (KD-) are less crucial for the binding on NRP-1 receptor and they could be replaced with alanine. This approach of structure-activity relationship (SAR) study has provided us information on the importance of each amino acid in the sequence and will serve-as a guide in the development of new peptides for neuropilin-1 targeting.

The third part of the thesis was related to the synthesis of a porphyrin and peptide building blocks through click chemistry technique, to form conjugates with different numbers of porphyrin and peptide attached to the platforms. This approach was taken as way to investigate the possibility of having more than one porphyrin in a platform to improve the photodynamic activity and also in parallel to investigate the ability of having more than one peptide in a platform to improve the targeting ability. Different factors influencing the synthesis yield of the porphyrin building blocks were investigated. As for the building blocks of peptide, two different synthesis approaches for its production were carried out: solid-phase and liquid-phase synthesis. All the products obtained were evaluated through mass spectroscopy and NMR analysis. The yield obtained for the building blocks differs: 96.5% for porphyrin-1-arm, 80.2% for porphyrin-2-arms and 76.8% for porphyrin-3-arms, whilst 82.2% for peptide-1-arm, 66.5% for peptide-2-

arms and 13.3% for peptide-3-arms were obtained. The photophysical characteristics of the porphyrin building blocks were also found to be preserved.

Résumé

La thérapie photodynamique (PDT) est un type de traitement du cancer qui offre de nombreux avantages. Une stratégie pour améliorer l'efficacité de la PDT est l'élaboration de photosensibilisateurs (PSs) de troisième génération, composés d'une molécule photoactivable couplée à un agent de ciblage. Les travaux de recherche de cette thèse portent sur l'amélioration de la sélectivité du traitement PDT en concevant des PSs ciblés. La première partie de la thèse est consacrée à l'étude d'un PS couplé à de l'acide folique (PS-FA). L'acide folique est une unité bien connue de ciblage qui se lie de façon efficace au récepteur de l'acide folique sur-exprimé à la surface de nombreuses cellules cancéreuses. Nous avons particulièrement vérifié la stabilité de l'acide folique sous l'influence des facteurs environnementaux. La deuxième partie est consacrée à l'étude du peptide KDKPPR conçu pour cibler neuropiline-1, un récepteur surexprimé dans les néovaisseaux. Plusieurs modifications du peptide ont été faites et les analogues ont été testés par des analyses ELISA afin d'évaluer leur capacité de liaison à la suite des modifications. La troisième partie de la thèse a consisté en la synthèse de porphyrines couplées à des blocs porteurs de 1, 2 ou 3 peptides grâce à la technique de chimie click pour former de multiples conjugués avec des nombres différents de porphyrines et peptides attachés aux plateformes.

Mots-clés : thérapie photodynamique ; administration ciblée de drogues ; Acide folique; KDKPPR ; Chimie click

Abstract

Photodynamic therapy (PDT) is a type of cancer therapy that could offer many advantages. One possible way to improve the effectiveness of PDT is the elaboration of third generation photosensitizers (PSs) which consisted of PSs coupled with targeting agents. This thesis focuses on improving the selectivity of PS delivery through designing targeted PS agents. The first part of the thesis deals with the study of a PS-folic acid (PS-FA). FA is a well-known targeting unit which bonds with high efficiency to folic acid receptor over-expressed on the surface of many cancer cells. We particularly checked the stability of folic acid under the influence of environmental factors. The second part is devoted to the study of KDKPPR peptide designed to target neuropilin-1, a receptor over-expressed in neovessels. Several modifications of the peptide were made and the analogues were tested through ELISA assays to evaluate their binding capability following the modifications. The third part of the thesis is related to the synthesis of porphyrin and peptide building blocks through click chemistry technique to form multiple conjugates with different numbers of porphyrins and peptides attached to the platforms.

Keywords: Photodynamic therapy; Targeted-drug delivery; Folic acid; KDKPPR; Click chemistry

Table of Content

Acknowledgement	2
Résumé	5
Abstract	7
Table of Content	10
List of Figures	14
List of Tables	18
List of Schemes	19
List of Abbreviations	20
Collaborations	23
Résumé détaillé	24
Chapter I: General Overview	29
[Cancer, Photodynamic Therapy and Drug Targeting]	29
1.0 General Introduction	29
1.1 Cancer and Its Therapeutics	31
1.1.1 General Overview	31
1.1.2 Development of Cancer: Cells, Genes and Mutations	32
1.1.3 Angiogenesis: Background review	34
1.1.4 Angiogenesis: The process	37
1.1.5 Neuropilin-1 receptor and cancer	41
1.1.6 Folate receptor and cancer	44
1.1.7 Treatment approach for cancer	45
A. Surgery	45
B. Chemotherapy	46
C. Radiotherapy	47
D. Immunotherapy	48
E. Hormone therapy	48
F. Bone marrow transplant	49
1.1.7 Current Anti-angiogenesis Treatment	49
1.2 Photodynamic Therapy	52
1.2.1 Historical background of photodynamic therapy	52
1.2.2 Overview of PDT	53

1.2.3	Components of Photodynamic Therapy	57
A.	Light	58
B.	Oxygen	60
C.	Photosensitizer	62
1.2.4	Classification of photosensitizers	63
1.2.5	Porphyrin: Historical Background and Current Advancement	68
A.	Structure of porphyrin	69
B.	Synthesis of Porphyrin	70
C.	Photophysical characteristics	75
1.2.6	Photodynamic action <i>in vivo</i>	77
1.3	Targeted Cancer Therapy: A Strategy in Improving the Delivery of Photosensitizer	79
1.3.1	Improving PS Delivery for PDT	81
1.3.2	Targeting with peptide	82
A.	DKPPR peptide	83
B.	Target application of DKPPR and KDKPPR in PDT	84
1.3.3	Targeting with folic acid	85
1.4	Objectives of Study	89
Chapter II: The Evaluation of Folic Acid Stability: As Free Molecule and as Conjugate for PDT Application		90
2.1	Introduction	90
2.1.1	Folic acid	90
2.1.2	Folic acid in cancer therapy	93
2.1.4	Conjugation with a Model Photosensitizer	96
2.1.5	Experimental approach: Design of Experiment	97
2.1.6	Statistical analysis	98
2.2	Results and Discussion	99
2.2.1	The solubilisation of FA and PS-FA	100
2.2.2	The evaluation of Folic acid stability	102
2.2.3	The evaluation of PS-FA conjugate stability	106
2.2.4	Statistical analysis	108
2.3	Conclusion and Future Perspective	112
Chapter III: Modification of KDKPPR Peptide to Investigate the Effect on its Binding on NRP-1 Receptor		113
3.1	Introduction	113

3.1.1	Peptides	113
3.1.2	Peptides and Solid-phase peptide synthesis	115
3.1.3	Peptides and drug development	119
3.1.4	KDKPPR peptide	121
3.1.5	Peptide modifications performed in this study	122
	A. Alanine-scanning	122
	B. Replacement of K2 lysine with arginine (KDRPPR)	123
	C. <i>Retro, inverso</i> and <i>retro-inverso</i> peptides	124
3.1.6	ELISA competitive binding assay	128
3.2	Results and Discussion	131
3.2.1	NMR analysis	133
3.2.2	ELISA competitive binding assay	135
3.3	Conclusion and Future Perspective	139
Chapter IV: Synthesis of Porphyrin (P1COOH) and DKPPR Peptide Platform through Click Chemistry		140
4.1	Introduction	140
4.1.1	Click chemistry	140
4.1.2	The advantages and disadvantages of click chemistry	146
4.1.3	Porphyrin-based click chemistry	147
4.1.4	Microwave-assisted click chemistry	150
4.1.5	Peptides in click chemistry	151
4.1.6	Synthesis plan	154
4.2	Results and Discussion	158
4.2.1	The synthesis of platform building blocks	158
4.2.2	Building porphyrin blocks through click chemistry	164
4.2.3	Photophysical properties	170
	A. Absorption	170
	B. Fluorescence	171
	C. Singlet oxygen	173
4.2.4	Building DKPPR blocks through click chemistry	175
4.2.5	Building the Porphyrin-DKPPR platform through click chemistry	183
4.2.6	ELISA Competitive Assay	184
4.3	Conclusion and Future Perspective	185
Conclusion		186

Materials and Experimental Section	190
References	221

List of Figures

Figure 1: Number of cancer cases and death in 2012. From [9]	31
Figure 2: Steps of cancer metastasis. From [13]	33
Figure 3: The complex mediators involved in angiogenesis. From [21]	37
Figure 4: The process of angiogenesis in GBM. From [22]	38
Figure 5: The three VEGF receptors. The function of VEGFR-2 in angiogenesis is amplified in the presence of neuropilin receptor as co-receptor. From [17]	39
Figure 6: The VEGFR-1, -2 and -3. Note the extracellular domain is folded in an immunoglobulin, IG-like manner. From [17]	40
Figure 7: The gene structure of VEGF-A which contained eight exons. Exons 6 and 7 encode for heparin-binding domains. From [18].....	41
Figure 8: The crystal structure of neuropilin-1 (B domain), rendered into secondary structure ribbon model. Image obtained from Protein Data Bank, structure code 2ORZ.	42
Figure 9: Average picomoles FR/mg of protein expressed in normal cells in comparison to cancerous cells. Adapted from [135]	44
Figure 10: History of chemotherapy development. From [46]	46
Figure 11: Anti-angiogenesis mechanism demonstrated by currently available drugs. From [36]	50
Figure 12: Milestones of PDT evolution. From [50].....	53
Figure 13: Schematic illustration of photodynamic therapy with the simplified Perrin-Jablonski's diagram. From [53]	54
Figure 14: The inter-relations and inter-connections between different disciplines of knowledge in PDT research. From [57].....	56
Figure 15: The steps involved in photodynamic therapy	57
Figure 16: Depth of light penetration at different wavelengths	58
Figure 17: Light penetration through tissues. Note that red light has the deepest penetration as compared to green and blue lights. From [54]	59
Figure 18: Backbones of porphyrinoid photosensitizers	64
Figure 19: Molecular structure of HpD ($n=1-9$).....	64
Figure 20: Molecular structures of heme (left) and chlorophyll A (right)	68
Figure 21: The porphine macrocycle and <i>meso</i> - position. Beta-positions are denoted by the asterisks (*)	69
Figure 22: Rothmund synthesis method of porphyrin. From [94]	70
Figure 23: Adler and Longo synthesis method of porphyrin. From [96].....	71
Figure 24: An example of reaction to produce symmetrical dipyrromethane.....	72
Figure 25: The synthesis steps of porphyrin as proposed by MacDonald and Woodward. X could be either hydrogen or carboxylic acid (as described in the text above)	73

Figure 26: Synthesis of porphyrin through [3+1] approach [89]	74
Figure 27: UV/VIS absorbance spectrum of porphyrin, substituted porphyrins, chlorins and bacteriochlorins. The intensity of QI band changed according to the type of photosensitizers	75
Figure 28: The fluorescence emission peaks of metallated porphyrin (blue line) in comparison to non-metallated porphyrin (red line).....	76
Figure 29: Mechanism of cell death through apoptosis	77
Figure 30: The differences between passive (A) and active (B) targeting. From [106]	79
Figure 31: Leaky vasculature (right) commonly associated with blood vessels surrounding tumours, in comparison to normal blood vessels (left). From [107].....	80
Figure 32: The 55-residues of carboxy-terminal heparin-binding fragments at the end of VEGF-A ₁₆₅ . Note the c-end rule terminal (R/K-XX-R/K).From Protein Data Bank, structure code 2VGH	83
Figure 33: Mechanism of drug-FA conjugate internalization. From [38]	86
Figure 34: Example of folic acid-drug conjugate. folic acid (module 1) conjugated to a drug (module 4) through a spacer (module 2) and a releasable linker (module 3). This conjugate will help to bring the drug to the targeted cell (image on the right) and the drug will be released inside the cell	87
Figure 35: Molecular structure of FA	90
Figure 36: The degradation products of FA. PABA: <i>p</i> -aminobenzoic acid, Glu: glutamic acid, FPT: 6-formyl pterin, PCA: pterin-6-carboxylic acid, PGA: <i>p</i> -aminobenzoyl-L-glutamic acid,.....	91
Figure 37: Molecular structure of methotrexate (above) and FA (below)	93
Figure 38: Molecular structure of folinic acid	94
Figure 39: Molecular structure of Vintafolide	94
Figure 40: Number of publications (per year) on the development of FR-targeted conjugates	95
Figure 41: One of the porphyrin-FA conjugate synthesized by Schneider and Nancy PDTeam. Red: FA, Green: spacer, Purple: Porphyrin.....	96
Figure 42: Survival of KB cells following phototoxicity TESTS. Grey cross: Unconjugated porphyrin, black square: Conjugate 1, black triangle: Conjugate 2. From [149]	96
Figure 43: Fisher, the pioneer and his book on Design of experiments (ninth edition 1971, first published in 1935).	97
Figure 44: Photodegradation induced by light at 365 nm of FA (red) and two different PS-FA conjugates (P1-FA (blue) and PS-FA (green)), as a function of time.	99
Figure 45: Steps in solubilising PS-FA. The conjugate is usually solubilised after agitation. Sonication was seldom needed	101
Figure 46: Elution of the three degradation products of FA under UV/visible absorbance.....	103
Figure 47: Diminution of FA concentration after light irradiation detected by fluorescence	103
Figure 48: RP HPLC Chromatogram of PS-FA.....	106
Figure 49: Degradation of fA from PS-FA conjugate. The pterin moiety was lost during the degradation	107
Figure 50: Definition of the new modalities for the factors time, temperature and medium.	109

Figure 51: Binary classification tree.....	110
Figure 52: The formation of peptide bond [167].....	114
Figure 53: L- and D-amino acids alanine	114
Figure 54: The synthesis of peptide in solid support is from C-terminus to N-Terminus.....	116
Figure 55: The steps involved in synthesis by SPPS. N-protecting group (NPG) is illustrated as red diamond; side-chain protecting group (SPG) is illustrated as arrows attached on the different amino acids	118
Figure 56: Solid phase synthesis of KDKPPR analogues by using Wang-resin (red circle)	119
Figure 57: Molecular structure of KDKPPR. The dotted lines separate the individual amino acid.....	121
Figure 58: The process of drug discovery from a native peptide. Alanine-scanning is a part at the beginning of the process [165]	122
Figure 59: The structure of lysine (right) and arginine (left)	123
Figure 60: Example of native L-peptide (A), <i>retro-inverso</i> (B), <i>inverso</i> (C) and <i>retro</i> peptide (D). From [209].....	124
Figure 61: Degradation products of tuftsin	127
Figure 62: The Different types of ELISA test. (Ag: Antigen). From [293].....	129
Figure 63: The TOCSY spectra of KDKPPR	134
Figure 64: Percentage of binding of each analogue of KDKPPR on NRP-1 receptor. Also features are tuftsin, DKPPR and K(P1)DKPPR.....	135
Figure 65: ELISA assay results for KDKPPR, KDRPPR, <i>retro</i> RPPKDK and <i>retro-inverso</i> rppkdk peptide.....	137
Figure 66: Types of click chemistry reactions. From [312].....	142
Figure 67: Examples of 1,3-cycloaddition reaction reported in the literature. From [313]	143
Figure 68: Huisgen's cycloaddition without the presence of copper catalysis (above) and with copper (I) catalysis (below). From [313]	144
Figure 69: Methods to introduce copper into a click reaction.....	145
Figure 70: Symmetrically substituted porphyrin and the production of capped porphyrin. From [324]..	147
Figure 71: An example of tetraglyco-porphyrin conjugate synthesized through click reaction	148
Figure 72: Porphyrin-cored glycodendrimer. From [328]	149
Figure 73: Illustration on heat transfer mechanism involved in conventional synthesis technique (left) and microwave (right). From [337].....	150
Figure 74: Triazole ring as amide bond bioisosters. The triazole ring also has three-dimensional planar structure that RESEMBLES an amide bond. From [343].....	152
Figure 75: Click chemistry applications in peptide-related fields [191].....	152
Figure 76: The 9 possibilities of platforms	155
Figure 77: Absorption spectra of P1-COOH and the different Porphyrin-Zn building blocks (in ethanol)	170

Figure 78: Fluorescence emission spectra of P1-COOH ($\lambda_{exc} = 414 \text{ nm}$) and different Porphyrin-Zn blocks ($\lambda_{exc} = 421 \text{ nm}$) in comparison to TPP as standard (in ethanol).....	171
Figure 79: Fluorescence lifetime for P1-COOH ($\lambda_{exc} = 414 \text{ nm}$) and different Porphyrin-Zn blocks ($\lambda_{exc} = 421 \text{ nm}$) (in ethanol)	172
Figure 80: Singlet oxygen production spectra of P1-COOH ($\lambda_{exc} = 414 \text{ nm}$) and different porphyrin-Zn blocks ($\lambda_{exc} = 421 \text{ nm}$) in comparison to Rose Bengal as standard (in ethanol)	173
Figure 81: Singlet oxygen production lifetime of P1-COOH ($\lambda_{exc} = 414 \text{ nm}$) and different porphyrin-Zn blocks ($\lambda_{exc} = 421 \text{ nm}$) (in ethanol)	174
Figure 82: The synthesis approaches to synthesize DKPPR-building blocks	176
Figure 83: The RP-HPLC chromatogram of P1-DKPPR purification. (BLUE: peaks detected at 423 nm, RED: peaks detected at 214 nm)	183
Figure 84: Percentage of bound VEGF ₁₆₅ after introduction of DKPPR (green) and porphyrin-DKPPR platform (blue) respectively	184

List of Tables

Table 1: API under clinical study at different phases as anti-angiogenesis agent.....	35
Table 2: The list of growth factors which have/possibly have interaction with b1/b2 extracellular subdomain of NRP-1. From [27, 28].....	43
Table 3: List of currently available PS and their properties. From [76].....	65
Table 4: Solvents used and their amount for solubilizing FA and PS-S-FA in this study.....	101
Table 5: Details on the RP-HPLC method used for FA analysis in comparison with the reference method.....	102
Table 6: Degradation of FA for all experiments.....	104
Table 7: Details on the method used during the analysis of FA and PS-FA.....	106
Table 8: Degradation of PS-FA for all experiments.....	108
Table 9: Confusion matrix computed with the validation data set.....	111
Table 10: List of peptides evaluated.....	131
Table 11: Synthetic yield of KDKPPR analogues.....	131
Table 12: retention time of KDKPPR analogues.....	132
Table 13: Comparison between mass expected and mass observed of KDKPPR analogues.....	133
Table 14: The EC ₅₀ of KDKPPR analogues prepared through Alanine-scanning as determined through ELISA assays after mathematical estimation with graphpad prism.....	136
Table 15: The EC ₅₀ values of modified peptides after mathematical estimation with graphpad Prism ...	138
Table 16: Different reaction conditions in the synthesis of P1-CO-NH-alkyne.....	162
Table 17: Different click reaction conditions between compound P1-CO-NH-alkyne and one-arm building block (10).....	166
Table 18: Different click reaction conditions between compound P1-CO-NH-alkyne and two-arm building block (11).....	168
Table 19: Different click reaction conditions between compound P1-CO-NH-alkyne and three-arm building block (12).....	168
Table 20: Molar extinction coefficient, ϵ of the synthesized products, in ethanol (L/mol.cm).....	171
Table 21: Fluorescence quantum yield, singlet oxygen quantum yield, fluorescence lifetime and singlet oxygen lifetime of the synthesized products, in ethanol (L/mol.cm).....	174
Table 22: List of different trials for the synthesis of DKPPR-blocks.....	182
Table 23: Modified design of experiments for the 56 experiments – Model Identification	195
Table 24: Modified design of experiments for the 33 experiments – Model Validation	196
Table 25: The purification condition for product 15	215
Table 26: The purification condition for products 17 , 18 and 19	217

List of Schemes

Scheme 1: Examples of 1,3-dipolar compounds. Above: nitrile oxide, below: azide	143
Scheme 2: Synthesis of 2-(2-azidoethoxy)ethyl methanesulfonate from diethylene glycol (MsCl: methanesulfonyl chloride, NaN ₃ : sodium azide)	158
Scheme 3: Synthesis of 3-azidopropan-1-amine. (NaN ₃ : sodium azide)	158
Scheme 4: Synthesis of one-arm building block from methyl-4-hydroxybenzoate	159
Scheme 5: Synthesis of two-arm building block from methyl-3,5-dihydroxybenzoate	159
Scheme 6: Synthesis of three-arm building block from methyl-3,4,5-trihydroxybenzoate	160
Scheme 7: Synthesis of meso-substituted porphyrin P1-COOH.....	160
Scheme 8: Introduction of alkyne functional group on porphyrin P1-COOH	161
Scheme 9: Metallation of porphyrin P1-COOH by zinc.....	163
Scheme 10: Click reaction to produce one- (product 10), two- (Product 11) and three-arms (Product 12) porphyrin blocks	164
Scheme 11: Introduction of alkyne functional group on the NH ₂ -terminal of aspartic acid. The example here is conducted on solid phase (black circle represent Wang resin).....	175
Scheme 12: Click reaction of DKPPR-alkyne and 4'	177
Scheme 13: Synthesis of modified building block 4''	178
Scheme 14: Synthesis of modified building block 5''	178
Scheme 15: Synthesis of modified building block 6''	179
Scheme 16: Synthesis of DKPPR-building blocks on solid phase (Approach 2)	180
Scheme 17: Synthesis of one-arm DKPPR block on liquid phase (Approach 3).....	181

List of Abbreviations

¹O₂	Singlet oxygen
5-ALA	5-Aminolevulinic Acid
ACS	American Cancer Society
ADC	Antibody-drug conjugate
Ala (A)	Alanine
ALL	Acute lymphoblastic leukaemia
API	Active pharmaceutical ingredient
APC	Adenomatous polyposis coli
Arg (R)	Arginine
Asn (N)	Asparagine
Asp (D)	Aspartic acid
ATRA	all- <i>trans</i> retinoic acid
COSY	Correlation spectroscopy
CRAN	Centre de Recherche en Automatique de Nancy
DCM	Dichloromethane
DMF	Dimethylformamide
DMSO	Dimethylsulfoxide
DNA	Deoxyribonucleic acid
DoE	Design of Experiment
DTE	Dithioerythritol
<i>e</i>	electrone
EC₅₀	Effective concentration half-maxima
EGFR	Epidermal growth factor receptor
ELISA	Enzyme-Linked Immunosorbent Assay
EPR	Enhanced Permeability and Retention
FA	Folic acid
FDA	Food and Drug Administration
FGF	Fibroblast growth factor
FMD	Foot and mouth disease

FPT	6-formyl pterin
FR	Folate receptor
GIT	Gastrointestinal tract
Gly (G)	Glycine
H₂O₂	Hydrogen peroxide
HBTU	<i>N,N,N',N'</i> -Tetramethyl- <i>O</i> -(1 <i>H</i> -benzotriazol-1-yl)uranium hexafluorophosphate
HGF	Hepatocyte growth factor
HO[•]	Oxidant-hydroxyl radical
HpD	Haematoporphyrin derivatives
<i>hν</i>	Light
<i>i.s.c</i>	Intersystem crossing
LC-MS	Liquid chromatography-coupled mass spectrometry
LCPM	Laboratoire de Chimie Physique Macromoléculaire
LDL	Low density lipoprotein
LED	Light-emitting diode
LRGP	Laboratoire des Réactions et Génie des Procédés
Lys (K)	Lysine
mAbs	Monoclonal antibodies
min	minutes
MMP	Matrix Metalloproteinase
NSCLC	Non-small cell lung cancer
NMM	<i>N</i> -methylnmorpholine
NMP	<i>N</i> -methylpyrrolidone
NMR	Nuclear Magnetic Resonance
NRP-1	Neuropilin-1
NRT-1	Neurotensin-1
O₂^{•-}	Superoxide anion radical
OS	Overall patients' Survival
PABA	<i>p</i> -aminobenzoic acid
PCA	Pterin-6-carboxylic acid
PDB	Protein Data Bank
PDGF	Placenta-derived growth factor

PDGFR	Placenta-derived growth factor receptor
PEG	Polyethylene glycol
PFS	Progression-Free Survival
PGA	<i>p</i> -aminobenzoyl-L-glutamic acid
PIGF	Placental growth factor
PLGF	Placenta Growth Factor
PPIX	Protoporphyrin IX
Pro (P)	Proline
PDT	Photodynamic Therapy
PS	Photosensitizer
ROS	Reactive oxygen species
RP- HPLC	Reversed Phase High Performance Liquid Chromatography
rt	Room temperature
S_0	Ground state
S_1	Excited singlet state
SPPS	Solid Phase Peptide Synthesis
Streptavidin-HRP	Streptavidin-Horseradish Peroxidase
T_1	Triplet state
TAF	Tumour Angiogenesis Factor
TFA	Trifluoroacetic acid
TGF	Transforming growth factor
TIPS	Triisopropylsilane
TKI	Tyrosine kinase inhibitor
TMB	Tetramethylbenzidine
TOCSY	Total Correlation Spectroscopy
TPC	5-(4-carboxyphenyl)-10,15,20-triphenylchlorin
TPP	5-(4-carboxyphenyl)-10,15,20-triphenylporphyrin
UV	Ultraviolet
VEGF-A₁₆₅	Vascular Endothelial Growth Factor-A ₁₆₅
VEGFR	Vascular Endothelial Growth Factor Receptor

Collaborations

Laboratory	Personnel
LCPM, Nancy (UMR 7375)	Régis Vanderesse (<i>Director of thesis</i>) Samir Acherar (MC) Mathilde Achard (T) Eugenia Longarela del Hoyo (Bac)
LRGP, Nancy (UMR 7274)	Céline Frochot (<i>Co-Director of thesis</i>) Philippe Arnoux (IE) Francis Baros (CR) Ludovic Colombeau (Post-Doc) Zahraa Youseff (D) Mathilde Lobry (MSc) Pierre Althusser (MSc)
CRAN, Vandoeuvre-lés-Nancy (UMR 7039)	Cédric Boura (MC) Thierry Bastogne (Pr) Thibaut Peterlini (MSc)

Résumé détaillé

Le cancer est une maladie résultant de la prolifération anarchique de cellules qui se multiplient indéfiniment. Ces cellules sont capables d'envahir le tissu normal avoisinant, de le détruire puis de migrer et coloniser d'autres tissus – on parle alors de métastases. La prolifération est rendue possible, entre autre, par le fait que les cellules cancéreuses ne répondent plus au signal d'autodestruction (les facteurs pro-apoptotiques) reçu par la cellule par des «récepteurs de mort».

Les traitements classiques du cancer sont: la chirurgie qui consiste à retirer les parties du corps envahies par les tumeurs ; la radiothérapie qui utilise les rayonnements ionisant émis par certains éléments radioactifs pour détruire les cellules anormales ou du moins ralentir leur progression et la chimiothérapie qui implique l'utilisation de produits chimiques ayant un effet direct sur les cellules malades, soit en les détruisant, soit en empêchant leur prolifération.

Malgré leur efficacité, toutes ces techniques présentent de nombreux inconvénients : la chirurgie est en générale trop invalidante pour le malade (même si des progrès sont faits pour diminuer la gêne occasionnée), tandis que la radiothérapie et la chimiothérapie manquent de sélectivité et touchent également les tissus sains.

Puisque le cancer est la deuxième cause de mortalité chez l'homme (après les maladies cardiovasculaires), on comprend l'intérêt de la thérapie photodynamique (PDT). Il s'agit en effet d'une technique innovante qui a été récemment acceptée en clinique pour traiter un certain nombre de cancers et ne présentant pas tous les inconvénients des autres traitements.

La PDT repose sur une accumulation plus ou moins sélective d'une molécule photo-activable (le photosensibilisateur ou PS) dans les cellules tumorales ou les néovaisseaux alimentant les tumeurs, suivie d'une exposition à une longueur d'onde appropriée de lumière pour activer le photosensibilisateur. Lorsqu'il est activé par irradiation lumineuse ou RX, le PS interagit avec l'oxygène moléculaire pour conduire à la production d'espèces réactives de l'oxygène cytotoxiques, en particulier une espèce de courte durée connue sous le nom d'oxygène singulet. La PDT engendre des réactions apoptotiques et nécrotiques au sein de tumeurs traitées et produit des effets microvasculaires menant à l'inflammation et à l'hypoxie.

La thérapie photodynamique (PDT), parfois appelée photochimiothérapie, est une forme de photothérapie impliquant la lumière et une substance chimique photosensible, utilisée en conjonction avec de l'oxygène moléculaire pour provoquer la mort cellulaire (phototoxicité). La PDT a prouvé sa capacité à tuer des cellules microbiennes, y compris les bactéries, les champignons et les virus. La PDT est couramment utilisée dans le traitement de l'acné et autres

maladies cutanées. Elle est utilisée en clinique pour traiter un large éventail de maladies, y compris la dégénérescence maculaire liée à l'âge, le psoriasis, l'athérosclérose et a montré une certaine efficacité dans les traitements anti-viraux, y compris l'herpès. Il traite également certains cancers malins comme le carcinome de la tête et du cou, du poumon, de la vessie et de la peau en particulier. La technologie a également été testée pour le traitement du cancer de la prostate.

La principale caractéristique d'un agent photosensibilisant est sa capacité à s'accumuler préférentiellement dans le tissu malade et induire un effet biologique souhaité par l'intermédiaire de la génération d'espèces cytotoxiques. Les critères spécifiques des PS peuvent être résumés ainsi :

- Concernant l'aspect chimique, des synthèses simples avec des rendements transposables.
- une bonne stabilité chimique avec une composition connue et constante.

Concernant les caractéristiques photophysiques des photosensibilisateurs, elles doivent être appropriées avec

- un coefficient d'extinction élevé dans l'infrarouge (600-850 nm) pour une plus grande pénétration de la lumière dans les tissus plus profonds.
- un temps de vie relativement long et une énergie élevée de l'état triplet et un rendement quantique élevé eu formation d'oxygène singulet.
- Une faible cytotoxicité en l'absence de lumière. (Le photosensibilisateur ne doit pas être nocif pour le tissu cible jusqu'au traitement par la lumière).
- Un faible photoblanchiment

Enfin, concernant les propriétés pharmacodynamiques et pharmacinétiques, les PS doivent répondre aux critères suivants :

- Une clairance rapide après traitement
- Une bonne solubilité dans les milieux biologiques, ce qui permet une administration intraveineuse.
- Une accumulation préférentielle dans les tissus malades par rapport aux tissus sains.

Ces photosensibilisateurs de première ou deuxième génération souffrent néanmoins d'un certain nombre d'inconvénients tels une solubilité trop faible ou un manque de sélectivité pour les tissus tumoraux. Une stratégie pour améliorer l'efficacité de la PDT est l'élaboration de photosensibilisateurs de troisième génération, composés d'un PS couplé à un agent de ciblage. Les agents de ciblage peuvent être des peptides, des anticorps monoclonaux, des LDL, des sucres.... Il est également possible d'utiliser des systèmes d'administration avancés tels que des

liposomes ou des nanoparticules. Ces stratégies permettent de délivrer directement le PS aux sites tumoraux.

Ces travaux de thèse ont porté sur l'amélioration de la localisation du PS à travers le design de constructions moléculaires composées d'un PS couplé à une unité d'adressage. Le chapitre II de la thèse porte sur l'étude de l'acide folique (AF), une unité de ciblage qui se lie efficacement aux récepteurs à l'acide folique (RF) sur-exprimés à la surface de nombreuses tumeurs.

L'acide folique (FA) est une petite molécule, également connue sous le nom de vitamine B9. C'est un composé essentiel impliqué dans de nombreux processus biochimiques importants chez l'homme, principalement sous sa forme ionique. L'AF est disponible à la fois naturellement et synthétiquement. Les dérivés d'AF naturellement disponibles chez l'homme, les plantes et les aliments d'origine animale sont sous une forme réduite et sont plus stables que l'AF synthétique, mais ils ont une faible biodisponibilité. L'AF est cependant largement utilisée comme vecteur pour le traitement et le diagnostic ciblé.

De nombreuses applications cliniques ont été effectuées avec des médicaments ciblés par l'acide folique en particulier dans le domaine de la recherche anticancéreuse. En effet, le récepteur de folate (RF) est une cible antitumorale prometteuse car elle est surexprimée par 40% des tumeurs solides et est absente dans la plupart des tissus sains. Les thérapies ciblées dirigées vers le récepteur de l'acide folique sont étudiées dans plusieurs types de cancer, y compris le cancer du poumon, mais à l'heure actuelle, le cancer épithélial ovarien est l'indication la plus étudiée pour le développement de ce type de traitement.

Dans le domaine de la PDT, le développement d'un conjugué d'acide folique lié à un PS pour cibler les RF pour le traitement du cancer de l'ovaire est une stratégie prometteuse. En effet, en dépit des stratégies de traitement (chirurgie et la chimiothérapie) qui sont souvent utilisés dans le cadre clinique pour le traitement du cancer de l'ovaire, les taux de récurrence restent élevés. 60% des femmes en rémission développent une récurrence dans un délai de cinq ans. Par conséquent, le développement de la PDT ciblée par l'acide folique et associée à la chimiothérapie conventionnelle, la radiothérapie et la chirurgie, pourrait diminuer ce taux de récurrence. Par ailleurs, la thérapie photodynamique pourrait faire partie d'une gestion innovante des métastases péritonéales à la suite d'un cancer de l'ovaire. Sa capacité à traiter les lésions superficielles disséminées sur une grande région en fait un excellent candidat qui pourrait permettre d'assurer la destruction de la maladie résiduelle microscopique en complément de la chirurgie. Cette recherche fait l'objet d'une collaboration étroite entre la PDTeam de Nancy et ONCOTHAI (INSERM-Lille). Cependant de nombreuses données de la littérature font état de l'instabilité de l'acide folique sous l'influence de plusieurs facteurs qui incluent la lumière, la haute température, la présence d'oxygène et le milieu. Récemment, nous avons soumis une revue

intitulée « Is Folic acid an ideal targeting agent ? »; elle est présentée dans l'Annexe 9.

Nous avons particulièrement vérifié la stabilité de l'acide folique sous l'influence des facteurs environnementaux tels que la lumière, l'oxygène, le milieu, le temps et de température. Les expériences ont été réalisées en utilisant un plan d'expériences et les résultats ont été analysés statistiquement. D'une manière générale, on constate que le conjugué PS-acide folique présente un profil de stabilité amélioré par rapport à la molécule d'acide folique non couplée. Une publication de ces travaux sera prochainement soumise.

La deuxième partie est consacrée à l'étude du peptide DKPPR ciblant la neuropiline-1 (NRP-1), un récepteur surexprimé dans les néo-vaisseaux. Ce peptide a été découvert par notre équipe et est issu d'une étude par modélisation moléculaire suivie de tests ELISA et d'analyses *in vivo*. DKPPR a d'abord été conçu sur la base de la séquence de la tuftsine (TKPR), un ligand connu du NRP-1 mais aussi sur la base de la séquence terminale du VEGF-A₁₆₅ se liant à l'héparine. Il a été montré que ce peptide avait une très bonne affinité pour NRP-1 et a donc été choisi comme base pour la suite de nos travaux. Deux publications ont porté sur ces travaux et sont en les Annexes 10 et 11.

Par ailleurs, dans le cadre d'une étude parallèle, nous voulions greffer le peptide et le photosensibilisateur simultanément sur des nanoparticules. Il n'était pas possible d'utiliser le NH₂ epsilon de la lysine comme point d'ancrage du PS car cette lysine doit conserver son intégrité pour une bonne reconnaissance. Cela nous a conduits à modifier DKPPR en lui ajoutant une lysine supplémentaire à l'extrémité N-terminale sur laquelle nous pouvions greffer le PS sur l'amine en position δ. De manière surprenante l'ajout de cette lysine (ou de la Lys-PS) ont grandement favorisé la reconnaissance par NRP-1 comme cela a pu être évalué par ELISA. L'hexapeptide KDKPPR est devenu alors le peptide d'intérêt de la PDTeam.

Pour affiner plus encore la reconnaissance, plusieurs modifications ont été faites sur ce peptide pour connaître l'importance de chaque acide aminé sur l'affinité du peptide pour NRP-1. Les acides aminés ont été remplacés l'un après l'autre par une alanine (alanine-scanning). Tous les analogues ont été testés grâce à des tests ELISA et il a été constaté que les quatre derniers acides aminés (-KPPR) sont essentiels pour l'affinité et le remplacement de ces acides aminés par l'alanine provoque une importante perte d'affinité dans l'ordre de KDKPPA > KDKPAR = KDKAPR > KDAPPR. Seul l'acide aspartique ne semble pas jouer un rôle essentiel sur la reconnaissance et pourrait être remplacé par un autre acide aminé. Enfin, la lysine supplémentaire semble n'avoir qu'une faible incidence sur la reconnaissance puisque ADKPPR et KDKPPR se lient pratiquement de la même façon. L'amélioration par rapport au pentapeptide de base DKPPR vient sans doute plus de l'addition d'un acide aminé que de sa nature même. Dans notre cas, puisque cette lysine sert à greffer le photosensibilisateur, il ne sera donc pas question de la remplacer.

La troisième partie concerne la synthèse de plateformes portant un nombre variable de porphyrines zinguées (1, 2 ou 3) et un nombre variable de peptides DKPPR (1, 2 ou 3) en utilisant la chimie click et plus précisément la cycloaddition 1,3-dipolaire de Huisgen catalysée par les sels de cuivre. L'intérêt de cette approche est de pouvoir étudier la possibilité d'avoir plus d'une porphyrine pour améliorer l'activité photodynamique et, en parallèle plus d'un peptide pour améliorer la capacité de ciblage. La construction de ce type de plateformes nécessite la préparation préalable d'acides benzoïques substitués par 1, 2 ou 3 oligo-éthylèneglycols azidés qui permettront l'ancrage de 1, 2 ou 3 propargylporphyrines. Ces synthèses ne présentent aucune difficulté mais ont cependant demandé quelques mises au point.

Différents facteurs influençant le rendement de synthèse des blocs de porphyrines ont été étudiés. En particulier, nous avons montré que le choix du solvant et surtout l'irradiation microonde pouvait améliorer grandement la cycloaddition-1,3. Les trois blocs porteurs de porphyrine(s) ont pu être obtenus avec des rendements satisfaisants (77-96%) avec une difficulté de synthèse croissante avec le nombre de porphyrines à coupler. Les caractéristiques photophysiques des différents blocs porteurs de porphyrine(s) ont également été mesurées et aucune différence notable n'a été détectée entre ces plateformes et la porphyrine pure.

En ce qui concerne les blocs porteurs de peptides, deux approches différentes de synthèse ont été réalisées: en phase solide et en phase liquide. Tous les produits obtenus ont été caractérisés par spectroscopie de masse et par RMN. Les rendements de synthèse de ces blocs varient de 13 à 97%. Une publication est actuellement soumise à Tetrahedron, elle est dans l'annexe 12.

Finalement, une condensation entre la plateforme à une porphyrine et une plateforme à un peptide a été réalisée et le composé a été soumis à un test ELISA. Le complexe porphyrine-DKPPR conserve sa capacité à cibler NRP-1 mais avec une capacité réduite par rapport à DKPPR seul (EC_{50} : 150 μ M par rapport à 18,3 μ M pour DKPPR). Ce résultat demande cependant à être confirmé.

Chapter I: General Overview

[Cancer, Photodynamic Therapy and Drug Targeting]

1.0 GENERAL INTRODUCTION

The classical and conventional chemotherapy of cancer utilizes systemically administered drug which will be distributed throughout the body system once introduced into circulation. This brings about many disadvantages such as high dose requirement because the drug is being distributed and partitioned around the body. The distribution and partitioning of these toxic drugs cause the development of adverse drug reactions commonly associated with chemotherapy. Hence, many researchers tend to move towards developing targeted drug delivery as this is believed to have better outcome in terms of patient recovery [1-3].

Targeted drug delivery is not a new concept. Paul Ehrlich in the early 20th century has proposed a theory called the “magic bullet”, which he defined as “*compounds which would have a specific attraction to disease-causing microorganisms by seeking them out and destroying them whilst avoiding other organisms and having minimal undesired/harmful effects on the patient*” [4]. This gives rise to the ideas of utilizing active targeting in the therapy of different diseases, and in the interest of this study for cancer therapeutics.

Photodynamic therapy (PDT) is a potentially advantageous modality that has shown great chances and improvements of treatment efficacy, safety and reduces toxicity as compared to chemotherapy. It could be considered as one step closer towards realization of the “magic bullet” idea due to the fact that the ‘drug’ or the photosensitizing agent administered having no or low toxicity in the absence of light and hence could offer a safer alternative and reduces the risk of toxicity [2]. However, with regard to the earliest photosensitizers (the first and second generations) developed or under study, mostly showed lack of selectivity towards cancer cells and had the tendency to accumulate in the skin and other healthy tissues. This would subsequently cause skin photosensitivity reaction upon exposure to light. In an attempt to improve the selectivity of the photosensitizers, third-generation photosensitizers are being developed which includes a targeting agent conjugated with a photosensitizer of second generation.

This thesis consists of four main chapters; the first (current chapter) describes the essential backgrounds and updates on cancer, photodynamic therapy (PDT) and the basis of drug targeting, with special interest on the targeting of Folic acid and Neuropilin-1 receptor for photodynamic therapy application. The needs and importance of research on cancer and its therapy is discussed, and also the potential that PDT has for the improvement of cancer therapy.

The three following chapters were on the three projects conducted during the course of the work (Chapter II, III and IV). The first and second projects evolve around the evaluation of targeting vehicle for PDT. Folic acid was chosen first of all as a targeting moiety and a stability evaluation was performed on free folic acid molecule and on folic acid-conjugated photosensitizer. The second part is on a study of a peptide KDKPPR which was found to target Neuropilin-1 (NRP-1) receptor [5, 6]. The importance of each amino acid in the sequence was determined through a technique called ALA-scanning. The third project is on the development of a third generation photosensitizer. A porphyrin-based photosensitizer was conjugated with a targeting peptide (DKPPR) *via* click chemistry approach. The approach proposed has the advantage of producing platforms of porphyrin-peptide with different number of porphyrins and/or peptides in the platforms. Further details will be described in the following chapters under the respected topics of interest.

1.1 CANCER AND ITS THERAPEUTICS

1.1.1 General Overview

Cancer in medicine is a term used to describe malignant tumours or neoplasm. Cancer can basically affect any part of the body. Studies on cancer cells have revealed that there are differences among cells subpopulation from the same tumour; they vary in terms of their ability to metastasize, drug response, immunogenicity and growth rate, and hence this shows their heterogeneity in terms of functions and phenotype. The differences in terms of phenotyping are believed to be due to both the genetic and non-genetic variability contained in the tumour cells. Although cancer cells could arise from mutations due to environmental and other non-genetic factors, cancer is widely believed to be a genetic-related disease caused by mutations on susceptible genes, such as the oncogenes and tumour-suppressor genes [7].

There are actually more than 200 different types of cancer, from which about 85% are carcinomas. Carcinomas are cancers of the epithelium and among the most common carcinomas are breast, prostate, lung and colon cancers. Another 6.5% comes from cancer of the blood; the lymphoma and leukaemia, and cancer of the lymph glands, whilst cancers of the muscle, bone and fatty tissues contributed to approximately 1%. The balance 7.5% is of the rarer cancers comprising of brain tumours and multiple myeloma [8].

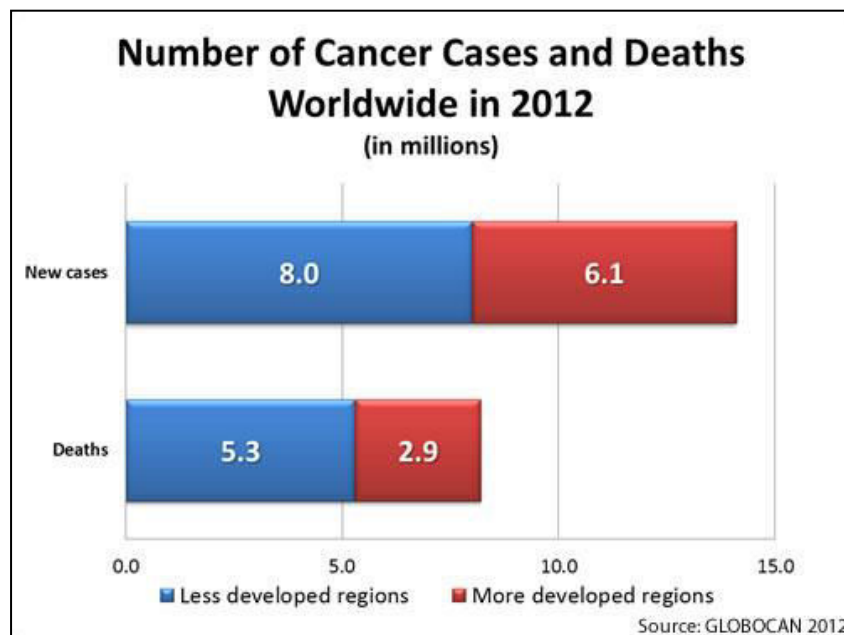


Figure 1: Number of cancer cases and death in 2012. From [9]

Based on the most recent worldwide cancer statistic available from the WHO which was for the year 2012, cancer has caused 8.1 million of deaths in that year alone (Figure 1). Among the adults, lung cancer caused the highest number of deaths, 1.59 million followed by liver and stomach cancer at around 700,000 deaths [10]. Leukaemia on the other hand causes the highest number of deaths among children.

The approach taken in the development of therapeutic for cancer has evolved throughout the years. Although statistically there were only 5% success rate of oncology drugs in clinics, researchers continue to work and efforts are put into finding useful drugs in the management of cancers. The low success rate is attributed to many different factors: poor pharmacokinetics and bioavailability of the drugs, insufficient activity *in vivo* and also high toxicity. Improvement have been made, and specific targeting drugs are actively under research and development based on the knowledge we have on the many different receptors that we could use to target cancers, thanks to the on-going researches conducted to understand the mechanism of this killer disease [11].

1.1.2 Development of Cancer: Cells, Genes and Mutations

Based on the latest finding, cancer is now regarded as an evolving ecosystem. It adapted itself to the surrounding and the available resources in order to ensure its existence and growth are not disrupted. The progression of tumours is largely determined by the tumour microenvironment. The signals delivered from various sources such as from immune cells, endothelial cells and modifier genes would determine either the tumour will progress or stay dormant, or either the initial cancerous lesion will get destroyed or progresses into malignancy [12]. The difference in resources available to tumour cells due to the unique tumour architecture and properties could also be the reasons for their continuous survival.

Cancer cells divide uncontrollably, are undifferentiated, have atypical cell structures and do not function like normal cells. The cells do not have the same function as the organ from where they originally divided; rather they display invasiveness and compete for nutrients from the surrounding normal cells which subsequently caused nutritional deprivation of the normal cells and thus killing them. They would usually induce the formation of new blood capillaries through a process called angiogenesis once they achieve certain sizes, to get a more constant supply of various resources for their growth. Subsequently, these cancerous cells will invade adjoining parts of the body and spread to other organs in a process called metastasis [10].

Figure 2 describes the steps involved in cancer metastasis. In (a), cells reduce adhesion to neighbouring cells and subsequently clear a path for migration into the stromal cells (b). In order to allow its movement into blood vessels, the cells would induce endothelial cell retraction by releasing compounds such as VEGF or cause endothelial cell death by releasing reactive oxygen species and molecules such as MMPs (c). The cancer cells then either express a receptor that could bind to metastasis-supporting sites (d) or the cells would bind to platelets (e) to protect them from the immune system. Upon finding a suitable new environment, the cells would exit the bloodstream (f) by causing endothelial cell retraction or death and finally induce the release of necessary growth factors by the surrounding cells to support their growth (g) [13].

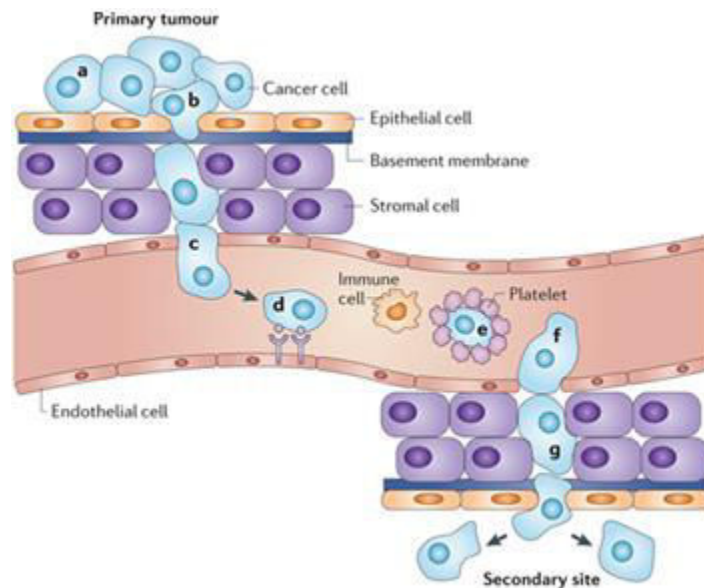


Figure 2: Steps of cancer metastasis. From [13]

The genes that are susceptible to mutations as mentioned before could be divided into three types. Metaphorically, they are known as the caretaker, the gatekeeper and the landscaper genes, and the mutation on these genes usually causes hereditary-related cancers [14]. Caretaker genes are not tissue specific and hence they usually control the genome of multiple tissues. Its function is crucial in maintaining the stability of tissue growth through producing substance that preserves the genome stability. The mutation on caretaker genes will lead to genome instability and subsequently loss of tissue growth control. However, changes on caretaker genes alone is insufficient to cause cancer [15].

The second type of gene, the gatekeeper gene is more tissue specific. It has control over proliferation, differentiation and apoptosis of cells and hence under normal functional condition, it has the ability to maintain the tissue stability and cell numbers. Since gatekeepers are tissue specific, it is believed that they could serve as tumour biomarkers. As an example, the mutation on the APC gene is a useful biomarker for colorectal cancer. It was found that large bowel cancer that arises in young individuals is nearly 100% in those that inherited the mutated APC gene [15, 16]. Finally, landscaper genes as the name implies are responsible in providing a suitable microenvironment for tumour growth. The microenvironment will have the ability to re-program the tumour cells so that they can be controlled and act as normal cells [15].

Mutations on a single gene will not cause a full-blown cancer; instead multiple mutations usually happened on cellular lineage leading to the progression of tumour growth into malignancy and invasion. It is also very interesting to note that in recent years, quantitative methods with mathematical models have been developed to evaluate the genetic instability that could lead to tumour development [7]. By predicting such possibility, earlier detection and treatment could be carried out and hence increasing the chance of survival.

1.1.3 Angiogenesis: Background review

Angiogenesis is the formation of new blood capillaries from existing vasculatures. It is the hallmark mechanism in normal bodily functions such as during wound healing, embryonic development (vasculogenesis) and reproduction, menstrual cycle and also blood vessel formation in adult [17]. Unfortunately, it is also a mechanism utilized by cancer cells and various ischemic and inflammatory diseases in maintaining their pathological function and in order to draw-in nutrients and oxygen needed to support their growth [18].

The concept of angiogenesis was first augured in early 1970s, when Dr Judah Folkman proposed several hypotheses on the presence and the importance of angiogenesis on tumour survival, and the possibility of developing anti-angiogenesis drugs as a way of treating cancer. His hypotheses include (1) Angiogenesis is not essential for very small tumours. Up until the size of around 1-2 mm in diameter, the cancer cells could obtain oxygen and nutrient that are necessary for their growth through simple passive diffusion from nearby blood vessels; (2) Once their need becomes more than those available from simple diffusion, the tumour cells have the ability to induce the sprouting and formation of blood capillaries from nearby blood vessels, and hence providing the infinite growth capability in addition to metastatic spread ability as well; (3) A specific factor produced by the tumour mass itself called 'tumour angiogenesis factor' (TAF) is believed to be responsible for inducing the formation of blood capillaries; (4) The inhibition of the TAF factor ought to be possible as a method of supressing tumour growth. In addition it must also be possible to inflict damage on the newly formed blood vessels. If the latter strategy is

feasible, there will be some structural differences between the normal and the tumour-induced capillaries which will allow targeting of active pharmaceutical ingredients (API); (5) The anti-angiogenesis treatment would not be curative, but instead is a kind of *dormancy-inducing*. In this way, the treatment will cause continuous regression of the tumour mass until the size of 1-2 mm when they could survive without direct blood supply [19].

All these hypotheses are generally accepted in current time, after vigorous fundamental research and drug development works were carried out on angiogenesis. There are several contributing factors to the increased interest on angiogenesis research and among all is the discovery of certain factors that play a role in angiogenesis, such as the VEGFR and the related factors and receptors. Different angiogenesis factors have been identified to date and this includes the EGF, VEGF, TGF- α , TGF- β and angiogenin [20]. A big number of APIs are being tested for anti-angiogenesis therapy in various clinical phases. Table 1 below was constructed based on data available on www.clinicaltrials.gov (there are also a number of completed studies that was not included). Among the completed studies, some molecules were unfortunately have to be discarded such as SU5416 and TNP-470 (Table 1) due to their inability to offer positive outcomes [19], which means that more work is needed in finding effective anti-angiogenesis agents.

Table 1: API under clinical study at different phases as anti-angiogenesis agent

Drug	Mechanism of action [Type of cancer]	Company	Status
PHASE I			
COL-3	MMP inhibitor (tetracycline derivative) [Refractory metastatic cancer]	Collagenex, NCI	Completed (2003)
AMG 706	Mechanism unknown [Advanced solid tumours]	Amgen	Completed (2006)
Combretastatin	Causes apoptosis of endothelium during proliferation [Advanced solid tumour]	Oxigene	Completed (2007)
PTK787/ZK222584	VEGFR tyrosine kinase inhibitor [Refractory/advanced cancer]	Novartis	Completed (2009)
PF-00337210	Mechanism unknown [Advanced solid tumours]	Pfizer	Completed (2011)
PHASE II			
SU5416	VEGFR signal blockage	Pharmacia	Terminated (2002) [discarded]
TNP-470	Endothelial proliferation inhibitor [Adenocarcinoma of pancreas]	TAP Pharmaceuticals	Terminated (2004) [discarded]

EMD121974	Integrin antagonist [Glioblastoma multiforme]	EMD Serono	Completed (2007)
Squalamine	Na/H exchange inhibitor [Advanced prostate cancer]	OHSU Knight Cancer Inst.	Completed (2007)
AG-013736	Tyrosine kinase inhibitor of VEGFR and PDGFR [Anti-angiogenesis for metastatic thyroid cancer]	Pfizer	Completed (2009)
Thalidomide	VEGF blockage (probable mechanism) [Anti-angiogenesis in leukaemia]	Celgene	Completed (2010)
PHASE III			
IM862	[Kaposi's sarcoma]	Cytran	Terminated (2001) [discarded]
AG3340	MMP inhibitor [Advanced NSCLS]	Pfizer	Completed (2001)
Marimastat	MMP inhibitor	ILEX Oncology Service, Inc.	Completed (2004)
Neovastat/AE941	MMP and VEGFR inhibitor [Metastatic kidney cancer] [NCSLC]	Aeterna	Completed (2007)
SU5416	VEGFR signal blockage	Pfizer	Completed (2007)
PHASE IV			
Endostatin	Endothelial cell proliferation inhibitor [NSCLC]	Tianjin Medical University Cancer Inst. and Hosp.	Completed (2015)

1.1.4 Angiogenesis: The process

Angiogenesis involves the coordination of multiple factors from cells and their surroundings. Figure 3 illustrates the complexity involved [21].

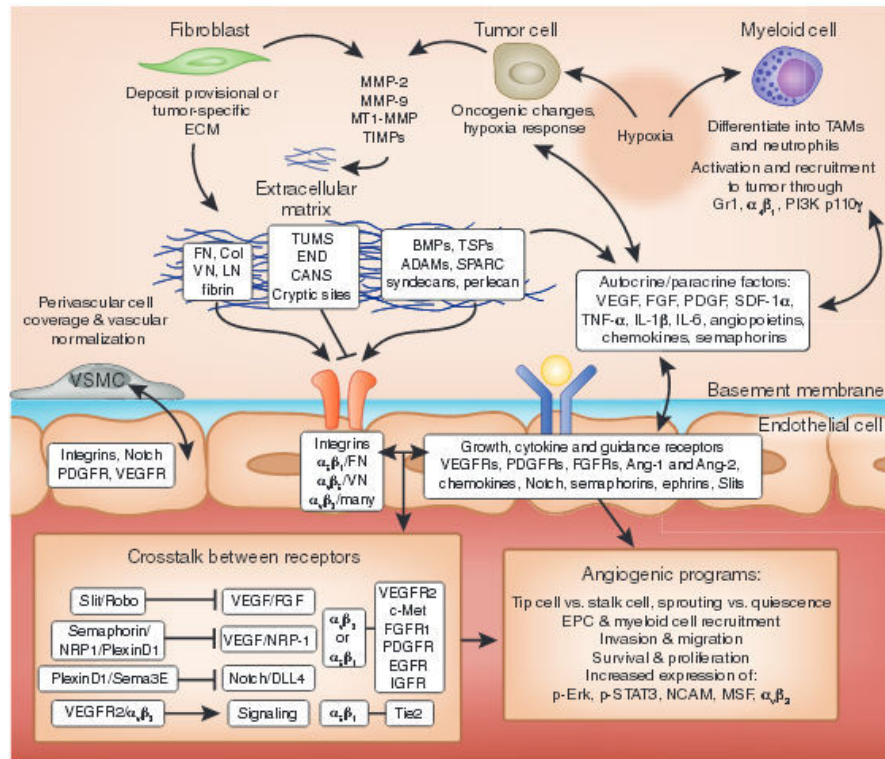


Figure 3: The complex mediators involved in angiogenesis. From [21]

In the process of angiogenesis, vascular endothelial growth factor or VEGF is an important pro-angiogenic factor. The release of this factor by the cancer cells can induce the formation of new blood vessels (neo-vessels) towards them, sprouting from the available ones nearby. Figure 4 illustrates the process involved in angiogenesis, based on the steps of angiogenesis in glioblastoma multiforme.

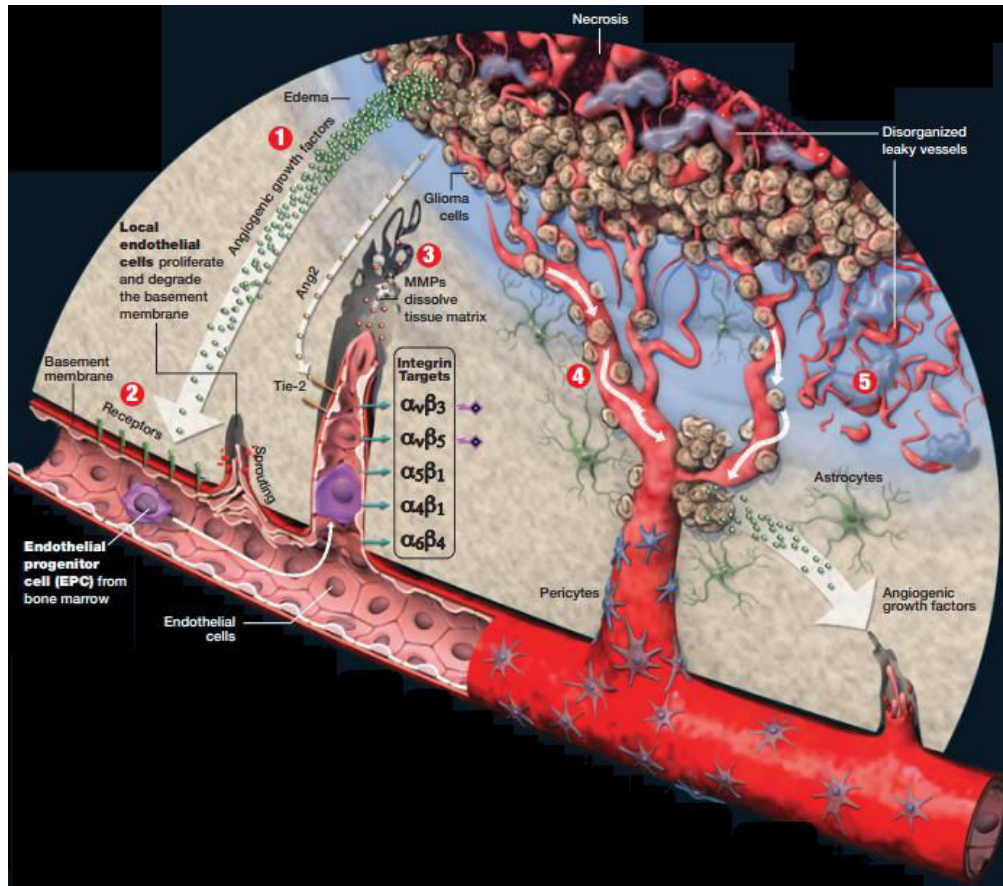


Figure 4: The process of angiogenesis in GBM. From [22]

The process of angiogenesis is elaborated in brief in Figure 4 which consists of 5 steps. In (1), due to low oxygen supply to the growing cancer cells (hypoxia), they release growth factors that could activate the nearby endothelial cells. These growth factors will then induce proliferation of endothelial cells towards the cancerous lesion (2). In order to reach the cancer cells, the new blood vessels need to pass through the surrounding tissues. This is achieved by secreting a substance called matrix metalloproteinase (MMP) which can dissolve the surrounding tissue matrix as presented in (3), hence enabling the migration of new blood vessels. In (4), the cancerous cells then migrate from the primary tumour tissues along the main blood vessel and induce the formation of other new blood vessels. This condition was further worsened in (5) by the leakage of protein and fluid from the hyperpermeable tumour neo-vessels into the brain tissues, causing edema and increased interstitial fluid pressure.

As described before, VEGF is among the most important factor in angiogenesis. It is a dimeric glycoprotein of 34 - 42 kDa and there are five different forms of VEGF identified so far in mammals [17, 18]. These forms are alphabetically coded as VEGF-A, VEGF-B, VEGF-C, VEGF-D and placenta growth factor, PLGF. In a normal adult, VEGF-A mRNA as an example, could be found in abundance in the heart, kidney, lung and adrenal gland [18].

The VEGFs interact with a type of tyrosine kinase receptor called vascular endothelial growth factor receptor, VEGFR. The VEGFR is highly expressed in the vascular system since its function is primarily located at the endothelial cells, although it has also been found to be expressed in non-endothelial cells [17]. There are three known isoforms of VEGFR: VEGFR-1, VEGFR-2 and VEGFR-3. Each VEGFR has different functions. VEGFR-1 is responsible for vascular stabilization; VEGFR-2 has a function in angiogenesis whilst VEGFR-3 is responsible in lymphangiogenesis process (Figure 5).

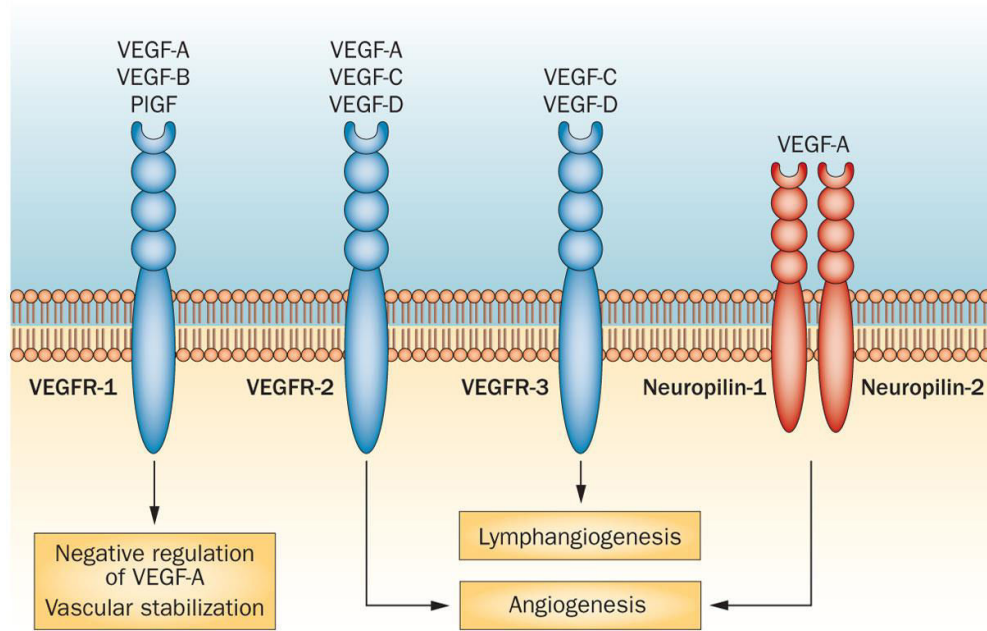


Figure 5: The three VEGF receptors. The function of VEGFR-2 in angiogenesis is amplified in the presence of neuropilin receptor as co-receptor. From [17]

Structurally, the VEGFRs are composed of an extracellular domain, a single transmembrane region, a juxta-membrane domain, a tyrosine kinase domain which is split by a 70-amino acids kinase insert and a C-terminal end. The extracellular domain is formed by roughly 750 amino acids which are organized into seven immunoglobulin-like folds (Figure 6). This specific structure of VEGFRs has a role in its function and binding of the specific VEGF growth factor [17].

VEGF-A and VEGF-C interact with VEGFR-2 and hence these two forms of growth factor have a role in angiogenesis. The VEGF-A undergoes several alternative splicing and this gives rise to seven different VEGF-A isoforms in human, in which they have different biological functions. These isoforms are known as VEGF-A₁₂₁, VEGF-A₁₄₅, VEGF-A₁₄₈, VEGF-A₁₆₅, VEGF-A₁₈₃, VEGF-A₁₈₉ and VEGF-A₂₀₆. Among these seven isoforms, VEGF-A₁₂₁ and VEGF-A₁₆₅ are the most predominant forms produced by most cells [17, 23].

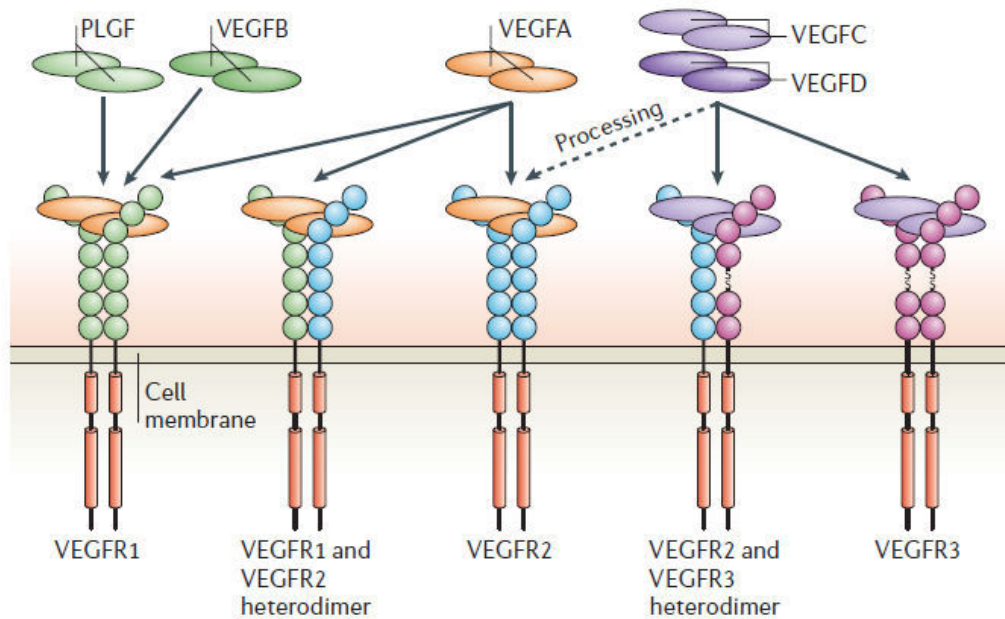


Figure 6: The VEGFR-1, -2 and -3. Note the extracellular domain is folded in an immunoglobulin, IG-like manner. From [17]

In the pathology of cancer, VEGF-A is produced by the cancer cells themselves or by macrophages. Upon production, most of the VEGF-A isoforms bind tightly to the extracellular matrix due to the presence of heparin-binding domain in their structure. However, the absence of one heparin-binding domain in VEGF-A₁₆₅ and lack of heparin binding domain in VEGF-A₁₂₁ render them diffusible and hence are able to move towards their targeted receptor, in this case the VEGFR-2 located on the endothelial cells of the vascular system, to exert their effect [18, 24]. The interaction of VEGF-A₁₆₅ with VEGFR-2 was found to be amplified in the presence of heparin and this is believed to have been caused by the formation of complex between the heparin with VEGF-A₁₆₅ and VEGFR-2 through the heparin binding domain of the VEGF-A₁₆₅. This effect on the other hand could not be seen with VEGF-A₁₂₁ because of lack of heparin binding domain in its structure (Figure 7) [17, 25].

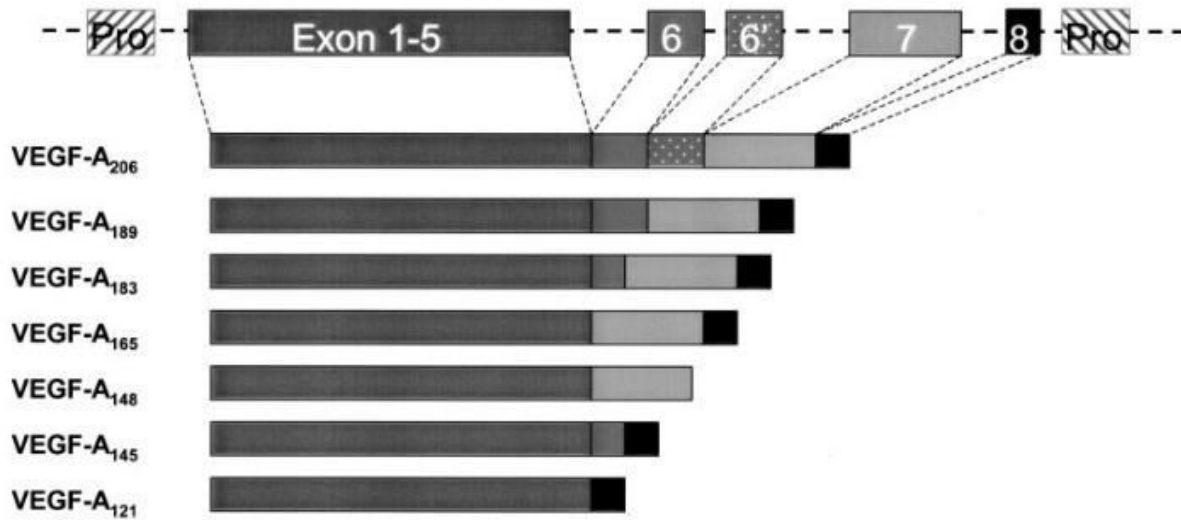


Figure 7: The gene structure of VEGF-A which contained eight exons. Exons 6 and 7 encode for heparin-binding domains. From [18]

Besides the VEGFR-2 tyrosine kinase receptor, VEGF-A also binds to other receptors (which act as VEGFR-2 co-receptor) to enhance angiogenesis with the most important being the Neuropilin-1 [17]. The binding of VEGF-A with VEGFR-2 in the presence of Neuropilin-1 will produce higher signals which will induce the formation of more blood vessels for the tumour cells. The subject of Neuropilin-1 is discussed in details in the following sub-topic.

1.1.5 Neuropilin-1 receptor and cancer

The neuropilins are a type of transmembrane glycoproteins with 120-140 kDa in size and were found to be a player in many different physiological and pathological processes. There are two known homologues of neuropilins: the Neuropilin-1 and Neuropilin-2. Neuropilin-1 (NRP-1) is known to be involved in angiogenesis, cancer pathogenesis, cardiovascular development, immunity, neuronal guidance and cell migration, whilst Neuropilin-2 (NRP-2) has fewer known functions which include mediation of axon guidance. NRP-1 commonly functions by being a co-receptor for many different growth receptors including the VEGFR-2 [26].

In the light of discovery of NRP-1 function in angiogenesis, it was also reported that NRP-1 is overly-expressed in new blood vessels formed by tumour cells and hence it is indeed a good target for anti-cancer therapy. NRP-1 has the ability to increase vascular permeability and to promote angiogenesis, which subsequently permits the growth and spreading of tumour cells. It was reported that the over-expression of NRP-1 in tumour vasculature could be associated with advancement of tumour progression and poor clinical outcome [26].

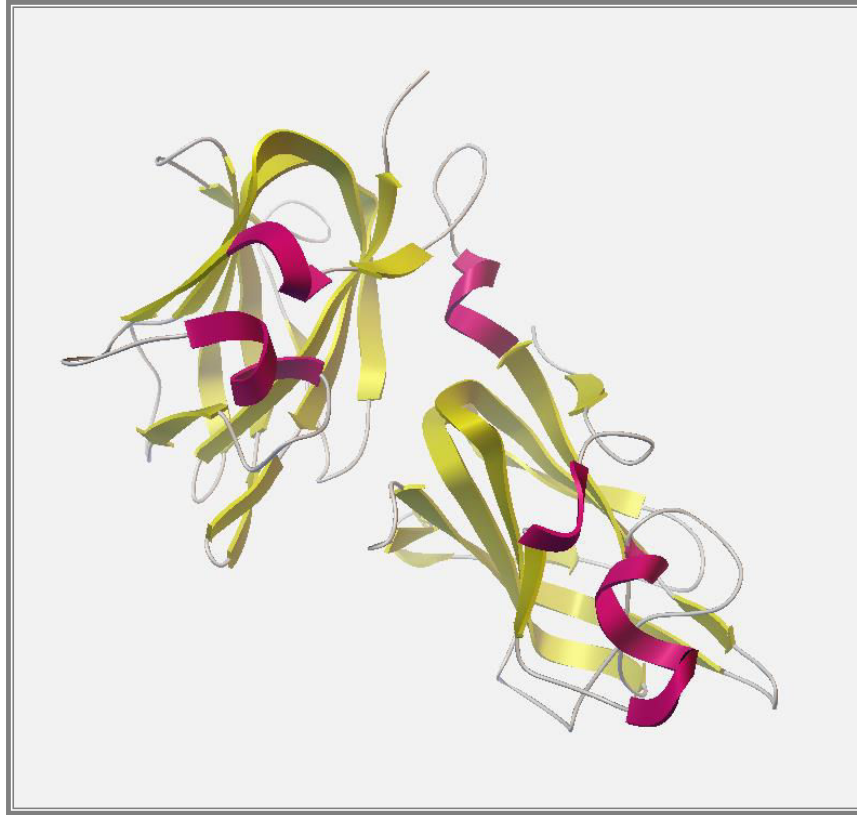


Figure 8: The crystal structure of neuropilin-1 (B domain), rendered into secondary structure ribbon model. Image obtained from Protein Data Bank, structure code 2ORZ

Structurally, NRP-1 has a short intracellular cytoplasmic residue, a short transmembrane domain and a large extracellular domain which could be divided into A, B and C subdomains. The A subdomain is an *N*-terminal complement-binding CUB domain (a1/a2), the B subdomain is the coagulation factor V/VIII domain (b1/b2) whilst C is a meprin domain. Figure 8 illustrates the B subdomain of NRP-1 in a secondary structure as obtained from the crystal information published in Protein Data Bank. The B subdomain plays a major role in the NRP-1 function as a co-receptor for different growth factors, which are listed in Table 2 [26, 27].

Table 2: The list of growth factors which have/possibly have interaction with b1/b2 extracellular subdomain of NRP-1. From [27, 28]

Ligand / growth factor	Effect
Vascular endothelial growth factor (VEGF-A _{165/145})	The formation of VEGFR-2/NRP-1 complex is enhanced by VEGF-A ₁₆₅ which acts as a bridging molecule. This subsequently improves the pro-angiogenic effect of VEGF-A ₁₆₅
Transforming growth factor beta (TGF-β)	NRP-1 binds and activates the latent complex of LAP-TGF-β.
Hepatocyte growth factor (HGF)	The binding of HGF with NRP-1 increases the signalling of c-Met and hence promoting angiogenesis and endothelial cell proliferation.
Placenta-derived growth factor (PDGF)	This growth factor promotes expression of NRP-1 which increases mobilisation of vascular smooth muscle cells and hence angiogenesis. <i>(possible interaction)</i>
Fibroblast growth factor-2 (FGF-2)	The binding of FGF-2 with NRP-1 enhances the growth stimulatory effect of FGF-2 and pro-angiogenic activity <i>(possible interaction)</i>
Placental growth factor (PIGF)	PIGF through its receptor NRP-1 promotes angiogenesis and tumour growth

VEGF-A₁₆₅ binds to the B subdomain of NRP-1, and possibly to the VEGFR-2 simultaneously. As the NRP-1 does not have any signalling effect, it was proposed that the NRP-1 is a co-receptor for VEGFR-2. A study by Whitaker *et al.* (2001) had found that the activity of VEGF-A₁₆₅ on VEGFR-2 was enhanced in the presence of NRP-1 receptor [29]. This double interaction of VEGF-A₁₆₅ towards both VEGFR-2 and NRP-1 was found to have enhanced angiogenesis activity on the endothelial cells that express both receptors, in comparison towards cells that express VEGFR-2 alone [30].

In uterus, the expression of NRP-1 is very significant since this is the place for physiological angiogenesis [31]. It was also found that there is a three- to five-folds increment of NRP-1 mRNA expression in the prostate tumour tissues as compared to normal prostate tissues [32]. These evidences further reinforce the fact that NRP-1 does have a role in tumour progresses and angiogenesis [23]. In addition, Latil and co-workers (2001) have suggested that the level of NRP-1 and VEGF expression could be used as the prognosis marker of cancer, specifically in prostate cancer. They found that VEGF over-expression could be correlated with stage 2 cancer, whilst over-expression of NRP-1 represented an advanced disease and a high Gleason grade, which correspond to an aggressive disease [32].

NRP-1 is known to be abundant in the area of tumours because of the fact that tumour cells induce the formation of neo-vascularisation around themselves in ensuring more nutrients and oxygen molecules are obtained for their survival. Fakhari *et al.* (2002) have reported that the NRP-1 and -2 receptors are being up-regulated in all stages of cancer (stage I until IV) for human neuroblastoma and would be a good target for anti-angiogenic treatment from the early stages of

cancer [33]. Other publications had also reported that the expression of NRP is up-regulated in many different tumours and their vasculature networks [34, 35].

1.1.6 Folate receptor and cancer

Folate receptor (FR) is a cell-surface membrane-bound receptor protein, a type of glycosylphosphatidylinositol-anchored receptor which is responsible to transport folic acid into cells through a process called endocytosis. There are at least four subtypes of FR α , β , γ/γ' and δ , and among them the FR α is the most abundant. FR α expression is usually amplified in the epithelial cells of cancer, whilst FR β is more common on myeloid leukaemia and on macrophages activated in relation to chronic inflammatory disease [36, 37].

The FR α has a limited expression on the surface of normal cells. Cells of lungs, brain, kidneys, small intestine, breast, endometrium and ovary are known to express this receptor, but at a very low level [38]. On the surface of certain cancerous cells however, the expression of FR is of abundance to meet the demand of rapidly dividing folate-deprived cells. As illustrated in Figure 9, the level of FR expression was found to be significantly elevated especially in ovarian cancer cells. It was found that more than 80% of epithelial ovarian cancer cells expressed this receptor with 10- to 100-fold higher than the normal expression [39]. It is being expressed in similarly high manner either in newly developed or recurrent ovarian cancer. However, there are also small cases whereby FR α is not expressed in ovarian cancer, although this is rare as compared to those with high FR α expression.

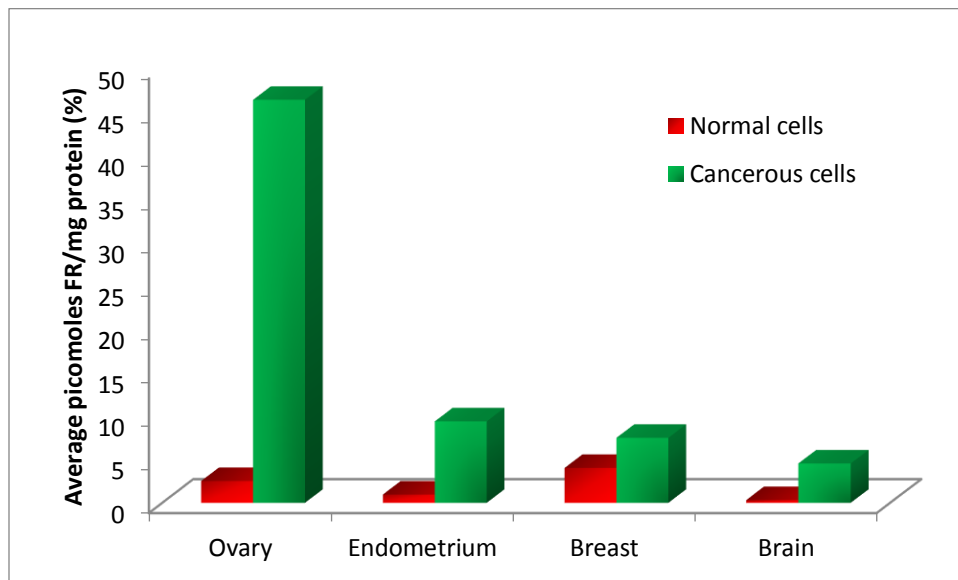


Figure 9: Average picomoles FR/mg of protein expressed in normal cells in comparison to cancerous cells. Adapted from [135]

This receptor was first isolated from a sample of ovarian cancer tissues nearly 15 years ago and since then it was recognized as a valuable tumour marker for ovarian cancer [40]. The level of FR α expression demonstrates biological aggressiveness and can be correlated to the overall prognosis of patients [38]. This has opened up an excellent opportunity to improve the efficiency of anti-cancer therapeutics delivery by using this receptor as a target point. It is also noteworthy that the FR α expression is strongly correlated with the grade and histological stage of tumours; higher expression of FR α were found on metastasized and highly undifferentiated cancers as compared to the localized and lower grade ones [36, 37, 41].

1.1.7 Treatment approach for cancer

In the current clinical practice, there are many different therapeutic options available for clinicians and patients to choose from, depending on cancer type and stage. The treatment of cancer involves complex parameters and is principally aimed at destroying as many cancerous cells as possible, extend the survival of patients and at the same time maintain their quality of life. The most common treatment includes surgical intervention, chemotherapy and radiation therapy [42]. The other less common therapies are immunotherapy, hyperthermic-type of therapy, stem cell transplant, laser treatment, photodynamic therapy and blood product donation and transfusion. It is also a common practice to combine two or more of these therapeutic options in order to obtain the maximal benefit from the therapy. The following subsections will describe these treatment options in detail.

It is also interesting to note that there is also an approach called the *watchful waiting* in the case of cancers that are very slow in progression such as prostate cancer. In this situation, clinicians could choose to maintain active surveillance and do not start any therapy. However, all of these available options need to be weighed accordingly, prioritized and individualized [43].

A. Surgery

Surgery remains as the main approach in cancer therapy especially for small and localized solid tumours in their early stages, which are usually contained in one area. During surgery, the tumour and some normal tissues around the cancerous tissues will be removed in order to ensure that all cancer cells are eliminated. Surgical intervention commonly needs to be combined with chemotherapy or radiotherapy as either adjuvant (surgery as first treatment step), or neo-adjuvant treatment (surgery is conducted after a treatment with chemotherapy or radiotherapy to shrink the tumour size). Indeed, there is no one standard approach for treating cancers and it is highly dependent on the status and condition of the patients and the cancers involved.

Surgery is impossible to be effective as a single treatment for metastasized cancers. In this state of disease, treatment options that could work throughout the body are more preferred and this would include chemotherapy, biological therapies such as immunotherapy and hormonal therapies.

B. Chemotherapy

The word chemotherapy takes a meaning of *drug treatment* and hence in general meaning, this includes all therapy involving drugs such as antimicrobial and other drug-based treatment. Figure 10 illustrates in brief the history of chemotherapy since the early of 20th century. Paul Ehrlich who is known as the father of chemotherapy introduced Salvarsan® in the early 1900s as an antimicrobial chemotherapy. Many years after, during World War II, scientists observed that the person who was exposed to nitrogen mustard significantly lost their white blood cell counts [44]. This has led to the research and discovery of mustard as anti-cancer agent in the treatment of lymphoma by Alfred Gilman and Louis Goodman in 1940s [45].

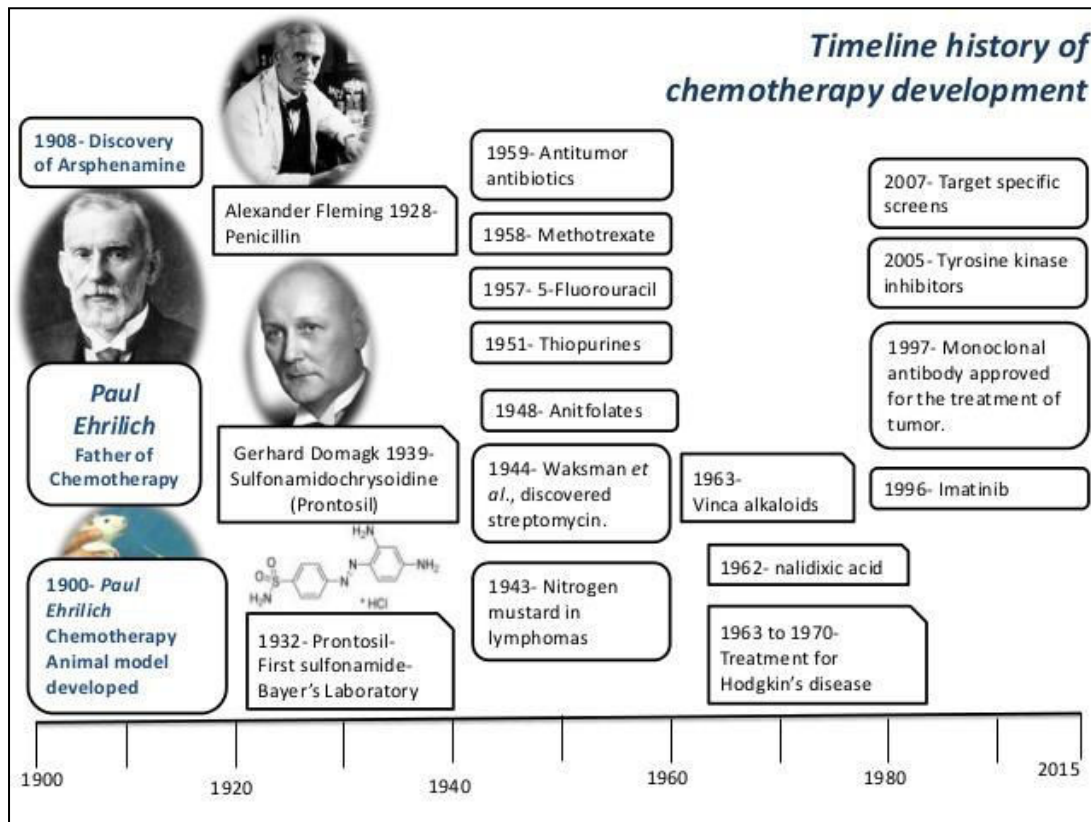


Figure 10: History of chemotherapy development. From [46]

With specific interest for cancer therapy, chemotherapy could be defined as treatment involving administration of cell killing (*cytotoxic*) drugs into the body. Currently, there are more than 100 different cytotoxic drugs available and this number is increasing as more drugs are being discovered and produced. However, certain cytotoxic drugs remain as the first line of treatment due to their effectiveness, despite having bad adverse drug reactions.

The choice of cytotoxic drugs to be used during chemotherapy is dependent on different factors and these include the type of cancer, stage of cancer, its metastasis status and the general health of the patient. Sometimes due to different reasons, a combination with other intervention is needed, such as with surgical intervention and/or radiotherapy technique. Chemotherapy as single treatment modality could be effective in the treatment of haematological neoplasm such as leukaemia and lymphomas which are considered to be a widespread cancer from the beginning. In other types of cancers, chemotherapy is likely to be more effective in tumour killing when used in adjunct with other treatment modalities.

The available treatment with chemotherapy today presents a challenge in balancing between the destructive effect on cancerous tissues and the undesired effect on normal healthy cells. This includes destruction on the body immune system and high-replicating cells such as hair follicles and the lining cells of gastrointestinal tract. The safety and efficacy of chemotherapeutic drugs are known to be influenced, to some extent, by the variability of genetically related factors in pharmacokinetics and pharmacodynamics. Hence, the latest researches and medical approaches are trying to exploit the genetic information of patients in order to improve the response towards chemotherapy. Through advancement of clinical practice and research findings, cytotoxic drugs with better toxic profiles are available for cancer patients, providing improved clinical outcome and better overall treatment experience.

C. Radiotherapy

Radiotherapy has become an important part of cancer treatment. According to American Cancer Society (ACS), more than half of cancer patients have undergone radiotherapy during their course of treatment and this shows that radiotherapy has a significant contribution in cancer treatment.

The basis of radiation involves transfer of energy by waves or stream of particles. This energy will cause damage to the genes of the targeted cells and this will subsequently lead to cell death and tumour shrinkage. Radiation's effect is more obvious on rapidly dividing cells, which is the characteristic of tumour cells. It is less cytotoxic on cells that are dormant or has low-dividing rate. However, radiotherapy will nevertheless causes damage on healthy cells during the course of the treatment, and it is of importance for clinicians to balance between cytotoxic effect

on cancerous cells and the damage that could be suffered by normal cells. Current advancement in medical technology has enabled the delivery of radiation specifically on the lump of tumours and minimizes the radiation received by the neighbouring cells and hence reducing the unwanted adverse reactions.

D. Immunotherapy

Immunotherapy is a biological-approach that is carried out in two ways, either by stimulating the body's own immune system to destroy cancer cells or by administering synthetic immune-system molecules such as peptides and proteins. It could be used on its own with some cancers but with the others, it is more effectively used when combined with other treatment modalities. Some examples of currently available immunotherapeutic products are monoclonal antibodies and cancer vaccines [43, 47].

Monoclonal antibodies are available in different forms: the naked monoclonal antibodies are useful to boost body immune system, whilst conjugated monoclonal antibodies are useful as targeting agents and are used in combination with chemotherapy and radiotherapy. Cancer vaccines on the other hand are made from cancer cells themselves; the presence of key antigen on the vaccine could induce attack from the body immune system itself against the cancer cells. As an example, a vaccine is available for the treatment of advanced prostate cancer under the name of Provenge®. It does not have the ability to cure prostate cancer and it can only prolong the survival of patients for a number of months [47].

E. Hormone therapy

Hormone-based therapy is commonly used in the treatment of breast and prostate cancer. In the treatment of breast cancer, hormone therapy is used for patients that are tested as positive for hormone receptors to reduce the chances of recurrence and it is usually started after the completion of chemotherapy and radiotherapy, where necessary. There are different hormonal products available in the clinical setting and this includes tamoxifen and aromatase inhibitors such as anastrozole.

In the case of prostate cancer, hormonal therapy (androgen deprivation) is useful in the treatment of advanced disease. It is commonly used as the first-line treatment for advanced prostate cancer and it could help to control cancer for a long period of time. It could also be used in combination with chemotherapy and/or radiotherapy [43].

F. Bone marrow transplant

Bone marrow transplant is a method commonly used in the treatment of blood-related cancer such as leukaemia. The transplanted cells could be donated by a person who has a closely-matched tissue type with the patient's. This is called allogeneic bone marrow transplant and is recommended for patients who are characterized as having a high-risk disease and also for patients who relapse after remission. This treatment approach is also applicable in patients who do not attain remission after courses of chemotherapy [43].

1.1.7 Current Anti-angiogenesis Treatment

In the current clinical setting, there are already a number of anti-angiogenesis therapy agents available for the treatment of angiogenesis in metastatic cancer, as adjuvant and also neo-adjuvant therapy. Vasudev and Reynolds in a review in 2014 summarized the current available treatments and future direction of anti-angiogenesis therapy. In a simplified way, they described three different classes of drugs that are available in clinical settings with different mechanisms of action as illustrated in Figure 11; (1) agents that bind to VEGF ligands and subsequently impede its binding to their receptors, examples being Bevacizumab that binds to VEGF-A ligand and Aflibercept that binds to VEGF-A, VEGF-B and PLGF; (2) monoclonal antibodies, Ramucirumab that directly binds on VEGFR-2 and block signalling through the receptor; (3) the tyrosine kinase inhibitors (TKI) such as Sorafenib, Sunitinib and Pazopanib that block the activity of VEGFR-1, VEGFR-2 and VEGFR-3 (as explained before, VEGFR are tyrosine kinase receptors) [48].

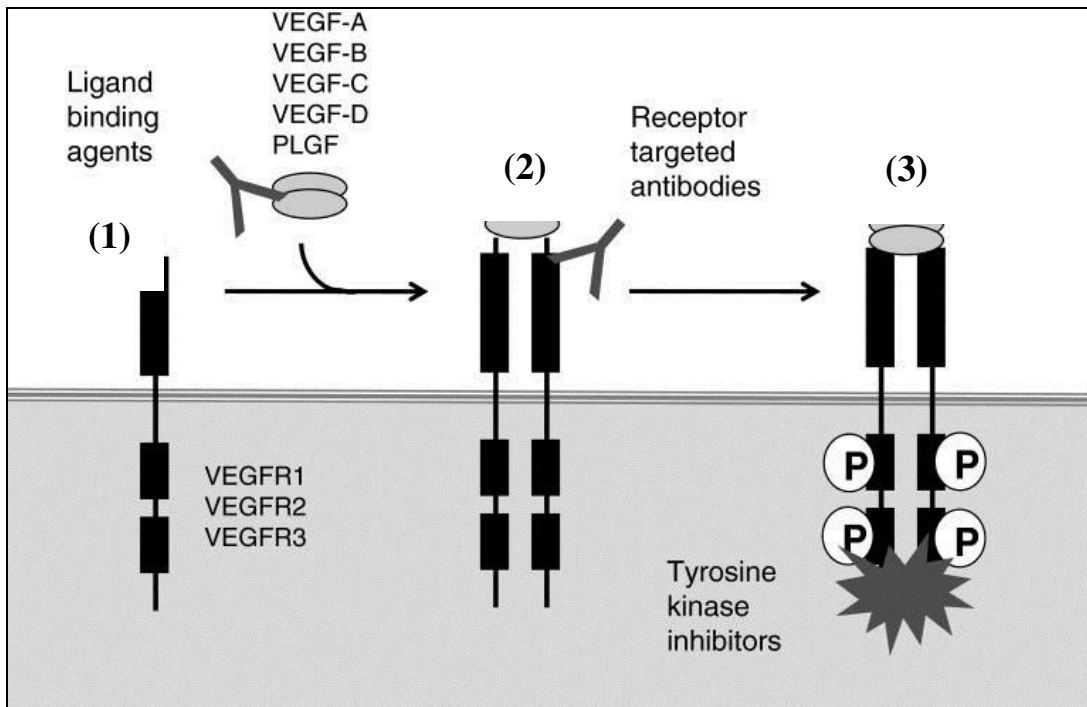


Figure 11: Anti-angiogenesis mechanism demonstrated by currently available drugs. From [36]

Agents from class (1) and (2) are used in combination with other available chemotherapy drugs whilst class (3) drugs, the TKIs have shown single-agent activity in a few treatment indications. Treatment responses were varied; while one agent might be effective in some metastatic cancer, it may not show improvements in the others. Based on a number of clinical trials conducted on anti-angiogenesis agents, it was evident that a treatment combination of bevacizumab with paclitaxel/carboplatin may be effective in improving the progression free survival (PFS) and overall survival in ovarian cancer, but the same combination did not show any improvement in melanoma [48]. In general, although the data on anti-angiogenesis treatment is promising, there are several types of cancers that the treatment is consistently failing at improving the overall patients' survival (OS). This includes breast, prostate, melanoma and pancreatic cancers.

In order to prolong the survival period and achieve effective therapy, there is a need to find effective drugs combination. As an example in a clinical trial for metastatic prostate cancer, the combination of Docetaxel with Bevacizumab shows improvement in PFS while instead, the combination of Docetaxel with Aflibercept showed no improvement on PFS. It is still unclear as to why this happened, as there are also many unresolved questions regarding drug combinations and choices. More studies are needed to understand the mechanism of drug combination in current practice of anti-angiogenesis therapy [48].

As mentioned before, there are a number of different solid tumours in which the anti-angiogenesis therapy has already been indicated. These tumours have extensive neo-vasculatures that could be the target of anti-angiogenesis therapy. Among these solid tumours, glioblastoma multiforme (GBM) is the most vascularised. However, there are still limited anti-angiogenesis agents that could be used to treat GBM. The growth and histological progression of GBM relies greatly upon angiogenesis and thus anti-angiogenic treatment is one of the feasible ways to combat this disease [22].

In clinics, bevacizumab is the first approved agent for GBM treatment. In combination with another chemotherapy agent (Irinotecan), this therapy has shown 50% PFS for six months, much improved as compared to Irinotecan alone, only between 9-12%. However, there is preliminary evidence that shows possible rebound in angiogenesis following the therapy. In such cases, it is necessary to have a more effective treatment to cater to this relapse problem.

More research is indeed needed to improve the current available therapy. It is also very interesting to explore other therapeutic means in support of the conventional chemotherapy and the currently available anti-angiogenesis drugs. In recent years, greater interests are being shown on the utilization of photodynamic therapy as anti-angiogenesis. The presence of several important receptors as discussed before (NRP-1 and VEGFR-2) could be good targets to deliver photosensitizer directly towards the neo-vessels. Perhaps, this approach can offer much improvement and further extend the PFS following therapy. Subsequent sub-chapter will describe in detail on PDT and current advancement in PDT research. The combination of PDT and targeted therapy is of interest and it is among the objectives of this thesis to develop a conjugate of photosensitizer and peptide to target NRP-1 receptor with specific application in the treatment of GBM.

1.2 PHOTODYNAMIC THERAPY

1.2.1 Historical background of photodynamic therapy

Treatment of skin disease in the presence of light has been used since 1400 BC. Earlier Egyptian, Indian and Chinese civilisations used light in the treatment of psoriasis, rickets and skin cancer. This was later known as phototherapy. Phototherapy uses either ultraviolet (UV) or visible light, and could be performed with or without a photosensitizer (PS). Whenever a PS is not in-use, phototherapy is commonly applied for the treatment of dermatological problems such as eczema, neonatal jaundice and in the treatment of vitamin D deficiency. Photochemotherapy is another concept of treatment which is done in the presence of a photosensitizer, usually the psoralens. It is commonly employed in the treatment of psoriasis, atopic dermatitis, *alopecia areata* and many other kinds of skin problems [3].

Photodynamic therapy is actually a type of photochemotherapy in which light, photosensitizer and molecular oxygen are required for treatment.. In the beginning of the twentieth century, treating diseases with light started to gain interest, and the first oncological application of chemical and light in cancer treatment was realized in 1903, during which eosin and light were used to treat skin cancer.

Ten years after, in 1913 Frederic Meyer-Betz conducted the first PDT test on himself by injecting 200 mg of haematoporphyrin into his body and subsequently exposing himself to sun light. He experienced swelling and photoreaction especially in the light-exposed areas of his body, such as hands and face. Since then, many discoveries were made (Figure 12) throughout the years, and in 1975, Dougherty et *al.* successfully treated skin cancer by using haematoporphyrin derivative (HpD) in 98 out of 113 patients in his study. The studies that followed afterwards showed that this technique is effective in treating early-stage cancers but failed to produce better outcome due to the problem of targeting and specificity [49].

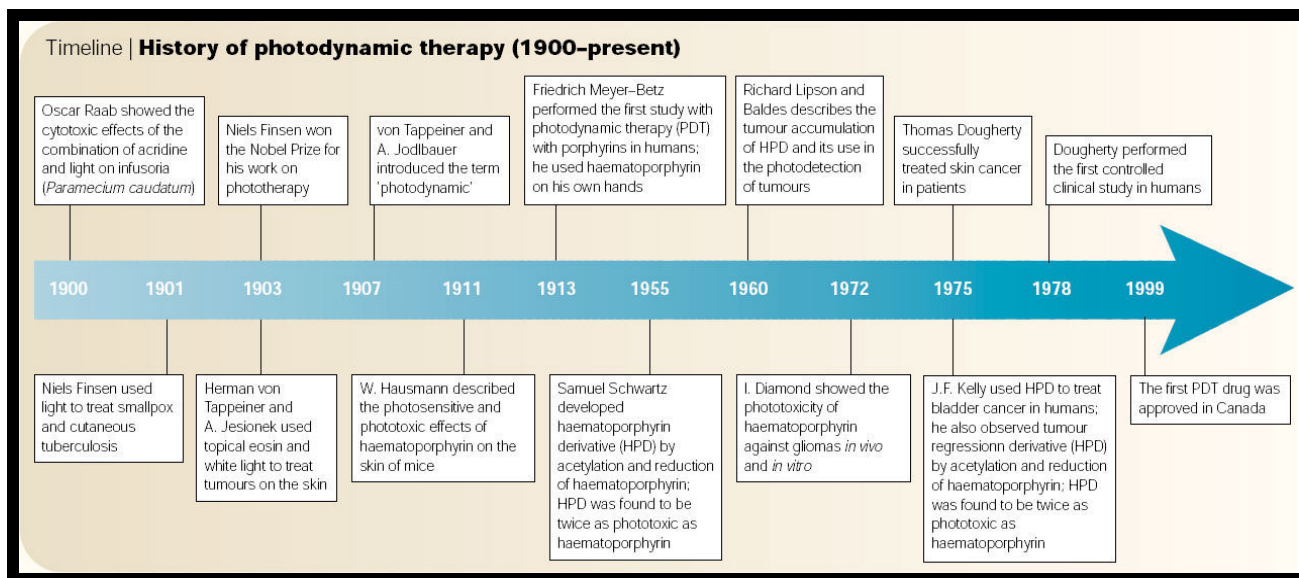


Figure 12: Milestones of PDT evolution. From [50]

Much improvement has been made since then, and many other agents were developed with different targeting capabilities. With the current modern technologies and more specific agents, photodynamic therapy is believed to have its own potential in treating cancer patients, especially those in the early stages of the disease.

1.2.2 Overview of PDT

Despite the number of researches done and the advancement in the knowledge of cancers and their treatments, there has only been slight improvement in the clinical outcome of patients post-treatment [51] and hence this calls for different treatment modalities to complement the conventional available methods. One of the promising key modalities is photodynamic therapy (PDT) technique. Ever since the potential of PDT in cancer therapeutics became more promising after Dougherty clinical success in 1975, more research and development works are being realized to date.

PDT is a combination of drug-device system. It is formed by the combination of three components: photosensitizer (PS), molecular oxygen and light of specific wavelength. Individually, these components have very low toxicity, but when they are combined together, they could produce reactive oxygen species (ROS) namely singlet oxygen which can induce cell death through apoptosis and necrosis [51]. The concept behind the application of PDT is indeed very interesting and safer as compared to the conventional therapies. Figure 13 illustrates the photodynamic action through the Perrin-Jablonski's diagram. A PS is excited to its singlet state upon absorption of light at an appropriate wavelength. The PS in this singlet state would then

undergo an internal transition into an excited triplet state, which has a longer life-span and lower energy state as compared to the singlet state. The energy of the excited triplet state can be transferred onto molecular oxygen (substrate) of the surrounding medium through type II reaction, whilst an electron or hydrogen can also be transferred to the substrate through type I reaction. Both reactions lead to the formation of reactive oxygen species (ROS). These entities are extremely toxic upon contact with biomolecules such as amino acids and DNA, causing damage and destroying nearby cells [52].

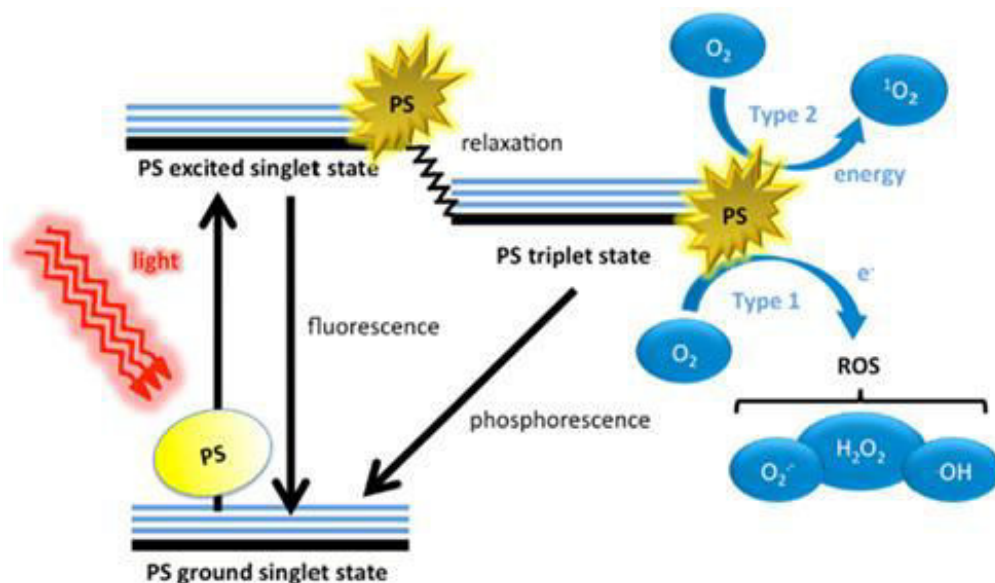


Figure 13: Schematic illustration of photodynamic therapy with the simplified Perrin-Jablonski's diagram. From [53]

There are several factors which are believed to govern the effectiveness of PDT which include the type and concentration of the PS used, the drug-light interval (time between the administration of PS and the light exposure), total light dose and its fluence rate, and also the oxygen concentration at the tumour site [51].

PDT is a very promising treatment and its potential has called for much wider applications in cancer therapy. This could be attributed to the various advantages that are being associated firmly with PDT, one of the most evident being its ability to reduce treatment-related toxicity [50]. PDT could help to prolong survival in patients with inoperable cancers and increase their quality of life significantly, besides reducing the long term morbidity of patients [54]. PDT also has the ability to induce immunogenic response which could further assist in antitumor activity. It could be used in combination with other treatment modalities such as chemotherapy, radiotherapy and surgical interventions [51]. There are also studies suggesting that synergistic effects are observed when PDT is combined with radiotherapy in which more

cancer cells are destroyed as compared to both treatment modalities being used on its own [55, 56]. In addition, unlike radiotherapy PDT could be used repeatedly without long-term complications since it uses non-ionizing radiation and will does not cause direct damage on DNA [57].

Generally, PDT is a good therapeutic option for diseases that are hyper proliferating [58]; it can be used in dermatology for the treatment of psoriasis which is characterized by high proliferation rate of the skin tissues, in cancer which is caused by uncontrolled cells growth and also against microbes which have faster growth rate as compared to the mammalian cells [59]. Despite being relatively underutilized in clinical cancer therapy, PDT has shown quite impressive successes in the treatment of several numbers of cancers, which include non-melanoma skin cancers, *actinic keratosis*, early lung cancers, oral and larynx early cancers, prostate and gynaecological cancers [60].

Although there are many advantages, there are also a few disadvantages of PDT. The localization of PS proves to be unbeneficial for the treatment of metastatic tumour, especially since metastasis is the most common cause of death in cancer patients. In addition, some agents of PDT could cause discomfort and pain to patients, besides prolong skin photosensitization [54]. These disadvantages are the limitation of PDT application which will be reduced or eliminated by more advance researches that are currently underway.

Recently, researchers from different domains are complementing each other for obtaining significant finding and bringing PDT forward. In a 2008 review, Timothy Zhu and Finlay categorized basic PDT research into five domains which are (1) light sources, light transport and light delivery into tissues, (2) PDT dosimetry, (3) optical and anatomic imaging, (4) development of new photosensitizers and (5) the biology of PDT. All these five domains are actually interconnected due to the dynamicity of photochemical reactions involved in PDT (Figure 14) [57].

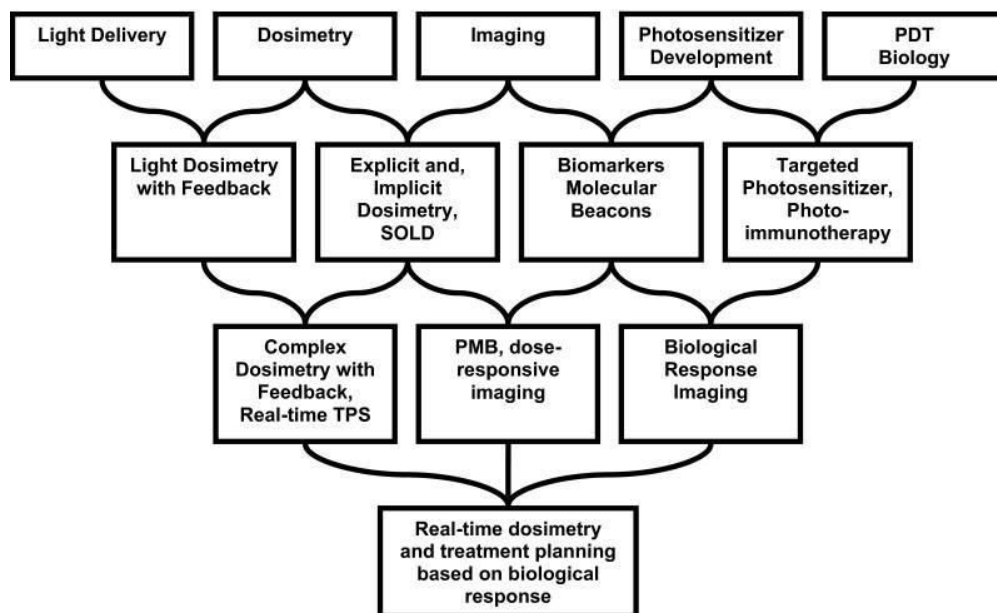


Figure 14: The inter-relations and inter-connections between different disciplines of knowledge in PDT research. From [57]

In the recent years, excellent research findings were actually made by inter-discipline collaborations. The combination of skills and knowledge from different fields are crucial in providing the right drug (PS) for the right patient at the right time, which is the most basic idea in pharmaceutical and medical practice. As presented in Figure 14, from a set of unrelated fields at the top row, the collaborations between different professionals comprising chemists, biologists, physicists and medical professionals have made significant contributions to the growing knowledge and technique for PDT, and making PDT a reality. The second row in the figure described the integration of two fields and the current state-of-the-art research whilst the third row illustrates the future direction of research. The fourth row shows the ultimate direction of all different research fields.

1.2.3 Components of Photodynamic Therapy

The three components of PDT are light, oxygen and photosensitizer. It is interesting to note that these components individually have very low toxicity, but when they are combined in the right conditions and environment, they proved to be very toxic. Figure 15 illustrates in a simplified manner the steps involved in PDT, beginning from the administration of PS, light irradiation and subsequently the destruction of cells that follows.

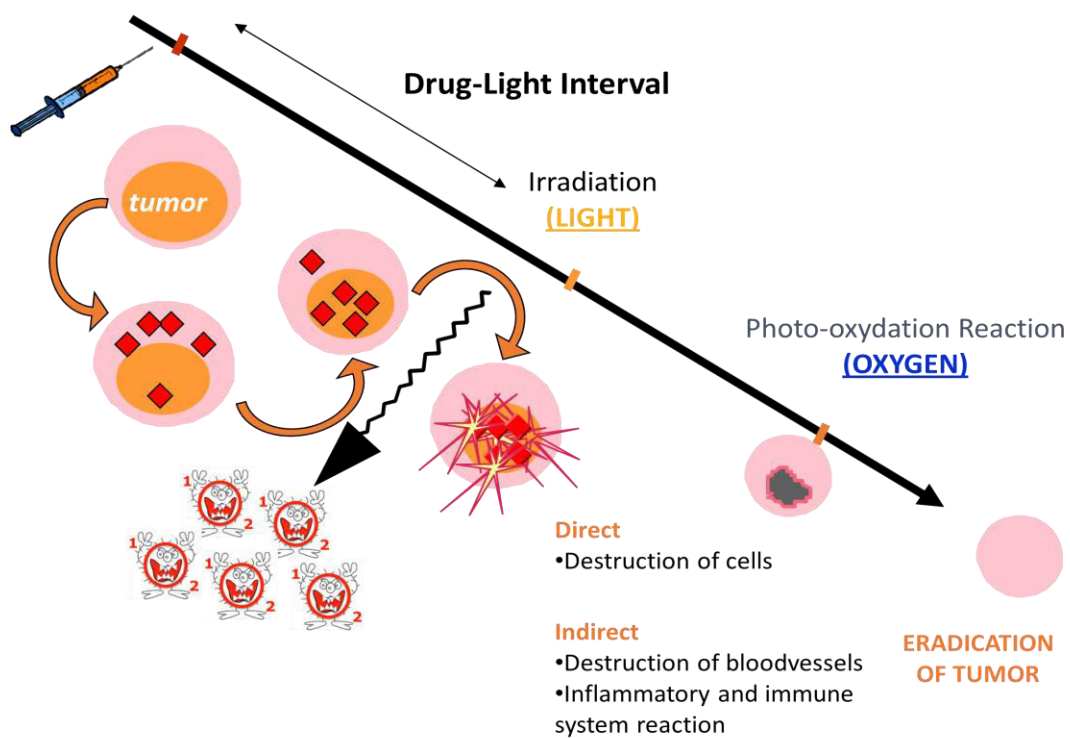


Figure 15: The steps involved in photodynamic therapy

A. Light

Therapeutic window of PDT refers to the wavelength of light that can be used during irradiation. The extent of tissue penetration by light differs depending on the type of tissue and wavelength of light used. There is actually no specific light wavelength that is most suitable for PDT. The wavelength of light chosen will largely depend on several factors, which includes the characteristics of tumour such as the location (superficial or deep seated), type of tissue, size, accessibility, PS absorption and the availability of the laser [51].

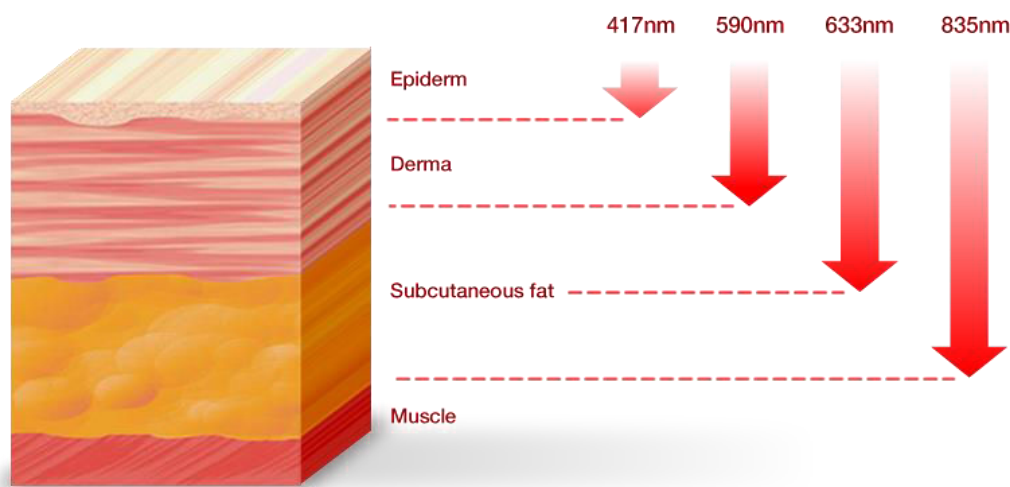


Figure 16: Depth of light penetration at different wavelengths

The effective penetration depth of light at 630 nm is about 2-3 mm and this means that it could penetrate until the dermis layer and the upper part of subcutaneous fat. At longer wavelength of 700-800 nm, the depth increases to 5 or 6 mm near to the muscle layer (Figures 16 and 17). Different lights are used depending on the type of cancer, for examples, blue light for dermatology applications, green light for the treatment of oesophagus cancer and red light for lung and prostate cancers. However besides absorption by PS, endogenous molecules present in the body are also absorbing a big part of the photon delivered especially in the blue wavelength. In the red however, a better penetration of light into the tissues could be observed with less absorbance by endogenous molecules. This means that for the treatment of deep-seated tumours, red light is preferred as compared to blue light.

In practice, the range of light used usually does not exceed 900 nm. This is because the energy content of photons at higher wavelengths is not sufficient to induce singlet oxygen generation. Light is mostly used in between 650 and 850 nm and this is called the “Therapeutic Window of PDT” [3, 61, 62].

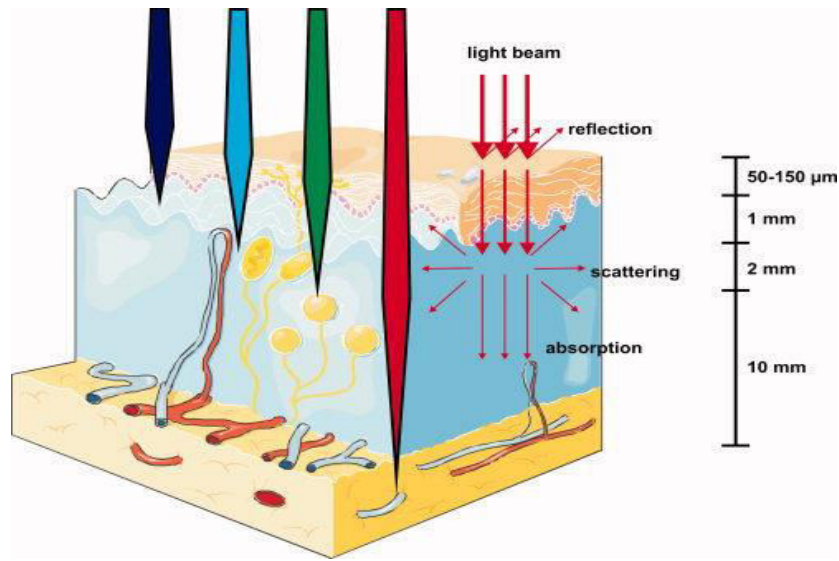


Figure 17: Light penetration through tissues. Note that red light has the deepest penetration as compared to green and blue lights. From [54]

In the practice of PDT, the PS used needs to be administered prior to light exposure in a precisely and carefully determined time length, called the drug-light interval. This interval is important because high accumulation of PS in disease tissues as compared to normal tissues is achieved during this interval, and if this time length is exceeded, the accumulated PS will start to leave the targeted tissues, hence reducing the efficiency of treatment afterwards. Furthermore, if light is administered too early, the amount of PS presence in disease tissue would not be sufficient. Light should be applied once the PS ratio between diseased and healthy tissues is at the highest, therefore minimising damages that could occur to the healthy cells [4].

Several types of light sources are used, such as argon or copper pumped dye lasers, double laser consisting of potassium titanyl phosphate/yttrium aluminium garnet medium, solid state laser and light emitting diodes (LED) [3]. Diode lasers are currently being designed to be used as a light source for PDT. They are small, simple to install, have automatic dosimetry and calibration features, longer operational life and are cost-effective. LED provides narrow spectral bandwidth and high fluence rate, whilst dye lasers are large and more inefficient in comparison to the other two [51].

Delivering the light to the targeted cancer cells is also an interesting feature which is continuously under study and investigation. Endoscopic light delivery is an efficient technique developed which has enabled the delivery of light into hollow structures such as in the treatment of early and advanced lung cancer, oesophageal cancer and superficial gastric cancer [63, 64]. Recently, the development of light tissue is also of interest. A research group at Inserm Medical Research Centre in Lille, France is developing a method to deliver light through a flexible light textile for the application of PDT for *actinic keratosis*, with the ability to provide a more uniform

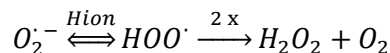
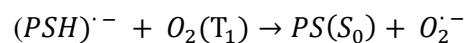
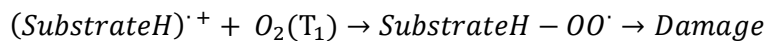
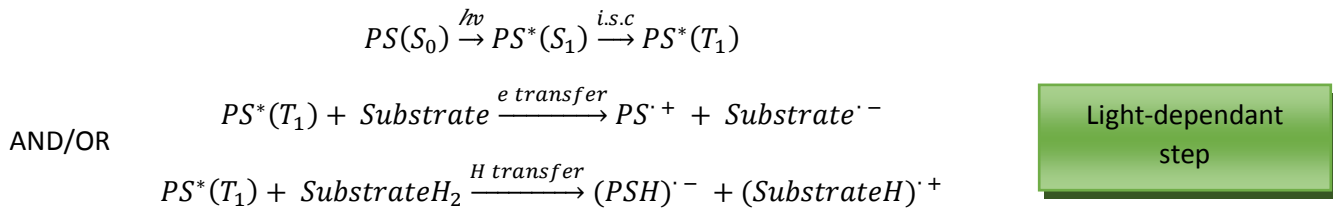
light application and a lower effective light dose. This technique is currently under evaluation and is believed to be able to provide better PDT applications as compared to conventional techniques [65].

Day-light PDT is another useful light application technique available to date for the treatment of *actinic keratosis*. In this approach, sunlight is used as the light source and it is a convenient technique especially for patients with large areas of affected skin. This technique however needs to be guided with respect to the influence of weather and seasons based on different geographical locations, in order to ensure sufficient amount of light is received by patients for an effective PDT [66].

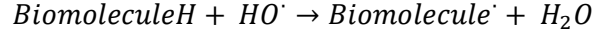
B. Oxygen

Oxygen is the killing source in photodynamic therapy. An excellently targeted photosensitizer and light at the highest precise wavelength have no effect at all on tumour cells and vasculatures without the presence of oxygen at the tumour site.

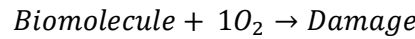
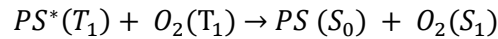
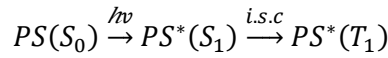
As mentioned before, there are two types of mechanism for ROS production. Type I is also known as “electron transfer” mechanism. It comprises of direct interaction of excited PS with an organic molecule (substrate) in the microenvironment of cells. This interaction leads to the reduction of the PS by acquiring a hydrogen atom or electron and forming a radical. The reduced PS will then undergo auto oxidation which produces a superoxide anion radical ($O_2^{\cdot -}$). A one-electron reduction subsequently produces hydrogen peroxide (H_2O_2), which in turn will undergo another one-electron reduction in the presence of transition metals such as ferrous (II), forming a powerful oxidant-hydroxyl radical (HO^{\cdot}).



Dark step



Type II mechanism involves energy transfer and is much simpler than Type I. Generally, most PSs in their ground state have two electrons with opposite spins and these electrons are located at the most energetically favourable molecular orbital. When the PS absorbs light, an electron is promoted to a higher energy level. PS can emit the excess energy as heat and/or fluorescence. In another way, intersystem crossing will happen to the excited singlet PS which will lead to the formation of the excited triplet PS. The PS in this triplet state is much more stable and will decay to the ground level. At the same time it can also transfer its energy to oxygen molecules. Singlet oxygen is then formed.



A photosensitizer is estimated to generate between 10,000 to 1,000,000 molecules of singlet oxygen in following cycles before becoming inactive, which will happen through bleaching, oxidation and other inactivation reactions [67]. Quantum yield of singlet oxygen (1O_2) is an important parameter to assess photosensitization phenomenon [67]. This could be determined by evaluating the number of photons used to produce 1O_2 in comparison to the number of photons absorbed; during the same length of time. The singlet oxygen population lifetime is the duration in which the singlet oxygen exists. This lifetime determines the distance that the singlet oxygen could diffuse to react and to exert its toxic effect on the surrounding biomolecules. Among the biomolecules that could react with singlet oxygen are unsaturated lipids, cholesterol and α -amino acid derivatives which form the most parts of cell membranes. Hence, it was predicted that cell membrane damage is an important damage mechanism inflicted by PDT.

C. Photosensitizer

A photosensitizer is a molecule which when excited by light, has the ability to use the irradiating energy to induce photochemical reactions which eventually produce lethal cytotoxic species which includes reactive oxygen species. These lethal cytotoxic species could subsequently result in cell death and tissue destruction [3, 4]. Some molecules are capable of performing the function of photosensitizers but they need to have common characteristics: the ability to absorb light energy and the ability to transfer this energy to adjacent molecules which commonly are organic substrate or oxygen [4].

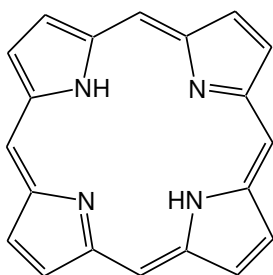
One of the most important advantages of PDT is given by its potential selectivity. There are actually two mechanisms that contribute to its selectivity: the ability to induce preferential uptake of the PS by the diseased tissue and the ability to confine the PS activation by selectively illuminating the specific diseased tissue regions. However, not all PS molecules are being taken up preferentially by diseased tissues. As an example, the uptake of 5-aminolevulinic acid (ALA) into tumour cells is influenced by several abnormalities possessed by these cells, such as decreased level of iron and increased permeability of abnormal keratin, leading to the accumulation of ALA and subsequently protoporphyrin IX in the cells [68].

The essential properties of a photosensitizer are believed to be [51, 69]:

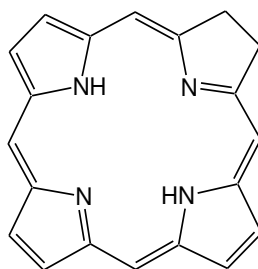
- a. Contains only a single pure compound and known composition to allow quality control analysis during production,
- b. Have high absorption peak between 600 and 800 nm (compounds with red to deep red in colour), and strong absorbance with high extinction coefficient at excited wavelength,
- c. Have high quantum yield for the oxidative process, especially for singlet oxygen,
- d. Have high photochemical reactivity, able to produce high quantum yield of triplet state and long triplet-state lifetime,
- e. Have low manufacturing cost and good stability in storage,
- f. Should have minimal dark toxicity and become cytotoxic in the presence of light at specific wavelength,
- g. Preferentially retained in diseased tissues and subsequently have rapid clearance from the body to prevent systemic toxicity.

1.2.4 Classification of photosensitizers

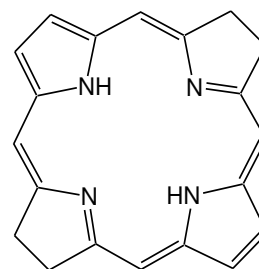
Photosensitizers could be broadly classified into two types: the porphyrinoids and non-porphyrin dyes PS. The porphyrinoid PS are porphyrins, chlorins, bacteriochlorins, pheophorbides, bacteriopheophorbides, texaphyrins and phthalocyanines. The non-porphyrin dyes PS are such as anthraquinones, phenothiazines, xanthenes, cyanines and curcuminoids [3]. Figure 18 shows the backbones of the main porphyrinoid-based photosensitizers.



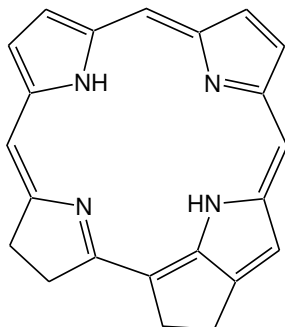
Porphyrin



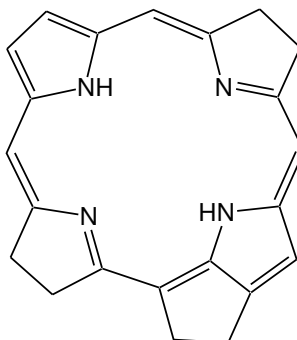
Chlorin



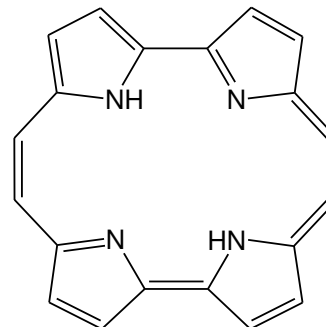
Bacteriochlorin



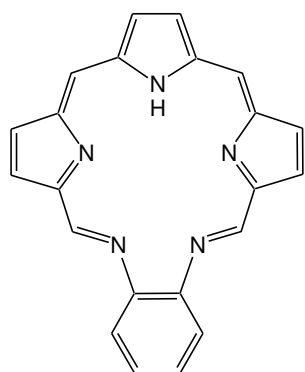
Pheophorbide



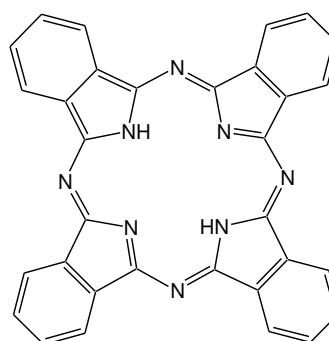
Bacteriopheophorbide



Porphycene



Texaphyrin



Phthalocyanine

Figure 18: Backbones of porphyrinoid photosensitizers

Photosensitizers are classified based on their generations. Until now, there are four generations of PS and each higher generation has improved function and properties in PDT. The first PS approved to be used clinically as anticancer agent is Photofrin[®], a drug from a group called haematoporphyrin derivatives (HpD) (Figure 19). HpD was first described as a diagnostic agent in 1961 and its tumour-killing capability was described 11 years later [70].

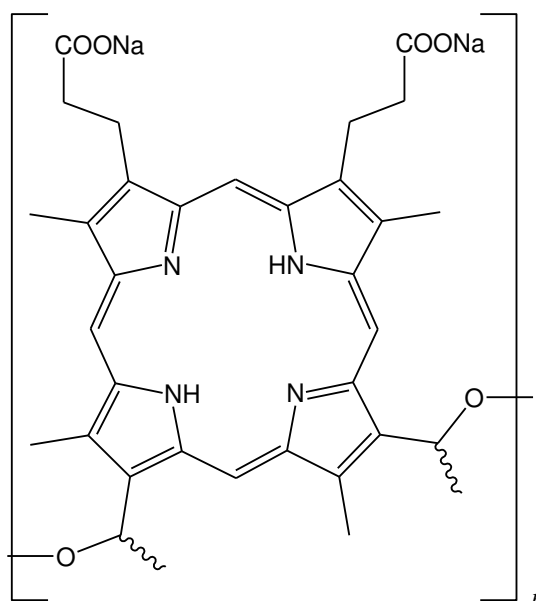


Figure 19: Molecular structure of HpD ($n=1-9$)

Following this finding, the efficacy of HpD in PDT was demonstrated shortly and this created a new history for PDT application in cancer treatment [71]. Photofrin® was purified from HpD and is approved by the FDA and other drug licensing authorities in Japan, Europe, Canada and about 40 other countries [51, 72]. Photofrin® was first approved in 1993 in Canada, for the prophylactic treatment of papillary bladder cancer. Since then, Photofrin® has become the most utilized photosensitizer in the clinical settings [50]. In Japan, PDT was approved for the treatment of early and advanced stages of lung cancer, and also for digestive and genitourinary tracts cancer. In the USA on the other hand, FDA has approved the use of Photofrin® for the treatment of obstructive oesophageal cancer and for microinvasive endobronchial non-small cell lung cancer for the cases where radiotherapy or surgery is not indicated [73].

Despite not having long-term safety issues, Photofrin® presents some disadvantages which includes a long lifetime in the body, around 4 to 6 weeks, causing prolonged skin photosensitivity. Its relatively low molar absorption coefficient at excited wavelength (635 nm) also causes the necessity of administering high drug and light dosage [50, 72]. These factors had caused the search for a better PS and the introduction of second and third generation of PS [74]. The second generation of PS consists of mainly chlorin, bacteriochlorin and phthalocyanines. Levulan®, Radachlorin®, Visudyne® and Foscan® are among those approved for clinical use in cancer-related and non-cancer related indications. Radachlorin® and Foscan® are chlorin-based, whilst Visudyne® is a benzoporphyrin. Levulan® on the other hand is 5-aminolevulinic acid or 5-ALA which is a prodrug and a precursor of porphyrin. It will eventually be activated and converted into its active form, called protoporphyrin IX [75]. Table 3 below listed the currently available first and second generation photosensitizers [76].

Table 3: List of currently available PS and their properties. From [76]

PS	Registered name	Indication	λ_{\max}	Manufacturer
First generation : Hematoporphyrin				
HpD partially purified, Porfimer sodium	Photofrin® IV	Oesophageal, bladder, gastric, cervix and	635	Concordia Lab, Inc. (Ontario, Canada)
	Photogem®	endobronchial non-small-cell lung cancer		Moscow Research Oncological Institute (Moscow, Russia)
Second generation : Protoporphyrin prodrug				
5- Aminolevulinic acid (5-ALA)	Levulan® Dermal	Actinic keratosis, basal cell carcinoma, head and neck cancer, gynaecological cancers	635	DUSA Pharmaceuticals, Inc. (MA, USA)
5-ALA-methylester (M-ALA)	Metvixia® Dermal	Actinic keratosis, basal cell carcinoma, Bowen's disease	635	Galderma Laboratories, L.P. (TX, USA)

5-ALA-hexylester (H-ALA)	Hexvix®	Bladder cancer diagnosis	375-400	PhotoCure ASA (Oslo, Norway)
	Cysview®			Photocure Inc. (NJ, USA)
5-ALA-benzylester	Benzvix®	Gastrointestinal cancer	635	<i>Not yet approved</i>
Second generation : Benzoporphyrin				
Verteporfin	Visudyne®	Age-related macular degeneration, pathologic myopia, histoplasmosis	689-693	Valeant Pharmaceuticals International Inc. (QC, Canada)
Second generation : Chlorins				
Temoporfin	Foscan®	Prostate, pancreatic and head and neck cancer	652	Biolitec Pharma Ltd. (Dublin, Ireland)
Talaporfin, NPe6, LS11	Aptocine®	Lung cancer and different types of solid tumours	664	Light Sciences (Washington DC, USA)
	Laserphyrin®			Meiji Seika Pharma Co. Ltd. (Japan)
Rostaporfin	Purlytin®	Rostaporfin (Under clinical trials)	664	<i>Under clinical trials</i>
Second generation : Phthalocyanines				
Aluminium phthalocyanine tetrasulfonate	Photosens®	Age-related macular degeneration, different cancers	675	General Physics Institute (Moscow, Russia)
Silicon phthalocyanine	Pc4	Actinic keratosis, Bowen's disease, T-cell non-Hodgkin lymphoma, skin cancers	670	Case Western Reserve University (OH, USA)
Zinc phthalocyanine	CGP55847	Actinic keratosis, Bowen's disease, skin cancer	675	Ciba-Geigy Ltd. (Basel, Switzerland) <i>Under clinical trials</i>
Second generation : Texaftrins				
Motexafin lutetium / Lutexaphyrin	Antrin®, Lutrin®	Prostate cancer and photoangioplasty	732	Pharmacylics Inc. (CA, USA) <i>Under clinical trials</i>
Second generation : Pheophorbide – A				
2-(1-hexyloxyethyl)-2-devinyl pyropheophorbide A	Photochlor®	Early oesophageal cancers, non-small cell lung cancer	665	Roswell Park Cancer Institute (NY, USA) <i>Under clinical trials</i>
Palladium-bacteriopheophorbide A	Tookad®	Recurrent prostate cancer	763	The Weisman Institute of Science (Rehovot, Israel)

Second generation : Purpurins				
Purlytin / Rostaporfin	Photrex®	Cutaneous metastatic breast cancer, basal-cell carcinoma, Kaposi's sarcoma and prostate cancer	660	Miravant Medical Technologies Inc. (CA, USA)
Second generation : Porphycenes				
9-acetoxy-2,7,12,17-tetrakis-(β-methoxyethyl)-porphycene	ATMPn	Psoriasis and non-melanoma skin cancer	610-650	Glaxo-Wellcome (NC, USA) and Cytopharm (CA, USA)

The agents that were described in Table 3 have indeed shown good properties as PS. Their incorporation as a treatment modality has lengthened the survival of patients and improve their quality of life, but they still lack the selectivity [4]. With the aim of increasing the selectivity, third generation PS was developed which is the derivative of second generation PS attached to a targeting moiety. The targeting moieties could be either biomolecules such as peptides, monosaccharides, LDL and antibodies, or also by embedding in nanoparticles [62, 74, 77]. This strategy is focused on developing a good delivery system in order to increase the selectivity and specificity of the PS and eventually increasing cellular uptake [4]. It is also possible to encapsulate or conjugate PS with nanoparticles and such approach is being taken in the re-formulation of available second-generation PS such as Visudyne® to further improve its efficacy in PDT [78, 79].

1.2.5 Porphyrin: Historical Background and Current Advancement

The word porphyrin originates from the Greek word porphura, which means purple. It is widely occurs in nature and is represented by chlorophyll and heme, which are also known as metalloporphyrins due to the presence of metal in the centre of their porphyrin rings (Figure 20). Ferrous (II) is known to be present in the centre of heme ring, and it was only in this form that the heme has the capability to bind oxygen for transportation in the blood. Chlorophyll on the other hand has magnesium as the central ring metal and the light capturing ability of plant for photosynthesis is actually magnesium dependant. Indeed, porphyrin-related molecules have contributed in multiple ways to the sustainability of living organisms including the respiratory and photosynthesis processes which are two of the most important processes in life.

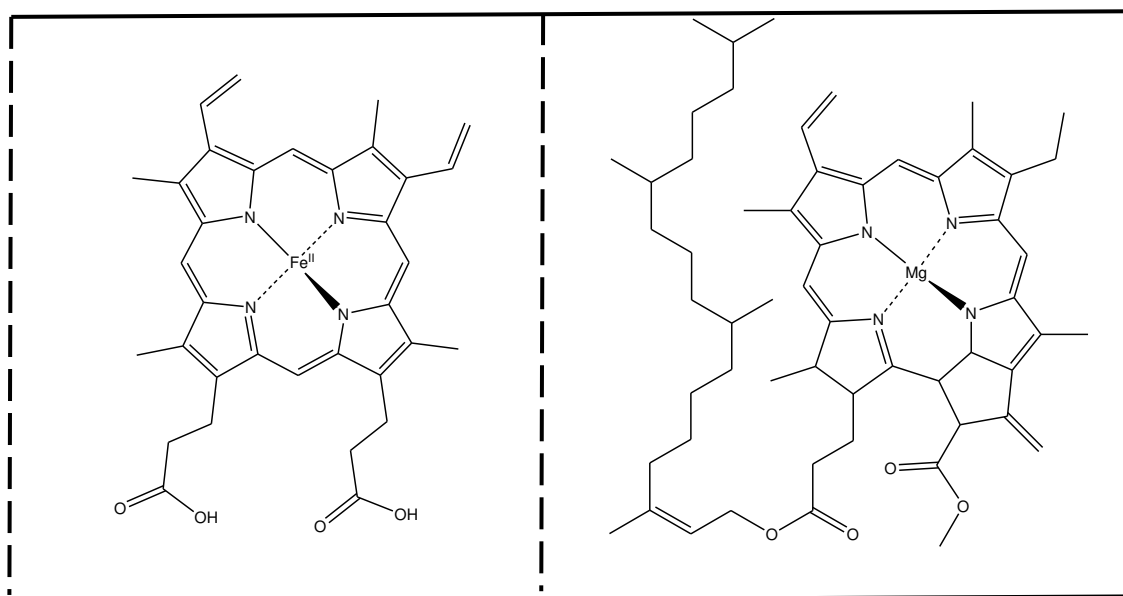


Figure 20: Molecular structures of heme (left) and chlorophyll A (right)

A. Structure of porphyrin

Porphyrin is a photoactive compound with a highly conjugated ring system. It has 22 π -electrons and 18 of them are delocalized in the macrocycle. This aromatic ring system is very stable and this is the reason that it is easily found in nature. The macrocycle is built from four pyrrolic sub-units connected by four methylene bridges, and this heterocyclic skeleton is known as *porphine* (Figure 21).

Due to the fact that all the atoms in the ring is sp^2 -hybridized, this ring system is flat and has a trigonal planar in shape. It has a large open cavity in the inside with four nitrogen atoms facing the centre. The presence of these nitrogen atoms enabled the porphine to form stable complexes with small metal ions such as zinc, copper, palladium, magnesium and ferrous, among all. The conjugated macrocycle could be substituted at the *meso*- and/or β -positions with non-hydrogen atoms or groups, and the *porphine* will be known as porphyrins [4].

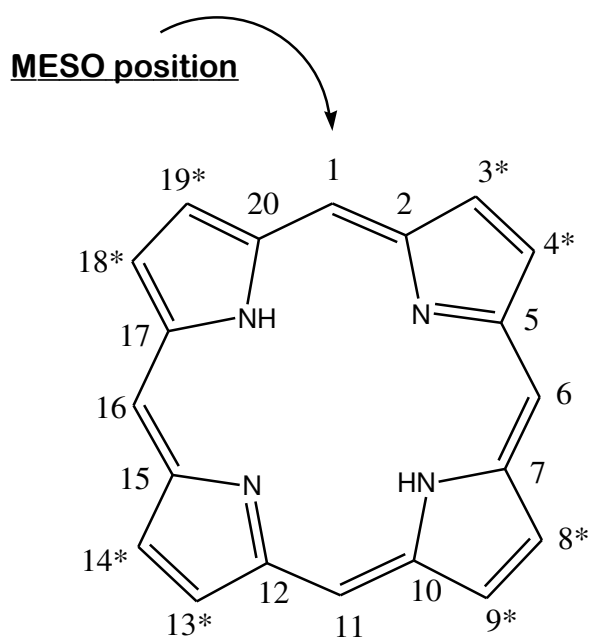


Figure 21: The porphine macrocycle and the *meso*- position. Beta-positions are denoted by the asterisks (*)

B. Synthesis of Porphyrin

The synthesis of *meso*-substituted porphyrin is of much interest. This is due to the fact that the presence of a possible substitution position on the side of porphyrin ring could render the porphyrin capable of carrying attached functional groups with specific functions such as a targeting agent. *Meso*-tetraphenylporphyrin as an example has been used in different model studies due to its attractive characteristics and potentially wide applications [80].

Due to extensive researches conducted in finding the best synthesis method, many different techniques are available in the literature and the most famous ones include Rothmund (1935), Adler (1964) and Lindsey (1979) methods. Among these famous porphyrin synthesis methods, Lindsey's has the best capability in large scale synthesis with higher product yields, but at a higher cost in terms of price and environmental effect [81]. These factors have unfortunately restricted its application and hence the earlier synthesis methods by Rothmund and Adler are still of importance. Many improvements have been made like the synthesis on solid support [82], the use of microwave irradiation [83-86] or by using building blocks such as the 2 + 2 [87, 88] or 3 + 1 synthesis approach [89, 90].

I. ROTHEMUND METHOD (1935)

The synthesis hypothesis by Rothmund is based on the fact that porphyrin is an aromatic compound which is stable, hence the reaction between pyrrole and aldehyde at high temperature would lead to the formation of porphyrin by thermodynamic control (Figure 22) [80]. He was the first person who successfully synthesized tetraphenylporphyrin. His synthesis technique involves condensation and oxidation processes. The reaction started from pyrrole and benzaldehyde in a sealed tube, in the presence of pyridine at high temperature (140 – 220°C). The reaction time was very long, about 24 to 48 hours with less than 10% yield [80, 91-93]. Although this method is far from perfection, this first reported method in 1935 could be seen as a stepping stone for the development of newer synthesis techniques with better efficiency and higher yield.

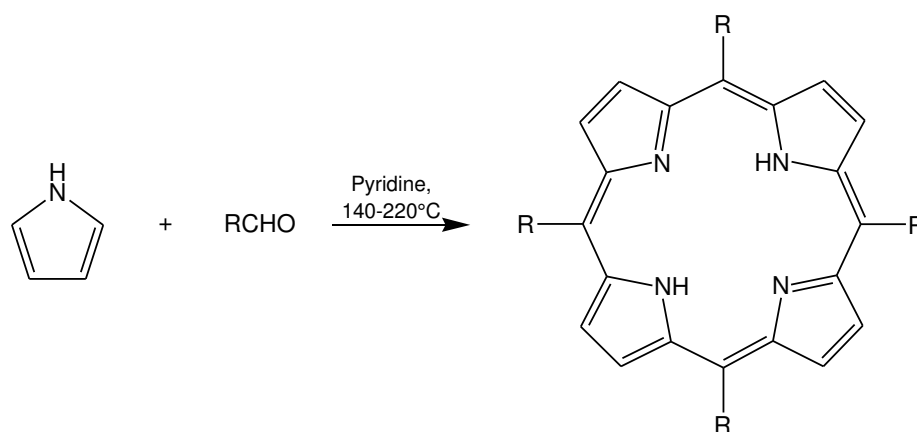


Figure 22: Rothmund synthesis method of porphyrin. From [94]

II. ADLER AND LONGO METHOD (1964)

In the Adler method which was developed nearly 30 years later, the reaction of aldehyde and pyrrole were conducted in refluxing propionic acid at 141°C for 30 minutes in an open vessel [80] and the porphyrin crystals were isolated at the end of the reaction by cooling, with about 20% yield (Figure 23). This method has the advantage of being easy, milder and is capable of producing numerous different *meso*-substituted porphyrins [92]. It allows the utilization of a greater variety of aldehydes and hence different symmetrical *meso*-tetraarylporphyrins could be produced [95], besides being able to increase into bigger synthesis scales [80, 96].

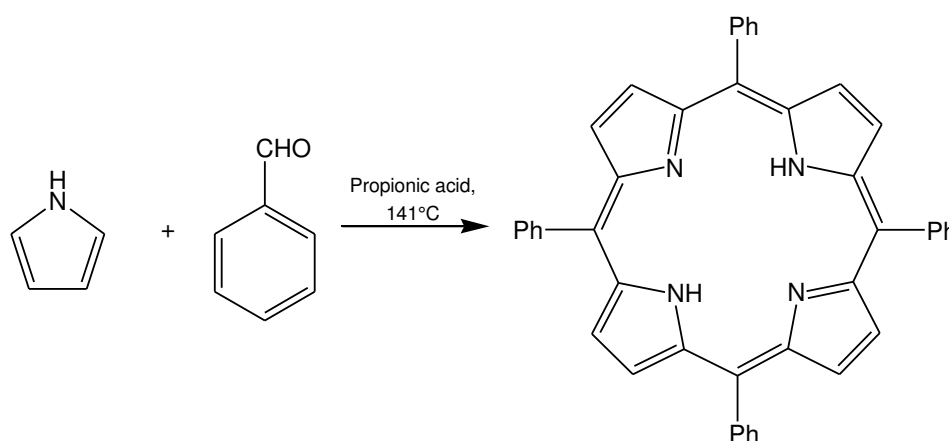


Figure 23: Adler and Longo synthesis method of porphyrin. From [96]

However, there are still some problems that could be associated with this synthesis method. The relatively rigorous experimental condition was proven to be a failure when benzaldehyde with highly sensitive functional groups was used. The reaction also produces a high amount of tar as side product and this is difficult to remove especially in the conditions whereby the synthesized porphyrin does not crystallize or precipitate post-reaction. In addition, the reproducibility of the reaction was also found to be poor [80].

III. LINDSEY METHOD (1979)

Lindsey group in 1979 has managed to improve the synthesis method proposed by Rothmund and came out with a method of synthesizing substituted tetraphenylporphyrin compounds in dichloromethane, in the presence of boron trifluoride etherate, $\text{BF}_3 \cdot \text{Et}_2\text{O}$ as the catalyst and *p*-chloranil as the oxidizing agent. The strategy that was taken was centred on the following criteria: (1) tetraphenylporphyrinogen should be the thermodynamically-favoured product when pyrrole and benzaldehyde are condensed under appropriate conditions; (2) very high temperature is not necessary for the formation of porphyrin because pyrrole and benzaldehyde are both reactive molecules.

Lindsey's group has proven that these hypotheses are generally valid. They used a maximum of 39°C in their synthesis method and obtained around 45-50% of yield and this yield could approximately be obtained by synthesis scale between 25 mL until 1L. This is indeed a good improvement in the methodology of porphyrin synthesis. They have also outlined the fact that the yield of synthesized porphyrin is dependent on several factors which includes presence of water in the solvent, concentration of pyrrole, benzaldehyde and acid, duration of condensation period and choice of oxidant and acid catalyst [80]. All these factors were evaluated by their group and they came out with a general method which has been adapted by our research team in the preparation of porphyrin P1-COOH. This will be described later-on in the following chapters.

VI. THE MACDONALD [2 + 2] PORPHYRIN SYNTHESIS METHOD

This method usually utilizes dipyrromethane as an intermediate and this is the most common pathway to synthesize porphyrin. The dipyrromethane molecules could be classified as either symmetrical or unsymmetrical, depending on the starting molecule prior to the condensation reaction. As an example in Figure 24, the condensation on two molecules of bromoethylpyrrole in hot methanol produces a symmetrical substituted dipyrromethane. Catalytic hydrogenation of the benzyl ester group produces carboxylic acid and this is followed by formylation of the carboxylic group with Vilsmeier reagent to form the final diformyldipyrromethane. The formyl group (-CHO) is the source of bridging carbons in the MacDonald [2+2] porphyrin formation [97].

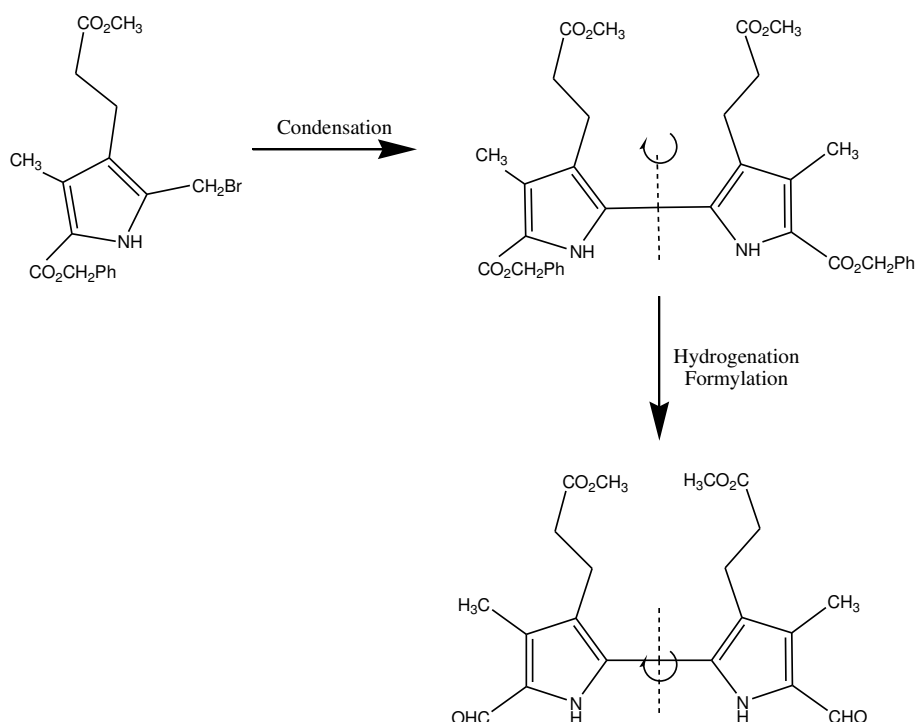


Figure 24: An example of reaction to produce symmetrical dipyrromethane

MacDonald and Woodward independently demonstrated that the condensation of 5,5'-diunsubstituted dipyrromethanes or related dicarboxylic acids with diformyldipyrromethanes in the presence of an acid catalyst forms porphodimethenes. As illustrated in Figure 25, this reaction followed by subsequent oxidation gave the corresponding porphyrin and the yield of products obtained was usually very satisfactory. This concept served as the basic foundation for the synthesis of porphyrin *via* the [2+2] synthesis method [98].

This reaction also necessitates the involvement of at least one symmetrical building block in order to avoid formation of mixed isomeric porphyrins. MacDonald and his team have shown that with at least only one symmetrical block, the formation of substituted porphyrins could be achieved. It is necessary to have an aldehyde functional group in one of the building blocks and the second building block could have merely hydrogen or carboxylic acid in the connecting side chain [97-99]. Figure 25 describes an example of complete porphyrin synthesis steps proposed by this method.

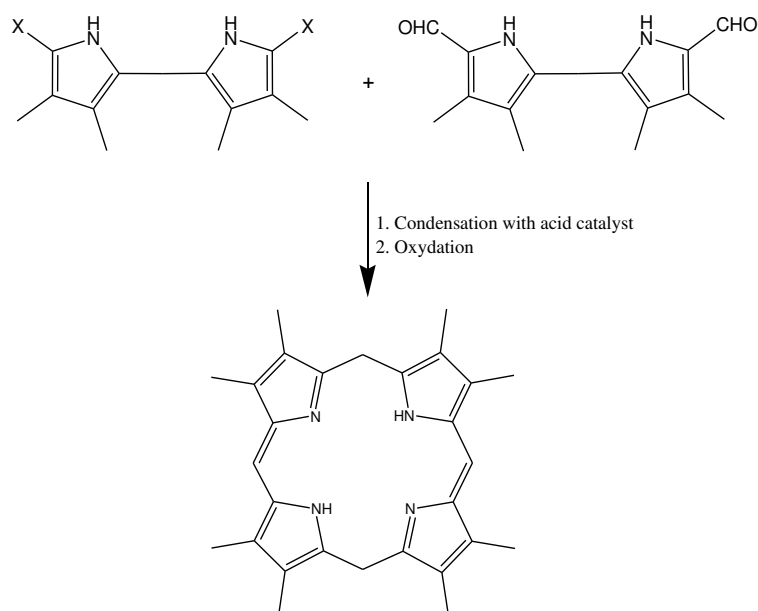


Figure 25: The synthesis steps of porphyrin as proposed by MacDonald and Woodward. X could be either hydrogen or carboxylic acid (as described in the text above)

V. 1 + 3 METHOD

Boudif and Momenteau in 1994 reported the first porphyrin synthesis approach with [3+1] technique, in which they used a tripyrrane and 2,5-diformylpyrrole [100]. This method employs the basic chemistry approach as in the [2+2] technique but the utilization of 3-pyrrole open-ring system with a monopyrrole unit enables the synthesis of porphyrin with unique functionality. This desired function group will usually conjugate with the monopyrrole unit and will be inserted at the final synthesis stage. At the beginning, Boudif and Momenteau used *bis*-propionic porphyrins with diformylpyrrole (Figure 26). But afterwards, several other

groups such as Sessler's and Lash's expanded the applicability of this synthesis method and much more diverse porphyrin molecules could be synthesized [97, 98].

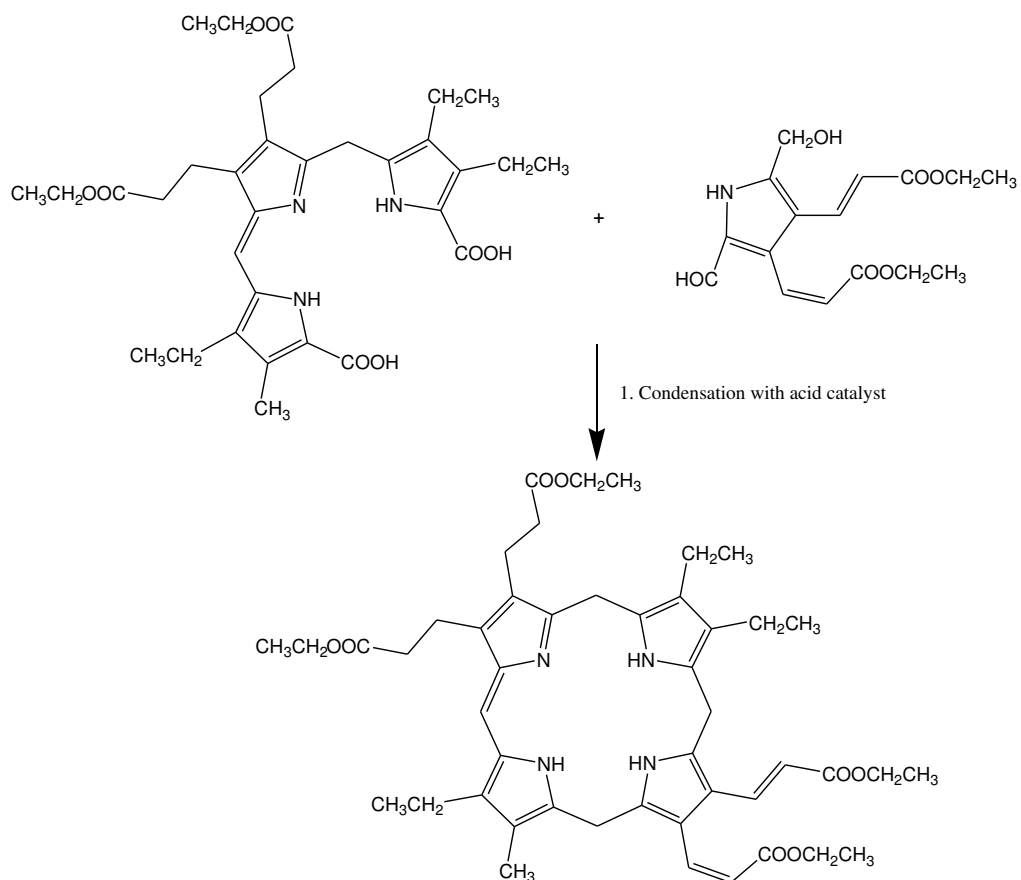


Figure 26: Synthesis of porphyrin through [3+1] approach [89]

C. Photophysical characteristics

Figure 27 illustrates the UV/Visible absorbance of different PSs: porphyrin, chlorin and bacteriochlorin as some examples. The electronic absorption bands of porphyrin could be divided into two types of bands, the B-band and the Q-bands. The B-band is also known as Soret band; it is a very intense band between 380 nm to 500 nm. The Q-bands on the other hand appear at longer wavelengths, between 500 nm and 700 nm, and consist of four much weaker peaks in comparison to the Soret band [101].

Metallation of porphyrin is also of interest. This could be done by using several metals such as zinc, copper and palladium. The type of metals incorporated in the porphyrin ring was also found to have influence on the photochemical and photophysical characteristics of porphyrin [75]. The insertion of metal in the porphyrin ring usually changes the pattern of the Q-bands. Because the ring becomes more symmetrical than it was in the free porphyrin, the Q-bands will be simplified into only two Q-bands at 557 nm and 597 nm [101].

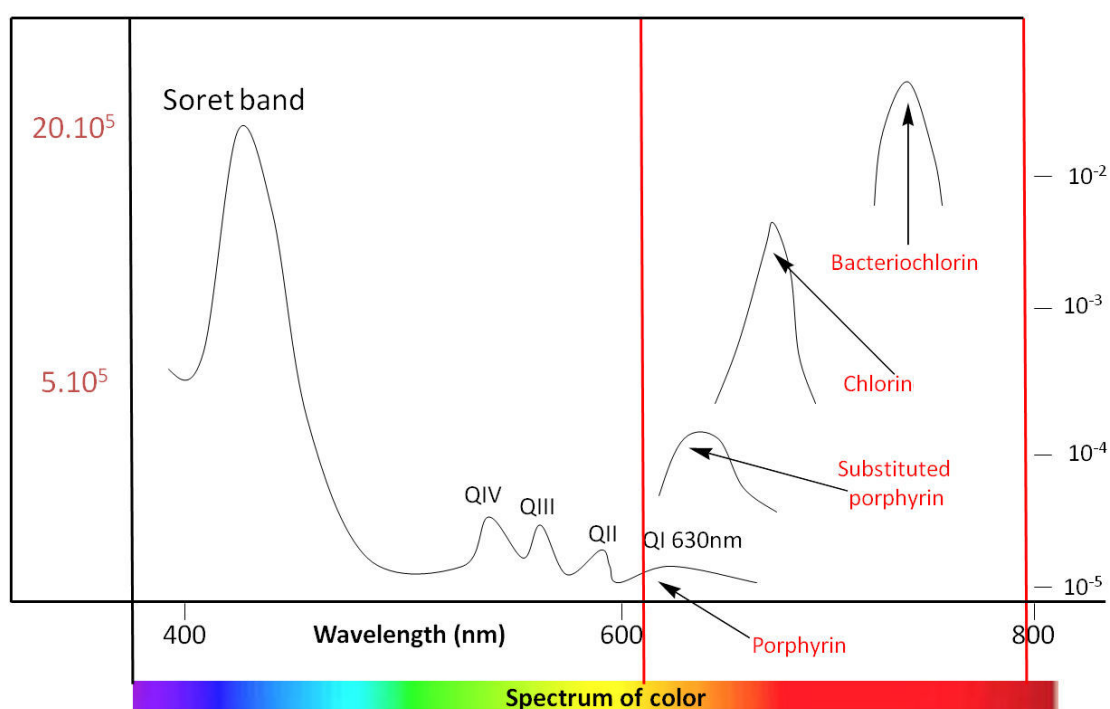


Figure 27: UV/VIS absorbance spectrum of porphyrin, substituted porphyrins, chlorins and bacteriochlorins. The intensity of QI band changed according to the type of photosensitizers

In addition to UV/visible absorbance characteristic, porphyrin also shows interesting fluorescence and singlet oxygen production capability. Non-metallated porphyrin has two fluorescence peaks: the first one with a maximum at around 650 nm and the second one at a

maximum of 720 nm. Metallation causes changes and shifting of the fluorescence peak and this change depends on the type of metal inserted into the porphyrin centre. In the case of zinc-metallated porphyrin, shifted fluorescence peaks could be observed at 603 nm and 655 nm (solution in ethanol), with lower fluorescence intensity as compared to non-metallated porphyrin (Figure 28). The production of singlet oxygen on the other hand is not significantly affected by metallation and in general, the singlet oxygen quantum yield of porphyrin is around 60% (solution in ethanol) in comparison to Rose Bengal as the standard.

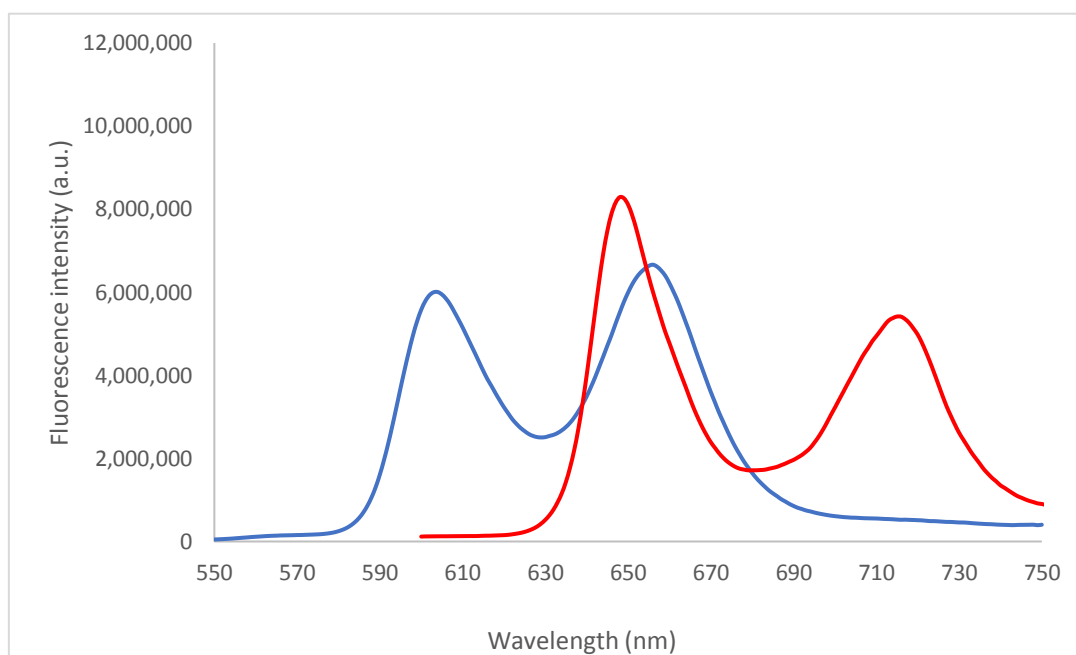


Figure 28: The fluorescence emission peaks of metallated porphyrin (blue line) in comparison to non-metallated porphyrin (red line)

Central-metallated porphyrin and in particular gold porphyrin are also being intensively investigated over the last decade. For example, Che *et al.* (2003) developed four different types of Gold (III) meso-tetraarylporphyrin complexes and compared those with a Zn(II) tetraphenylporphyrin (TPP) complex on *in vitro* anti-proliferative capability. Their finding was remarkable: the IC_{50} of the Gold (III) complexes were between 0.1 to 1.5 μ M and it has about 100-fold higher cytotoxicity *in vitro* than the Zn(II) complex [102]. They also reported that this series of Gold(III) complexes induced p53-dependent apoptosis of several cancer cell lines; KB-3-1, HL-60, HepG2, SUNE1, HeLa, KB-V1 and CNE1.

1.2.6 Photodynamic action *in vivo*

The administration of currently available PS for PDT in clinical settings could be done through intravenous, intraperitoneal or topical route, and once it is administered, it is allowed to localize in tumour cells over several hours or days, depending on the type of PS and tumour. The fluorescence from the PS can also be used to diagnose and pinpoint the location of the tumour [3].

Cell death that happens after PDT treatment is believed to be through combination of different pathways. Three major events that are known to happen following PDT are direct cell damage, vascular shutdown and activation of immune response [103]. PDT mediates tumour cell damages through all three classical cell death mechanisms: apoptosis, necrosis and autophagy-associated cell death [3].

Apoptosis, or Type I cell death is a programmed cell-death which is mediated by caspases. The organelles from the cell cytoplasm are engulfed by apoptotic bodies and the cell will overall shrink before the membrane integrity is lost (Figure 29). This is the most highly in-used mechanism in PDT. Type II cell death is known as autophagy-associated cell death, during which the cytoplasm is filled with two-membrane autophagic vacuoles. Type III cell death is necrotic cell death. Generally, necrosis is defined negatively as a type of cell death that lack both Type I and Type II cell death characteristics [51, 104].

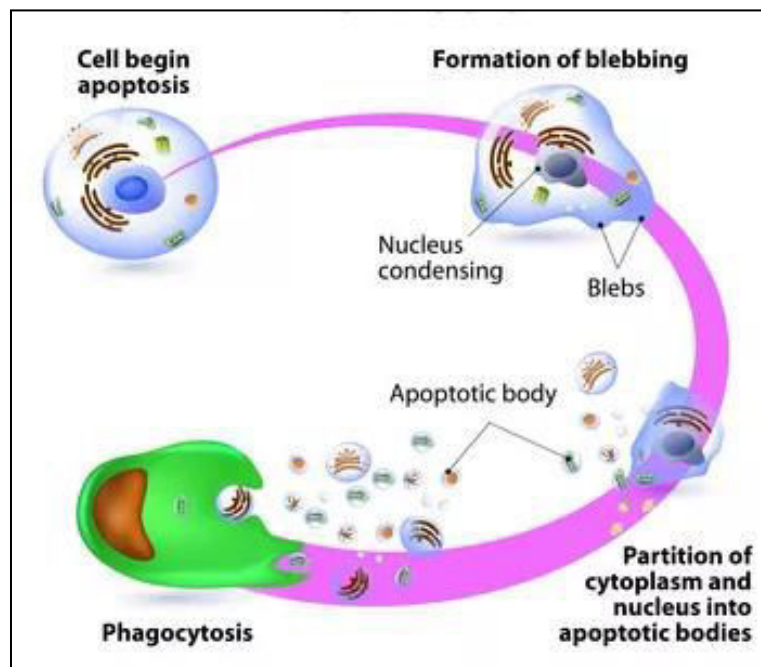


Figure 29: Mechanism of cell death through apoptosis

Unlike chemotherapy and radiotherapy which target the cells' DNA itself, PDT primarily exerts its killing effect through damaging targets other than the DNA, and the specific targets depends on the localization of the PS within the cancerous cells and this varies among different PS and cell types. As examples, Photofrin[®] was found to localize near and within the lipid layers [105]. Chlorin NPe6 prefers lysosomes, whilst the benzoporphyrin derivatives target mitochondria and *m*-tetrahydroxyphenylchlorin targets mitochondria, endoplasmic reticulum or both. These different types of accumulation are believed to cause different mechanism of cell death. As an example, pyropheophorbide and PpIX which are localized in the mitochondria upon internalization into cells could cause damages to mitochondria directly and eventually leads to cell death *via* apoptosis [57, 105].

Besides having in-cell localization of photosensitizers, some PS could also be retained in the vasculature or being directed to target the vascular endothelial cells. In this case, the damage that happens following PDT is believed to be through vascular damage, thus depriving the cells from oxygen supply and nutrients thus eventually causing cell death. Research has also shown that the actual response to PDT is not necessarily confined to the cells where singlet oxygen is presence, but PDT can also invoke physiological and immunological reactions as well [57].

From the explanation above, it is hence obvious that the target points of PSs are very important in determining their effectiveness. Since the time-activity of singlet oxygen is very short (10-300 ns), the singlet oxygen that is generated by nearby PS has a very limited range of diffusion and also limited time to travel to desired target sites. Its site of generation is the site that it could inflict damage upon [51, 52]. Hence, it is very important to ensure site-specific delivery of PS to achieve the optimum effect following PDT. This is the basis behind the development of targeted PS for the improvement of its delivery.

1.3 TARGETED CANCER THERAPY: A STRATEGY IN IMPROVING THE DELIVERY OF PHOTSENSITIZER

Targeted drug delivery is important in improving the safety and efficacy of therapeutic agent, especially since one of the most important underlying problems in cancer therapeutics is the inability to deliver the active therapeutic substance directly to the tumour cells with little or no collateral damage. Thus the approach of targeting could be useful in making the anti cancer therapy less invasive, especially since the major barriers against therapy success are the dose-limiting toxicity of the drug and development of drug resistance. Hence, the addition of a targeting agent may be able to help and improve the delivery of anti-cancer therapeutics [36]. Generally, targeting in drug delivery could be divided into two types: (1) **passive** and (2) **active** targeting, which could be simply explained by the presence and absence of targeting moiety attached on the drug entity, respectively (Figure 30).

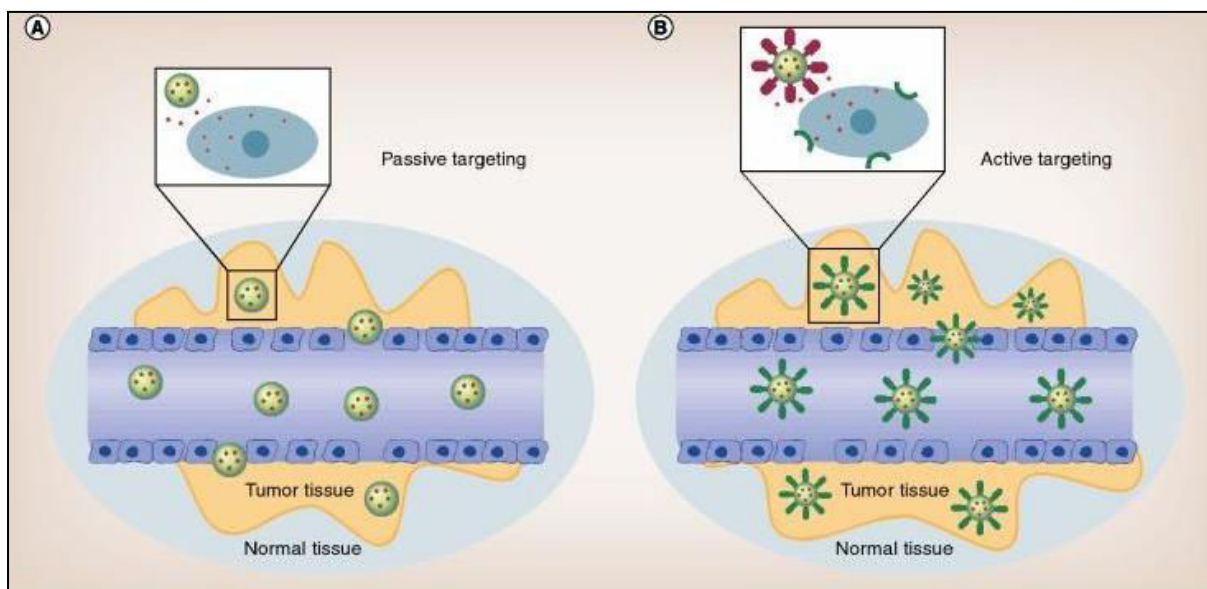


Figure 30: The differences between passive (A) and active (B) targeting. From [106]

I. PASSIVE TARGETING

Passive targeting exploits the environmental condition of the tumour which is usually different than normal cells. Their vasculature is usually leakier, and not well formed as those surrounding normal cells (Figure 31). Drugs could reach the tumour through the Enhanced Permeability and Retention (EPR) effect. In the field of PDT, passive targeting is applicable with nanoparticles such as liposomes, micellar systems and polymeric capsules to facilitate the transportation and incorporation of the PS into tumour cells.

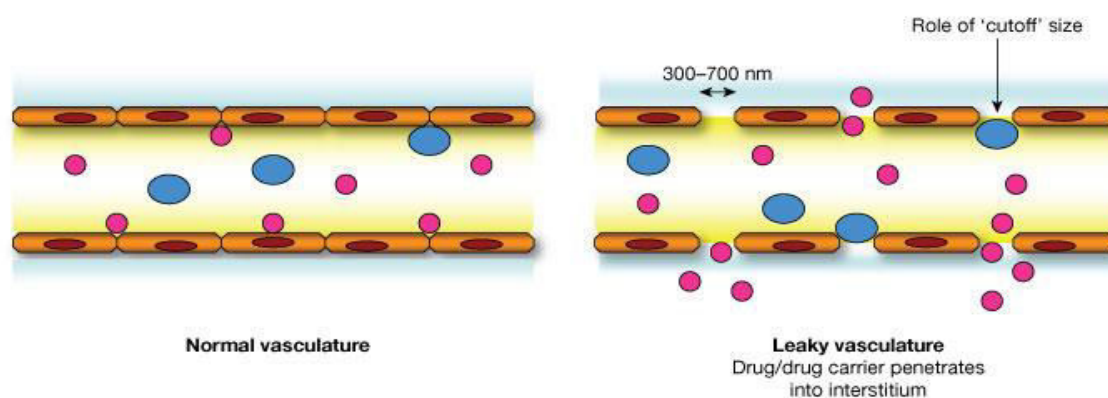


Figure 31: Leaky vasculature (right) commonly associated with blood vessels surrounding tumours, in comparison to normal blood vessels (left). From [107]

II. ACTIVE TARGETING

In **active targeting**, the delivery of drug to targeted sites is based on molecular recognition, by using specific ligands conjugated to the drug which binds on appropriate receptors expressed by cells at the targeted site (Figure 30). The targeted receptors for these ligands are usually over-expressed by cancerous lesions (direct action) or its vasculatures (indirect action). Several receptors are useful in active targeting, and they include the transferrin receptors, epidermal growth factor receptor (EGFR), human epidermal growth factor receptor, integrins, somatostatin/growth hormone receptor, glucose transporter, insulin receptor and folate receptor. Folate receptor is an important target in anti-cancer treatment. It is one of the most explored receptor in cancer targeting and is believed to hold good potential in improving the delivery of therapeutics [108, 109].

The approach of active targeting enables the administration of lower effective dose of drugs. This is because as the majority of drugs administered could be delivered to its target (a role played by the targeting ligands), there will be less drugs being unnecessarily distributed

to other sites, hence lowering the quantity of drug is needed to exert the similar effect in comparison to the same drug without a targeting ligand [110].

1.3.1 Improving PS Delivery for PDT

The therapeutic effect of PDT could be enhanced by, (1) direct illumination of the target tissue; (2) strategic timing of light dose administration; (3) topical administration the PS and (4) chemical manipulation of the photosensitizer molecules [4]. Strategy (4) in particular has captured much interest in recent years. Ever since the discovery and introduction of porphyrin molecules as effective photosensitizers, many efforts have been made to generate PSs with better safety and improved efficacy profiles.

A number of researches and studies were already conducted on PSs or PSs-vector systems which targets some of the receptors mentioned earlier, including the epidermal growth factor receptors [111, 112], transferrin receptors [113-115], folate receptors [116, 117] and insulin receptors [118]. Our PDT team in Nancy has also described in several publications on the conjugation of chlorin (PS) to peptides as targeting vectors (ATWLPPR, DKPPR and TKPPR) which have shown good targeting capability against NRP-1 receptor [5, 6, 119-122].

Peptides are thought to be good candidates from the bio-mimetic point-of-view because they could have a specific interaction with cell membrane besides being easily solubilised in aqueous medium [123] and hence could simultaneously improved the water solubility of PSs. In the design of third generation PS, the use of peptides as the targeting agent has been under the ‘spotlight’ for being potentially useful and utilizable for better delivery of PS [67]. Besides peptide, folic acid is another useful anti-cancer targeting agent. As mentioned before, the abundance of folate receptor on the surface of cancer cells present as an opportunity to be exploited as a target for drug delivery. This will be further explained in subsequent sub-topics and chapter.

This thesis will focus on active targeting technique involving two different molecules: peptide and folic acid. Targeting by peptide is “**active, indirect targeting**” due to the fact that the peptide used is targeting the neo-vessels formed during angiogenesis. The targeting by folic acid on the other hand is “**active, direct targeting**” because folic acid is directly targeting the cancer cells themselves. The development of PS conjugated with these two different targeting strategies is of high interest to obtain effective targeting system.

1.3.2 Targeting with peptide

By definition, peptides are short biopolymers consisting of not more than 50 amino acids which are linked by amide or peptide bonds. Because they are short, they do not have a real tertiary structure and they have the advantages of better tissue permeability, rapid internalization, good receptor binding, high tissue clearance and mild antigenicity. These factors ensure that they are good candidates as targeting agents for drug delivery of typically any drug. An interesting feature in using a peptide is its ability to have both targeting and delivery capabilities, which means that a drug molecule associated or linked with a targeting peptide could be specifically delivered and internalized into its targeted cells [124].

In recent years, ligands with a peptide sequence containing R/K-XX-R/K were reported to have enhanced cellular penetration. In 2009, Teesalu *et al.* conducted a random phage screening analysis for peptides binding to prostate cancer cells and found that peptides with terminal arginine (or sometimes lysine) residues, commonly in the form of R/KXXR/K have good cell penetration. Further research revealed that the C-terminal arginine was crucial for the activity; its activity will be eliminated if another amino acid was added or the carboxyl group is blocked by an amide group, and hence this kind of peptide is called C-end rule. These C-end rule peptides were subsequently shown to be good candidates as ligand for NRP-1 receptor [125]. In addition, it was also discovered in the literatures that the “XX” is preferred to be equal to PP (proline-proline) or PR (proline-arginine) to give optimal organization at the active site of the NRP-1 receptor [126].

Teesalu and co-workers also reported that they noted a unique and important function of the peptides that follow the C-end rule; they have the ability to penetrate and internalize into tissues and cells. They found that the cargo attached to such peptide could escape from the vasculature and spread into the surrounding vicinity, suggesting that the peptide could bring along its conjugated therapeutic agent through vascular and tissues to exert its intended effect [125]. This information is indeed very interesting and important which could augment the role of this peptide, in this case KDKPPR, in targeted drug delivery for cancer therapeutics. By using this peptide, it may also be possible to extend the application of photodynamic therapy into deep-seated tumours which were difficult to achieve before.

Furthermore, it is very interesting to note that the VEGF-A₁₆₅ which targeted NRP-1 have a C-end rule terminal sequence which enables it to interact with the b1 domain of NRP-1 receptor and subsequently causing the cascade of events leading to cellular internalization and vascular leakage [125]. Keyt *et al.* (1996) reported that the 55-amino acids residues at the C-end of VEGF-A₁₆₅ (Figure 32) are important in stimulating endothelial cells proliferation. Upon cleavage of the 55 residues by plasmin, the VEGF-A₁₁₀ that is produced has significantly lower endothelial cell mitogenic potency; more than 100-fold diminution was observed [127].

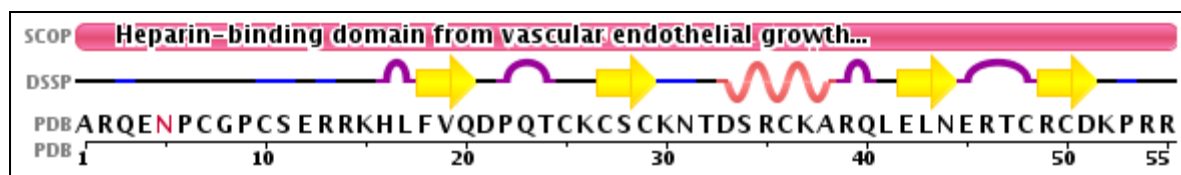


Figure 32: The 55-residues of carboxy-terminal heparin-binding fragments at the end of VEGF-A₁₆₅. Note the c-end rule terminal (R/K-XX-R/K). From Protein Data Bank, structure code 2VGH

A. DKPPR peptide

DKPPR is a peptide discovered by our research team in Nancy by Ezatul Ezleen Kamarulzaman through elaborate works involving docking simulation studies followed by *in vitro* and *in vivo* experiments. The binding capability of DKPPR peptide on NRP-1 was reported [5, 6] and this finding supports the R/K-XX-R/K theory described in other publications as explained earlier. DKPPR was initially assembled based on the sequence of tuftsin (TKPR), a known ligand of NRP-1. It was also designed based on the terminal sequence of heparin binding domain of VEGF-A₁₆₅ (Figure 32), with slight modification on the fourth amino acid from arginine into proline. Apart from DKPPR, ten other peptides were also evaluated in the study including DKPRR, TKPPR and TKPRR in the search of a suitable NRP-1 targeting agent. From docking simulation study and ELISA test, it was found that DKPPR has excellent binding capability on NRP-1 receptor, better than DKPRR.

This peptide was subsequently conjugated with a chlorin-type PS with different spacers: aminohexanoic acid, PEG-9 and PEG-18 to investigate the influence of different length of spacers on their binding ability. The EC₅₀ of the different conjugates were not significantly different among each other (~30 μM), although this value is much higher than the free DKPPR peptide (18 μM). This finding is interesting in which it depicts that the presence of a conjugated PS may cause reduced activity perhaps due to some conformational hindrance at the site of the receptor. The relatively big molecular size of the PS may nevertheless contribute to this problem.

From a subsequent *in vivo* experiment, the conjugate was found to have good bio-distributions in important organs including liver, spleen and kidney. It is known that NRP-1 is expressed in normal liver cells [128] and this shows the potential that this peptide holds in improving the delivery of conjugated PS. But due to the fact that the animal model is of healthy models, no data is hence available on specific targeting of the conjugates towards NRP-1 receptors *in vivo* [6, 129]. The two publications that were published are included in the Appendices 10 and 11 of this thesis.

Following the discovery of DKPPR, as part of a parallel study we aimed to graft the DKPPR peptide and a model photosensitizer simultaneously on nanoparticles. The amino group on the side chain of lysine provides the possibility of coupling a PS on the peptide (through a spacer), but due to the fact that perhaps the lysine available in the structure (DKPPR) may be needed for its interaction with NRP-1 (as has been proven in this thesis and will be described later on in Chapter III), a supplementary lysine was introduced at the *N*-terminal of the peptide sequence, and hence KDKPPR was created.

The presence of the *N*-terminal lysine allowed the functionalization of the δ -amine and coupling of the PS on the peptide. Surprisingly, the addition of this lysine (and its conjugation with the PS) was found to have improved binding on NRP-1 receptor as determined by ELISA assays conducted. The data on ELISA assay is described in more detailed in Chapter III.

B. Target application of DKPPR and KDKPPR in PDT

As mentioned above, the two peptides DKPPR and KDKPPR discovered were found to have good targeting capability on NRP-1, which is a receptor known to have an important function in angiogenesis and nervous system development. Many solid tumours demonstrate up-regulation of NRP-1 expression, and human glioblastoma is one of them [130]. To date, the anti-cancer treatment of glioblastoma multiforme is among the most difficult, due to the nature of the tumours which involves the brain and the malignant aggressiveness of the tumour.

PDT is believed to have the ability to offer an advantage in the treatment of glioblastoma multiforme. The presence of good targeting agent such as the mentioned peptides will definitely help to deliver the conjugated PS precisely to the tumour site in the brain, which is difficult to treat with surgical or chemotherapy approach. Several preliminary *in vivo* studies have already been conducted involving PS-peptide conjugate with other peptides such as ATWLPPR on xenograft animal models with gliomas, and the studies have shown promising results with improved tumour level of the PS-peptide conjugate as compared to PS alone and better visualization of the tumours and its peripheral margins [119, 131].

With the improved ability of NRP-1 targeting by DKPPR and KDKPPR, it is believed that the utilization of these peptides as targeting agent will be able to increase the delivery of conjugated PS. Hence, this is the ultimate target of this project; the development of PS-peptide conjugate with the aim of improving PS delivery towards the glioblastoma multiforme tumour tissues.

1.3.3 Targeting with folic acid

As mentioned earlier, FR is a very promising target to deliver anti-cancer agent. There are two approaches that could be used in targeting FR; the first is based on the development of anti-FR antibody and the second is by using folic acid (FA) as a receptor ligand, with conjugation to a drug or diagnostic agent. In the initial works involving FR targeting, monoclonal antibodies (mAbs) were used and they showed some advantages over FA as targeting agent, especially since their binding is unaffected by the presence of FA molecule in the environment. However, due to the preference of utilizing low molecular weight molecules as targeting ligand, folic acid is much preferred and used widely as compared to mAbs in FR targeting [36]. The FA itself is useful as a targeting agent due to its inexpensiveness, low toxicity, non-immunogenicity and easiness to be conjugated with other carrier and molecules, besides its good stability during storage and after *in vivo* administration [132].

The second approach is also a versatile strategy in FR-targeted drug delivery because FA could be coupled to different therapeutic agents without compromising its targeting capability. In addition, there is substrate specificity between FA and the FR α , providing higher chances of delivery [38]. It was reported that FA's affinity towards FR α is 10-times higher as compared to FR β , and 4-times more than FR γ [36].

Figure 33 illustrates the internalization mechanism of FA-drug conjugates into cells. The internalization of FA-drug conjugates is achieved through endocytosis. Upon interaction of FA with the receptor which is located within a caveolae, the complex of drug-FA will be internalized into the cytoplasm together with the receptor. They will stay attached to each other and as the pH of the endosome approaches pH 5, FA will be detached from the receptor and the associated drug will be released into cytoplasm to exert its effect. In addition to the FRs, there are also folate receptor carriers on cell surface, which are only known to transport unconjugated FA. These carriers however are not very useful in the delivery of FA-drug conjugate [108].

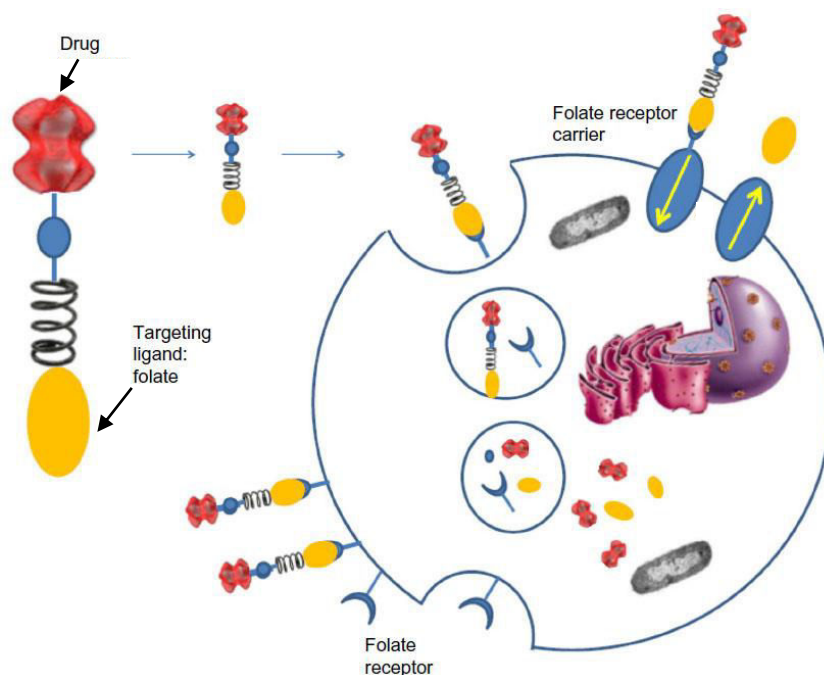


Figure 33: Mechanism of drug-FA conjugate internalization. From [38]

There are many techniques described in the literature on folic acid conjugation for cancer targeting. This includes conjugation on the surface of various carriers such as nanoparticles and liposomes besides direct conjugation between folic acid and molecules such as chemotherapeutic drugs, proteins and oligonucleotides. As an example, Feng *et al.* (2015) reported on the conjugation of folic acid with $\text{TiO}_2\text{-SiO}_2$ nanoparticles. Through a cell internalization study, they observed that the conjugated nanoparticles bind on the folate receptor of human nasopharyngeal epidermoid cancer, KB cells, showing that the conjugate has indeed a cancer cells targeting capability [133]. A number of chemotherapy drugs were also being conjugated directly with folic acid such as paclitaxel, mitomycin C and vinca alkaloids. In general, it was reported that the conjugates have shown higher affinity towards FR and have also shown selective cytotoxicity against FR-expressed cells [36, 134]. Figure 34 illustrates an example of a vinca alkaloid-folic acid conjugate under investigation called Vintafolide (Merck & Co).

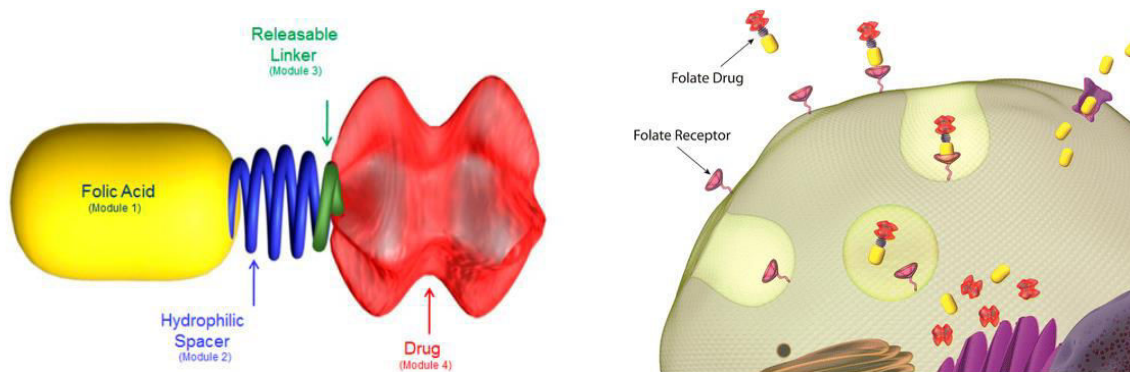


Figure 34: Example of folic acid-drug conjugate. folic acid (module 1) conjugated to a drug (module 4) through a spacer (module 2) and a releasable linker (module 3). This conjugate will help to bring the drug to the targeted cell (image on the right) and the drug will be released inside the cell

The relatively small size of drug-folic acid conjugates as compared to nanoparticles- or liposomes-conjugated folic acid gave a better chance for the former to access FR expressed cells. As for the latter, they have much limited access to FR on solid tumour due to their much bigger size. However in terms of internalization, they will still be internalized efficiently by tumour cells or tumour-infiltrating macrophages. This means that these macrophages could be a second vehicle to aid in the delivery of nanoparticles-conjugates FA into non-FR expressing tumour cells [36].

In the field of PDT, the development of PS-folic acid conjugate to target FR α for the treatment of ovarian cancer is a very promising strategy. This is because albeit the treatment strategy (surgery and platinum-based chemotherapy) that are available currently in clinical setting for the treatment of ovarian cancer, the recurrence rates remained high: 60% of women in remission develop recurrence within the period of five years. Hence, the development of targeted PDT with folic acid could help to bring conjugated PS to the tumour microenvironment, and with the application of PDT coupled with conventional chemotherapy, radiotherapy and surgery, it is believed that the recurrence rate could be decreased significantly [135].

Qualls and Thompson who were the first in using folic acid for PDT, have prepared liposomes containing phthalocyanine with folic acid as targeting agent, also against KB cells. They observed that after irradiation, the phototoxicity induced by the FA-liposome was superior as compared to free phthalocyanines or untargeted liposomes [136]. Stallivieri *et al.* (2015) published a comprehensive review on the application of folic acid in PDT. In terms of direct conjugation between folic acid and active substance, folic acid is usually conjugated either with or without a spacer *via* its glutamic acid moiety. Several types of spacer are being reported in the literature with the most common being polyethylene glycol, PEG of different lengths. Through analysing the available literatures, it was evidential that all the PS conjugated with folic acid has improved affinity towards FR regardless of the PS nature [109].

Although targeted drug delivery is very promising, there is an important factor that limits the effectiveness of targeted therapy: the abundance of targeted receptor on cell surface. Targeted drug delivery is thought to be much more effective for drugs with high potency or low effective concentration. However there are reports on methods to increase the expression of receptors on cell surface. As an example, the expression of folic acid receptor was found to be increased by using agents such as dexamethasone or all-*trans* retinoic acid (ATRA). This could be a useful approach in improving the delivery of drug conjugated with folic acid [36].

All these data available are shows that folic acid is indeed very useful, has high potential in cancer targeting and is also applicable in PDT. Albeit all the advantages associated with folic acid as drug targeting agent, it suffers a major stability problem. The folic acid molecule is highly sensitive towards various environmental factors including light, thermal and oxygen, making the synthesis and handling involving folic acid to be difficult. Hence to address this problem, a stability study involving folic acid as single molecule and in conjugation with a PS was conducted as part of this thesis.

1.4 OBJECTIVE OF STUDY

This thesis aims to improve PDT application for the treatment of solid tumours through two different approaches: direct targeting and indirect targeting. The direct targeting could be achieved by using folic acid as the targeting vehicle against any folate receptor-expressing tumours such as ovarian cancer. Indirect targeting on the other hand aimed to target NRP-1 receptor expressed by vascular network surrounding tumour cells, by using peptide as the targeting agent. The research projects conducted were based on these topics. Hence the objectives of the thesis are outlined as below:

- i. To evaluate the stability of folic acid molecule as a targeting agent and a novel photosensitizer-folic acid conjugate intended for the treatment of ovarian cancer through the Design of Experiment (DoE) approach.
- ii. Design of platforms with porphyrin and peptide as a targeting agent towards NRP-1 receptor
 - ii.a Improvement of DKPPR peptide through development of KDKPPR peptide as a way to improve the specificity of NRP-1 towards human glioblastoma multiforme tissues, and the evaluation of the importance of each amino acid in KDKPPR sequence through Alanine-scanning technique
 - ii.b Synthesis of different platforms of PS and DKPPR peptide through click chemistry technique to investigate the influence of different numbers of PS and peptide molecules in one platform on the efficacy and targeting capability of the platform towards human glioblastoma multiforme tissues for PDT application.

Chapter II: The Evaluation of Folic Acid Stability: As Free Molecule and as Conjugate for PDT Application

2.1 INTRODUCTION

This chapter describes a study on the evaluation of folic acid (FA) stability under different environmental conditions and stress. The objective is to get useful information on the optimal physical and chemical parameters for FA stability during storage, handling, chemical ligation and *in vivo* metabolism. The second part of this chapter is focused on stability evaluation of a photosensitizer-FA (PS-FA) conjugate, intended for targeted PDT. This targeting approach could help to improve the delivery of photosensitizers towards cancerous lesions which are known to have higher expression of folate receptor as compared to normal tissues. The PS-FA conjugate was synthesized in our laboratory and further explanations are available in the following subsections.

2.1.1 Folic acid

FA (Figure 35) is one of the essential vitamins for normal bodily function. It is also known as vitamin B₉, a water soluble vitamin which plays important roles in DNA metabolism, methylation and repair [108]. FA is available from both natural and synthetic origin. Naturally produced FA has a lower stability as compared to the synthetic one; and it also has lower bioavailability. Due to its biological function which is very important, FA is commonly fortified in food to ensure sufficient intake by people and hence preventing health issues related to FA deficiencies such as anaemia [137].

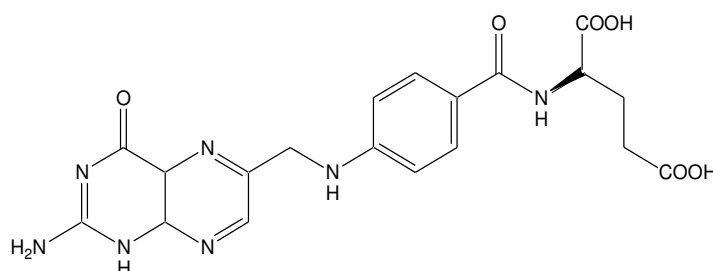


Figure 35: Molecular structure of FA

Some early studies on FA showed that although FA is classified as water-soluble vitamin, its solubility profiles differ depending on the pH and/or the temperature of the dissolving media. Pfiffner *et al.* reported that FA has a solubility of 0.16 mg / 100 mL at pH 3, 25°C and increased to 100 mg / 100 mL at 100°C. He also observed that FA is not soluble in most common organic solvents but have relative solubility in acetic acid, phenol and pyridine [138]. In another study by Scheindlin *et al.* who studied pharmaceutical formulation of FA showed that a solution of 2.5 mg FA in 4 mL water at pH 5.1 precipitated after one week, showing that an initial solubility would not mean a permanent stability. They concluded from this study that a stable formulation of FA could be prepared with a minimum concentration of 2.5 mg in 4 mL with a pH between 8 to 9 [139, 140]. This physicochemical property of FA is important because of the influence it has on the stability of FA.

The research involving FA and its derivatives such as tetrahydrofolate has become of wide interest due to the important roles that it plays especially in cancer therapy and targeting. As mentioned earlier in Chapter One, FA has a big potential in the targeting of ovarian cancer, due to the presence of abundant FA receptors on the surface of ovarian cancer cells [38]. However, among the vast body of data available on FA, it is generally known and recognized that FA in one way or another suffers from instability, which is a problem that needs to be carefully taken into account.

From the literature, many environmental factors were reported to have detrimental effects on FA stability. This includes light, high temperature, presence of oxygen and type of solution medium, among all. The degradation of FA was found to produce truncated FA moieties which cause partial or complete loss of activity. Three most common degradation products formed are 6-formylpterin (FPT), pterin-6-carboxylic acid (PCA) and *p*-aminobenzoyl-L-glutamic acid (PGA) (Figure 36) [141].

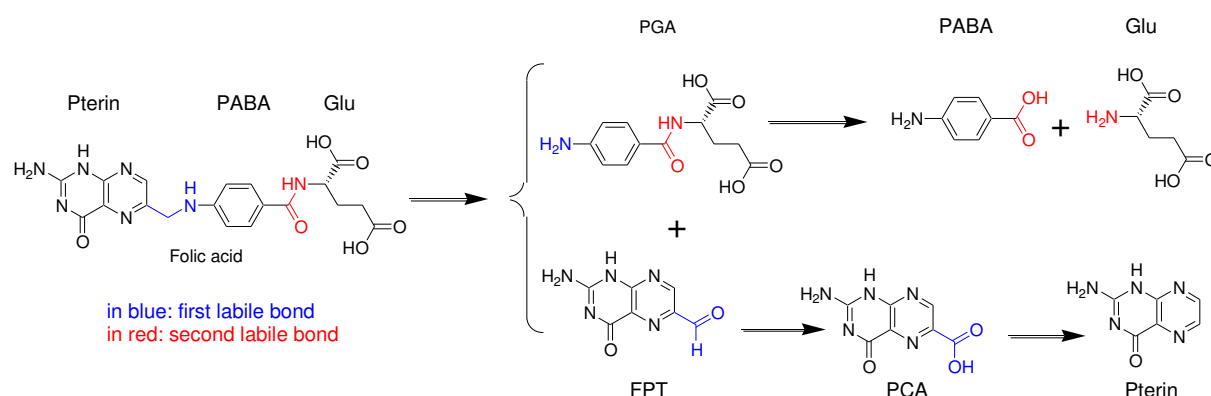


Figure 36: The degradation products of FA. PABA: *p*-aminobenzoic acid, Glu: glutamic acid, FPT: 6-formyl pterin, PCA: pterin-6-carboxylic acid, PGA: *p*-aminobenzoyl-L-glutamic acid,

Extensive information is available regarding the degradation products of FA following many years of research done on this molecule. This includes the degradation pathways

following its exposure to the different factors that cause its degradation. In general, the major products are as illustrated in Figure 36, however in some cases more specific products could also be recovered, such as the degradation caused by electron beam whereby 6-(hydroxymethyl)pterin and *N*-(4-nitrobenzyl)-L-glutamic acid were found to be formed [142]. Recently, we submitted a review article entitled “*Is folic acid an ideal targeting unit?*” regarding the stability of FA and the major factors involved in its degradation. This paper is available in [Appendix 9](#) at the end of this thesis.

During the handling of FA in laboratories, some precautionary measures are usually taken in order to prevent FA degradation. Reducing agents such as ascorbate, β -mercaptoethanol, dithiothreitol and dithioerythritol could be added but some loss of activity should still be expected. Jones and Nixon (2002) reported that ascorbate was found to be more protective than DTE, providing 53-times higher stability of tetrahydrofolate at 4°C. They attributed this stability to the removal of oxygen by ascorbate because the presence of oxygen is indeed disastrous for FA [143].

With regards to drug-related research and development, stability is indeed a big issue because an unstable molecule will lose its affinity leading to the lost of its activity. In addition, a higher development cost will incur, which will ultimately become a burden for patients and indirectly for the nations. This project is thus a step that was taken in evaluating the stability of FA; to investigate the most important factors that influence the degradation of FA. This will then be compared with the stability of FA in conjugation with a photosensitizer molecule, to determine if a chemical conjugation could help to improve the stability of FA.

The novelty of this study lies on the application of Design of Experiment (DoE) to evaluate the different factors that are known to influence FA stability. Based on the literature review conducted, it was discovered that in all the studies available, the stability of FA was evaluated in only one, or maximum two environmental factors. In this study however, all the common factors were pooled together and evaluated through the utilization of DoE approach to determine the most important factor that influence FA stability. This can contribute to a clearer view on ways to improve FA stability through controlling the exact environmental factors.

2.1.2 Folic acid in cancer therapy

FA has a wide application in the clinical practice of cancer therapy. It has been in the spotlight ever since the discovery of folate receptor as a potentially effective targeted receptor in the 1940s by Sidney Farber with countless reports of positive outcomes in cancer therapy involving FA and its derivatives. Farber studied the effect of antagonising folate receptor by using analogues of FA in the treatment of acute lymphoblastic leukaemia (ALL) in children and he discovered that the analogues that he used (aminopterin and amethopterin) blocked the function of folate receptor and hence producing improvement of ALL in the children treated. This serves as a ground-breaking finding in anti-cancer treatment. The analogue amethopterin is still in use up to this day and is known as methotrexate; one of the most essential drugs recognized in basic health system (Figure 37) [144-146].

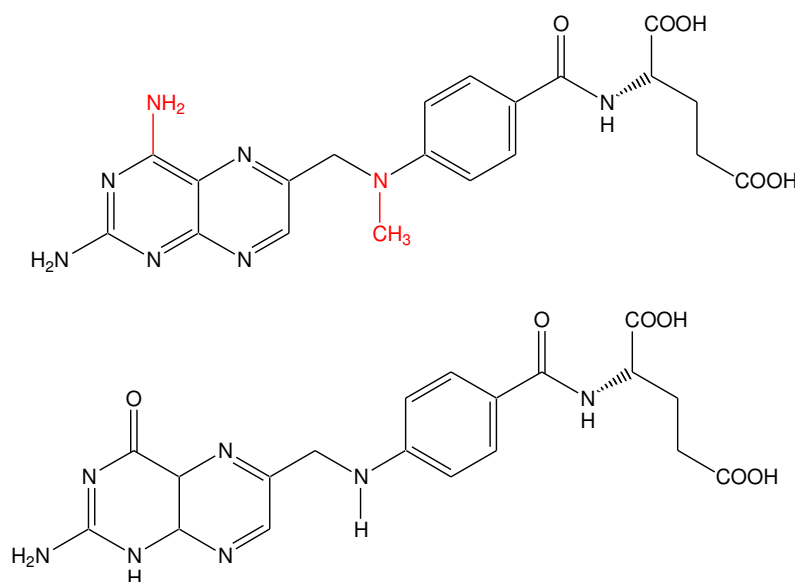


Figure 37: Molecular structure of methotrexate (above) and FA (below)

The molecular structure of methotrexate resembles closely of FA molecular structure. The modifications done on the pterin moiety has no disruption on the binding capability of methotrexate on folate receptor and subsequent blockage of folate function could be observed as reduction of cell tumour viability. However in current clinical practice, the administration of methotrexate is usually followed by FA or folinic acid (Figure 38), another analogue of FA, after a specific time-length, in order to prevent adverse drug reaction that might be caused by methotrexate. This is due to the fact that methotrexate has no specificity towards cancer cells, although the majority of folate receptor are expressed on the surface of cancerous cells, the remaining folate receptors antagonized by the drug need to be 'saved' by the administration of FA at the end of treatment time-length. Hence in this case of treatment, folic/folinic acid is also known as 'rescue drug'[147].

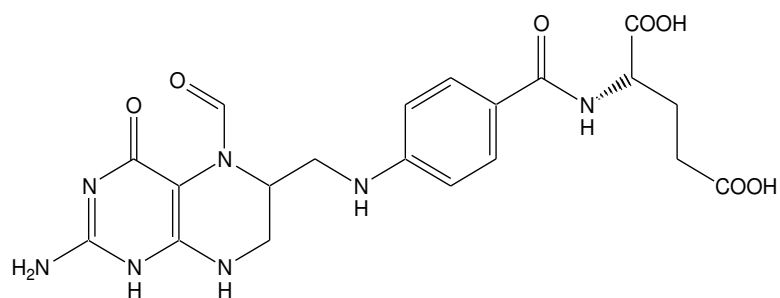


Figure 38: Molecular structure of folic acid

In addition to this application, folic acid is also used with a different mechanism of action in the treatment of colon-related cancer with 5-Fluorouracil. Folic acid is routinely administered before 5-Fluorouracil to enhance the activity of this drug. It acts through inhibition of thymidylate synthase, an enzyme which is important in DNA bio-synthesis and this inhibition will ultimately leads to DNA damage. FA has indeed been contributing and has significant involvement in cancer therapy for decades.

In the field of targeted imaging and cancer drug targeting, a number of agents are also being re-formulated with FA. Anti-cancer agents such as vinca alkaloids are conjugated with FA through chemical ligation through a disulfide cleavable linkage, producing Vintafolide (Figure 39) which is the first FA-drug conjugate that enter clinical trial as a therapeutic agent. Along with Vintafolide, an imaging agent called Etarfolatide is also in clinical trial which is a technetium (^{99m}Tc)-labelled imaging agent for FR status determination [38]. Etarfolatide consists of conjugated FA-technetium which has the ability to show functional FR, helping in determining the status of cancerous lesion around the body [148].

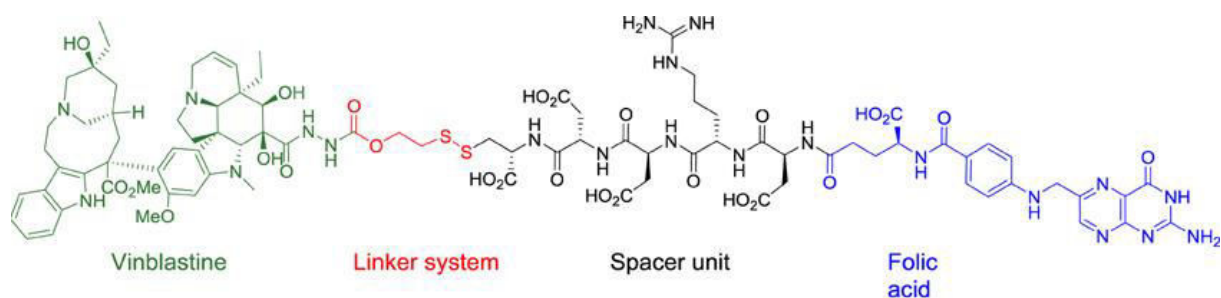


Figure 39: Molecular structure of Vintafolide

In recent years, with emerging interest in the potential of PDT in cancer therapy, researchers in chemistry-related fields turned to focus on synthesizing conjugates containing FA and photosensitizers (PS). Different types of PS were used with different approaches. This includes direct conjugation with or without spacers and also by conjugation on nano-carriers such as nanoparticles, in the presence of specific substances on the surface of the carriers to render them stealth and deliverable to the targeted cancer cells. Stallivieri *et al.* reviewed on the different publications available on the subject and they managed to assemble 29 publications until 2013 with 2 products are currently patented. Between 2013 and 2016, more publications were recorded (Figure 40) as revealed from a search done on publications indexed by Web of Science. More than half of these publications were published between 2012 and 2016, showing strong efforts are currently being carried out worldwide in producing such conjugates and it is believed that the number will increase in the coming years [109].

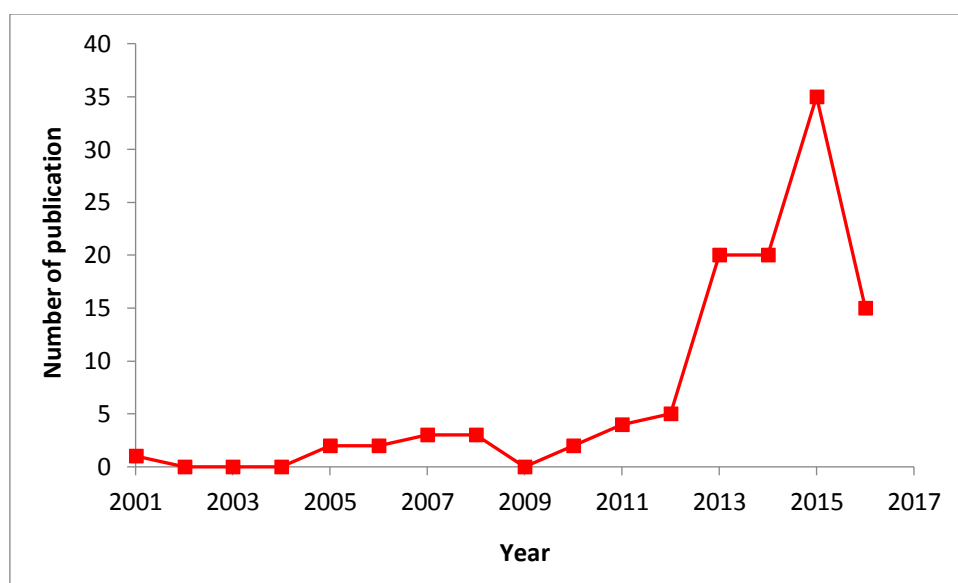


Figure 40: Number of publications (per year) on the development of FR-targeted conjugates

2.1.4 Conjugation with a Model Photosensitizer

In 2005, Schneider and the Nancy PDTeam [149] reported their attempts in producing PS-FA conjugates and the evaluation of the conjugates' photophysical properties and cytotoxicity. In their study, porphyrin (5,10,15,tri(*p*-tolyl)-20-(*p*-carboxyphenyl)porphyrin) was used as the photosensitizer. The conjugates were prepared by using hexane-1,6-diamine (conjugate 1) and a short PEG chain, 2,2'-(ethylenedioxy)-bis-ethylamine (conjugate 2) as the spacers (Figure 41), and they showed good fluorescence quantum yields.

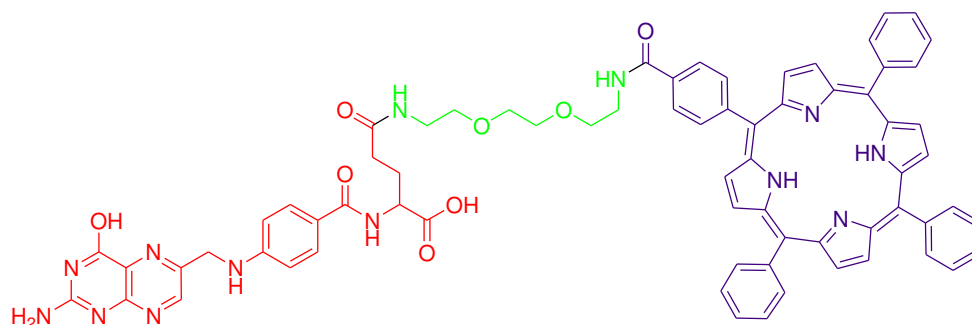


Figure 41: One of the porphyrin-FA conjugate synthesized by Schneider and Nancy PDTeam. Red: FA, Green: spacer, Purple: Porphyrin

The phototoxicity of the conjugates was tested on KB cells which indicated that conjugate 2 has a significantly improved phototoxicity as compared to the non-conjugated porphyrin (Figure 42). The selectivity of FA targeting by using this porphyrin-FA was maintained even with the presence of conjugated porphyrin and this finding offered a potentially effective treatment approach combining both targeting by FA and PDT technique [149].

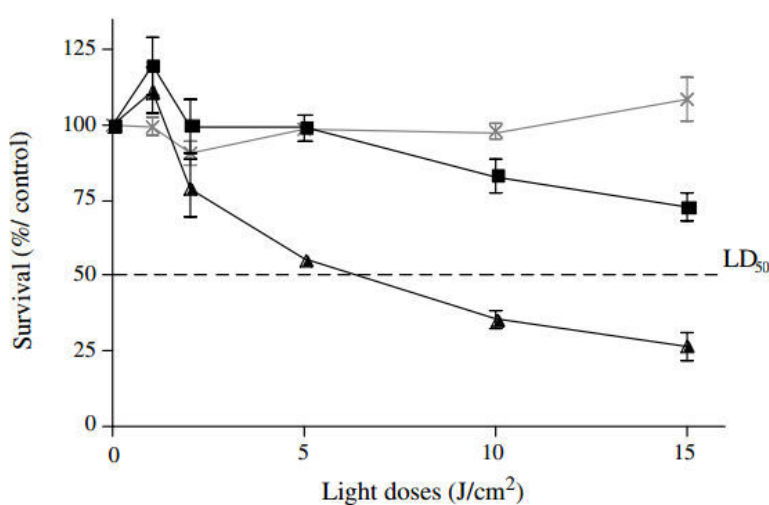


Figure 42: Survival of KB cells following phototoxicity TESTS. Grey cross: Unconjugated porphyrin, black square: Conjugate 1, black triangle: Conjugate 2. From [149]

In another study by Gravier et al. [117], they reported on the synthesis of a chlorin (*m*-THPC) linked to FA via a Boc-monoprotected 2,2'-(ethylenedioxy)-bis-ethylamine as the spacer. The conjugate showed good selectivity for cancerous versus normal cells (5:1) and enhanced uptake by targeted cancer cells by two-fold. However, the conjugate was found to be degraded in storage at cold temperature and in the absence of light. The purification of freshly prepared conjugate gave a mixture of degraded and non-degraded product and the reasons for this degradation became a question.

2.1.5 Experimental approach: Design of Experiment

Design of Experiment or DoE was first described by Sir Ronald A. Fisher in 1935. It was one of the early modern-day works on DoE and statistical analysis in science and it was explained in his book, *The Design of Experiments* [150] that these techniques are important in order to validate experimental results, interpretation of the results and to validate conclusion that is drawn from the result (Figure 43). Specifically, DoE is a useful technique that allows researchers to carry out minimal number of experiments while still having the most important information, and the relative influence and interactions of factors on the results obtained can be determined accordingly with specific analysis [151]. DoE allows researchers to organize experiments based on the most important questions to be answered while minimising cost and at the same time having control on experiment uncertainties [152].

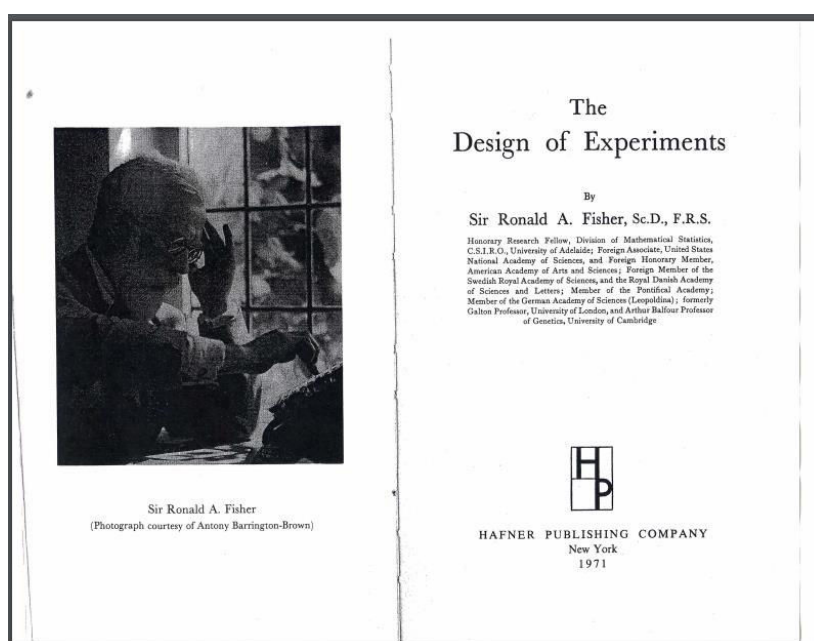


Figure 43: Fisher, the pioneer and his book on Design of experiments (ninth edition 1971, first published in 1935).

It is a type of problem solving approach that is designed to be structured, systematic and rigorous, and at the same time able to obtain valid, defensible and acceptable conclusions. It could be described in short, as a method to evaluate the relationships between different factors (input variable) and responses (output variable) [153].

In general, there are four main fields in DoE applications; (1) comparative, (2) screening or characterizing, (3) predicting and (4) optimizing. DoE is being used (1) *comparatively* to evaluate the ability of a single factor change to result in a positive or negative outcome of a process or condition. The second field, (2) *screening or characterizing* is useful in determining the most important factor affecting the outcome of a process or condition. In addition, DoE also allows building of mathematical model from the experimental results, thus enabling good (3) *prediction* of outcome from a process or condition affected by the same factors investigated in the experiments. It is also possible to use the DoE technique in (4) *optimizing* the setting of process parameters and subsequently determining the importance of each factor in obtaining optimized process response [153].

Due to the fact that there are many factors that could influence the degradation of FA and PS-FA, the DoE approach is considered as an effective method to determine the importance of these factors. The experimental design that was taken enables the evaluation of the factors through a very minimal number of experiments with the capacity of obtaining reliable results. Hence, the application of DoE in this study aims to primarily screen and determine the important factors affecting the stability of FA and PS-FA to give ideas on their stability under the tested conditions.

2.1.6 Statistical analysis

The degradation state of any active pharmaceutical ingredient may be influenced by a large number of parameters that can be interlinked. Since it is difficult to understand all their possible permutations and effects on the stability of the final drug product, statistical design of experiment methods are extensively applied in chemical process design to help process engineers to understand the effects of possible multidimensional combinations and interactions of various parameters on final drug quality [117, 154, 155].

The originality of this application is to examine the case of a binary output variable (stability of a molecule). In other terms, the DoE methodology is adapted to solve a classification problem. A binary classification test is aimed at classifying the result obtained in two groups: yes/no, high/low and etc. There are two terms that have to be understood: sensitivity and specificity. The two terms are statistical measures used to assess the performance of a binary classification test. Sensitivity, also called the true positive rate, measures the proportion of positives that are correctly identified as such while specificity, also called the true negative rate, measures the proportion of negatives that are correctly identified as such.

2.2 RESULTS AND DISCUSSION

Preliminary study conducted by our PDTeam suggests that it would be possible to reduce the degradation of FA by a judicious choice of spacers and by forming conjugates of drug-FA. As a way to get initial ideas on the degradation of FA and PS-FA conjugates, a study comparing the effect of light on the degradation of the molecules was conducted.

Figure 44 shows the percentage of photo-degradation of free FA and two different PS-FA conjugates as a function of time. The degradation values were determined by using analytical RP-HPLC. The photodegradation was induced by using a visible light (or UV-A) at 365 nm (5 mW/cm²) in DMSO as solvent. From the graph, it clearly show that free FA is rapidly degraded upon irradiation while the two conjugates are more stable, especially PS-FA which remains relatively unchanged after 2 hours.

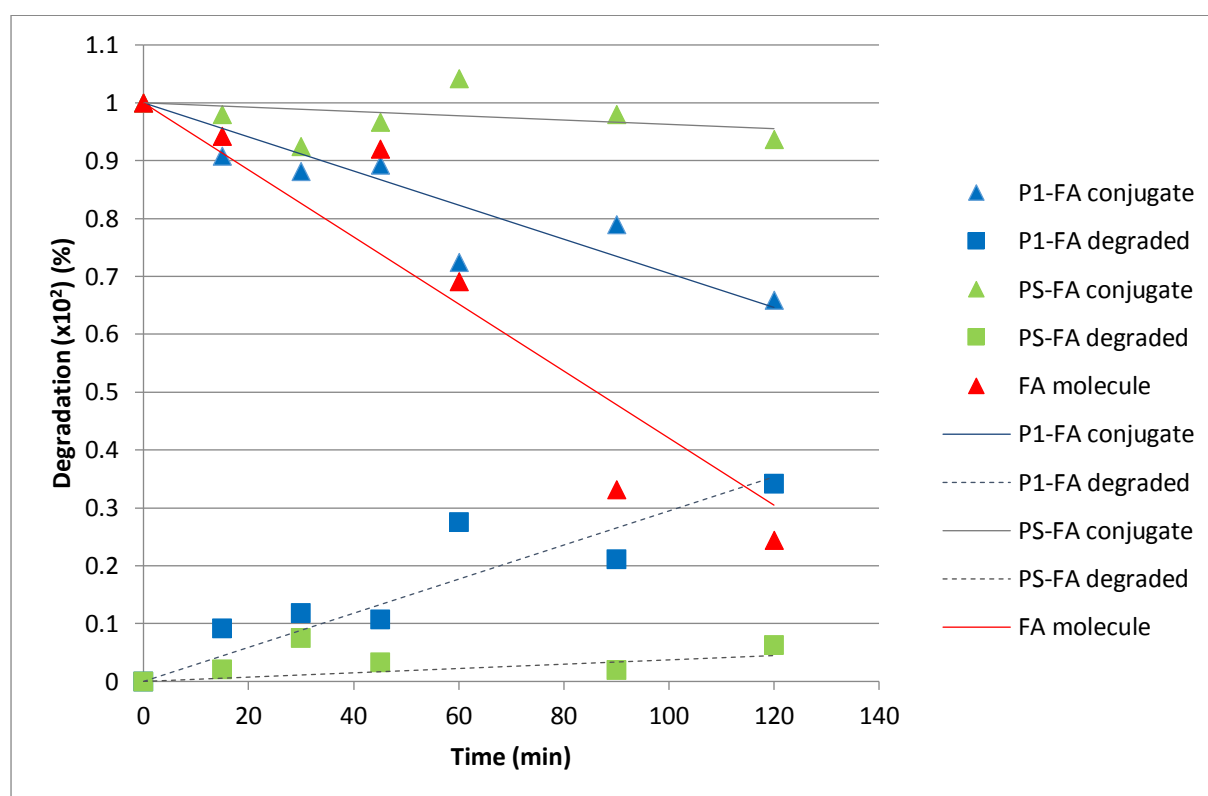


Figure 44: Photodegradation induced by light at 365 nm of FA (red) and two different PS-FA conjugates (P1-FA (blue) and PS-FA (green)), as a function of time.

This interesting finding of PS-FA stability is of interest to us and currently a patent filing for this product is underway. More recently, we described the assessment of PS-FA specificity for peritoneal metastasis of epithelial ovarian cancer for the application of intraperitoneal photodynamic therapy [156-158]. In our ongoing research, we observed the degradation or chemical modifications of our conjugates (the degradation was actually of FA into pterin and PABA).

In the binding of FA on its receptor, It is known that the glutamic acid (Glu) moiety of FA is exposed to the external environment of the receptor, while the pterin moiety is responsible for binding to the receptor pocket. This means that the integrity of the FA structure as a whole is very important, especially for its function as a targeting agent to ensure that the drug chemically linked to the Glu moiety of FA is delivered to the targeted receptor, which will then interact with the pterin moiety. As far as we know, there is only one publication (Tend *et al.* 2013) [159] in which the authors relate the potential photolytic transformation of FA..

Due to confidentiality and patenting works that are underway, the nature of the PS will not be disclosed in this thesis. Nevertheless, the type of PS conjugated is not of a concern yet due to the fact that the point of the study is to evaluate the effect of conjugation on FA stability. Hence, for the purpose of reporting in this thesis, the conjugate will be called PS-FA: *photosensitizer-folic acid*.

The experimental conditions for the evaluation of FA and PS-FA stability were hence developed with the aid of Design of Experiment (DoE). By consulting Pr. Dr Thierry BASTOGNE (CRAN, UMR 7039, CNRS, Université de Lorraine), a computer-aided design of experiments based on 26 different conditions was proposed and implemented. This is in comparison to the 768 conditions if a complete set of evaluations was to be done. The 26 experiments were conducted in triplicates. 14 were on the evaluation of FA stability whilst 12 were on PS-FA stability.

2.2.1 The solubilisation of FA and PS-FA

Solubilising FA was proven to be a challenge especially at lower pH medium. This is in accordance to available literature which describes similar occurrence. As an example, Younis *et al.* reported the solubility study of FA in different pH buffer media at 37°C [160]. They described that the solubility of FA is very minimum at acidic pH (1 mg/L at pH 3) and increases as the pH increases (18 mg/L at pH 10). It is hence understood that the difficulties in solubilising FA at low pH media could be expected and due to this problem, perhaps the stability study of FA in such medium (pH 4) was compromised.

PS-FA has a different solubility profile as compared to FA alone. Due to the presence of a PS, it was already projected that the conjugate could only be solubilised in DMSO and at a lower concentration as compared to FA. Its solubility in methanol and the tested buffer medium is also very poor. After conducting a solubility study with the conjugate, it was decided that the conjugate will be solubilised first in DMSO to help its dissolution and subsequently the respected medium will be added. Figure 45 described the steps taken in solubilising PS-FA conjugate.

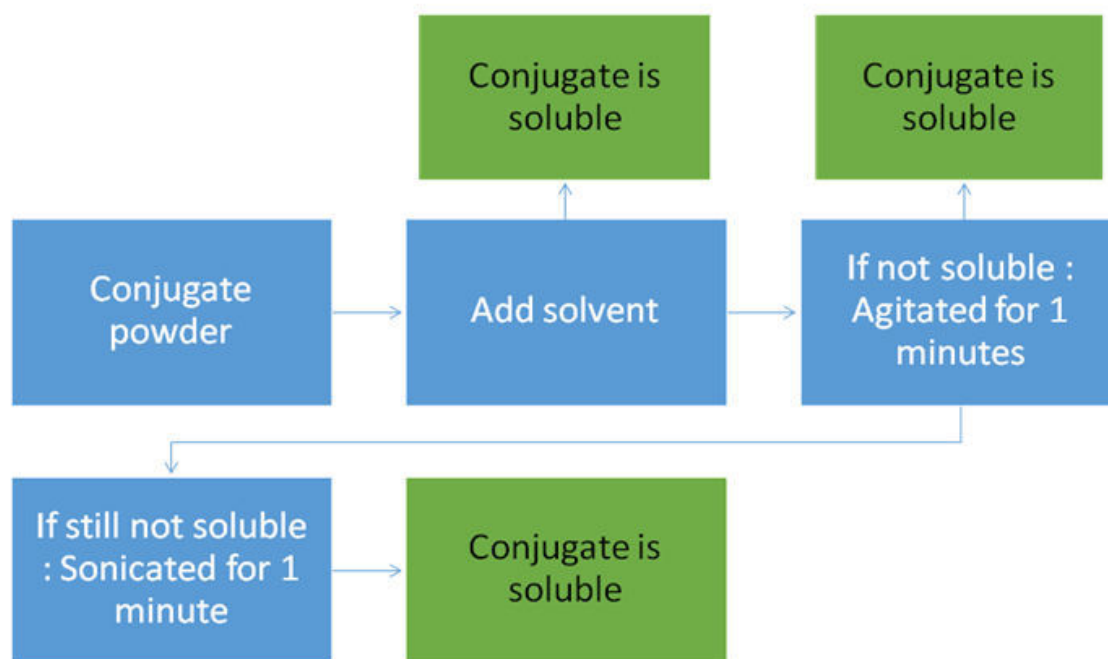


Figure 45: Steps in solubilising PS-FA. The conjugate is usually solubilised after agitation. Sonication was seldom needed

Hence, after considering the factors mentioned above, the solutions of FA and PS-FA in the respected solvents were made as summarized in Table 4.

Table 4: Solvents used and their amount for solubilizing FA and PS-S-FA in this study

Substance	Tested media	Amount of compound (mg)	Percentage (DMSO : Tested media)	Final concentration (mg/5mL)
FA	DMSO	1	100%	1.00
FA	Methanol	1	10% : 90%	1.00
FA	Buffer pH 4	1	25% : 75%	0.25
FA	Buffer pH 7	1	100%	1.00
FA	Buffer pH 10	1	100%	1.00
PS-S-FA	DMSO	0.5	100%	0.50
PS-S-FA	Methanol	0.5	25% : 75%	0.50
PS-S-FA	Buffer pH 4	0.5	25% : 75%	0.50
PS-S-FA	Buffer pH 7	0.5	25% : 75%	0.50
PS-S-FA	Buffer pH 10	0.5	25% : 75%	0.50

2.2.2 The evaluation of Folic acid stability

Different techniques including UV/Visible spectrophotometer and HPLC with UV/visible and/or fluorescence detector were reported in the literature as useful in detecting FA and its degradation products. With the aim of obtaining the most reliable results from the experiments conducted, it was decided that HPLC analysis would be the most suitable technique with both UV/visible and fluorescence detection.

A method reported by Araujo *et al.* (2012) was chosen as a reference [161] and as outlined in Table 5 it is being adapted accordingly. Based on this method, a mixture of methanol and water was used as the eluting solvent, and formic acid was added at a concentration of 0.1%. The addition of formic acid is beneficial in improving the resolution of peak during elution.

Although technically trifluoroacetic acid or TFA is more efficient for this purpose, TFA is a much stronger acid and is more destructive as compared to formic acid. Our research team has also discovered preliminarily that TFA could cause degradation of FA or complexes containing FA in the HPLC chain during analysis.

Table 5: Details on the RP-HPLC method used for FA analysis in comparison with the reference method

	Method by Araujo <i>et al.</i> (2012)			Method used for FA analysis		
Column	Agilent-XDB 5 Phenyl (250 × 4.6 mm)			Agilent-Pursuit 5 C18 (150 × 4.6 mm)		
Solvent	Water/Methanol/0.5% Acetic acid			Water/Methanol/0.1% Formic acid		
Gradient	Time (min)	Water (% conc.)	Methanol (% conc.)	Time (min)	Water (% conc.)	Methanol (% conc.)
	0	100	0	0	99	1
	10	100	0	45	40	60
	56	40	60	46	40	60
	60	40	60	50	99	1
	61	100	0			
	70	100	0			
Flow rate	1 ml/min					
Detector	UV/Visible and mass spectra			UV/Visible and fluorescence		
Detection wavelength	UV/Visible (nm)	<i>not specified</i>		UV/Visible (nm)	255, 270, 280	
				Fluorescence (nm)	λ_{EX} : 280, λ_{EM} : 450	

The three degradation products of FA, 6-formyl pterin (FPT), pterin-6-carboxylic acid (PCA) and *p*-aminobenzoyl-L-glutamic acid (PGA) were found to be eluted at the same time during RP-HPLC analysis (Figure 46). This became a hindrance to separate them in order to evaluate the amount of each degradation product separately.

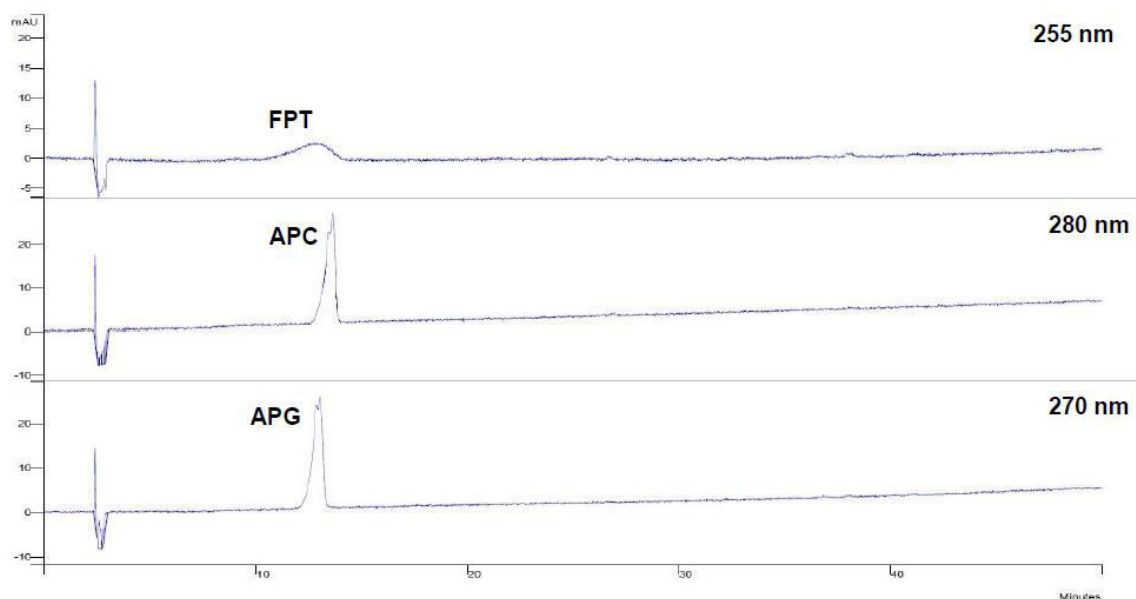


Figure 46: Elution of the three degradation products of FA under UV/visible absorbance

The peak of FA was found to be well separated at 28 minutes. The diminution of this peak was hence taken as a reference to evaluate the amount of FA degraded at the end of each experiment (Figure 47).

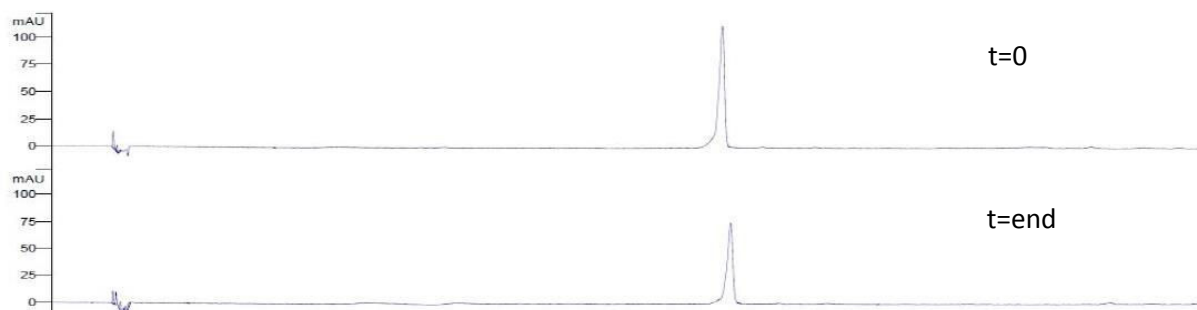


Figure 47: Diminution of FA concentration after light irradiation detected by fluorescence

Due to the inability to quantify the degradation product accurately, it was decided that the analysis of FA degradation will be a semi-quantitative analysis. The amount of degraded FA is determined relative to the initial amount of FA available in the solution. In order to achieve this, a fresh solution of FA at the same concentration as the experimental solutions (4.5×10^{-4} M) was prepared every day to serve as a reference for the initial concentration. Based on this reference concentration, the amount of degraded FA was calculated in percentage.

$$\% \text{ FA degradation} = \frac{\text{Area of peak (HPLC)} - \text{Area of peak (sample)}}{\text{Area of peak (HPLC)} - \text{Area of peak (FA reference)}} \times 100$$

The detail data on FA degradation from the experiments conducted are presented in [Appendix 1](#). Table 6 shows the results obtained on the analysis of FA stability.

Table 6: Degradation of FA for all experiments

Exp.	Condition					Percent degradation, % (± SD)
	Light	Oxygen	Temp	Medium	Time	
A	No	No	RT	DMSO	1 hr	11 (±13.0)
D	Yes	Yes	40°C	DMSO	15 min	29 (± 13.3)
E	Yes	No	RT	MeOH	15 min	14 (± 6.1)
F	No	Yes	4°C	MeOH	24 hr	27 (±14.4)
I	No	Yes	RT	Buffer pH 4	24 hr	60 (± 20.4)
K	No	Yes	4°C	Buffer pH 4	1 hr	68 (± 16.1)
L	No	No	-20°C	Buffer pH 4	1 hr	22 (± 38.9)
N	Yes	No	RT	Buffer pH 7	24 hr	99 (± 0.4)
O	No	Yes	RT	Buffer pH 7	1 week	16 (± 16.7)
Q	No	Yes	-20°C	Buffer pH 7	15 min	28 (± 6.8)
U	No	No	-20°C	Buffer pH 10	1 week	0 (± 14.1)
V	Yes	Yes	40°C	Buffer pH 10	24 hr	30 (± 14.7)
X	No	No	4°C	Powder	15 min	25 (± 7.9)
Z	No	No	40°C	Powder	1 week	13 (± 3.9)

Among the 14 experiments conducted, Experiment N gave the highest degradation of FA. In buffer pH 7 in the absence of oxygen, light alone could cause nearly 100% degradation of FA after only 24 hours at room temperature, which is in accordance to a study reported by Liang *et al.* These authors investigated the effect of sunlight exposure on FA stability at different pH values, and it was found that after only 2 hours, 85% of FA was degraded in buffer media pH 6 and 9, whilst 63% was degraded in pH 3. This means that at a higher pH, the presence of light could cause detrimental effect on FA stability [162].

Experiment E has the same condition as Experiment N in terms of light, absence of oxygen and temperature, but in methanol in comparison to buffer pH 7 for Experiment N. It showed in average 14% degradation in just 15 minutes. We could hence make a projection that in 24 hours, FA will be completely degraded. The type of medium is believed to be of importance in causing degradation for both Experiment N and E. In buffer pH 10, even in the presence of oxygen, only 30% of FA degradation was observed after 24 hours.

Experiment U gave the lowest percentage of degradation. It showed that the combination with absence of light and oxygen, very low storage temperature (-20°C) and pH 10 buffer would be the excellent conditions for long-term FA storage. Experiment Z showed that even at 40°C, only 12.6% of FA was degraded after one week, indicating much better stability could be achieved if the FA solid is stored at very low temperature in the absence of light and oxygen.

Comparing Experiment N and Experiment V would be a good indicator that FA has a better stability in pH 10 as compared to pH 7. Although the experimental condition in Experiment V is harsher as compared to N, the average percentage of degraded FA was lower. Solubilisation in pH 4 buffer media consistently showed very low stability. Experiment L as an example was having the mildest experimental condition, but 21.5% of FA was degraded in only 1 hour. This is in agreement by the results reported by other studies. As examples, Dick *et al.* reported that the stability of FA reduced in pH lowers than 5, with an observed degradation of 50%, 20% and 5-10% for pH 1, 2 and 3-4 respectively [163]. O'Broin and co-workers also reported on the half-life of FA stability in different buffer system: they found that at pH higher than 5, FA shows a half-life of more than 700 hours, whilst at pH lower than 4, the half-life dramatically reduced to 24-64 hours [164]. The experiments denoted by letters I, K and L which corresponded to the experiments in buffer pH 4 showed the highest standard deviation among all experiment conditions. This could be due to the presence of residual insoluble small particles which has made the measurement process difficult.

2.2.3 The evaluation of PS-FA conjugate stability

The analysis of PS-FA necessitated some modification on the method used for FA analysis. This is due to different solubility profile of the conjugate as compared to FA and different detection characteristics due to the presence of a photosensitizer in the complex. Table 7 described the method used in comparison to FA analysis (Subsection 2.2.2).

Table 7: Details on the method used during the analysis of FA and PS-FA

	Method used for FA analysis			Method used for PS-FA analysis		
Column	Agilent-Pursuit 5 C18 (150 × 4.6 mm)			Agilent-Pursuit 5 C18 (150 × 4.6 mm)		
Solvent	Water/Methanol/0.1% Formic acid			Water/Methanol/0.1% Formic acid		
Gradient	Time (min)	Water (% conc.)	Methanol (% conc.)	Time (min)	Water (% conc.)	Methanol (% conc.)
	0	99	1	0	90	10
	45	40	60	25	0	100
	46	40	60	35	0	100
	50	99	1	40	90	10
Flow rate	1 mL / min					
Detector	UV/Visible and fluorescence			UV/Visible and fluorescence		
Detection wavelength	UV/Visible (nm)	255, 270, 280		UV/Visible (nm)	255, 400, 670	
	Fluorescence (nm)	λ_{EX} : 280, λ_{EM} : 450		Fluorescence (nm)	λ_{EX} : 400, λ_{EM} : 670	

Figure 48 shows the general RP-HPLC chromatogram obtained. The non-degraded PS-FA was eluted first at 30.89 minutes followed by the degraded PS-FA (31.94 minutes). The second peak was found to be of the degraded PS-FA based on mass analysis, which did not show the presence of PS-FA. The pattern of elution is also similar to the degradation of P1-FA: the degraded conjugate is eluted after P1-FA.

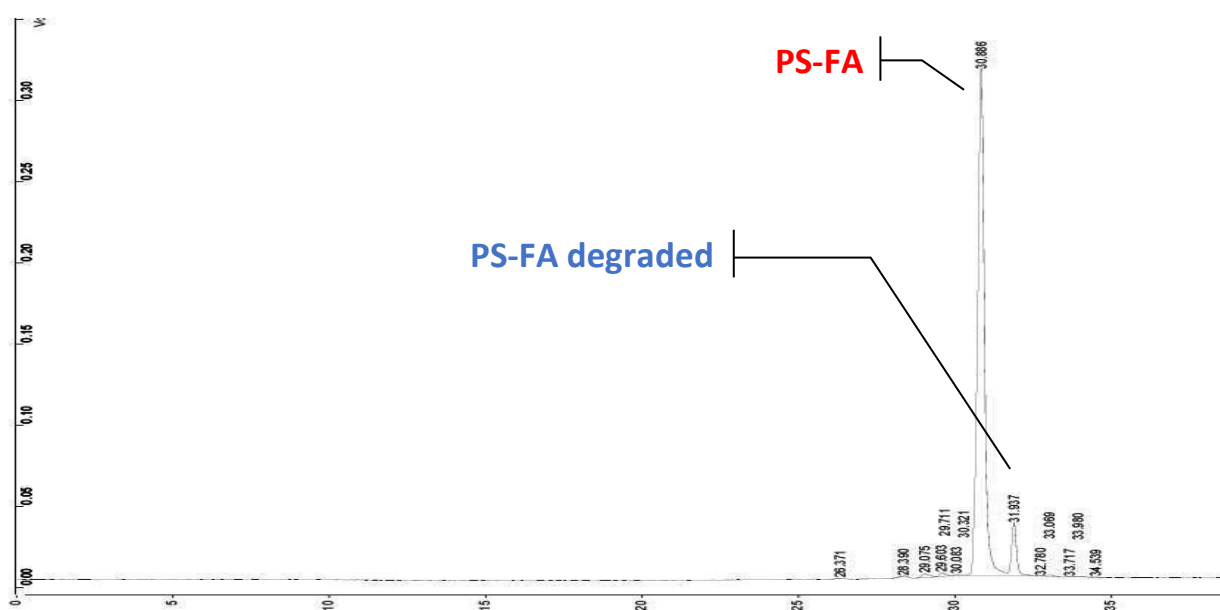


Figure 48: RP HPLC Chromatogram of PS-FA

The percentage of PS-FA degradation was calculated based on the following formula:

$$\% \text{ PS - FA degradation} = \frac{\text{Area of (PS - FA) degraded peak (HPLC)}}{\text{Area of (PS - FA) peak} + \text{Area of (PS - FA) degraded peak (HPLC)}} \times 100$$

Our preliminary studies conducted on other photosensitizer-FA conjugates demonstrated that the pterin moiety from FA is lost from the conjugate following degradation, as illustrated in Figure 49.

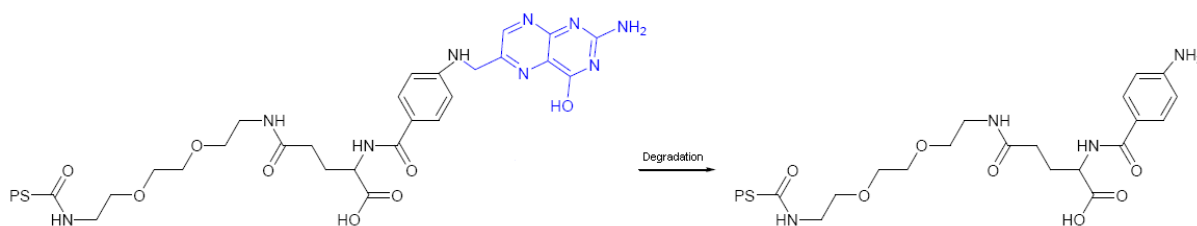


Figure 49: Degradation of fA from PS-FA conjugate. The pterin moiety was lost during the degradation

From the results obtained on the stability of PS-FA conjugate, it was found that the conjugate has better stability as compared to FA alone. In general, only between 3 to 6% degradation was observed for all the conditions except one, Experiment J (Table 8). In this condition, the PS-FA was exposed to light for one week, in pH 4 buffer solution. The nature of PS is in general light-sensitive and hence this result is not surprising. Acidic condition is also unfavourable to FA molecule and might have caused the degradation of FA. Experiment R and W which also involved light exposure showed lower degradation perhaps due to shorter exposure time.

A general comparison between the stability of FA and PS-FA shows that the FA in the conjugate has a better stability. This is an interesting point because the same phenomenon has been observed in the field of food chemistry, in which it was being reported on the stabilization of 5-methyltetrahydrofolate and tetrahydrofolate by complexation with folate-binding protein (FBP). The stability of 5-methyltetrahydrofolate was increased more than 1000-times in phosphate buffered solution pH 7 at 4°C, and no significant degradation of bound folate after more than 400 days. The authors of the publication also proposed that binding folate to other molecules could also increase its stability [143].

Table 8: Degradation of PS-FA for all experiments

Exp.	Condition					Percent degradation, % (± SD)
	Light	Oxygen	Temp	Medium	Time	
B	No	Yes	4°C	DMSO	1 week	3 (±0.8)
C	No	No	-20°C	DMSO	24 hr	4 (± 1.9)
G	No	Yes	-20°C	MeOH	1 week	4 (± 0.3)
H	No	No	40°C	MeOH	1 hr	6 (±1.9)
J	Yes	No	RT	Buffer pH 4	1 week	49 (± 3.6)
M	No	No	40°C	Buffer pH 4	15 min	4 (± 2.1)
P	No	No	4°C	Buffer pH 7	24 hr	4 (± 0.9)
R	Yes	Yes	40°C	Buffer pH 7	1 hr	4 (± 0.2)
S	No	Yes	RT	Buffer pH 10	15 min	4 (± 0.9)
T	No	No	4°C	Buffer pH 10	1 hr	4 (± 1.6)
W	Yes	Yes	RT	Powder	1 hr	4 (± 0.5)
Y	No	Yes	-20°C	Powder	24 hr	3 (± 1.4)

2.2.4 Statistical analysis

The statistical analysis was conducted with all the data from both FA and PS-FA degradation. The measured response variable, Y corresponded to the degradation level of the tested molecule: Y=0 for conditions that indicate low degradation (< 45% degradation) and Y=1 for conditions that indicate high degradation (>45% degradation).

In total, there are [26*3 = 78 experiments]. In addition to these experiments, 4 additional experiments were also conducted [4*3 = 12 experiments] with different experimental conditions as of the initial 78 experiments. Thus a total of 90 experimental results are available. However, due to some experimental problems occurred, one experiment was eliminated and hence, the total experiments assessed statistically are 89.

The 89 experiments were further divided into two groups; (1) model identification and (2) model validation. 56 experiments were grouped to be used in the model identification, and the remaining 33 experiments were used in model validation. The analysis protocol of the design of experiment consisted of six qualitative factors and one binary response (see Experimental section). This complete protocol was designed with Nemrod software [154], which is based on computer-aided design finally reduced to get the minimal number of experiments such that the variance inflation factor is lower than two.

The statistical problem addressed in this study is a classification problem and it was decided that a classification tree model will be beneficial to describe the collected experimental data. This modeling technique can be very sensitive to the different number of modalities between the six studied factors. However, it is important to remember that such classification tree is a black-box representation and not a mechanistic model. Its goal is to classify but not to explain. To overcome that potential lack of robustness, modalities of factors *Time*, *Temperature* and *Medium* have been further transformed into only two-level variables, as indicated in Figure 50.

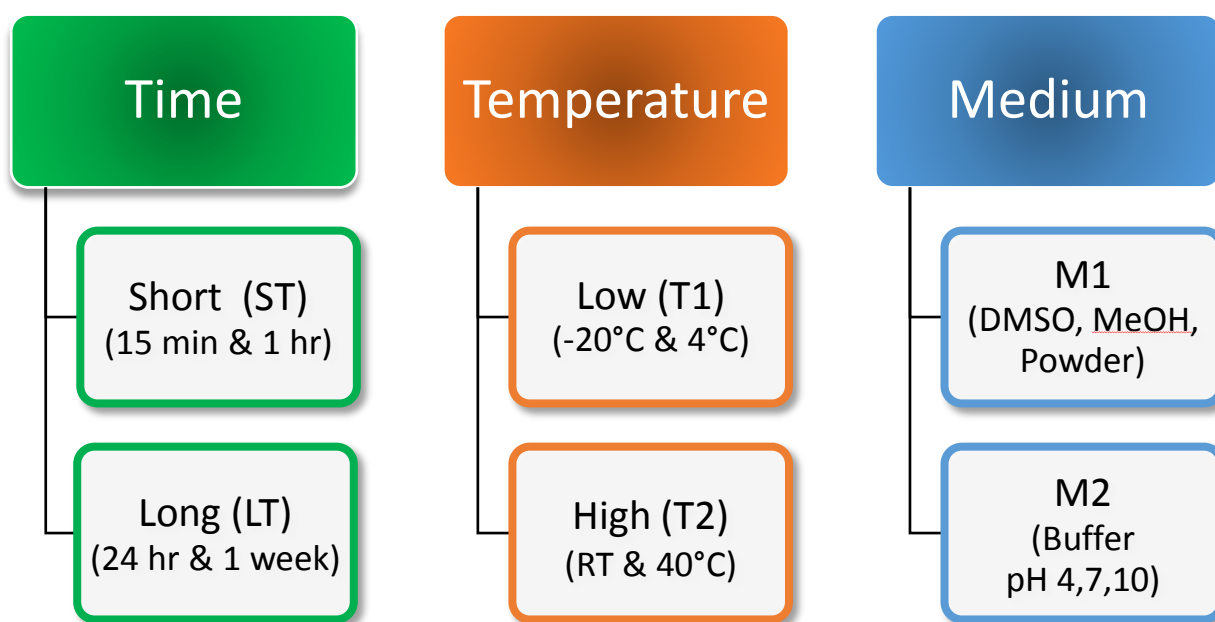


Figure 50: Definition of the new modalities for the factors time, temperature and medium.

Figure 51 shows a classification tree built from the data collected during the 56 first experiments (model identification). Statistical analysis conducted on this set of data has chosen four factors as the most discriminating for the classification: light, oxygen, temperature and molecule.

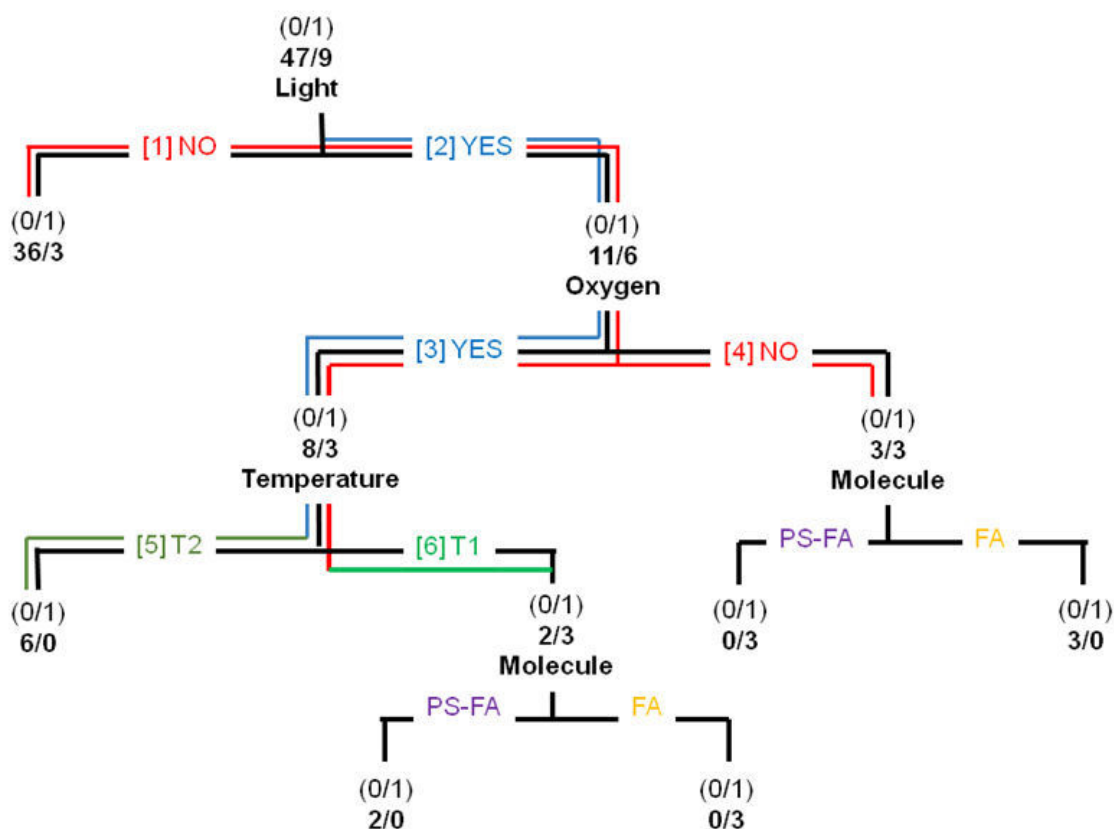


Figure 51: Binary classification tree

From the 56 experiments, light was found to be the first most discriminating factor and it is shown that the absence of light mainly explains the non-degradation. In the absence of light (branch 1), 36 experiments showed no degradation and only three showed degradation. A small number of experiments remained: 17 (from 56). These 17 experiments will be further discriminated based on subsequent factors. However, due to the small number of experiments left (17/56), the effect of the other three subsequent factors could not be surely interpreted.

From the 17 experiments left, 11 showed no degradation, and by taking the oxygen factors into account, the presence of oxygen (Branch 3) caused degradation in three cases, whilst eight showed no degradation. At high temperature (T2), six showed no degradation (branch 4). At lower temperature (branch 5), three showed degradation and two showed no degradation. The two experiments correspond to experiments involving PS-FA molecule and the remaining three involved FA. In branch 6, the absence of oxygen showed degradation in three experiments and non-degradation in another three. The degradation was shown by PS-FA and the non-degradation by experiments involving FA.

From the binary classification, it can be understood that in the presence of light alone, PS-FA could show degradation, but not FA. Degradation of FA could happen in the presence of light and oxygen, and perhaps with the influence of storage medium, although media is not being considered in the binary tree. Such classification is useful in providing information to predict the behavior of the molecules in certain environmental conditions.

Table 9 presents the confusion matrix used to assess the classification performance of the previous model. This matrix was built from the 33 experiments grouped in the model validation set.

Table 9: Confusion matrix computed with the validation data set

		MEASUREMENT	
		Non-degraded	Degraded
PREDICTION	Non-degraded	27	6
	Degraded	0	0

From the 33 experiments, 27 showed non-degradation, as predicted by the model developed based on the first part of the statistical analysis (model identification). However, there are 6 experiments that showed degradation but are not predicted by the model. From Table 9, it is clear that the prediction model developed is very specific but not sensitive. In other terms, it predicts very well the non-degradation of the drug but not its degradation.

As mentioned earlier, a classification tree such as the Binary classification tree is a black-box representation with a goal to predict classification but not to explain. Moreover it has been identified from a relatively small number of experiments. To improve its sensitivity, new study factors should be integrated and to confirm the effect of the four discriminating factors, additional trials could be carried out.

2.3 CONCLUSION AND FUTURE PERSPECTIVE

This study allows us to define the parameters that influence the stability of FA and a model of photosensitizer-FA conjugate under several environmental conditions. In general, FA as single molecule showed lower stability than the conjugate of PS-FA. This is indeed a good point because it is now known that a PS-FA conjugate has the needed stability to be used as therapeutics in PDT application.

The results obtained may be further improved statistically by conducting a deeper study with more inclusion factors such as longer storage time and also in other media as well. There may be also an advantage to conduct another stability study of the PS-FA conjugate *in vivo*, to see the half life of this conjugate and to assess whether the conjugate is stable for the duration of time needed for PDT. Currently, this PS-FA conjugate is under patenting work and is also under preliminary *in vivo* study to examine its fluorescence generating capability and PDT efficacy.

Chapter III: Modification of KDKPPR Peptide to Investigate the Effect on its Binding on NRP-1 Receptor

3.1 INTRODUCTION

This chapter describes an experimental approach taken in the evaluation of KDKPPR as an NRP-1 targeting peptide. It relates to an experimental work-up conducted on a technique called “Alanine-scanning” (Ala-scan). In order to achieve several objectives regarding the stability and structure-activity relationship of a peptide, the Ala-scan approach was performed to define the importance of each amino acid in the sequence of KDKPPR for its binding on NRP-1. The peptide KDKPPR was modified through replacements with alanine on each amino acid and the affinity of each peptide was evaluated through ELISA assays. Subsequently, this chapter also describes the receptor affinity of a *retro* peptide (RPPKDK) and a *retro-inverso* peptide (rppkdk) prepared based on KDKPPR. Another peptide KDRPPR with an arginine-substituted lysine was also evaluated.

3.1.1 Peptides

The number of naturally-occurring peptides identified to date is huge; more than 7000 were already identified and they play important roles in different body mechanisms. They act as neurotransmitters, growth factors and hormones, as ligands in modulating cell function and as anti-infective, to name a few. Given their active *in vivo* function, peptides now serve as a very interesting starting point in the design of novel therapeutics and due to their specificity, they have shown good safety profile and excellent efficacy and tolerability in human [165].

There are 20 well-known amino acids that form the life in human. These amino acids are different in terms of their molecular sizes, side chain functionalities, charges and polarities which contribute significantly to their biological action [166]. The combinations of these different amino acids form different peptide molecules with specific functions. Through the formation of peptide bonds, vast diversified peptides and proteins are formed. Peptide bond is constructed through dehydration process in which a water molecule is released during the reaction and an amidic liaison between two amino acids is established (Figure 52).

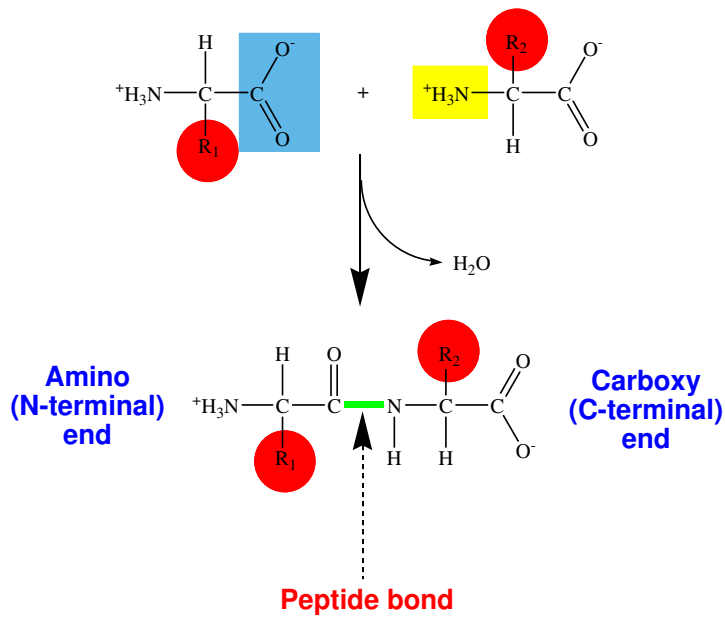


Figure 52: The formation of peptide bond [167]

As mentioned before, these amino acids have different molecular sizes with different acidic-basic properties and different charges on the molecule. Among all the amino acids, Alanine (A, Ala) is the simplest and smallest chiral amino acid, whilst Glycine (G, Gly) is the smallest in terms of molecular size.

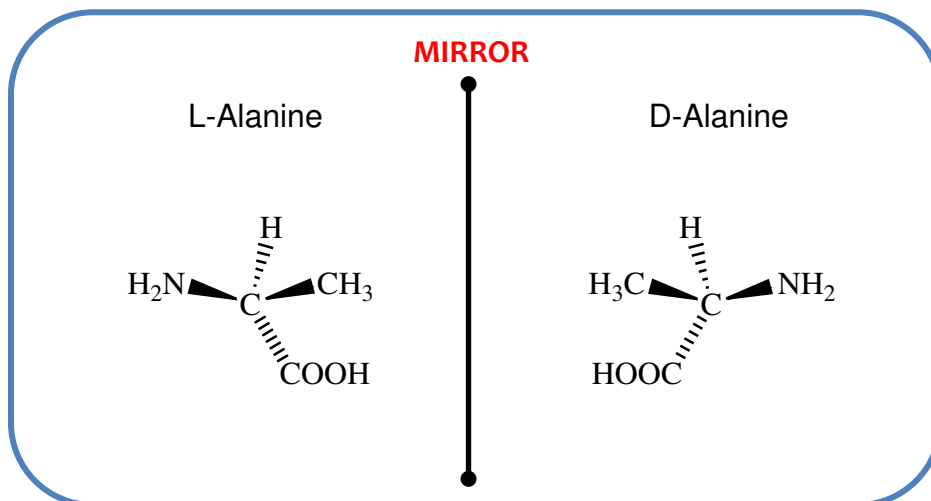


Figure 53: L- and D-amino acids alanine

There are two different configurations of amino acids that could be found naturally: L or *S*- and D or *R*- configurations, which are essentially the mirror image of each other (Figure 53). Proteins and most peptides that could be acquired naturally are in the form of L-configurations, whilst D- configurations peptides and proteins are found in some animals such as in spiders' venom, neuropeptides from snails and some hormones from crustaceans [168, 169]. The D-amino acids are formed in cells following post-translational alterations of the L-

amino acids. All amino acids that have a chiral carbon will have these two different configurations, and this means all except glycine. The α -carbon of amino acid serves as the chiral centre (Figure 53).

3.1.2 Peptides and Solid-phase peptide synthesis

Peptides are small proteins but with no tertiary, three-dimensional structures as is the characteristic of proteins. Medium size peptides could have secondary structures. The utilization of peptide-based therapeutic agents is gaining much attention in many different fields of pharmaceuticals, owing to the improvement in its production techniques, the ability to reduce its metabolic breakdown and also the feasibility of different administration routes. Although there are some problems that could be associated with peptides *in vivo*, they have more advantages as compared to proteins and antibodies. Indeed, they have less immunogenicity and higher chances for tissue penetration due to their smaller size, better stability profile and lower manufacturing cost [170]. Although some restrictions do exist, the application of peptides has nevertheless advances, with a lot of protein- or peptide-based drug products already available in the clinics. More than 60 peptide-based products are approved currently by FDA, around 140 drugs are currently in clinical trials and more than 500 peptide molecules are in pre-clinical stage [165].

The introduction of modern peptide synthesis technique in the last few decades has contributed to the increasing application of peptides in therapeutics. Solid-phase peptide synthesis (SPPS) is a significant breakthrough and more researchers have opted for this technique due to its ease of usage, feasible and reliable production of peptide. During the initial years, solid phase protocol was only devoted to peptide synthesis. The organic chemists considered this method as not very reliable because the intermediaries were neither isolated, nor characterised. The biologists and pharmacologists, who were in great need of numerous new molecules for the design of new drugs, encouraged the chemists to reconsider their position. In fact, the implementation of robotic high-throughput screening which enables the testing of thousands of compounds per day was the reason why there is a high demand of fast compounds production. Methods which promise shorter time or lower production cost were then eagerly taken up. This is clearly the case with combinatorial chemistry and multiple parallel syntheses technique such as the solid-phase synthesis which is well suited to perform reactions in parallel, because it readily enables the automated performance of multistep synthetic sequences. Solid phase synthesis technique has enabled the synthesis of up to 50 amino acid-length peptides and the synthesis is usually conducted in an opposite direction (*C*- to *N*-terminus) than the native peptide synthesis in cells (Figure 54) [166].

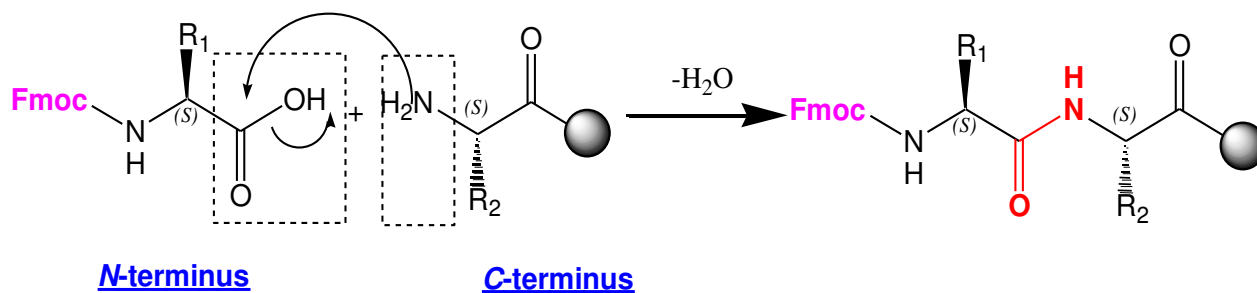


Figure 54: The synthesis of peptide in solid support is from C-terminus to N-Terminus

Solid phase peptide synthesis or SPPS technique was first introduced by Robert Bruce Merrifield in 1963 [171] using Boc strategy, whereby he reported a new peptide synthesis technique by adding in stepwise manner a sequence of amino acids to a solid polymeric particle and removing the final synthesized peptide from the polymeric support. He used cross-linked polystyrene beads as the support resin and had successfully obtained the expected peptide (LLGV peptide) in relatively pure form. One year later, Merrifield synthesized, on solid support, the nonapeptide bradykinin (RPPGFSPFR) in 8 days with 68% yield [172, 173]. Later on, his team continued to synthesize longer peptides (ribonuclease [174], insulin [175] and others) by the same technique.

Among the important milestones of the SPPS include the introduction of hydrogen fluoride-cleavage in 1967 [176], the butylated hydroxyanisole, BHA-resins for peptide amides synthesis [177], the introduction of Fmoc-protecting group in 1970 [178], Wang-resin in 1973 [179], the concept of orthogonal protection schemes [180] and the introduction of resins for the synthesis of fully protected peptide fragments [181-185].

The utilization of solid support has enabled the automation of this technique. The automated peptide synthesizer was first developed in 1968, five years after the introduction of solid phase synthesis method. This has render peptide synthesis to be more facile and efficient. With the advancement of technology, many different types of synthesizers were developed. Generally, there are three types of automated synthesizer, (1) parallel synthesizer, (2) batch synthesizer and (3) continuous flow synthesizer.

The (1) parallel synthesizer enables simultaneous synthesis of different peptides in small scales, which is useful in structure-activity relationship studies. Bigger quantities of a single peptide could also be produced by preparing parallel synthesis of the same peptide. (2) Batch synthesizer allows the synthesis of peptides at bigger scale, up to kilograms in one synthesis. However, such machine could only produce one or two peptides of different sequences at one time. It could also have a mechanical agitation to ensure mixing. (3) Continuous flow synthesizer uses pump to circulate the reaction solution through the column containing resin beads. This machine commonly possess a monitoring mechanism to

ensure that each process is completed before proceeding to next steps [186]. In our study, we used a parallel synthesizer (ResPep XL, Intavis AG Bioanalytical Instruments, Germany).

Figure 55 illustrates the synthesis steps and cycles as is commonly conducted during a solid phase peptide synthesis process. The first step in the process which is anchoring the first amino acid is usually done commercially. There are two different types of protection groups, (1) *N*-protecting group (NPG) and (2) side-chain protecting group (SPG). The NPG in solid phase peptide synthesis is also known as “temporary” protecting group. It is usually Fmoc-group which is base-labile, allowing easy removal by piperidine during the synthesis steps.

The SPG instead is known as “permanent” protecting group because the protection will last until the end of the synthesis and will only be removed after the synthesis is completed. Hence the SPG is more acid-labile and can withstand multiple cycles of deprotection in order to ensure the side chain is always protected during synthesis. SPG could be formed by different types of protection, although is commonly by benzyl- or tert-butyl group. By having the amino acid protection in this way, it ensures the success of synthesis by having only one free amino group and one free carboxylic group at each time to form the peptide bond.

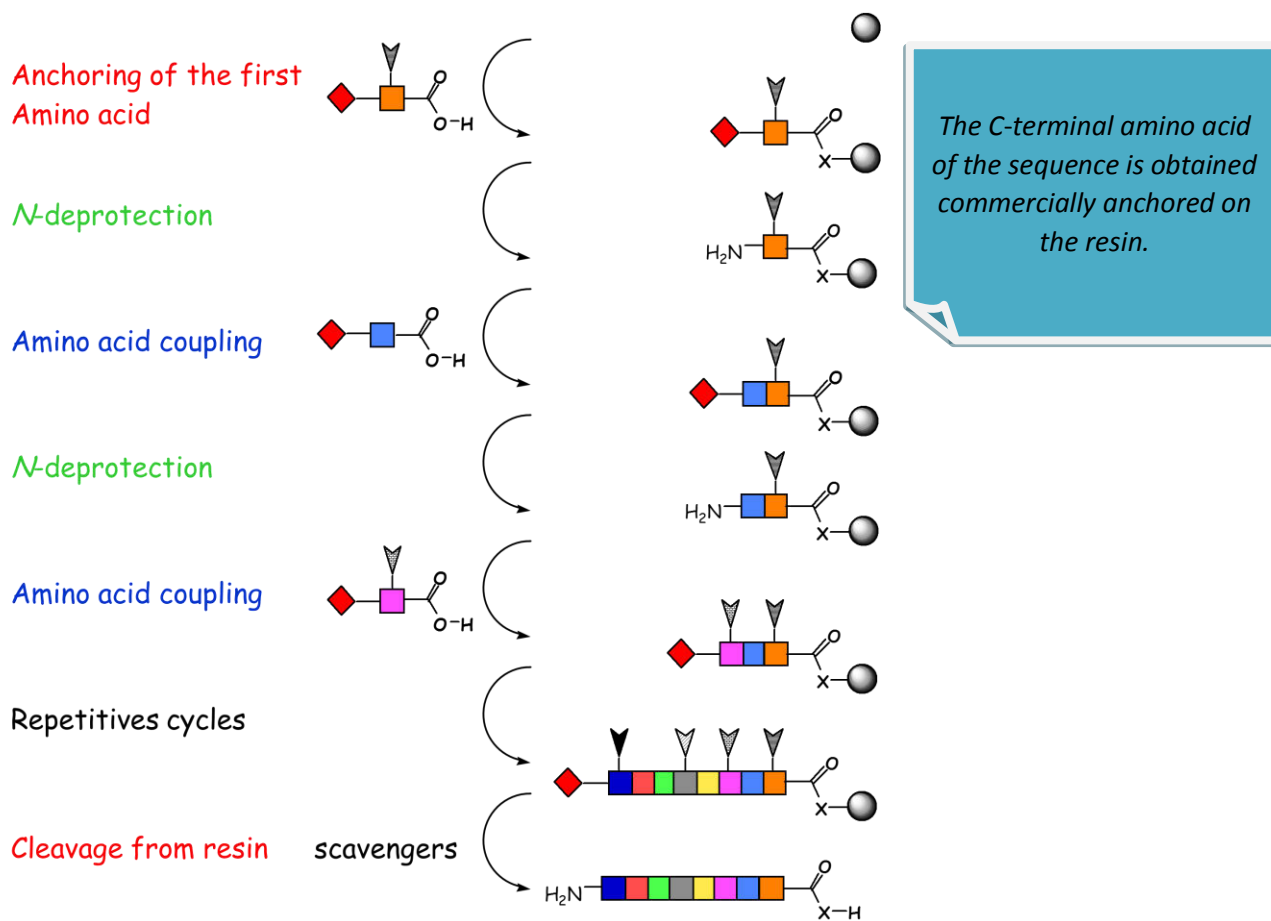


Figure 55: The steps involved in synthesis by SPPS. *N*-protecting group (NPG) is illustrated as red diamond; side-chain protecting group (SPG) is illustrated as arrows attached on the different amino acids

Generally, the SPPS technique could be divided into two steps, the *synthetic step* and the *cleavage step*, which is followed subsequently by purification of the peptide through chromatography techniques. The *synthetic step* consists of the assembly of protected amino acids in a number of reaction cycles depending on the number of amino acids to be added as described in Figure 55. Polymeric support, which is also known as resin is used as the support. Examples of commonly used resins are Wang resin (4-alkoxybenzyl alcohol resin) and 2-chlorotrityl chloride resin. Anchoring the first amino acid on the resin is already done on commercially available resin. The amino acid anchored on Wang-resin is Fmoc-protected, whilst for the amino acid anchored on 2-chlorotrityl resins does not have such protection.

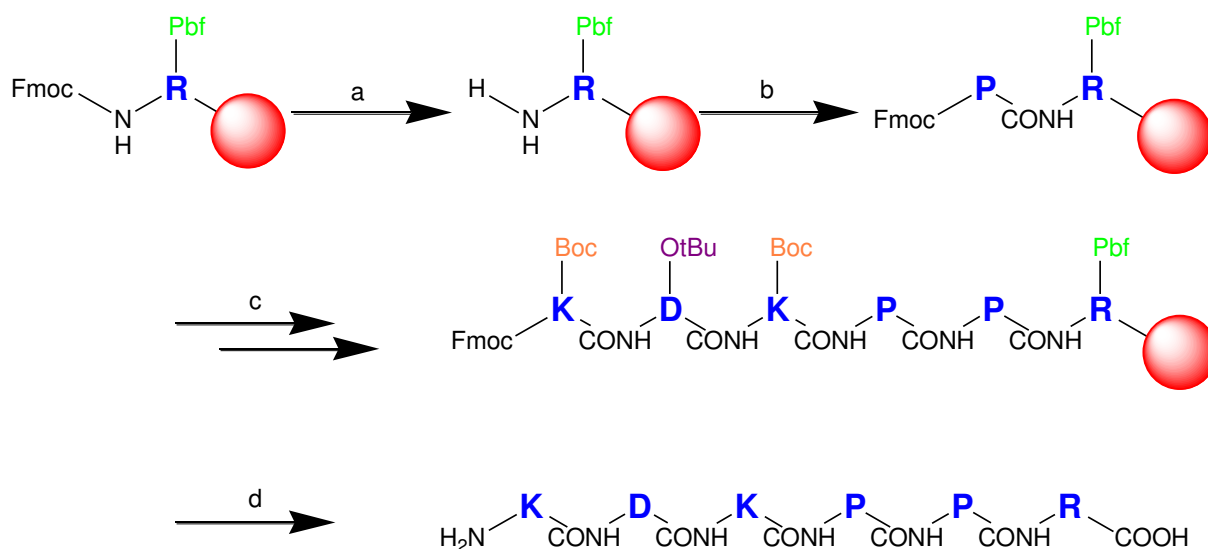


Figure 56: Solid phase synthesis of KDKPPR analogues by using Wang-resin (red circle)

Figure 56 illustrates the peptide synthesis of KDKPPR. Briefly in (a), the Fmoc-protection group of arginine anchored to Wang resin was removed by using 20% piperidine in DMF. This was followed by (b) in which the second amino acid, proline (Fmoc-Pro-OH) was coupled into the N-terminus of arginine in the presence of HBTU and NMM, in DMF. This was then followed by capping, in which the unreacted arginine (if any) was capped by acetic anhydride to block further reaction. This cycle was then repeated in (c), until all amino acid were coupled. Step (d) corresponds to the cleavage step. In this step, TFA is added into the reactor containing peptide attached to the resin, alongside triisopropylsilane (TIPS) and water at the ratio of 95(TFA): 2.5(TIPS):2.5(Water). TIPS and water are “scavengers”, able to quench the cationic or radical species produced during cleavage by TFA and subsequently prevent the alkylation of the peptide side chains. At the end of this process, the full-length peptide is obtained by filtration from the resin and precipitation in cold ether. The peptide is then purified by chromatography method.

3.1.3 Peptides and drug development

Peptides are long known to have good potential for many different roles in drug development and this includes as therapeutic agent and targeting moiety. However, native peptides are usually not suitable to be used directly as therapeutics due to several limitations which includes (1) easily degraded by peptidase in the gastrointestinal tract (GIT) and in blood circulation, (2) limited transportation ability through membranes and blood-brain barrier due to high molecular weight and unavailability of specific transport systems, (3) rapidly excreted either through liver or kidney and (4) their flexible characteristic enable interactions with other receptors besides the targeted receptor and hence may cause undesired side-actions [165, 187].

Due to these limitations, their biological applications are hindered and necessitate some modifications to improve their characteristics for *in vivo* applications. Hence, recent technology has come up with several solutions and advancement in ensuring better stability and improving the capability of peptides as therapeutics [165]. Approaches such as structure restraining could help to minimize binding to non-targeted receptors and subsequently enhance their activity at the targeted receptor. The addition of more hydrophobic residues could help to improve membrane crossing and cellular transportation whilst the modifications by using isosteres, cyclization and *retro-inverso* peptides could reduce the degradation by peptidase [165, 188]. With the aim of improving peptide stability especially to enzyme degradation, several approaches were found to be useful: (1) alteration of the amide bond, (2) cyclization and conjugation to a carrier molecule, (3) incorporation of non-proteinogenic amino acids such as β -Alanine (4) backbone modifications (5) terminal protection and (6) substitution with D-amino acids [189-191].

Among these protein- or peptide-based drug products, most of them are developed for two types of health problems: (1) metabolic disorders such as diabetes and obesity and (2) oncology. Hormones such as insulin and oxytocin are being used regularly and they have been contributing to the health of people in many wonderful ways. In the field of oncology, short peptide sequence products are available in the market. Product such as Lupron® (Leuprolide acetate) is used in the treatment of prostate cancer, fibroids and endometriosis. Lupron® contained a nonapeptide analogue pGlu-His-Trp-Ser-Tyr-D-Leu-Leu-Arg-Pro-NHEt derived from natural gonadotropin-releasing hormone and has been proven to be medically effective, just by looking at the sale figure that it made in 2013 alone: 1.73 billion USD worldwide. This indeed shows that such peptide-based product does have a big function and huge potential as therapeutics [165, 192].

Conjugation of peptides with molecules can enhance safety and efficacy profiles of therapeutics or theranostic agents. As an example, a neurotensin-1 (NRT-1) receptor peptide agonist was coupled to a radioactive ligand in order to improve the delivery of this ligand towards the targeted pancreatic cancer cells. This leads to the improvement of its therapeutic window with potentially higher and efficacious dosing of the radioactive ligand. This kind of approach is extensively under study especially in the field of oncology, with more than 20 peptide conjugates currently under clinical studies [165, 193].

3.1.4 KDKPPR peptide

As described in Chapter I, the discovery of KDKPPR peptide sequence was made unexpectedly. The addition of lysine at the *N*-terminal of DKPPR was for the purpose of conjugating a PS on the ϵ NH₂ group available on its side chain (Figure 57).

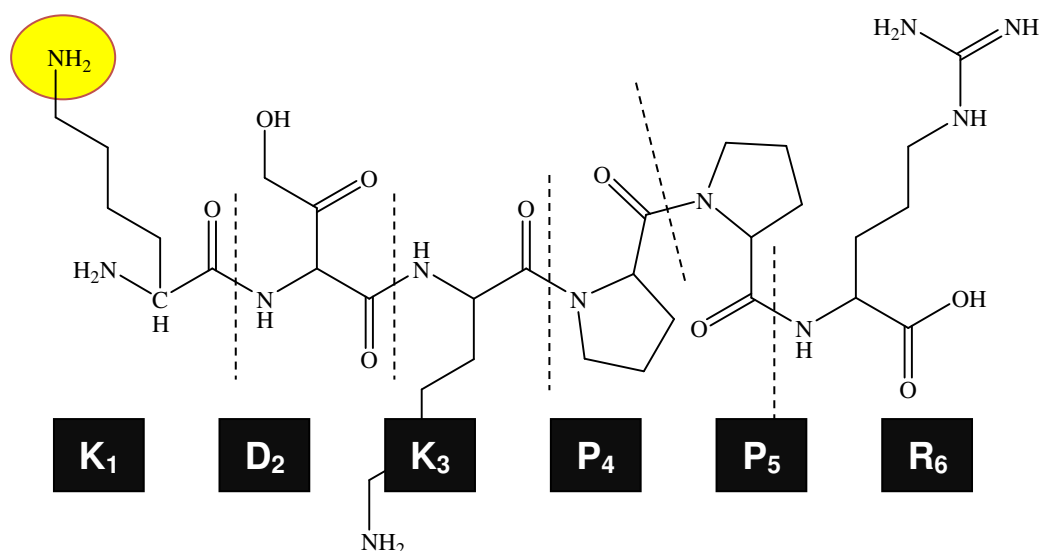


Figure 57: Molecular structure of KDKPPR. The dotted lines separate the individual amino acid

The molecular structure of KDKPPR is as illustrated in Figure 57. It is a very highly hydrophilic peptide due to the presence of four charged amino acids: two lysines (Lys, K) and one arginine (Arg, R) which are positively charged and one aspartic acid (Asp, D) which is negatively charged. The peptide is hence could easily be dissolved in water. As described in Chapter 1, KDKPPR fulfil the characteristic of *C*-end rule peptide (R/K-XX-R/K) which was found to be the strict rule followed in consensus by most peptides that have the ability to bind on NRP-1 receptor. This is in fact also the end sequence of VEGF-A₁₆₅ which is the ligand of NRP-1 receptor.

3.1.5 Peptide modifications performed in this study

A. Alanine-scanning

The utilization of peptide as therapeutic agent needs understanding of its function, or the structure-activity relationship. The role of each amino acid forming the peptides should be defined, especially their contribution on the overall stability and biological activity of the said peptides. Information regarding their contribution could help in understanding the interaction between the peptides and their receptors and hence if necessary, the design of analogues more selective for a needed mode of action could be carried out [194].

Ala-scan is a process done by sequentially and systemically substituting each amino acid in a peptide sequence with alanine (Ala, A) to evaluate the significance of each amino acid side chains in the binding or biological interaction of a peptide. By conducting Ala-scan, the amino acid responsible for the binding could be determined. Ala-scan is routinely used as a part of drug discovery process whereby the important sequence in a native peptide or protein will be determined and this sequence will be synthesized and developed as a potential drug molecule. This approach is called structure-based drug design (Figure 58) [165].

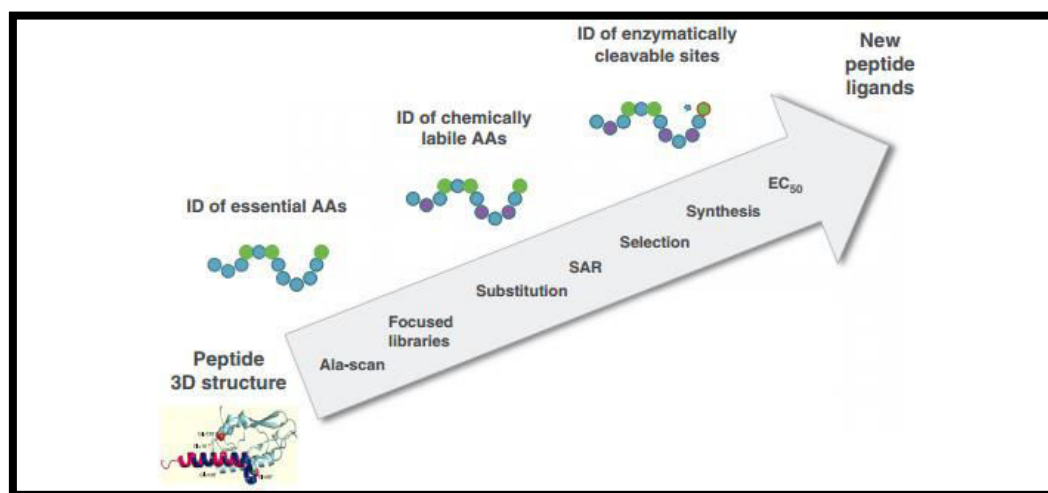


Figure 58: The process of drug discovery from a native peptide. Alanine-scanning is a part at the beginning of the process [165]

There are several reasons on why alanine is commonly being used as substitution for activity investigation and one of them is because alanine is the smallest chiral amino acid. As compared to the other amino acids, alanine is neutral and hence will not change the charge or the solubility of the peptide analogues [195]. Substitution with alanine will also preserve the configuration of the substituted amino acid and therefore the global conformation of the peptide analogues which is an important factor in the recognition by receptors [194]. In addition, since alanine side chain is extended only until β -carbon, substitution with alanine will remove the interaction of side chain beyond β -carbon without introducing new properties.

This will give a good estimation and a general idea on the importance of interaction between the amino acids in the native peptide sequence with their targeted receptor [196].

After substitution, the degree of activity of the substituted peptide would essentially be reduced as compared to the native peptide. This degree of activity reduction is taken as a relative measure to determine the importance of the amino acid being replaced. As an example, Scott *et al.* (2000) conducted an Ala-scan analysis on a peptide sequence derived from mEGF₍₃₃₋₄₂₎ which is an antagonist against the receptor laminin, a kind of basement membrane protein. They observed that the biological activity of the peptide was lost following the replacement with alanine; cell attachment, receptor binding and migratory response were significantly reduced [197].

However, there are also researchers who reported on the increase of binding affinity of the Ala-scan analogues as compared to its native peptide. As an example, Montigiani *et al.* (1996) observed an improved binding affinity of their analogues on calmodulin receptor as compared to the wild-type myosin light chain kinase (MLCK) 23-mer peptide. In addition, a 1000-fold increment of binding affinity was also observed in one case whereby an Asparagine (Asn, N) was replaced by alanine in the analogue [198].

B. Replacement of K2 lysine with arginine (KDRPPR)

Lysine (Lys, K) is a polar, positively charged amino acid. It could be substituted with other positively charge amino acids and arginine (Arg, R) in particular is usually favoured [199]. Figure 59 illustrates the molecular structures of the two amino acids. Their similarities lie on the presence of amine group in their side chain which contributes to their positive charge, and also on the size of their side chain though arginine is slightly bigger than lysine.

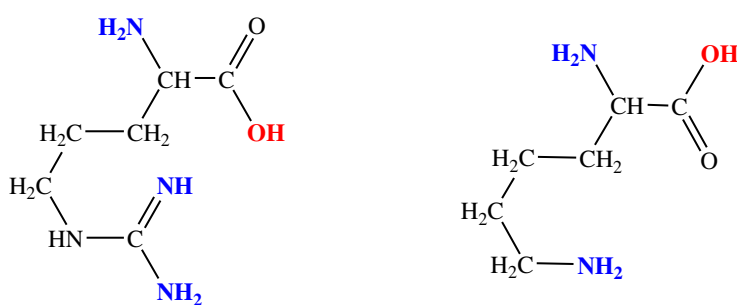


Figure 59: The structure of lysine (right) and arginine (left)

Substituting lysine by arginine in the peptide sequence could serve as a way to investigate the importance of lysine in its binding on the targeted receptor. The C-end rule as described in Chapter I also proposed that the sequence of **R/K**-XX-R/K is important in binding to the NRP-1 receptor. Hence it is also interesting to evaluate the effect of changing lysine at the third position in the peptide (KD**K**PPR) into arginine (KD**R**PPR).

Although substitution of lysine into arginine is normally favourable, the reverse could sometimes be disastrous. This is because due to the presence of multiple amine groups at arginine's side chain, it has the ability to form multiple hydrogen bonds with other amino acids in a protein for stabilization, or with an active targeting site for better interactions, which could not be imitated by lysine. Hence, in this kind of cases, the hydrogen interaction needed will be lost and subsequently the activity expected will be less or totally lost [199].

C. *Retro, inverso* and *retro-inverso* peptides

Chemical modifications of the peptide backbone allow the chance to favour certain conformations while maintaining the nature of the side chain which is often required for good recognition by the target. Thus pseudopeptides thus obtained often have a rigidified structure which sometimes induce a better affinity than the parent peptide [200]. The introduction of a pseudopeptide bond can also limit biodegradation by proteases and improve the pharmacokinetic properties [201-206]. There are many methods to modify a peptide backbone: these can involve isosteric or isoelectronic exchange units (such as peptoids, azapeptides and azatides) or the introduction of an additional fragment (such as hydrazinopeptides, β -peptides, α -aminooxy, sulfonopeptides and oligoureas). It is indeed relatively difficult to provide an exhaustive list .

One of the most common and interesting approaches in the investigation of peptide-receptor interaction is the modification of peptide backbone into a *retro*, *inverso* or *retro-inverso* peptides. These kinds of pseudopeptides have some advantages in comparison to the native peptide especially in term of stability improvement and in some cases, they have shown improved activity. Figure 60 shows an example of a *retro, inverso* (D-Peptide) and *retro-inverso* peptides as described by Guichard *et al.* (1994).

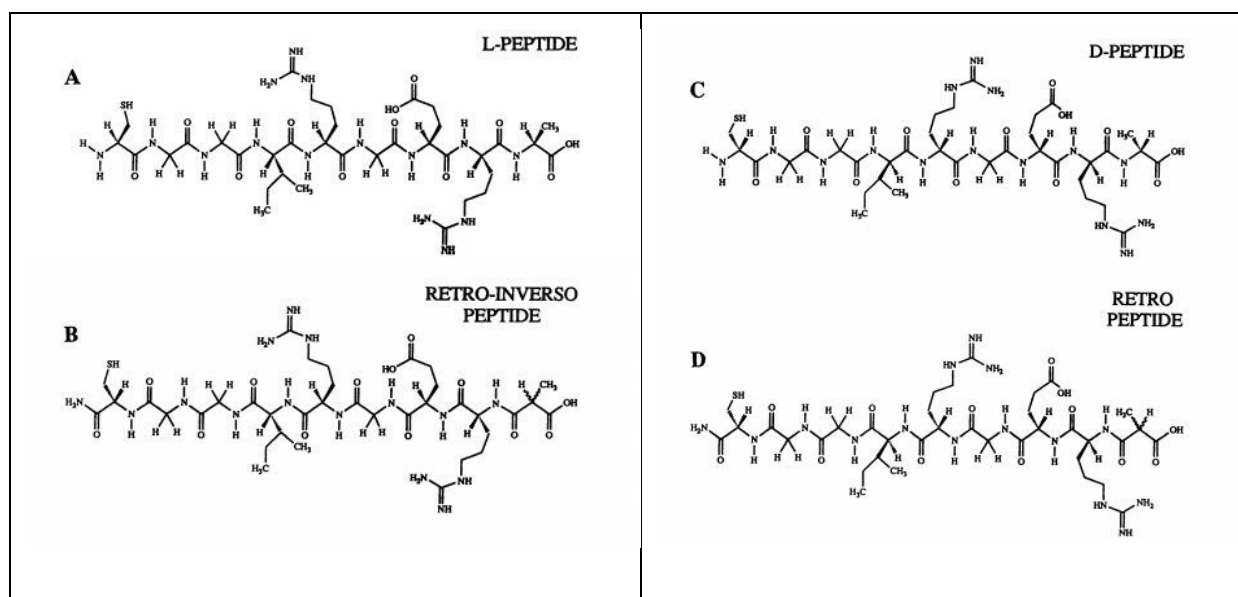


Figure 60: Example of native L-peptide (A), *retro-inverso* (B), *inverso* (C) and *retro* peptide (D). From [209]

Retro peptide is a peptide formed from L-amino acids with an inverted sequence as compared to its native sequence [210-212]. This reversal causes change in the topochemistry of the side chain, producing a non-complementary side chain in comparison to the native L-peptide. The charge structure of the peptide will also be changed due to the reversal of carboxy- and amino-terminal which may cause reduction in its biological activity [188]. Working on *retro* peptides however is interesting because it could give some ideas on the need of the peptide to form interaction with its receptor. By making the peptide in *retro* form and observing a reduced activity, it is evident that the conservation of carboxy- and amino-terminal on the right amino acid is crucial in order to preserve the activity of the peptide [213, 214, 215, 216, 217].

At the best of our knowledge there are only four *retro* peptides that exhibit good activity as described in the literature. Guichard *et al.* (1994) reported on the ability of *retro* IRGERA peptide to mimic the natural L-peptide and induce antibody recognition by IgG3 antibody in mouse. They also observed that the *retro* peptide had a slight improvement of stability against degradation by protease [209]. Another study by Nitsche *et al.* (2004) describes the ability of a *retro* tripeptide [R-Arg-Lys-Nle-NH₂] as a small molecular inhibitor on dengue virus protease enzyme and they have successfully shown that the *retro* peptide has a high inhibitory capability on the enzyme, better than its *retro-inverso* counterpart [218].

Inverso peptide is formed by substituting native L-peptide with D-peptide directly. Among the different modifications described in the literatures, this approach is a tempting and facile technique to be investigated. Peptides formed by D-amino acids have stronger peptide bond (towards peptidases) as compared to L-amino acids and hence show better stability against degrading enzymes such as proteases. It was found that peptides that are formed at least partially by D-amino acids can exhibit the same behaviour. However, direct substitution of L- into D-peptides were often found to cause loss of biological activity due to the conformational changes [214, 217] and only in few cases, *inverso* peptides can improve the biological effect [209, 215, 219].

The third type of modification, the **retro-inverso** peptide is a peptide in which the sequence of the amino acid and the chirality of the alpha-carbon are reversed and inverted. The amino acids used in the synthesis are those of D-amino acid, in reverse sequence and leading to inverted amide peptide bonds. The overall spatial orientation is hence unchanged, and so is the chirality of the side chains. The *retro-inverso* peptides have similar side chain topology with the native peptide [220] because conformationally, the D-amino acids are 'mirror image' of the L-amino acids that are normally produced biologically. This kind of peptide is also called all-D-*retro* peptides [221] *retro*-all-D-peptide or *retro*-enantio-peptide [220].

Inversion of the peptide sequence and changing the amino acids into D-enantiomers will usually preserve the biological activity. This is because the resulting side chain surface of the peptides remains the same between both L- and D-*retro inverso* peptides when the carboxy-terminus of L- becomes the amino-terminus and vice-versa. In total, the *retro-inverso* peptides have a reversed position of carbonyl and amine group in the peptidic bond while preserving the 3-dimensional position of side chain groups. The surface of the new peptide is hence largely unchanged as compared to the original L-peptide [222, 223].

There are several advantages that could be associated with *retro-inverso* peptides and this includes their ability to retain protein/peptides bioactivity while having much longer *in vivo* proteolytic stability. They also mimic the antigenic property of their L-peptides counterparts. Hence, in the field of vaccine development, *retro-inverso* peptides are believed to offer good potential as synthetic vaccine. Research has shown that the *retro-inverso* peptide derived from foot-and-mouth disease (FMD) virus is capable to induce the production of longer-lasting antibody titres in animal models as compared to the L-peptides or the antibodies induced by virus particle [221]. *Retro-inverso* peptides analogues are always of great interest in various scientific fields especially in pharmacology. During 2013 to 2015, no fewer than 60 publications with approximately 47 patents have been filed on products related to *retro-inverso* peptides [216, 224-280].

Among the pioneering works on *retro-inverso* peptide was the study of tuftsin and its *retro-inverso* analogues. Tuftsin is a tetrapeptide (H-Thr-Lys-Pro-Arg-OH) at the 289-292 sequence of leukonin heavy chain, a fraction of gamma-globulin protein. In natural conditions following cleavage by leucokinase enzyme, tuftsin is released from leukonin and is free to exert its effect which is usually related to immunomodulatory actions [281]. Interestingly, tuftsin peptide sequence is similar to the C-terminal sequence of VEGF-A₁₆₅ and as described in Chapter 1, VEGF-A₁₆₅ is the ligand for NRP-1 [281, 282]. Tuftsin is used as a reference in experimental works for ligand binding on this receptor. In X-ray crystal structure of NRP-1 as an example, tuftsin is co-crystallized in-complex with the receptor (PDB code: 2ORZ). There are some similarities in the amino acid sequence of tuftsin (TKPR), C-terminus VEGF-A₁₆₅ (DKPRR) and KDKPPR.

However, tuftsin is easily degraded *in vivo* into either H-Lys-Pro-Arg-OH or H-Thr-Lys-Pro-OH (Figure 61). This has led to the synthesis of its *retro-inverso* analogue as a way to improve its stability and indeed, it was shown in several studies that the analogue has a better stability while preserving the activity of tuftsin [281, 283, 284].

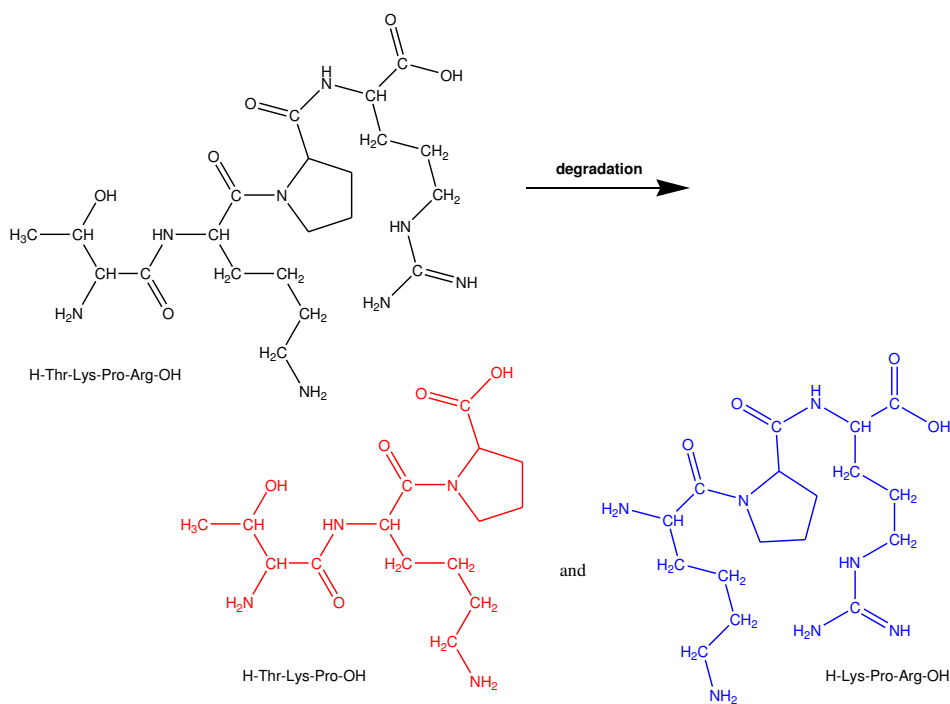


Figure 61: Degradation products of tuftsin

In 1991, Verdini *et al.* studied tuftsin and its partially modified *retro-inverso* analogue. The retro-inverso analogue was formed by inverting the bond between threonine and lysine from -CONH- into -NHCO-, yielding a stronger and more resistant bond against peptidase degradation. The native tuftsin molecule was found by Verdini team to have a half-life of around 8 minutes. However, with the partially modified *retro-inverso* peptide, they found that tuftsin has less than 2% degradation when incubated with 50 different human plasma samples for 50 minutes. Prolonging the incubation time to 360 minutes also has no significant increment on tuftsin degradation. They also showed that the biological activity of the analogue was well preserved. Thus, though the new pseudopeptide has some conformational changes as compared to the native, its biological activity was successfully preserved [188, 281].

There are also other studies on tuftsin and its *retro-inverso* analogue in immunomodulatory actions such as those reported by Becherucci *et al.* (1992) [283] and Paulesu *et al.* (1992) [284]. Paulesu reported that the effective concentration of the *retro-inverso* analogue of tuftsin is at 10^{-4} μM but even at femtomolar concentration, the analogue did show some activity. In this regard, they concluded that the retro-inverso analogue is very active, perhaps more active than the parent tuftsin by at least 10-fold. This phenomenon was attributed to its improved stability against degradation and hence a longer time to exert its effect [283].

3.1.6 ELISA competitive binding assay

Biological tests have been used in development of therapeutics as a way to predict the behaviour of molecules *in vivo*. Enzyme-Linked Immunosorbent Assay or ELISA is one of the most widely used bioanalytical test techniques in current research world which has been made available since more than 40 years ago [285].

ELISA is a developed technique enabling the quantitative determination of a substrate in sample. ELISA is famously known for immunological applications, and hence the substrates are usually antigens and antibodies. However since the application of ELISA is not restricted to merely immunology, the substrates could hence be any molecule that needs to be detected or quantified. Antibodies could be a protein, whilst the antigen could be any small molecule such as peptides, polypeptides or carbohydrates. The interaction between the antibodies and its antigen would be very specific through their 3-dimensional structures which will be complementary to each other and usually this will involve noncovalent linkage [286, 287]. ELISA is applied in a wide variety of disciplines; it could be used in biochemistry, pharmaceutical, forensic, clinical and bioanalytical chemistry laboratories. It allows the utilization of very small amounts of antigens, as low as picomolar (10^{-12} M) and femtomolar (10^{-15} M) [286].

In clinical settings, ELISA is useful in the detection of pregnancy, screening of HIV/AIDS, detection of hyperthyroidism and hepatitis C. In a much wider application, ELISA is also used in the detection of drug of abuse in body samples [288-290] and screening for contaminants in wastewater or soil [291, 292]. The easiness and simplified technique that is provided by ELISA has opened up the possibility of its applications in many different areas with fast and reliable quantitative results to be obtained in hand [287].

In general, ELISA tests are conducted in microtiter plates which need a very small amount of sample as described earlier. Traditionally-performed ELISA involves multiple washing steps which need to be done manually and it is tedious and complicated. To date, the latest technology is offering automated ELISA assay with automatic washing system besides enabling the coating of the microtiter plate automatically to reduce the set-up time of an ELISA assay. Coupled with a more sophisticated detection system such as by chemiluminescence and various fluorescent read-outs, ELISA continues to be the test of choice for many different applications ranging from detection of food plant pathogen to biomarkers analysis. More recently, a method based on beads (bead-based) and microfluidic platforms were introduced and will definitely take the conventional ELISA to a new level of applications [285].

There are four different types of ELISA tests: direct ELISA, indirect ELISA, sandwich ELISA and competitive ELISA are among the most famous. Each type of ELISA has different background concepts as illustrated in Figure 62.

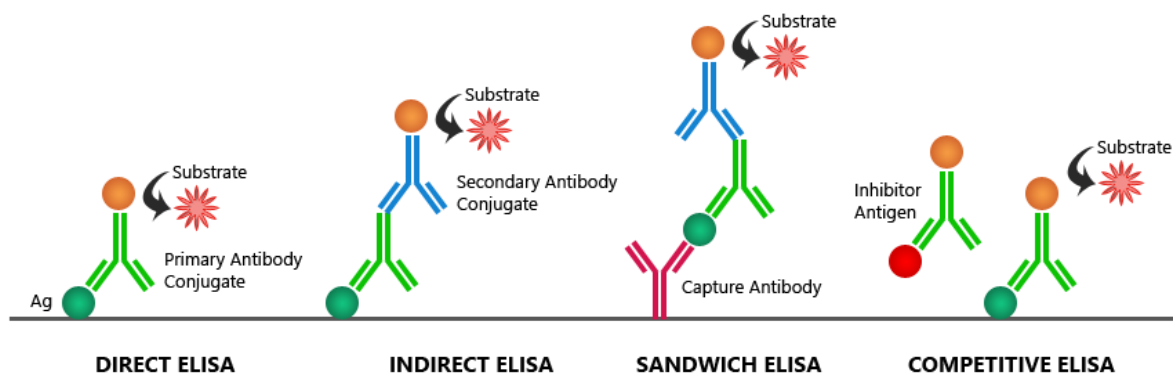


Figure 62: The Different types of ELISA test. (Ag: Antigen). From [293]

Among the different types of ELISA, the simplest, as expected, would be **direct ELISA**. In this technique, the antigen to be tested is coated on the surface of the microtiter well. Enzyme-conjugated antibody that is specifically complement to the antigen is added into the well and interacts with the antigen, resisting washing which removes the unbound antibodies. The addition of a substrate that induces colour changes acts as the reporter-enzyme and helps to determine the degree of binding of the tested antibody on the antigen coated on the well surface. Changes of colour upon reaction with the reporter-enzyme serves as an indicator of positive reaction and quantification is performed by using a plate-reader and a calibration curve prepared earlier.

Indirect ELISA is the reverse of direct ELISA. Antigen is also coated on the surface of the microtiter plate and a complementary antibody is added. Subsequently, a second antibody (an enzyme-conjugated antibody) linked with a reporter enzyme is added to help in the detection of positive reaction through colour changes. This is actually the basic principle in HIV detection. In this test, the presence of antibody in patients' serum is detected by interacting with HIV virus core (antigen) coated on the surface of the microtiter well. In the case whereby the antibodies against HIV is present in patients' serum, these antibodies bind on the surface of the antigen presence on the well and the addition of another enzyme-linked antibody which recognize the human anti-HIV antibody leads to the interaction with the bonded antibody. The addition of substrate causes colour changes noted as positive reaction.

Sandwich ELISA is more uncommon but is an important technique in biological studies. Sandwich ELISA utilizes multiple levels of antibodies. The first level of antibody is known as "capture" antibody. It is immobilized on the surface of the microtiter well and antigen to be detected is added. Following specific reaction time, another antibody is added which also has affinity on the detected antigen, hence the name sandwich ELISA. Subsequently, a third antibody which is enzyme-linked is added and catalyzes a colour change which indicates positive results. Technically and logically, this technique is unnecessary due to the fact that direct ELISA test is a similar technique with a much simplified way. However, sandwich ELISA offers an advantage of not having to purchase each enzyme-linked antibody

for analysis involving multiple numbers of different antigens to be detected. It is hence more cost-effective to use sandwich ELISA technique in this kind of situation.

The fourth type, **competitive ELISA** involves the addition of competing antibodies simultaneously and the antibody with a higher affinity will bind better on the antigen immobilized on the surface of the microtiter well. Positive result is given by the wells in which the signal of sample decreases when the second antibody is added. This is the type of ELISA assay used in this study.

Our PDT research group has been using competitive technique in evaluating the ability of our synthesized peptides or peptide-based conjugates to target different receptors including the NRP-1 [5, 119, 121]. The ELISA employed is not the conventional antigen-antibody reaction which is commonly known for ELISA; instead it is a **peptide-protein** interaction. Through this biological test, the binding capability of a tested peptide (**KDKPPR peptide in this study**) could be determined through its ability to compete and replace VEGF-A₁₆₅ which is the native ligand of NRP-1 (**protein**).

In this method, the NRP-1 receptor is immobilized on the surface of a 96-well microtiter plate. The native VEGF-A₁₆₅ ligand and tested peptide will then be introduced into the well. The ability of the peptide to bind on NRP-1 and displaced VEGF-A₁₆₅ is interpreted as the peptide's affinity towards the receptor.

3.2 RESULTS AND DISCUSSION

A complete suite of KDKPPR analogues was chemically synthesized by the solid phase peptide synthesis (SPPS) system. Another peptide sequence KDRPPR was also synthesized along with the *retro* RPPKDK peptide and *retro-inverso* rppkdk peptide. Table 10 below shows the details of the peptides evaluated.

Table 10: List of peptides evaluated

Compound	Denotation	Peptide sequence
1	Native	H ₂ N-Lys-Asp-Lys-Pro-Pro-Arg-OH
2	Alanine-analogue	H ₂ N-Lys-Asp-Lys-Pro-Pro- Ala -OH
3	Alanine-analogue	H ₂ N-Lys-Asp-Lys-Pro- Ala -Arg-OH
4	Alanine-analogue	H ₂ N-Lys-Asp-Lys- Ala -Pro-Arg-OH
5	Alanine-analogue	H ₂ N-Lys-Asp- Ala -Pro-Pro-Arg-OH
6	Alanine-analogue	H ₂ N-Lys- Ala -Lys-Pro-Pro-Arg-OH
7	Alanine-analogue	H ₂ N- Ala -Asp-Lys-Pro-Pro-Arg-OH
8	Arg/Lys substitution	H ₂ N-Lys-Asp- Arg -Pro-Pro-Arg-OH
9	<i>Retro</i>	H ₂ N-Arg-Pro-Pro-Lys-Asp-Lys-OH
10	<i>Retro-inverso</i>	H ₂ N-arg-pro-pro-lys-asp-lys-OH

The pure products obtained were weighed to evaluate the synthesis efficiency and the corresponding yield percentage was calculated as summarized in Table 11.

Table 11: Synthetic yield of KDKPPR analogues

Peptides	Yield (%)
KDKPPR	51%
KDKPPA	78%
KDKPAR	67%
KDKAPR	50%
KDAPPR	26%
KAKPPR	32%
ADKPPR	60%
KDRPPR	51%
RPPKDK	65%
rppkdk	49%

Table 12 summarizes the retention time of the peptides. All the peptides were eluted at between 3 and 8 minutes, during which the percentage of water in the eluting solvent is more than 90%. This showed that as expected, the peptides are very hydrophilic in nature and this fact is further supported by the characteristic of each amino acid which is influenced by the nature of their side chain. Lysine, aspartic acid and arginine are charged amino acids and the size of their side chain is big as compared to proline and alanine which are more hydrophobic. Hence, the presence of the charges from the three amino acids causes stronger interaction with water and renders the peptide to be more hydrophilic.

Table 12: retention time of KDKPPR analogues

Peptides	Retention time (min)*
KDKPPR	5.32
KDKPPA	6.48
KDKPAR	3.76
KDKAPR	4.27
KDAPPR	7.21
KAKPPR	5.20
ADKPPR	7.49
KDRPPR	5.02
RPPKDK	3.85
rppkdk	3.90

*Retention time is determined on a C-4 RP-HPLC Machery-Nagel Nucleosil 250/5mm with a gradient of 5-100% of acetonitrile in 25 minutes with a flow rate of 1 mL/min, monitored by UV/Vis absorbance at 214 nm (as described in Experimental section).

The retention times of KDKPPR, ADKPPR, KAKPPR, KDAPPR, KDKPPA and KDRPPR follow the general amino acid hydrophobicity coefficients described by several teams [294-296]. Concerning the *retro* and *retro-inverso* peptides, some publications have mentioned that these compounds exhibit a shorter retention time than that of the native peptide [252, 297]. This is in agreement with our results. In the particular cases of KDKAPR and KDKPAR it can be observed that the replacement of a proline by an alanine considerably decreases the retention time and confers the peptides to have a greater hydrophilicity. It can therefore be assumed that this particular behaviour is due to a total change in their conformation.

In order to further describe this phenomenon, one can imagine that the Proline-Proline sequence induces particular folded structures (particularly *cis-cis* conformation) in which ionic interactions between the *N*-terminal Lys₁ (or Asp₂) and Arg₆ may promote a pseudocycle. On the contrary, the replacement of one or the other proline by an alanine could lead to a more extended conformation. Yet it is known that the linear peptide has a shorter retention time than that of their cyclic analogous [298] and it can be expected that KDKAPR and KDKPAR follow a similar discrepancy even if we are dealing with pseudocycles. Furthermore, it is possible that molecular modelling approach could help to provide useful

indications on minimum energy conformation of the analogues hence helping to determine the possible intra-molecular interactions that may contribute to their hydrophilic/hydrophobic behaviour. However due to time constraint, this could not be completed especially since this was not the original purpose of our study and would undeniably require more time.

Table 13 summarized the mass of the analogues observed from mass analysis as compared to the expected mass. Details of the mass spectra obtained are available in [Appendix 3](#).

Table 13: Comparison between mass expected and mass observed of KDKPPR analogues

PEPTIDES	Mass expected		Mass observed	
	M ^[+]	M ^[2+]	M ^[+]	M ^[2+]
KDKPPR	740.43	370.72	740.45	370.72
KDKPPA	655.37	328.19	655.45	328.65
KDKPAR	714.42	357.71	714.43	<i>not seen</i>
KDKAPR	714.42	357.71	714.43	<i>not seen</i>
KDAPPR	683.37	342.19	683.39	342.19
KAKPPR	696.44	348.72	696.55	349.20
ADKPPR	683.38	342.19	683.38	342.19
KDRPPR	768.44	384.72	768.45	384.73
RPPKDK	740.43	370.72	740.44	370.73
Rppkdk	740.43	370.72	740.44	370.72

3.2.1 NMR analysis

Following the purification step, all of the peptide analogues were analyzed by NMR which showed good purity of the peptides obtained. Although in some peptides such as the *retro* RPPKDK, the NMR spectra showed the presence of water despite scrupulous precautions. This is nevertheless the feature of this peptide which is very hydrophilic in addition to the characteristic of DMSO-d₆ used for NMR analysis which is also water-attracting.

For each purified product, ¹H NMR, COSY and TOCSY spectra were generated in order to assign each amino acid present in the sequence. In this thesis, we did not attempt to determine the exact conformation(s) of the peptides due to the multiplicity of the signal sets. It is expected of the KDKPPR and its analogues to have multiple conformations due to the *cis/trans* isomerism of the Lys₃-Pro₄ amide bonds, which could give rise to a type IV β-turn or an inverse γ-turn as proposed by Nath *et al.* (2015) [299]. In addition, it is also well-known for the Pro₄-Pro₅ sequence to induce a high percentage of *cis-cis* conformation (as could be observed in 11.2% of well-defined protein structures in PDB [300]).

There are also multiple hydrogen bonds that could be formed between the side-chains of the amino acids in the peptide sequence. As examples, bonds could be established between $\text{Asp}_2(\text{OH}) \cdots \text{HN}_\epsilon(\text{Arg}_6)$, $(\text{Asp}_2)\text{OH} \cdots \text{HN}_\epsilon(\text{Lys}_3)$, $(\text{Lys}_1)\text{NH}_\epsilon \cdots \text{O}=\text{C}(\text{Arg}_6)$, $(\text{Lys}_1)\text{NH}_\epsilon \cdots \text{O}=\text{C}(\text{Pro})$ and $(\text{Pro}_1)\text{C}=\text{O} \cdots \text{HN}_\epsilon(\text{Arg}_6)$, and this causes difficulties in determining the accurate conformation of the peptides without further studies such as NOESY or ROESY and molecular dynamic simulations. An additional lysine at the *N*-terminus makes even more important the number of potential hydrogen bonds.

With regards to this thesis, the COSY and TOCSY analysis were made as a way of checking the sequence of the peptides. As an example, the TOCSY spectra and the attribution of signals of the native KDKPPR peptide is given below in Figure 63 and the spectra of the other peptides are available in [Appendix 4](#) at the end of this thesis.

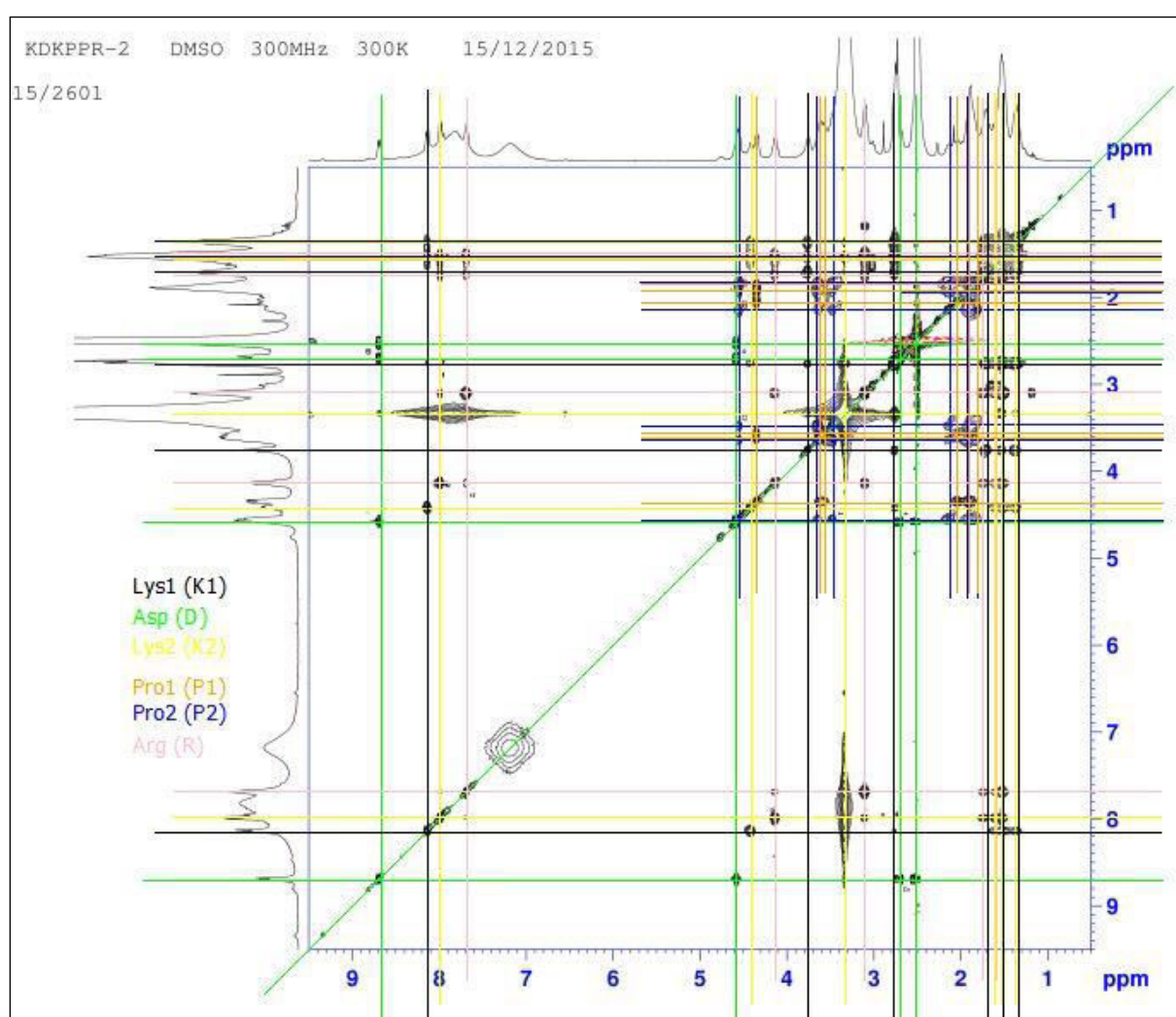


Figure 63: The TOCSY spectra of KDKPPR

3.2.2 ELISA competitive binding assay

Figure 64 illustrates the percentage of VEGF-A₁₆₅ binding on NRP-1 and Table 14 summarizes the EC₅₀ (half-maximal effective concentration) of all the Ala-scan analogues tested in comparison to the parent peptide and DKPPR.

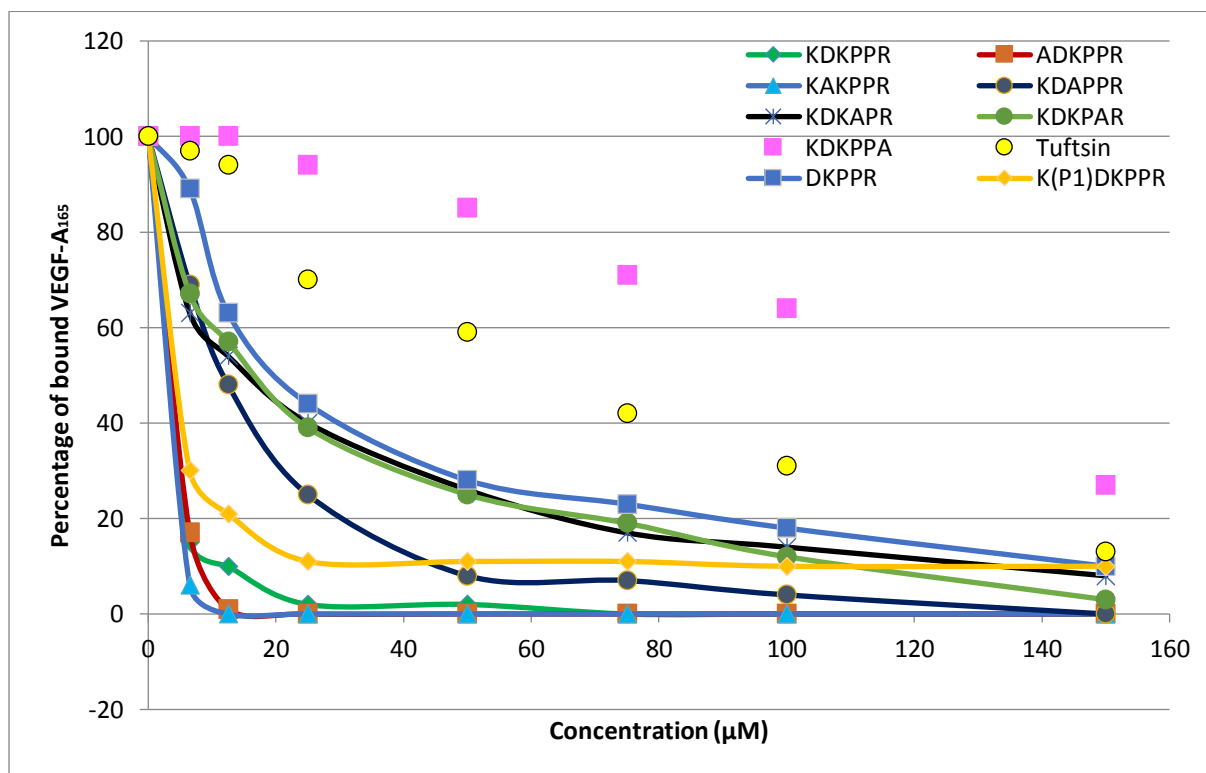


Figure 64: Percentage of binding of each analogue of KDKPPR on NRP-1 receptor. Also features are tuftsin, DKPPR and K(P1)DKPPR

As previously mentioned, a lysine was added at the *N*-terminus of the previous DKPPR sequence, giving the new sequence of KDKPPR. As shown in Figure 64, the affinity of KDKPPR is better than that of DKPPR (EC₅₀=6.0 µM and EC₅₀=18.3 µM respectively). This fact is comforted by the result obtained with ADKPPR in which a non-functionalized alanine has been added at the same position. This is a very important result because the same addition in the tuftsin TKPR (leading to KTKPR) induced a dramatic loss of activity [301]. Furthermore, we also confirmed that grafting of porphyrin P1-COOH at the εNH₂ of this supplementary lysine only has a weak effect on the NRP-1 receptor recognition and is still better as compared to tuftsin as a targeting peptide. The EC₅₀ values of both KDKPPR and K(P1)DKPPR are also the same, 6 µM for both molecules.

Table 14: The EC₅₀ of KDKPPR analogues prepared through Alanine-scanning as determined through ELISA assays after mathematical estimation with graphpad prism

Peptides	EC ₅₀ (μM)
DKPPR	18.3
KDKPPR	6.0
K(P1)DKPPR	6.0
KDKPP <u>A</u>	63.5
KDKP <u>A</u> R	27.3
KDK <u>A</u> PR	27.3
KD <u>A</u> PPR	13.4
K <u>A</u> KPPR	2.6
<u>A</u> DKPPR	4.7

The amino acid in the beginning of the sequence, **KDKPPR** is of lesser importance for efficient NRP-1 binding. The ADKPPR and KAKPPR have similar affinity than the native KDKPPR. As expected, among all of the analogues, KDKPPA presents the lowest activity, showing the crucial role of arginine at the C-terminus of the peptide sequence. Several peptides that have the ability to compete with VEGF-A₁₆₅ for NRP-1 such as tuftsin (TKPR), enhanced tuftsin (TKPPR) and A7R (ATWLPPR) also have the same C-terminal arginine as reported by Teesalu *et al.* (2009) [125]. This is in agreement with other publications on tuftsin, where it has been shown that the replacement of the C-terminus arginine by Arg-NH₂ [302], D-Arg, Lys [303], Gly, Ala or His [301] has induced a decrease in activity [299]. However, Teesalu *et al.* (2009) who proposed the C-end rule concept pointed out that there are rarely occasions in which lysine is presence instead of arginine at the C-terminus of the peptides which target NRP-1 receptor. However in most cases, the terminal carboxyl end is occupied by arginine [125]. Based on this report, the presence of arginine in the terminal carboxyl end is hence a very important feature and capping it with another amino acid or blocking the free carboxyl group by amidation will hamper the peptide's binding ability.

Substituting either one of the proline, P also causes a decrease of the peptide's affinity, probably because they induce a 3-dimensional structure of the peptide needed to ensure good binding on the receptor. Ala-exchanged at either one of prolines shows similar reduction of affinity, suggesting some equality on the function of prolines on the peptide's binding capability. The fact that proline is not charged and conformationally rigid and restricted may be a factor needed to have an effective binding of KDKPPR on the targeted NRP-1 receptor.

The results described thus are in agreement with the C-end rule described earlier on; an NRP-1 targeting peptide will need to have a sequence of K/R-XX-K/R. The two X in the centre are proline in this study, and the presence of both prolines is important. Although the middle amino acids in the C-end rule concept were noted as XX (R/K-XX-R/K), Teesalu *et al.* (2009) found through phage library screenings that peptides with prolines as the XX such as RGERPPR and RVTRPPR or proline and alanine such as RPARPAR showed efficient binding, more than 1,000 fold as compared to control [125]. The observation in this study

however is different. The replacement of either one proline with alanine (KDKAPR and KDKPAR) has lower activity as compared to the native KDKPPR.

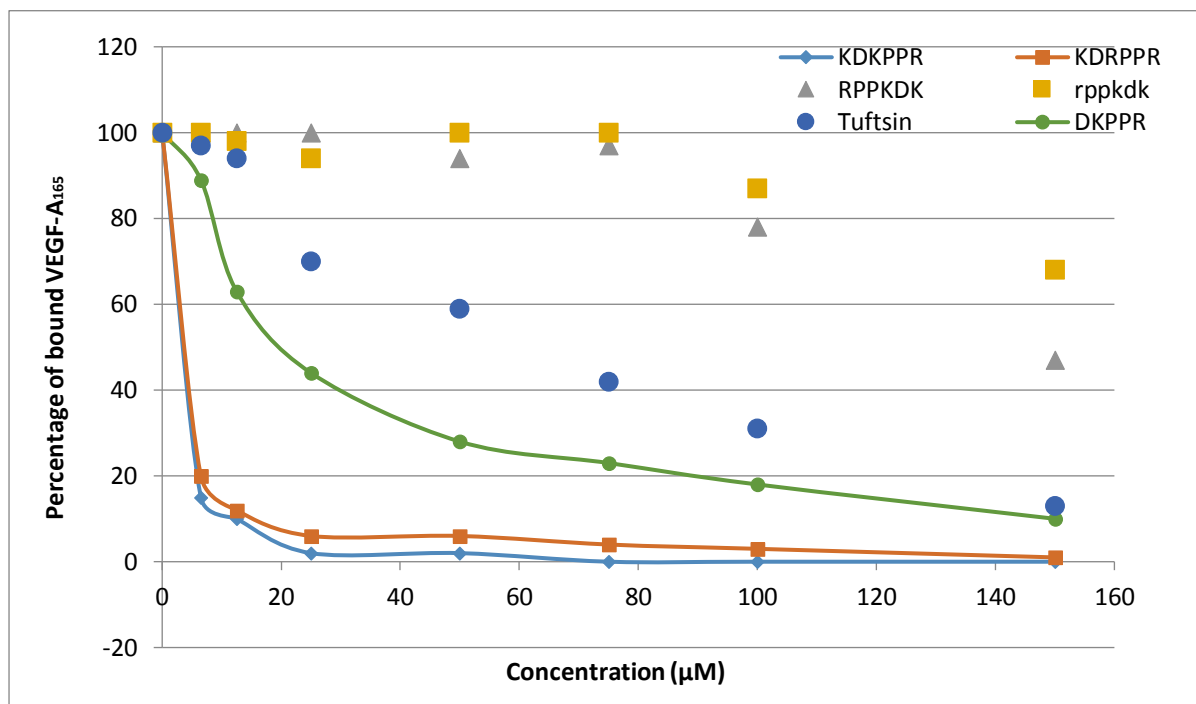


Figure 65: ELISA assay results for KDKPPR, KDRPPR, *retro* RPPKDK and *retro-inverso* rppkdk peptide

The lysine K3 in the middle of the peptide **KDK**PPR was substituted with an arginine to give **KDR**PPR. Figure 65 illustrates that the ability of KDKPPR and KDRPPR to bind on NRP-1 is similar to each other ($EC_{50}=6 \mu\text{M}$), showing that both lysine and arginine could be used interchangeably with no significant compromise on the binding ability. Substitution with alanine (**KDA**PPR) however is less favourable (Figure 64), suggesting the importance of charged side chain amino acid in this position for efficient binding.

Figure 65 also illustrates the binding of the *retro* RPPKDK and *retro-inverso* rppkdk peptides. The *retro* RPPKDK showed a higher binding affinity as compared to the *retro-inverso* peptide at high concentrations. Nevertheless, both *retro* and *retro-inverso* analogues showed lower affinity as compared to the native KDKPPR. Although the *retro-inverso* may have the advantage of better stability (which may be investigated and confirmed in future studies), the importance of stability versus the affinity will be evaluated to determine the possibility of using the *retro-inverso* rppkdk peptide in the place of its native KDKPPR. Table 15 below listed the EC_{50} values of the peptides presented in Figure 65.

Table 15: The EC₅₀ values of modified peptides after mathematical estimation with graphpad Prism

Peptides	EC ₅₀ (μM)
DKPPR	18.3
KDKPPR	6.0
KDRPPR	6.0
RPPKDK (<i>retro</i>)	78.0
rppkdk (<i>retro-inverso</i>)	85.0

With respect to the *retro* and *retro-inverso* peptides, it is very remarkable to know that *retro-inverso* all-D rppkdk peptide does not have the same affinity than the native KDKPPR. Since the retro peptide RPPKDK showed low affinity, there is a possibility that all-D rppkdk also showed low affinity unlike other *retro-inverso* peptides. This may be due to the binding of peptides on NRP-1 receptor involve chiral binding site, as proposed by Teesalu. They also described that in comparison to cell-penetrating peptides which are usually active in their D-forms, the C-end rule peptides uptake are dependent on specific recognition of L-peptides only [125].

3.3 CONCLUSION AND FUTURE PERSPECTIVE

In summary, the most important amino acids to be conserved for effective binding of KDKPPR on NRP-1 are the last four amino acids: K-P-P-R. Substitution of these amino acids with alanine causes reduction on its ability to replace VEGF-A₁₆₅ binding. A good binding on NRP-1 receptor will be possible to be achieved by using peptides that have the form of R/K-XX-R/K, with proline, P in the places of X. This study shows that the peptides that follow such consensus (ADKPPR, KAKPPR, and KDRPPR) have the best binding as native KDKPPR on NRP-1 as compared to the others.

In our publication [6], it was reported that the PS-conjugated-DKPPR was cleaved between aspartic acid, D and lysine, K producing [PS-conjugated-D] which was detected after 60 minutes *in vivo*. This phenomenon would render the peptide to lose its targeting ability towards NRP-1 receptor. To cater to this problem, a preliminary study is underway to investigate the potential of a new analogue K(d)KPPR with a D-aspartic acid as a possible way of improving the stability of the native peptide.

As a future outlook, it will be useful to conduct molecular modelling and molecular dynamic studies of the KDKPPR analogues in order to have a better understanding on the molecular conformation of the analogues in their interaction with NRP-1. This will help in deeper and further interpretation of their affinity towards the receptor as was discovered through ELISA assays, as presented in this chapter.

It would also be very interesting to investigate the *in vivo* stability of the three peptide analogues that present the best binding affinity on NRP-1 (ADKPPR, KAKPPR and KDRPPR). This is to ensure that their plasma half-life is long enough to enable the delivery of any conjugated drug and subsequently improve the clinical outcome of cancer patients. Since *retro-inverso* peptides are known to offer good potential as targeting agent with improved stability *in vivo*, it is necessary to also evaluate the stability of the peptides as a part of our study. It is of our highest interest to continue the study on this topic and this will be included in our future study plan. In the case of the peptides show low stability, it is also possible to synthesize a pseudopeptide as a way to improve the stability, if necessary.

Chapter IV: Synthesis of Porphyrin (P1COOH) and DKPPR Peptide Platform through Click Chemistry

4.1 INTRODUCTION

The approach of synthesizing conjugates between drugs molecules and a targeting moiety is of interest to many researchers. Different conjugates were already reported in the literature and this could be grossly divided into two types of conjugation approaches; (1) direct conjugations between drug and targeting agent, and (2) conjugation of targeting agent on the surface of drug-containing vehicles such as nanoparticles.

This chapter will describe the background and synthesis work-up on utilizing click-chemistry technique for direct conjugation of porphyrin and DKPPR, to form platforms with different number of porphyrin and DKPPR molecules each time, in each branch. A background on click chemistry will be discussed and the synthesis approach taken is detailed out in subsequent sections. The results obtained are also described and discussed accordingly.

4.1.1 Click chemistry

Nature offers diversity of secondary metabolites with magnificent architectures consisting of extensive carbon-carbon bonds networks. These secondary metabolites usually possess useful biological activities and would thus be good candidates for therapeutics. However, extracting these compounds are not easy; the laborious work often led to low yield besides being costly in terms of time and money. Hence, efficient synthesis technique in producing drug-like compounds such as those produced by nature would be very timely and beneficial.

However, such synthesis has never been easy especially since these secondary metabolites are usually huge and contain multiple functional groups. Hence, when Sharpless and co-workers introduced the concept of click chemistry in 2001, it was accepted widely in a matter of very short time and is applied in multiple research areas including in the synthesis of new drug molecules [304, 305].

George S. Hammond in a Norris Award Lecture in 1968 was quoted as saying [306]:

“The most fundamental and lasting objective of synthesis is not production of new compounds, but production of properties”

Through this point of view, it is not important to use a complicated synthesis technique to obtain any intended product if such product could be obtained through a much simpler way. This is the reason for the extremely wide acceptance of the click chemistry approach in product synthesis.

The concept of click chemistry was initially described in 1893 by A. Michael and in the early years of 1900's, Dimroth first reported the formation of triazole *via* cycloaddition of azide and acetylene. It was only in 1963 that the generality, scope and mechanism of this cycloaddition were fully realized after Rolf Huisgen's study and was later known as the Huisgen's 1,3-dipolar cycloaddition reaction. However the reaction produces non-stereospecific product mixtures of 1,4 and 1,5-disubstitution [304], besides requiring long reaction time, elevated temperature and high pressure. These factors lead to this useful reaction being ignored for decades [191].

In 2001, Fokin and Sharpless (in the United States of America), and Meldal *et al.* (in Denmark) have independently reported the efficiency of using copper (Cu) as a catalyst in this kind of reaction. Copper (I) was found to have the ability to accelerate the reaction by up to 10 million times and selectively produces only 1,4-disubstituted triazoles. Sharpless, Kolb and Finn (2001) later on described this as a *click reaction* and illustrated *click* as a reaction which is "spring loaded" for a single trajectory, especially since this reaction is usually driven by a high thermodynamic force and hence could be completed rapidly with high product selectivity [307]. Click reaction is then defined as a reaction that is modular, has a wide scope, produces high yields, clean and green, uses benign solvents, could be conducted in aqueous or organic environment, in solution or solid support, generates by-products that are non-toxic and could easily be purified *via* non-chromatographical methods [306, 308-310].

The introduction of click chemistry more than a decade ago has attracted interest of the scientific community and this has been manifested by the increasing number of click chemistry-related publications available to date. The incorporation of click chemistry in drug development research has contributed in improving the availability of active pharmaceutical compounds. This includes the synthesis involving biomolecules such as peptides and proteins which are easily damaged under harsh conditions and undeniably, click chemistry has become the reaction of choice [191].

There are different types of reaction that could be classified in the domain of click chemistry. The main ones are as listed below and illustrated in Figure 66 [306, 307, 311]:

- Nucleophilic opening of spring-loaded rings, examples being the epoxides and aziridines.
- Non-aldol carbonyl chemistry, example being the formation of ureas, oximes and hydrazones.
- Carbon-carbon multiple bonds addition reaction, especially oxidative addition
- Cycloaddition reactions, especially 1,3-dipolar cycloaddition reactions but also included the Diels-Alder reaction.

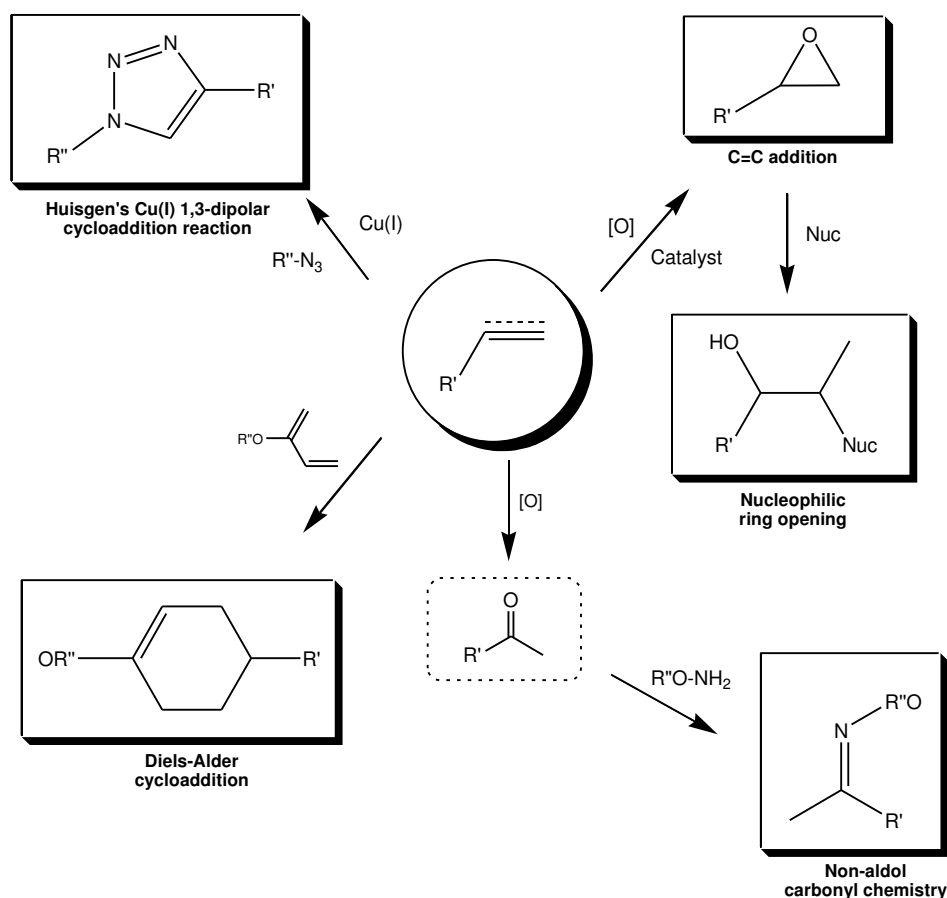


Figure 66: Types of click chemistry reactions. From [312]

1,3-dipolar cycloaddition and nucleophilic ring opening are the two click reactions most extensively studied to date. Nucleophilic ring opening involves the opening of a highly strained ring system such as aziridines, epoxides, cyclic sulphates, episulfonium ions and aziridinium ions, and among these structures, aziridines and epoxides are the most commonly applied in click reactions. The opening of the aziridines and epoxides rings produces regioselective products which are useful in the formation of diversified compounds and could be used in the synthesis of natural product derivatives. The 1,3-dipolar cycloaddition reaction

is the more widely used and it is also known as Huisgen's 1,3-dipolar cycloaddition reaction. Figure 67 describes some examples of this reaction.

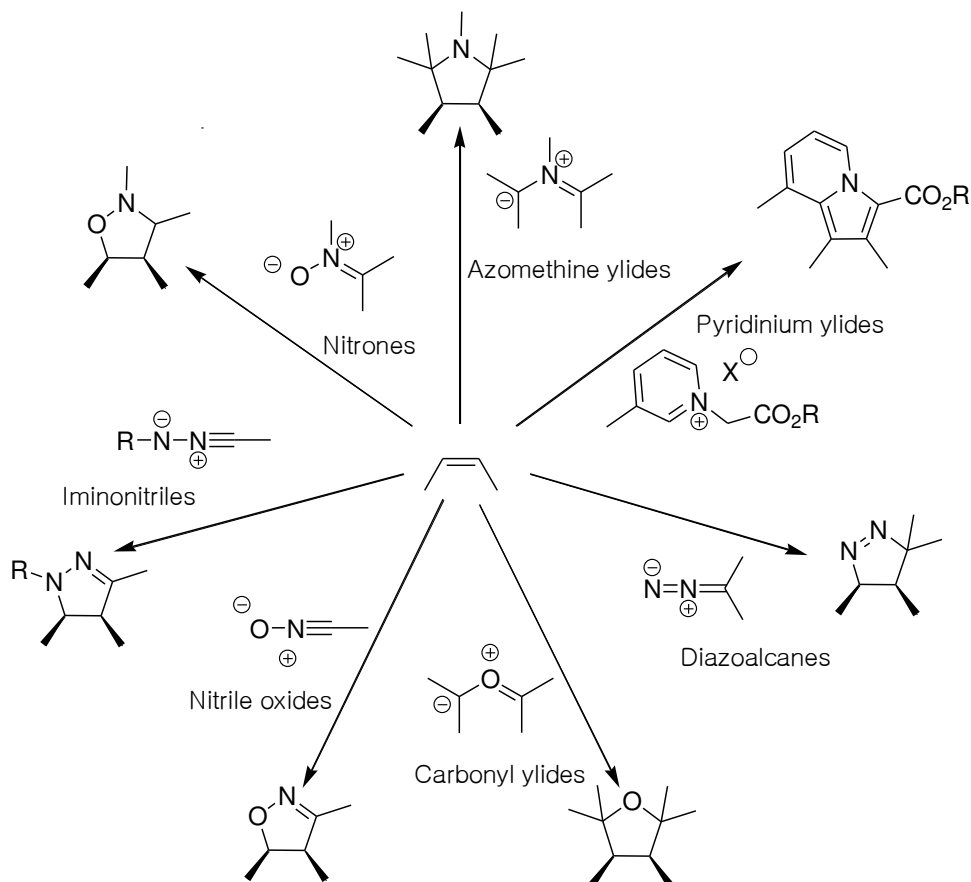
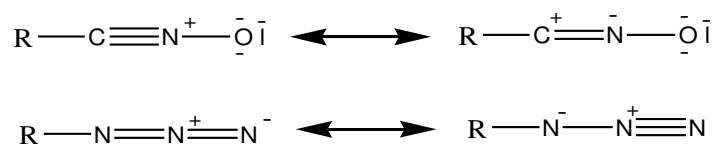


Figure 67: Examples of 1,3-cycloaddition reaction reported in the literature. From [313]

The Huisgen's 1,3-dipolar cycloaddition reaction is a reaction between a dipolarophile and a 1,3-dipolar compounds producing a 5-membered heterocycle rings. Examples of dipolarophile are alkenes and alkynes, whilst the 1,3-dipolar compounds are the compounds formed by one or more heteroatoms with at least one mesomeric structure of charged dipole (Scheme 1). Although there are many forms of functional azide and dipolarophiles that could be used for this reaction, the cycloaddition between a terminal alkyne and an azide has become the most famous click reaction [314].



Scheme 1: Examples of 1,3-dipolar compounds. Above: nitrile oxide, below: azide

As mentioned before, the Huisgen's cycloaddition reaction which was introduced in the 1960s did not produce stereospecific products. Interestingly, in the presence of copper (I)

catalyst as discovered by Meldel and Sharpless in the beginning of 21st century, the reaction proceeds in one direction and produces a product with single isomerism (Figure 68). This copper (I)-catalyzed 1,3-dipolar cycloaddition, also termed as [3+2] azide-alkyne cycloaddition is known as the “cream of the crop” of click reactions, so much that it is often directly being referred to as click chemistry itself [307, 311, 315]. It has the ability to combine two molecules with unsaturated functional groups, an azide and an alkyne, producing a variety of five-membered heterocycle rings [316]. The presence of copper as catalyst was found to reduce the activation energy barrier by 11 kcal/mol, pushing the reaction forward with high selectivity [305].

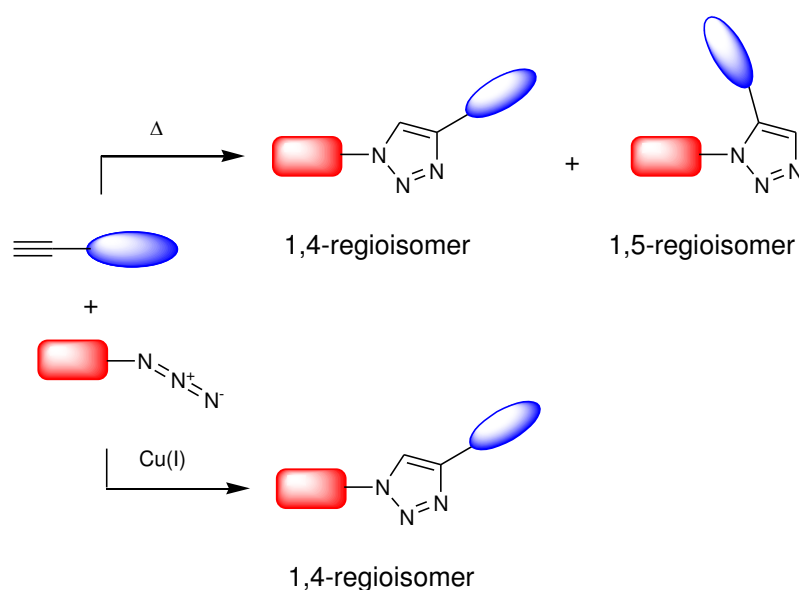


Figure 68: Huisgen's cycloaddition without the presence of copper catalysis (above) and with copper (I) catalysis (below). From [313]

The terminal alkyne and aliphatic azide involved in the reaction have high mutual reactivity, but individually, they are among the least reactive in organic synthesis besides showing inertness and stability towards other functional groups commonly found in biological molecules [314, 317]. Triazole ring that is formed is also known to present a good stability against acid/basic hydrolysis and in reductive/oxidative conditions, besides being relatively resistant to metabolic degradation [318, 319].

The added benefit of copper in accelerating the reaction has gathered interest from scientists of different fields including pharmaceutical sciences [305, 314], drug discovery [314], organic chemistry, inorganic chemistry, polymer chemistry [317] and biochemistry [311, 320]. This is perhaps due to its ease of handling, reliability and applicability to different reaction conditions.

There are four different ways of introducing copper catalyst in a click reaction, as illustrated in Figure 69. It can be used in the form of salt, copper (I) iodide and copper (I) trifluoromethanesulfonate benzene complex, (CuOTf.C₆H₆) are among others, but the reaction

would require the presence of nitrogen base such as triethylamine, pyridine and 2,6-lutidine and could sometimes generate unwanted diacetylene, 5-hydroxytriazole and *bis*-triazole by-products [317, 321]. A second approach is the use of a Cu^{II}/Cu⁰ system, in which Cu^I is formed through comproportionation (a reaction between two reactants of the same elements with different oxidation number, causing the elements to reach same oxidation number) of the Cu^{II}/Cu⁰ couple.

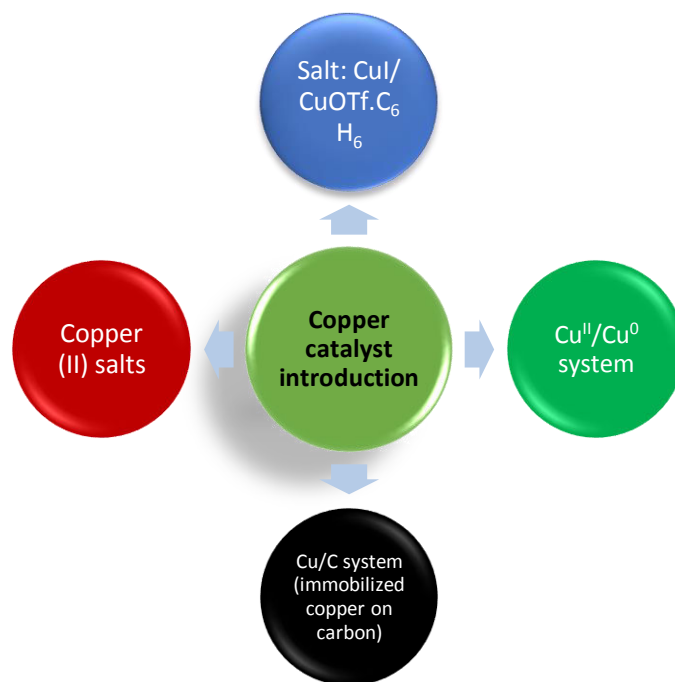


Figure 69: Methods to introduce copper into a click reaction

Thirdly, a Cu/C system which consists of copper immobilized on carbon is also useful. This is prepared by placing Cu(NO₃)₂.3H₂O and carbon black in water and mixing by sonication for 7 hours, and subsequently get activated by either using microwave heating or by the addition of triethylamine in the reaction mixture. The fourth method of copper (I) introduction is by using copper (II) salts such as copper (II) sulphate pentahydrate (CuSO₄.5H₂O) and ascorbic acid as the reducing agent. The production of copper (I) would then be done *in situ*. This last technique is the most preferable option to form 1,4-triazoles at room temperature in high yield [304, 321].

In the years following the introduction of click chemistry, a significant number of researches were conducted to further evaluate the ability of this technique and to search for possible modifications of the classic click technique. This has led to the development of other click chemistry-related reactions including copper-free click chemistry and ruthenium-catalyzed azide-alkyne cycloaddition [191]. The addition of these techniques has opened up a wider possible application in multiple fields which could not be achieved before due to the inability to use copper in their applications. For the scope of this thesis, copper (I)-catalyzed azide-alkyne cycloaddition was used and all discussions will be tailored to this reaction.

4.1.2 The advantages and disadvantages of click chemistry

The advantages of click chemistry are generally presented in its characteristics as listed before. Its characteristics have put this reaction to be one of the most reliable reactions in organic and synthetic chemistry. The large thermodynamic force that is included in the reaction caused virtually absolute conversion of reactants to a single product which necessitates only simple purification steps [308].

Azide and alkyne groups that are needed for the click chemistry reaction are thermodynamically favoured, high-energy and potentially reactive. Although they are reactive, biological molecules do not recognize them as reactants. This is very useful theoretically as this reaction could be conducted even in the presence of enzymes or other biological molecules *in vitro* or *in vivo*. Sharpless and co-workers have been building molecules through click reactions in the presence of specific enzymes' active site, in which the active site will act as a mould. They managed to come out with molecules that are at least as effective as the currently used drugs in the treatment of HIV and glaucoma [308].

The intrinsic properties of the triazole ring linker that is formed following click reaction also offer advantages. It contributes certain hydrophilicity which is favourable for *in vivo* applications. In addition, the triazole ring is also chemically stable and hence could improve the stability of the conjugate against enzymatic degradation. Furthermore, the cyclic structure of the triazole has the ability to direct the linked entities towards different directions and hence preventing them from interacting with each other, which is not the case of simple aliphatic linkage used conventionally [313].

Steric hindrance is one of the limiting factors in any chemical reaction. Interestingly, the steric bulkiness of the group attached to the azide or alkyne does not seem to affect the capability of triazole ring formation during click reaction [305]. This is also evident from numerous reports in the literature on the formation of supramolecular structures through click chemistry technique [322-324], providing facile technique for the synthesis of huge molecules such as fullerenes and dendrimers of multiple layers.

Although click chemistry is a compelling technique available for linking different groups, it is under-used especially in the development of clinical drugs. The presence of copper traces in the product of click chemistry intended for biological applications has potential toxicity risks (even at picomolar concentration) and hence caution needs to be exercised. Although copper is commonly used at a very low concentration and is removed during purification step, there is a need to ensure that copper is not retained in the final product [325]. Fortunately, the recommended health standard level of copper is known to be at 15 ppm, hence this limit should be respected in sample preparation intended for human use. Despite these drawbacks, click chemistry is nevertheless a useful tool in the field of drug discovery and drug delivery.

4.1.3 Porphyrin-based click chemistry

The utilization of click chemistry in synthesizing new PSs or PS-related conjugates is of interest, as a way to overcome the problem of lacking simpler synthesis protocol which is a known problem of PS synthesis. Click chemistry is believed to have the potential to improve the synthesis approach for PS. As reviewed by Dumoulin and Ahsen in 2011, the interest in utilizing click chemistry with tetrapyrrolic compounds such as porphyrin, chlorin, bacteriochlorin and phthalocyanines was only started around 2006, five years later after its description and the number of publications has increased exponentially over the next years. In the beginning, click chemistry was only used to combine an azide- or alkyne-functionalized macrocycles with another compound having the complementary function, but overtime, the research works were extended into combining different macrocycles to give di- or multi-nuclear structures, with symmetrical or asymmetrical derivatives (Figure 70) [324].

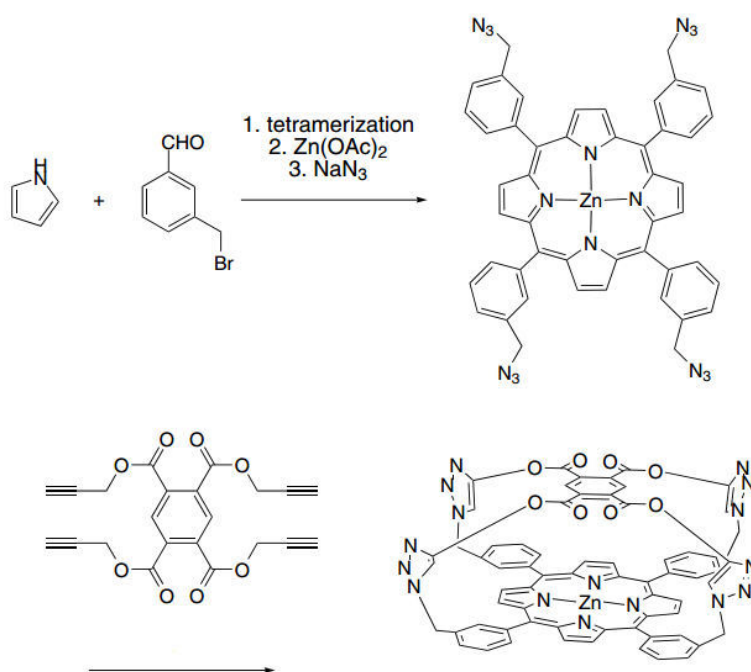


Figure 70: Symmetrically substituted porphyrin and the production of capped porphyrin. From [324]

Among the important benefit of utilizing click chemistry is the ability to conjugate certain groups such as sugars on a molecule to improve its properties including the physicochemical properties and targeting ability [313, 326]. The presence of sugar molecules attached to the PS can also improve its cell delivery through endocytosis. As an example, Hao *et al.* reported their attempts to synthesize porphyrin-sugar conjugates through click chemistry and subsequent investigation on cell internalization. They demonstrated that click chemistry was able to give their porphyrin-sugar conjugates in acceptable good yield at more than 80% after deprotection. Cell internalization study has shown that the number of attached sugar

moieties influences the type of cell organelles in which the conjugates accumulate: those with one moiety accumulated in endothelial reticulum whilst the conjugates with four sugar moieties preferred the lysosomes [327]. Figure 71 illustrates an example of a tetraglycoporphyrin conjugate obtained by Hao *et al.* There are many other studies reported and were reviewed in detail by our team [313].

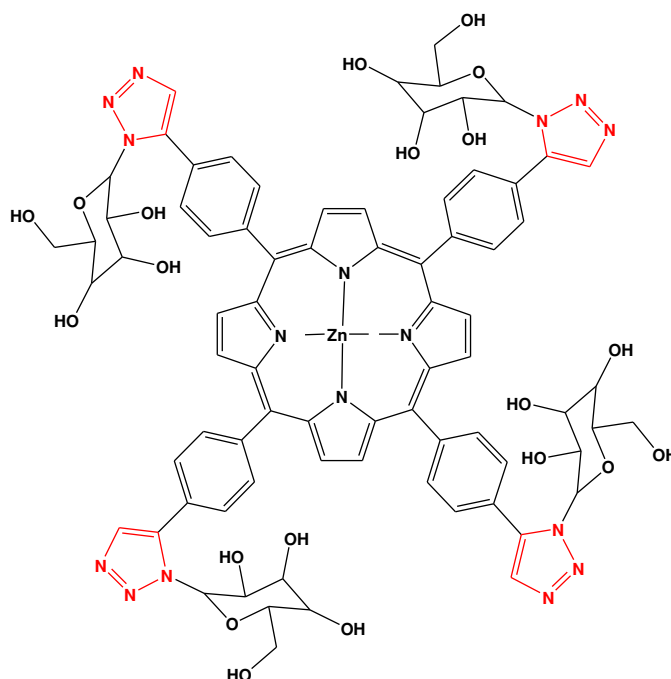


Figure 71: An example of tetraglyco-porphyrin conjugate synthesized through click reaction

In addition, click chemistry was also reported as being a useful technique in the elaboration of poly-glycoporphyrin through the synthesis of porphyrin-cored glycodendrimers. Kushwaha *et al.* synthesized the complicated poly-glycoporphyrin molecule with a porphyrin centre and multiple numbers of sugar molecules on the outside branch of the dendrimer as illustrated in Figure 72, acting as a targeting agent and helping in improving water solubility of the molecule. The success of the synthesis is usually dependant on the coupling efficiency of the sugar moieties into porphyrin framework, and hence click chemistry is indeed a suitable technique to be used due to its high efficiency [328].

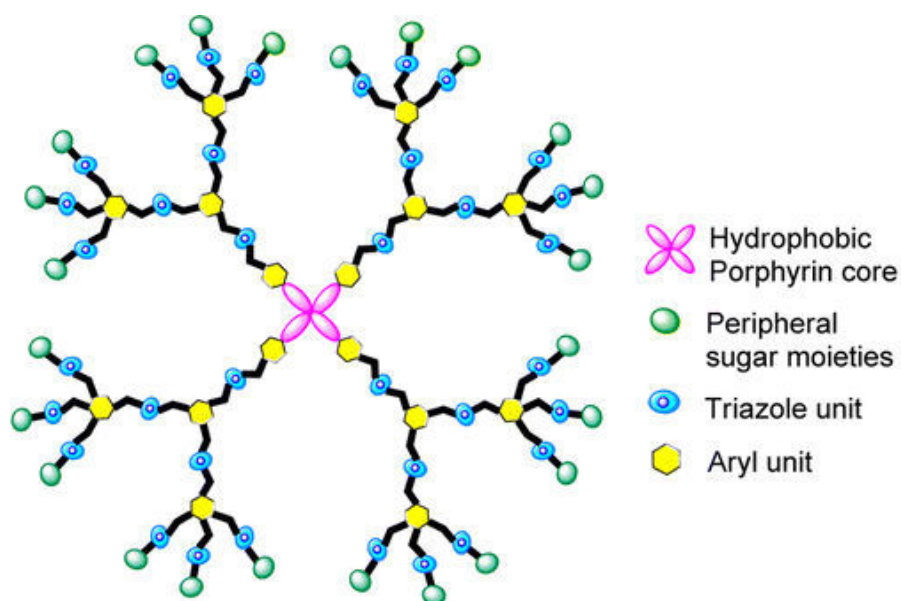


Figure 72: Porphyrin-cored glycodendrimer. From [328]

Bakleh *et al.* mentioned one limitation in copper(I) – catalyzed click chemistry: the copper ion used as the catalyst could insert into a non-metallated PS ring [329]. This is not favourable because the amount of copper available as catalyst is then reduced and hence lowers the yield of product obtained. The utilization of PS-metal complex on the other hand is more suitable to ensure optimal product yield and such complex is usually stable against displacement by copper during the reaction [329-331]. The metal could be removed at the end of the reaction by using acids such as TFA or hydrochloric acid [324].

More recently, there are also reports on methods to prevent copper insertion into porphyrin ring. A study by Daly *et al.* reported the use of tris(3-hydroxypropyltriazolylmethyl)amine as a stabilizing agent for copper (I) against insertion into porphyrin ring. Another useful approach to prevent this occurrence is by using a specific copper catalyst: 1,10-phenanthroline)*bis*(triphenylphosphine) copper (I) nitrate instead of the common copper (II) sulphate [332]. This approach however is not very widely applied, but can be very useful in porphyrin-related reactions which could not be treated with acid.

However, there are some concerns regarding the phototoxicity of PSs in the presence of triazole rings. There is limited number of studies which compared the phototoxicity of PSs synthesized through either click chemistry or conventional covalent linkage and it seems that the conjugates with triazole ring have shown reduced phototoxicity. To our knowledge, no reviews and very few papers have been dedicated to this issue. However in a study by Bakleh *et al.* [329], they reported that the porphyrin-peptide conjugates formed through the formation of triazole ring by click reaction showed very high singlet oxygen quantum yield (0.80 in ethanol), proving that the presence of the triazole ring did not disrupt the singlet oxygen production capability of the conjugated porphyrin. Two other articles on the other hand

described the direct comparison of the phototoxicity of clicked *vs.* covalently grafted conjugates and it seems that in these cases the presence of the triazole group induces a loss of activity [333, 334].

4.1.4 Microwave-assisted click chemistry

The utilization of microwaves in organic chemical synthesis started in 1986 with works pioneered by Gedye *et al.* [335] and Giguere *et al.* [336]. In these works, they reported considerable increase in rate of reactions while maintaining comparable yield of synthesized product. Following these reports, more and more organic syntheses were conducted under microwaves and three decades later in current time, nearly all organic synthesis reaction available have been tried and tested under microwave irradiation [337].

The application of microwave in organic synthesis has shown good capability to enhance reaction rate because the microwave irradiation energy could be absorbed by polar molecule selectively and it is not necessary to heat the reaction vessel first before the energy could reach the solvents and reactants. This leads to fast rising of temperature and instantaneous localized superheating of the reactants themselves, resulting in better thermal homogeneity of the sample and more efficient product synthesis. This is in comparison to the conventional synthesis technique with only thermal energy to drive the reactions forward (Figure 73) [337].

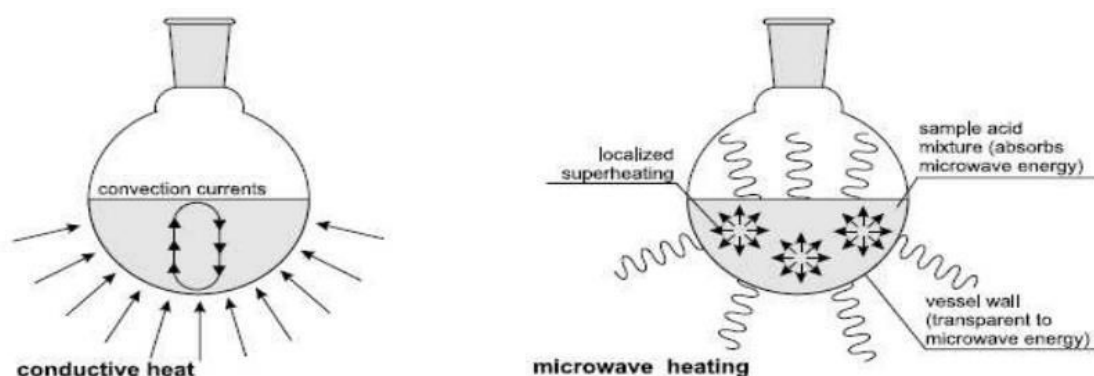


Figure 73: Illustration on heat transfer mechanism involved in conventional synthesis technique (left) and microwave (right). From [337]

The advantage of microwave irradiation as being fast and its ability to complete a synthesis in a fraction of time of those reactions utilizing conventional heating is excellent. [338]. The application of microwaves enables a cleaner, safer and more comfortable working environment. It also speeds up the optimization of synthesis reaction and improves overall preparation with recuperation of the intended products in a similar way as conventional synthesis technique. Many researchers have opted for this technique with different interesting

results. In the organic synthesis of PSs as an example, our team has described the synthesis of zinc 5-(4-carboxyphenyl)-10,15,20-triphenylporphyrin and zinc 5-(4-carboxyphenyl)-10,15,20-triphenylchlorin through microwave assisted technique. The reaction time was managed to be reduced significantly with comparable yield than the conventional synthesis method [83].

Microwave technique was also found to be useful in conducting click reactions. It has the ability to accelerate click reactions and to enable an even wider application with efficient synthesis [324, 329, 330, 339, 340]. Bakleh *et al.* (2009) showed good porphyrin-peptide clicked reaction by using microwave with a yield of 84% after only two minutes reaction at 85°C, in comparison to classical stirring method in which 24 hours were needed under similar reaction conditions to obtain 83% of synthetic yield [329].

4.1.5 Peptides in click chemistry

Ever since the introduction of click chemistry in 2001, the access to chemical reactions involving peptides has been much diversified. It opens up various possibilities to produce different structures in peptide scaffolds and hence could increase their potential applications in therapeutics. Even if peptides were not considered as very suitable therapeutic drugs in the past due to their low bioavailability and metabolic instability, they can be used as targeting agent because its role is limited to bringing the molecule of interest to its receptor, which is generally made in a short and sufficient time to carry out its role as "pilot" [191].

Besides the possibility of employing click chemistry in the synthesis of peptide-drug conjugates as specific disease targeting agent, click chemistry could also be used to modify the peptide molecule itself. The unique characteristics of the [1,2,3]-triazole ring is the key to the different roles that could be played by click chemistry in peptide-based therapeutics. It is recognized as having resemblance with the amide bond of peptides; the distance between substituent are relatively similar (3.8-3.9Å in amides and 5.0-5.1Å in [1,2,3]-triazole), dipole moments of ~4 Debye in amide and ~5 Debye in [1,2,3]-triazole, the lone pair of the three nitrogen mimics the lone pair presence on carbonyl oxygen of the amide bond, relative planarity and the ability to form hydrogen bonding is markedly higher by the triazole ring as compared to the amide bond (Figure 74) [191, 341, 342].

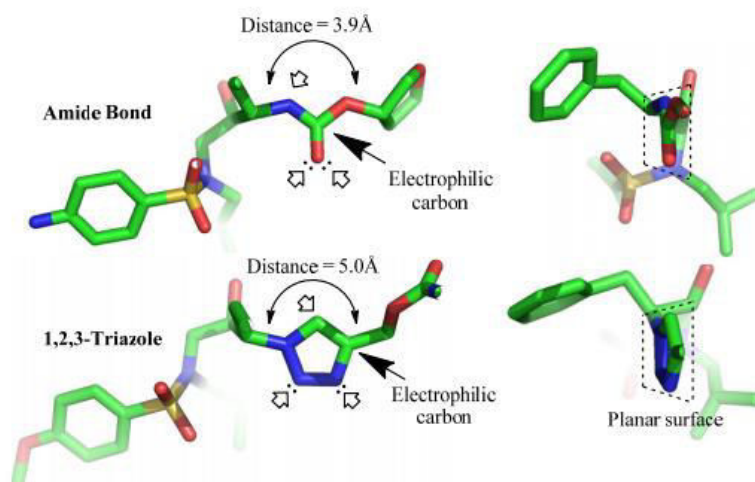


Figure 74: Triazole ring as amide bond bioisosters. The triazole ring also has three-dimensional planar structure that RESEMBLES an amide bond. From [343]

With this regard, the [1,2,3]-triazole ring can hence be used in peptide mimicry; to mimic disulfide bond, building components of peptides' secondary structures, conjugating functional groups together and is also useful in bioconjugations [191]. Click chemistry has also enabled the replacement of amide bonds in peptides, and hence allowing the synthesis of mimetic peptides and the cyclic counterparts [342]. These characteristics brought along multiple applications of click chemistry in the production of peptide-based therapeutics such as those illustrated in Figure 75.

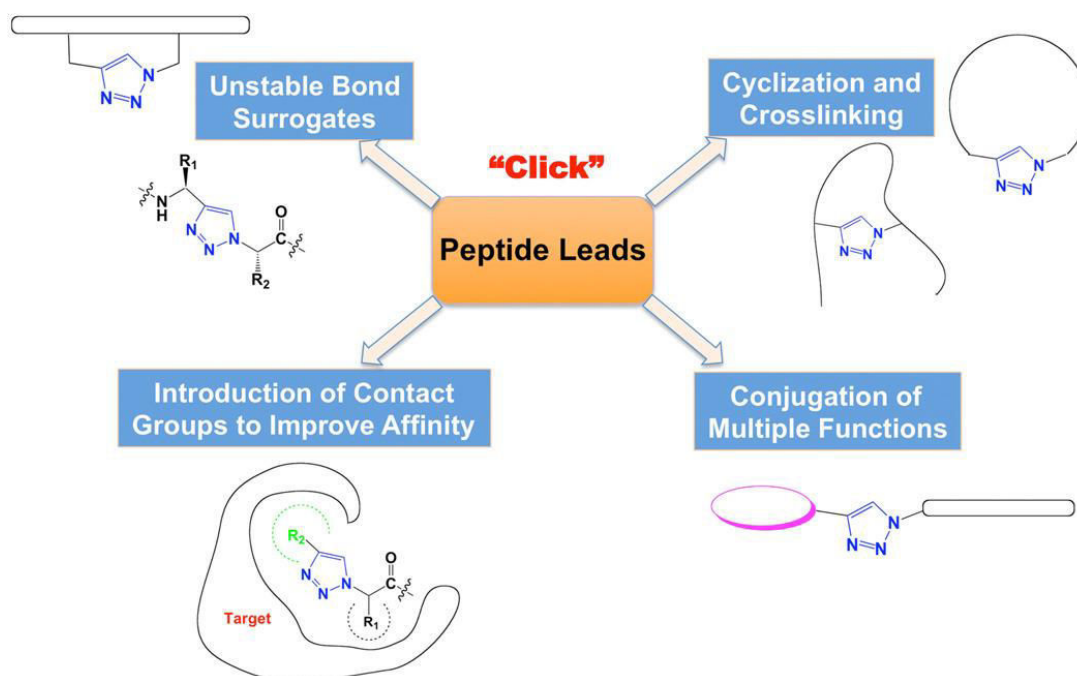


Figure 75: Click chemistry applications in peptide-related fields [191]

In addition, the [1,2,3]-triazole ring is also useful to crosslink and/or act as a linker to cyclise a linear sequence of peptide. This is important to improve its stability and at the same time rigidify the peptide structure into bioactive conformation which could be a way to improve the activity of peptide drugs. Through this method, the secondary structures of peptides could also be imitated through mimicry of β -turn and α -helix conformation and at the same time ensure that their activity will not be hampered [191].

4.1.6 Synthesis plan

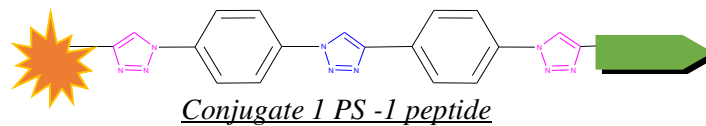
Synthesizing conjugates of a photosensitizer with targeting peptides are commonly done and many successful attempts were already reported in the literature including by our PDTeam research group in Nancy. However, the prospect of having conjugates with different number of photosensitizer and targeting peptides could open up the possibilities of having improved PDT activity and better targeting capability of the conjugate towards its receptor. Hence that becomes the topic of this chapter.

The synthesis work-up was divided into four parts:

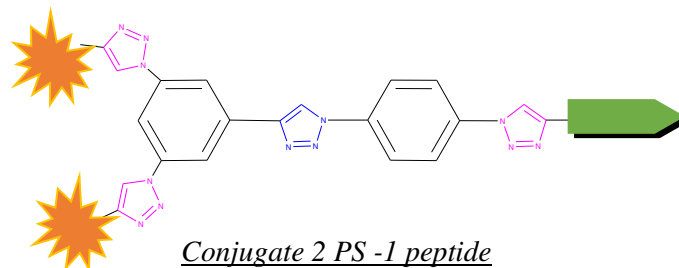
- a. The synthesis of platform building blocks,
- b. The synthesis of porphyrin and different porphyrin-platforms through click chemistry technique,
- c. The synthesis of DKPPR peptide and different DKPPR peptide platforms through click chemistry technique,
- d. The click reaction combining both platforms in (b) and (c).

Three different building blocks were synthesized in multiple steps giving blocks of one-, two- and three-arms. The blocks were then conjugated through click chemistry with porphyrin in step (b) and DKPPR peptide in step (c), yielding one-, two- and three-arms-porphyrin and one-, two- and three-arms-DKPPR peptide respectively. Following substitution of a carboxylic group with an azide group for porphyrin blocks and propargyl group for peptide block, these synthesized arms would be ready for conjugation with each other through another click reaction, giving 9 possibilities of different conjugates ($2^3 = 9$ different conjugates). All of these conjugates are illustrated in Figure 76. However due to time constraint, only one out of the nine conjugates was synthesized.

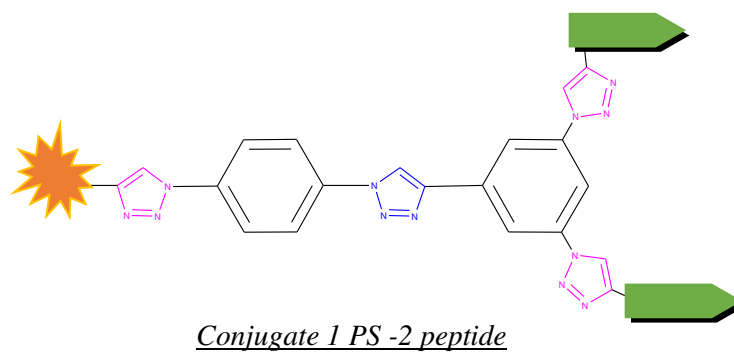
Possibility 1:



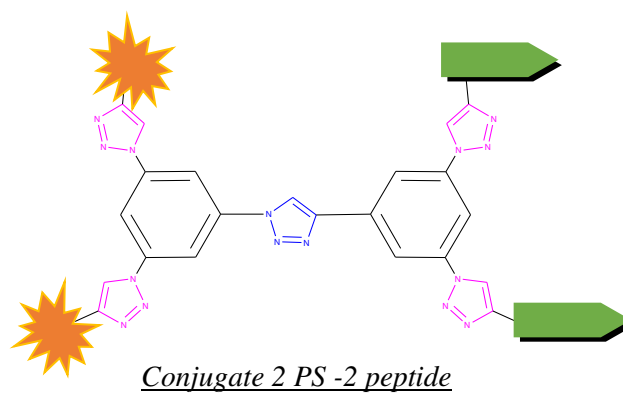
Possibility 2:



Possibility 3:



Possibility 4:



Possibility 5:

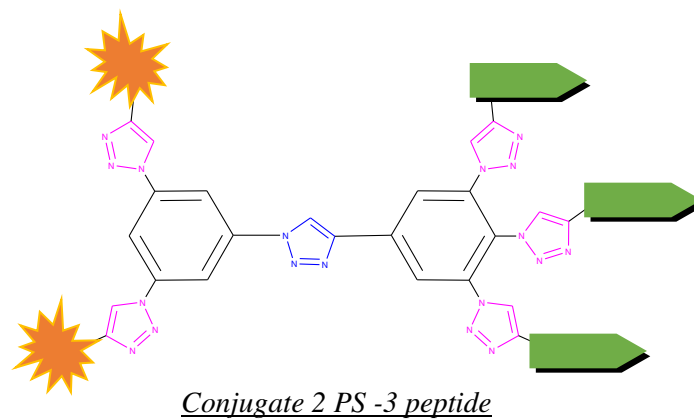
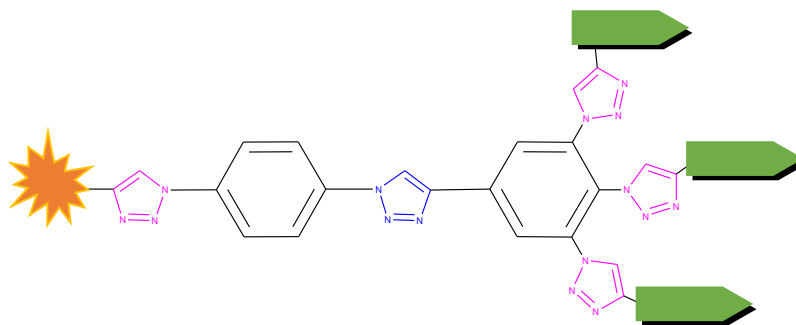


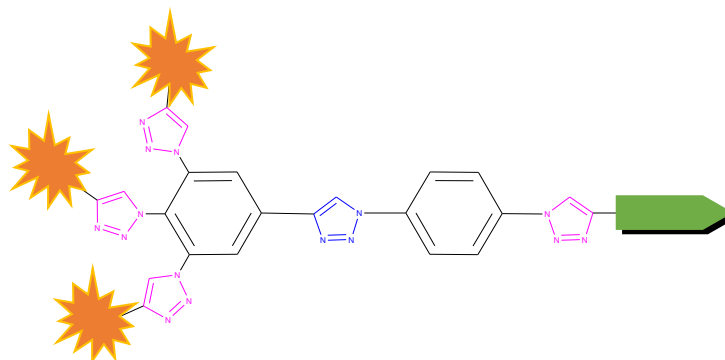
Figure 76: The 9 possibilities of platforms. (Green arrow: peptide, orange star: PS)

Possibility 6:



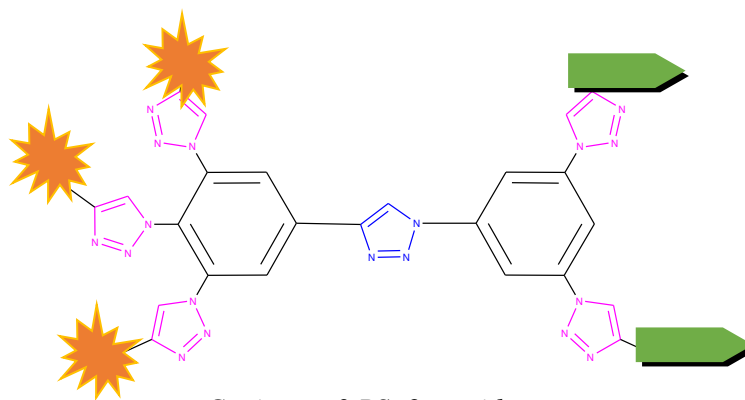
Conjugate 3 PS -1 peptide

Possibility 7:



Conjugate 1 PS -3 peptide

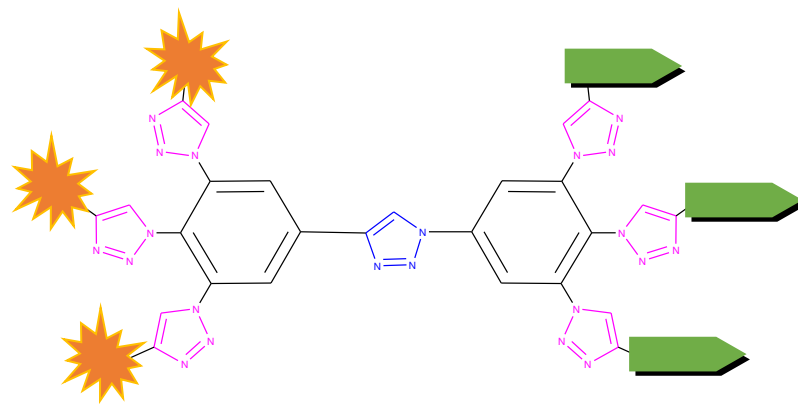
Possibility 8:



Conjugate 3 PS -2 peptide

Figure 76: *Continued*

Possibility 9:



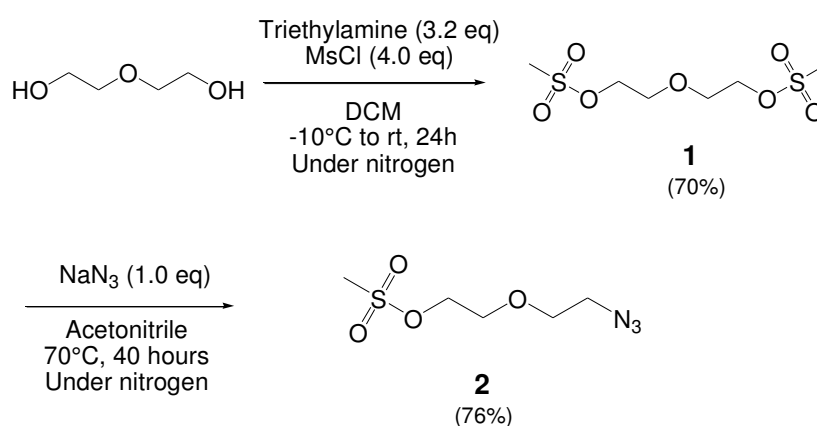
Conjugate 3 PS -3 peptide

Figure 77: *Continued*

4.2 RESULTS AND DISCUSSION

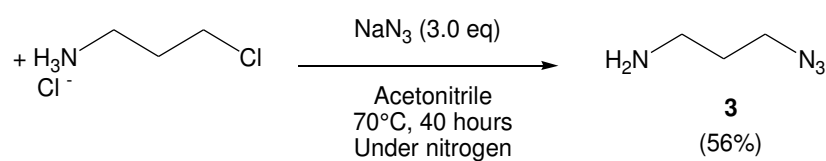
4.2.1 The synthesis of platform building blocks

Scheme 2 illustrated the beginning of the building blocks' syntheses which started with diethylene glycol (DEG). Methanesulfonyl chloride was used to substitute the two hydroxyl groups in DEG into sulfonate groups, giving compound **1** which will then be replaced with an azide group at one end through a reaction with sodium azide, leading to compound **2** with a good yield (76%).



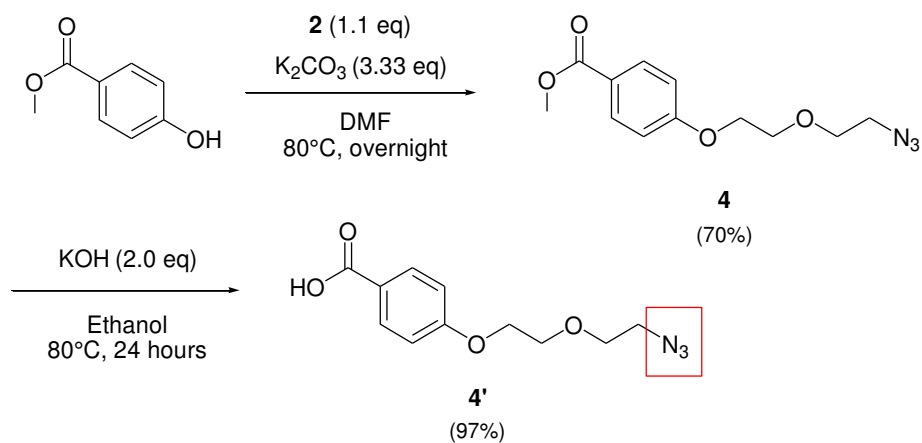
Scheme 2: Synthesis of 2-(2-azidoethoxy)ethyl methanesulfonate from diethylene glycol (MsCl: methanesulfonyl chloride, NaN₃ : sodium azide)

Separately, another azide-spacer (**3**) is synthesized (Scheme 3). Compound **3** is necessary in the second substitution of carboxylic group on porphyrin-blocks at the end of the synthesis work-up as a way to introduce an azide group into the blocks (refer product **10a**).

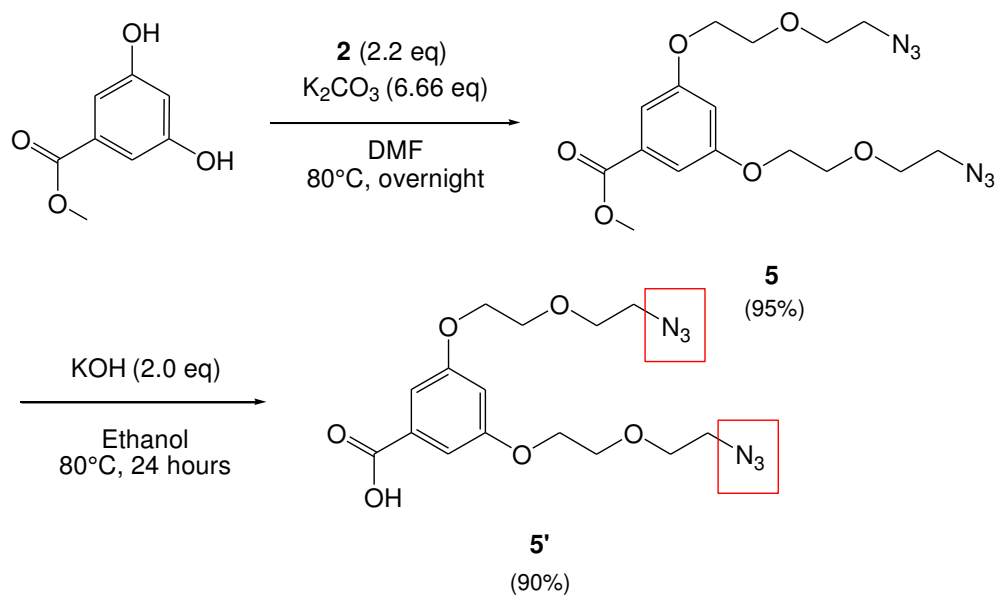


Scheme 3: Synthesis of 3-azidopropan-1-amine. (NaN₃ : sodium azide)

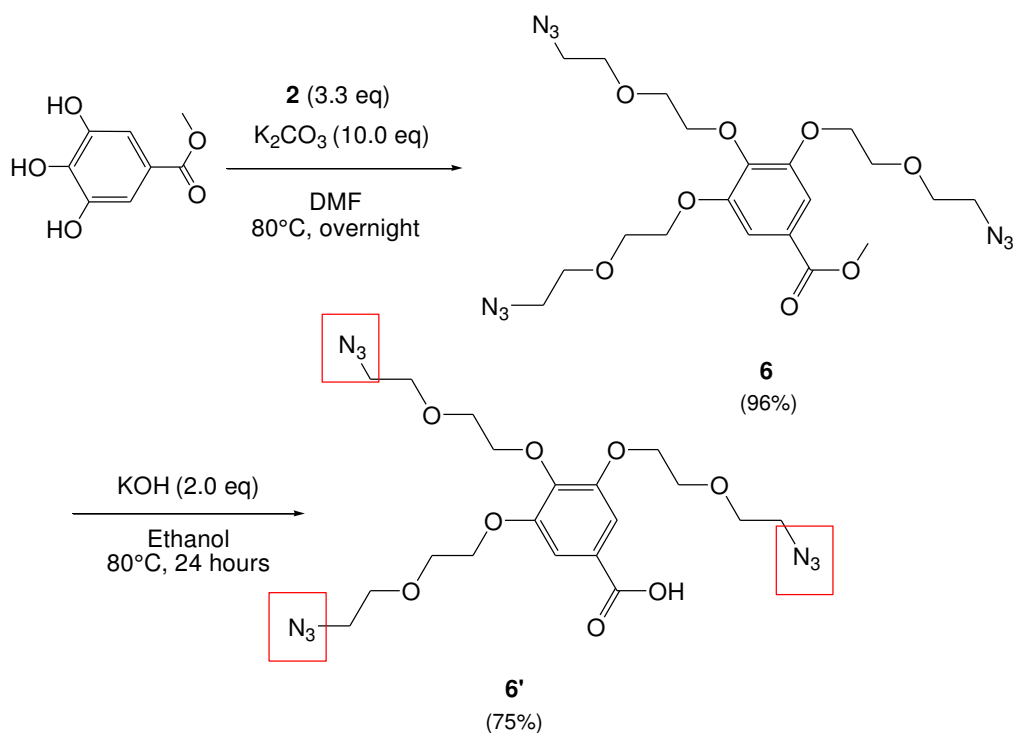
The intermediate spacer **2** subsequently reacted with methyl-4-hydroxybenzoate (Scheme 4), methyl-3,5-dihydroxybenzoate (Scheme 5) and methyl-3,4,5-trihydroxybenzoate (Scheme 6) to give the different building blocks **4'**, **5'** and **6'**.



Scheme 4: Synthesis of one-arm building block from methyl-4-hydroxybenzoate

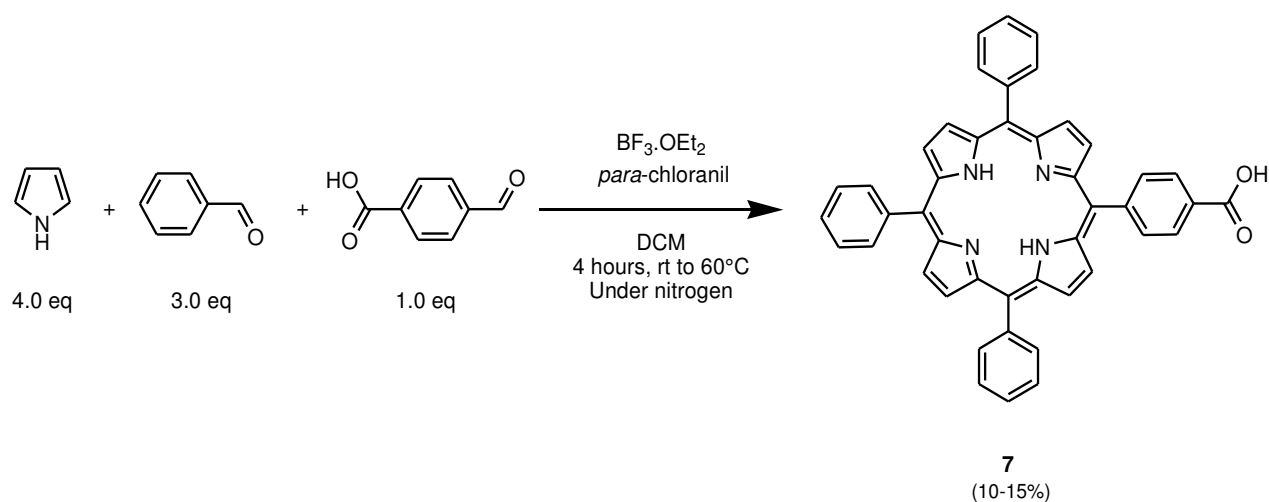


Scheme 5: Synthesis of two-arm building block from methyl-3,5-dihydroxybenzoate



Scheme 6: Synthesis of three-arm building block from methyl-3,4,5-trihydroxybenzoate

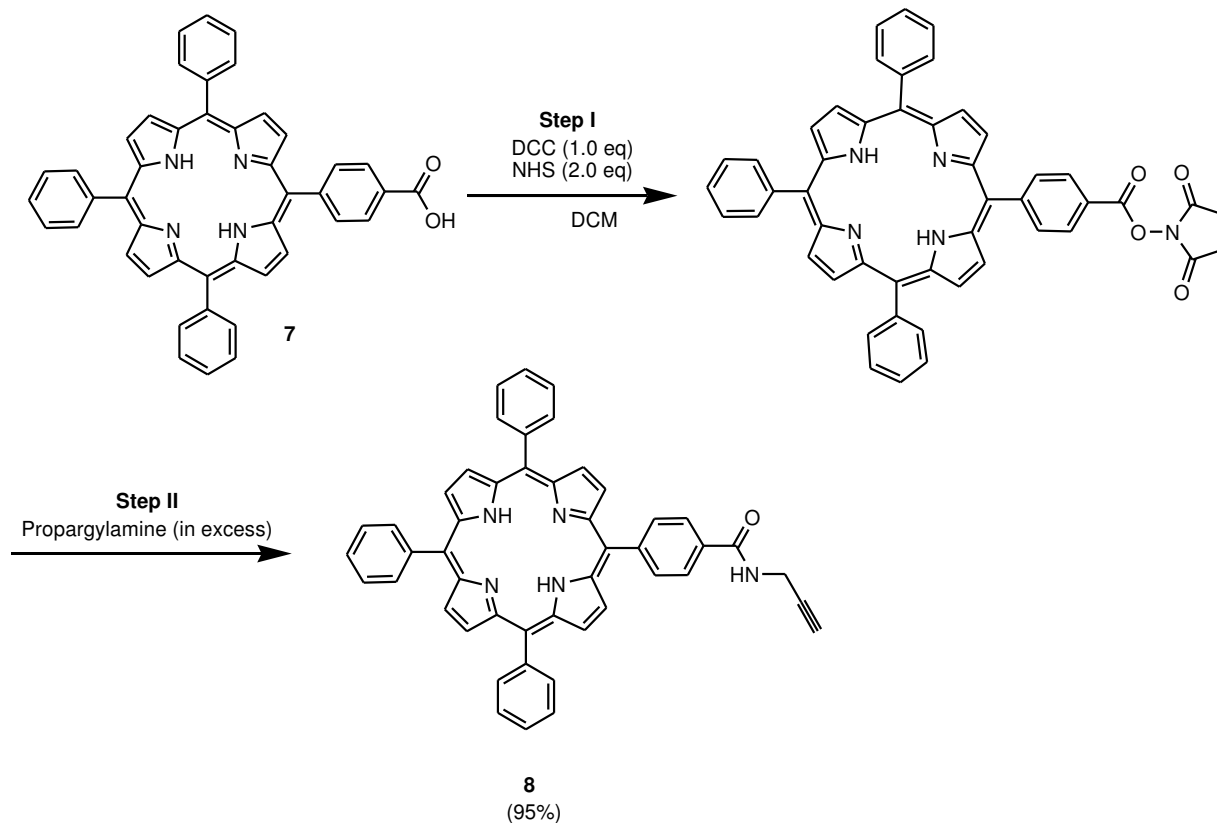
Separately, *meso*-substituted porphyrin P1-COOH (5-(4-carboxyphenyl)-10,15,20-triphenylporphyrin) was synthesized through modified Lindsay's method with a yield of 10-15% (Scheme 7).



Scheme 7: Synthesis of *meso*-substituted porphyrin P1-COOH

The carboxylic group of the porphyrin was activated into *N*-hydroxysuccinimide, NHS-ester to obtain P1-CO-NH-alkyne needed for click reaction with the azide functional group in the building blocks presented before (Schemes 4, 5 and 6). The reaction was conducted as a one-pot reaction with two reaction steps.

As illustrated in Scheme 8, **Step I** involves the formation of P1-CO-NHS and this was checked by TLC [(DCM/EtOH: 97/3) Rf: 0.77 for P1-CO-NHS as compared to Rf: 0.48 for P1-COOH]. **Step II** involves the addition of propargylamine directly into the reaction vessel which leads to the formation of P1-CO-NH-alkyne.



Scheme 8: Introduction of alkyne functional group on porphyrin P1-COOH

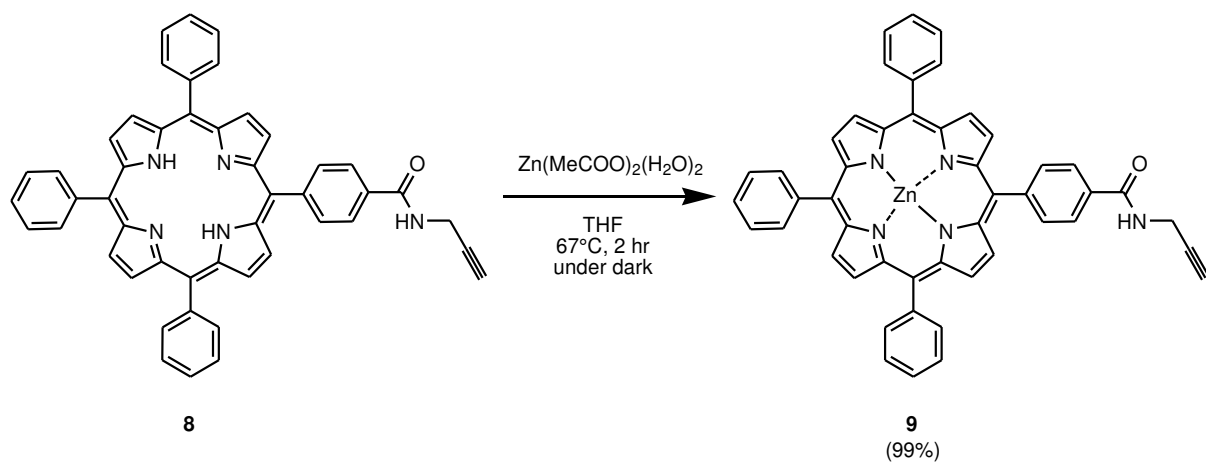
In order to optimize the synthetic reaction yield, different conditions were evaluated by changing the temperature and the reaction time for both steps. Table 16 describes all the reaction conditions tested and the corresponding yields obtained.

Table 16: Different reaction conditions in the synthesis of P1-CO-NH-alkyne

	STEP I		STEP II		Yield
	Temperature	Reaction time	Temperature	Reaction time	
Conventional stirring method					
E1	RT	4 hours	rt	24 hours	58 %
E2	RT	24 hours	rt	24 hours	66%
E3	RT	24 hours	40°C	24 hours	67%
E4	RT	4 hours	40°C	24 hours	66%
E5	40°C	4 hours	40°C	24 hours	69%
E6	40°C	24 hours	40°C	24 hours	95%
Microwave-assisted method					
E7	40°C	30 minutes	40°C	2.5 hours	65%

The reactions E1 to E6 listed in Table 16 were conducted through conventional stirring method, whilst reaction E7 was through microwave-assisted technique. As evidence from the results, all experiments gave in general between 50% and 70% of yield, except experiment **E6** which gave the highest of all. This shows that both time and reaction temperature are important factors to achieve the reaction with a good yield.

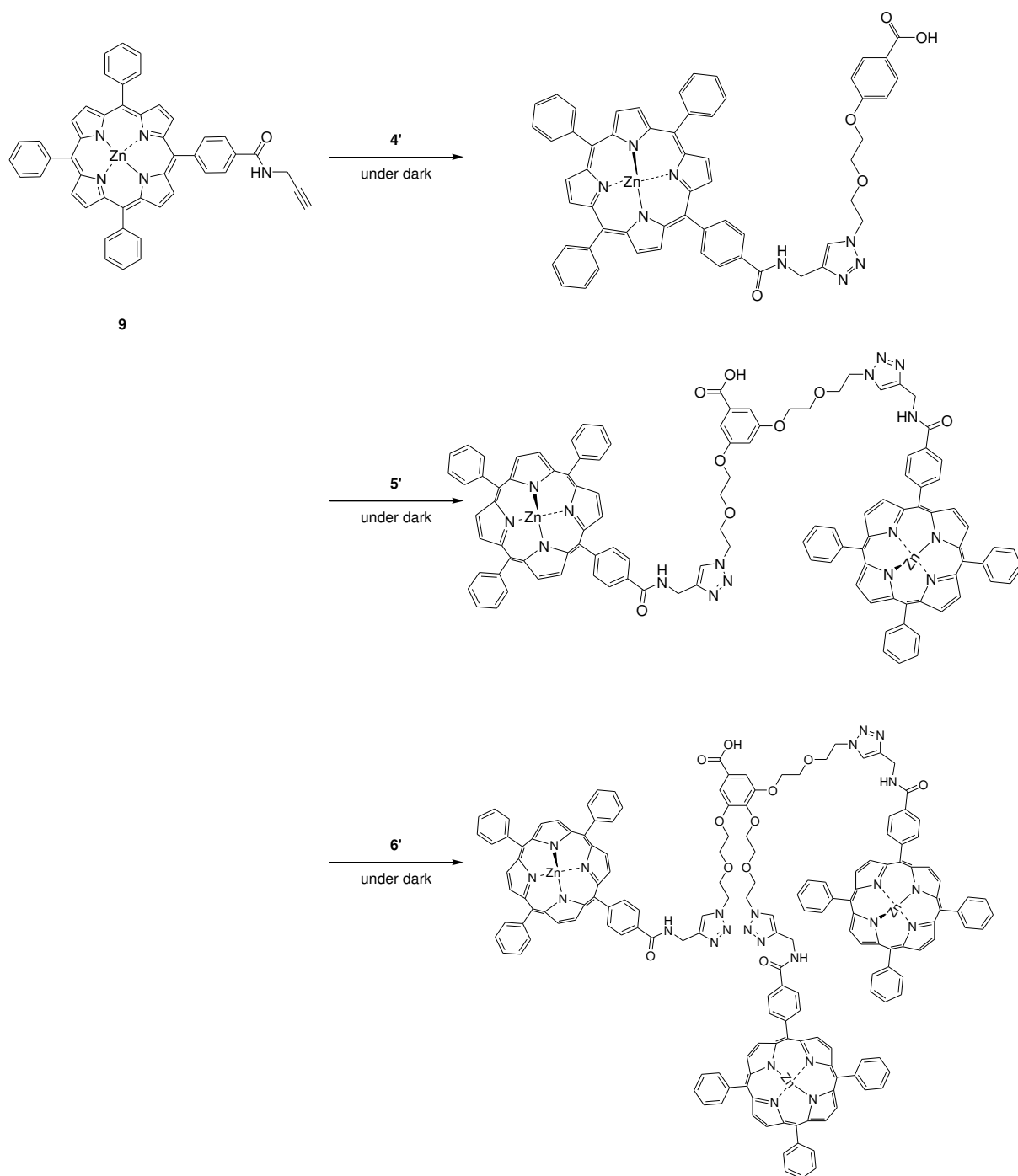
The P1-CO-NH-alkyne thus synthesized was metallated with zinc in order to protect the centre of the porphyrin ring against insertion of copper during click reaction. The metallation process was conducted following the method reported by our team (Colombeau *et al.* [344]). Briefly, the mixture of PS and zinc acetate dihydrate, $Zn(MeCOO)_2(H_2O)_2$ in THF is heated at reflux (67°C) for two hours and the complete metallation was monitored through UV/Visible spectrometry and TLC. The colour of the porphyrin product obtained following metallation is also useful in giving initial information on the presence or absence of metal. It was observed that the colour of porphyrin-Zn is bright purple; porphyrin-Cu is purplish red whilst the non-metallated porphyrin is dark purple. Scheme 9 illustrates the zinc metallation of P1-COOH conducted.



Scheme 9: Metallation of porphyrin P1-COOH by zinc

4.2.2 Building porphyrin blocks through click chemistry

Click chemistry reaction was subsequently conducted between the different building blocks (**4**, **5** and **6**) and porphyrin P1-CO-NH-alkyne-Zn (**9**) to give porphyrin-blocks with one, two and three porphyrin molecules, as illustrated in Scheme 10 (Detailed structure is available in Experimental section).



Scheme 10: Click reaction to produce one- (product **10**), two- (Product **11**) and three-arms (Product **12**) porphyrin blocks

The reaction was conducted in the presence of CuSO_4 as the catalyst and sodium ascorbate as reducing agent to convert copper (II) into copper (I). Different reaction conditions were tested to optimize the reaction yield. The click reaction of one-arm porphyrin block was taken as the study model. Table 17 details out the experimental conditions and percentage of yield obtained for the products.

Table 17: Different click reaction conditions between compound P1-CO-NH-alkyne and one-arm building block (10)

Solvent	Trial	Method	Temperature	Time	Nitrogen	Yield
DMF	E8	Mechanical stirring	rt	Overnight	No	7%
	E9	Mechanical stirring	rt	Overnight	Yes	10%
	E10	Mechanical stirring	50°C	Overnight	Yes	74%
	E11	Mechanical stirring	80°C	Overnight	Yes	74%
	E12	Microwave	50°C	45 minutes × 2*	No	42%
	E13	Microwave	80°C	45 minutes × 2*	No	59%
	E14	Microwave	50°C	45 minutes × 2*	Yes	86%
	E15	Microwave	80°C	45 minutes × 2*	Yes	88%
THF/Water (4:1)	E16	Mechanical stirring	rt	Overnight	No	10%
	E17	Mechanical stirring	rt	Overnight	Yes	19%
	E18	Mechanical stirring	80°C	3 hours	Yes	55%
	E19	Mechanical stirring	80°C	Overnight	Yes	96%
	E20	Microwave	80°C	45 minutes	No	88%
	E21	Microwave	80°C	45 minutes × 2*	No	96%
	E22	Microwave	80°C	90 minutes	No	91%
	E23	Microwave	80°C	90 minutes × 2*	No	97%

* (× 2) means that the catalyst was added again at the end of the first round of reaction.

Two different solvents were tested: dimethylformamide (DMF) and a mixture of tetrahydrofuran (THF) and water at 4:1 mixture. These solvent were chosen based on the data from the literature, in which it was found that many porphyrin-based click reactions were conducted in either DMF or THF/water. These studies have shown that a good and quantitative yield of products was obtained [345-348].

Two methods were used for the reactions: either by conventional stirring or by using the microwave, at an elevated temperature or at room temperature. The effect of nitrogen is also evaluated on the yield of the product, which has shown that reaction under nitrogen could significantly improve the yield as shown by trial E14 and E15 (as compared to E12 and E13).

In general, the reactions in THF/water give higher yields of product **10**. As expected, by comparing conventional stirring and microwave technique, the microwave technique gives a higher yield in a shorter time, which proves to be an effective synthesis technique. Between E21 and E23, there are no significant different in term of yield although the time of reaction in E21 is half of the time in E23.

Sodium ascorbate which is commonly used as the copper (II) reducing agent in click chemistry reactions may be having some drawbacks due to its low stability at high temperatures (and even at room temperature if left for a long time). Hence to overcome the risk of its degradation, we made successive additions of sodium ascorbate so that reactive ascorbate is continuously present in the reaction medium. This was found to be beneficial in increasing the overall product yield as evident from trial E21 (**96%**) (as compared to E20 (88%)) and E23 (**97%**) (as compared to E22 (91%)).

Based on the results obtained, the best conditions achieved by both solvent through the two synthesis methods (mechanical stirring and microwave) were adapted in the synthesis of two-arm porphyrin blocks and three-arm porphyrin blocks. Based on Table 17, the conditions hence chosen were E11, E15, E19 and E21 and the results are described in Table 18 and Table 19 for two-arm block and three-arm block respectively.

Table 18: Different click reaction conditions between compound P1-CO-NH-alkyne and two-arm building block (11)

Solvent	Trial	Method	Temperature	Time	Nitrogen	Yield
DMF	E24	Mechanical stirring	80°C	Overnight	Yes	59%
	E25	Microwave	80°C	45 minutes × 2*	Yes	37%
	E26	Microwave + Mechanical stirring	80°C rt	45 minutes × 2* 72 hr	Yes Yes	80%
THF : Water	E27	Mechanical stirring	80°C	Overnight	Yes	nd [#]
	E28	Microwave	80°C	45 minutes × 2*	No	nd [#]

[#]nd: not determined

* (× 2) means that the catalyst was added again at the end of the first round of reaction.

Table 19: Different click reaction conditions between compound P1-CO-NH-alkyne and three-arm building block (12)

Solvent	Trial	Method	Temperature	Time	Nitrogen	Yield
DMF	E29	Mechanical stirring	80°C	Overnight	Yes	nd [#]
	E30	Microwave	80°C	45 minutes × 2*	Yes	nd [#]
	E31	Microwave + Mechanical stirring	80°C rt	45 minutes × 2* 7 days	Yes Yes	68%
THF : Water	E32	Mechanical stirring	80°C	Overnight	Yes	nd [#]
	E33	Microwave	80°C	45 minutes × 2*	No	nd [#]
	E34	Microwave + Mechanical stirring	80°C rt	45 minutes × 2* 120 hr	Yes Yes	77%

[#]nd: not determined

* (× 2) means that the catalyst was added again at the end of the first round of reaction.

As presented in Table 18 and 19, the two- and three-arms blocks were more difficult to be obtained even by using the method proven to be effective for the synthesis of one-arm porphyrin block. Two-arm porphyrin block was only obtained in DMF at a lower yield as compared to the same reaction conditions for one-arm block. This is expected due to the fact that the coupling of more molecules into one building block will necessitate a stronger reaction condition such as higher temperature or longer reaction time. Thus, a subsequent reaction was conducted for E25; following the microwave irradiation, the reaction was left to stir for approximately 72 hours, yielding the expected product (E26) with 80% yield.

The reaction conducted in THF did not give the expected product despite multiple attempts. The molecule obtained following column purification was nevertheless analysed by ^1H NMR. The spectrum revealed that porphyrin was linked only on one of the arms. This shows that the choice of solvent is crucial. The type of solvent may help to improve the flexibility of the molecule and hence reducing the steric hindrance.

As for three-arms block, no product was obtained for all four initial reaction conditions. The huge molecular size also possesses a bigger steric hindrance as compared to the two previous molecules hence proving to be more difficult to be clicked with the incoming porphyrin molecule. Reaction E30 and E33 were then let to continue stirring at room temperature to allow more time for the reaction to take place and the expected product (E33) was obtained with 77% yield.

The porphyrin building blocks with one-, two-, and three-arm were successfully synthesized with the best yield of 97%, 80% and 77% respectively, and characterized by ^1H NMR and mass spectrometry.

4.2.3 Photophysical properties

A. Absorption

Figure 77 illustrate the absorption spectra of porphyrin P1-COOH and the three porphyrin blocks. As can be seen, the absorption spectra of the blocks differ from the spectrum of P1-COOH. The Soret band of P1-COOH is at 414 nm with four other Q-bands at 512 nm, 546 nm, 589 nm and 645 nm. The porphyrin blocks on the other hands show a Soret band at 421 nm and two Q-bands at 557 nm and 597 nm. These changes occur due to the metallation of porphyrin. Following metallation, the four Q-bands of porphyrin present in the visible region collapsed into two bands due to the formation of a more symmetrical ring, with no significant effect on the Soret band. The Soret band however is slightly shifted towards a higher wavelength.

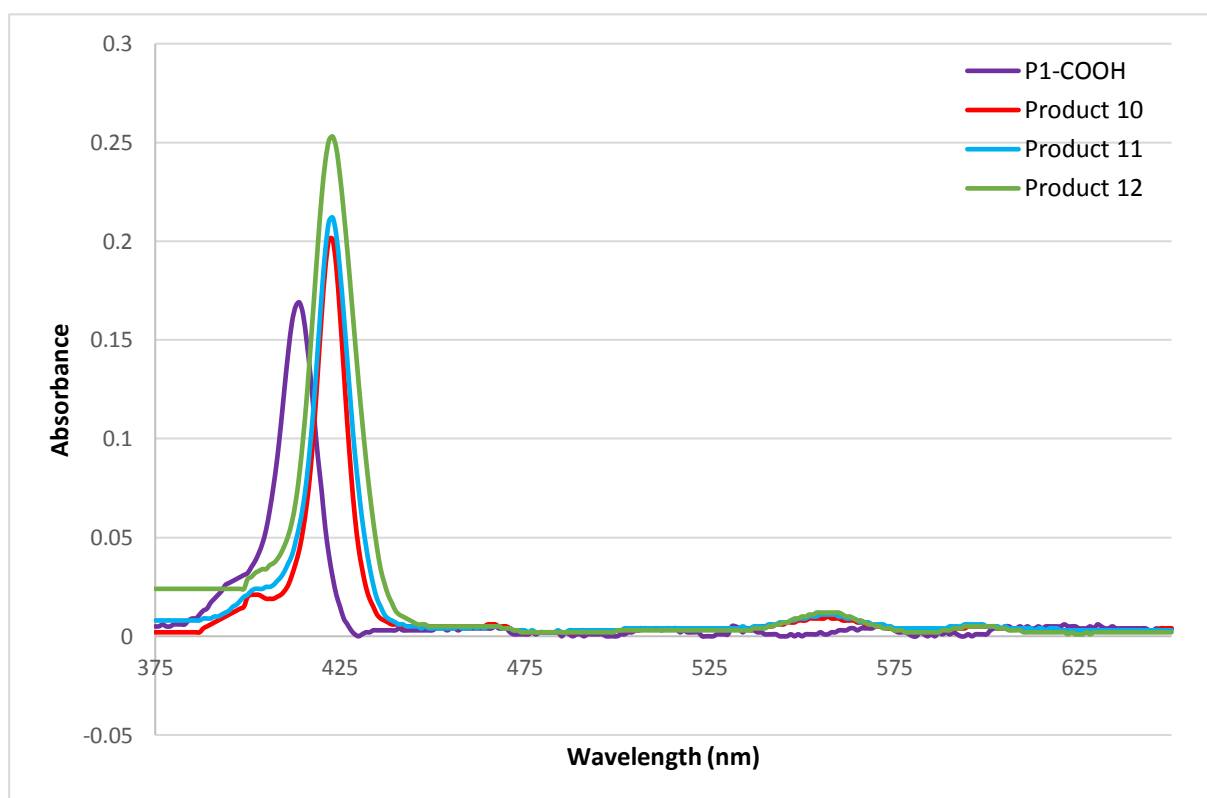


Figure 77: Absorption spectra of P1-COOH and the different porphyrin-Zn blocks (in ethanol)

The two Q-bands of the metallated porphyrin are called α and β , and their relative intensities can be correlated with the stability of a porphyrin-Zn complex. From Figure 77, it is evident that the porphyrin blocks demonstrated higher α band UV absorbance as compared to the β band. This means that the incorporated zinc is forming a stable square planar complex with the porphyrin [349]. Table 20 shows the molar extinction coefficient values of all the synthesized products.

Table 20: Molar extinction coefficient, ϵ of the synthesized products, in ethanol (L/mol.cm)

Product	Soret	Q _{IV}	Q _{III}	Q _{II}	Q _I	Q _a	Q _B
P1-COOH	414(173 304)	512(28 330)	546(17 560)	589(9520)	645(4230)	-	-
Product 10	421(245 332)	-	-	-	-	557 (60 205)	597 (4 000)
Product 11	421(250 243)	-	-	-	-	557(100 000)	597(10 000)
Product 12	421(266 839)	-	-	-	-	557(124 551)	597(10 000)

B. Fluorescence

The fluorescence emission of the building blocks was found to be lower than the standard TPP and from P1-COOH (Figure 78). This is expected due to the presence of zinc in the porphyrin ring which commonly causes reduction in fluorescence produced by photosensitizers. The wavelength of fluorescence emission was also shifted to lower wavelengths; at around 610 nm and 660 nm as compared to 660 nm and 720 nm for the standard TPP and porphyrin.

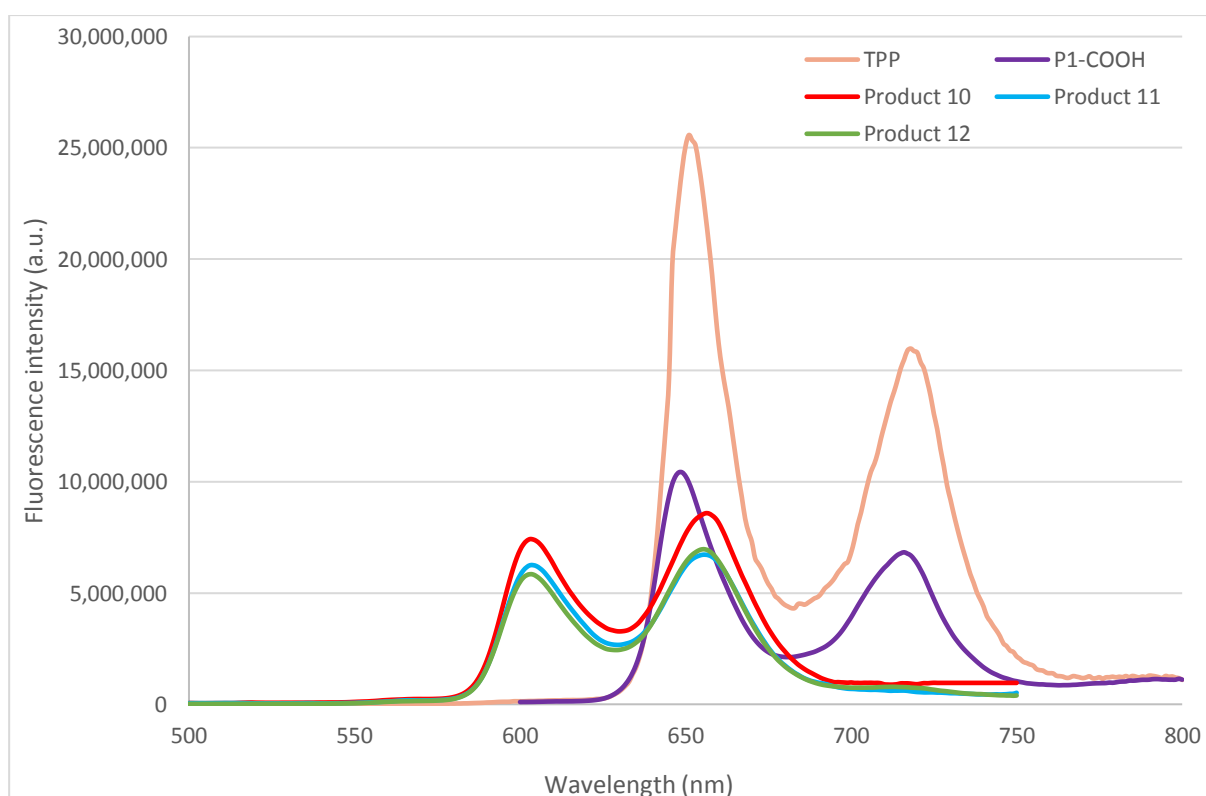


Figure 78: Fluorescence emission spectra of P1-COOH ($\lambda_{exc} = 414$ nm) and different porphyrin-Zn blocks ($\lambda_{exc} = 421$ nm) in comparison to TPP as standard (in ethanol)

Figure 79 shows the fluorescence decay of P1-COOH and the different porphyrin blocks. The fluorescence of the Products 10 and 11 was found to decay faster (1.9 ns) than Product 12, which decayed in between 2.2 to 10.6 ns. The fluorescence decay of Product 12 has some similarities with that of P1-COOH (10 ns).

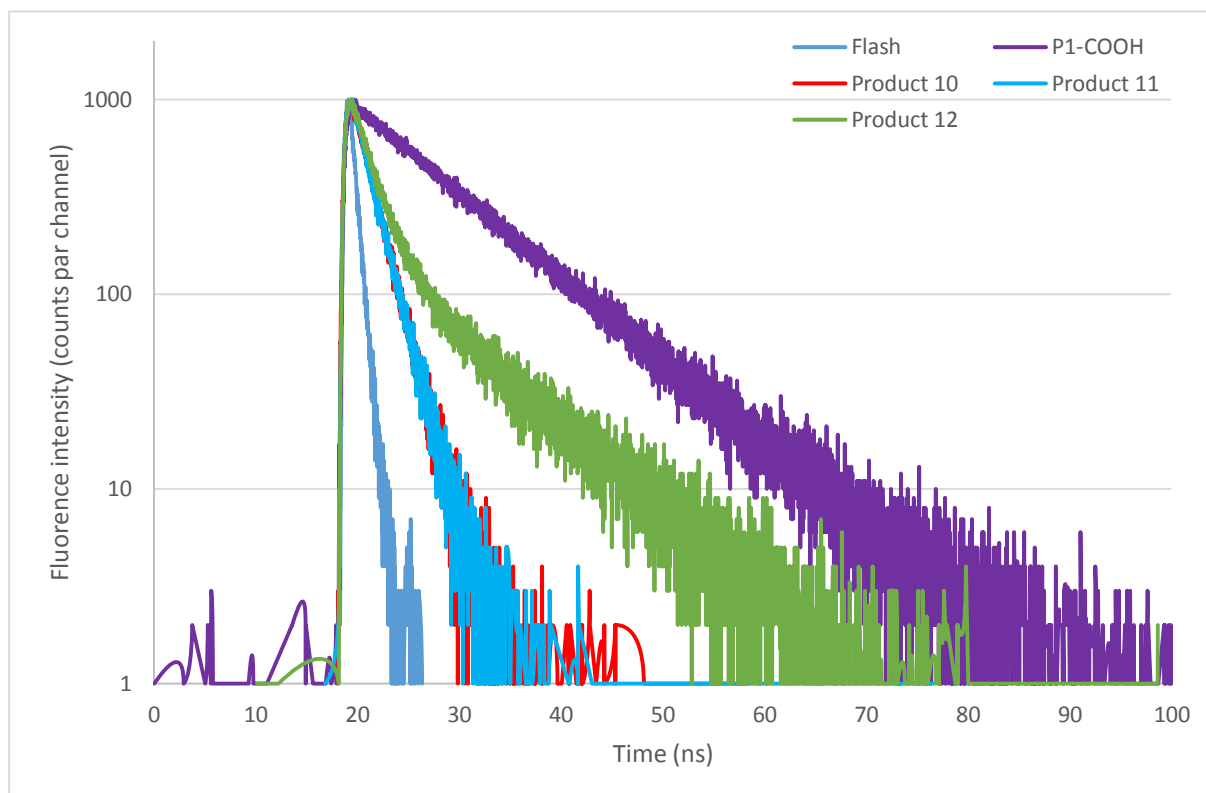


Figure 79: Fluorescence lifetime for P1-COOH ($\lambda_{exc} = 414$ nm) and different porphyrin-Zn blocks ($\lambda_{exc} = 421$ nm) (in ethanol)

C. Singlet oxygen

Singlet oxygen production was detected in the infrared region, following excitation of the porphyrin (at 414 nm) and the porphyrin blocks (at 421 nm). The spectra show a bell-type graph, with the maximum emission at 1270 nm. Figure 80 illustrate the singlet oxygen production spectra of the products. The porphyrin blocks show similar singlet oxygen production ability with the standard and porphyrin, although Product **10** shows much higher singlet oxygen quantum yield as compared to Product **11** and **12**.

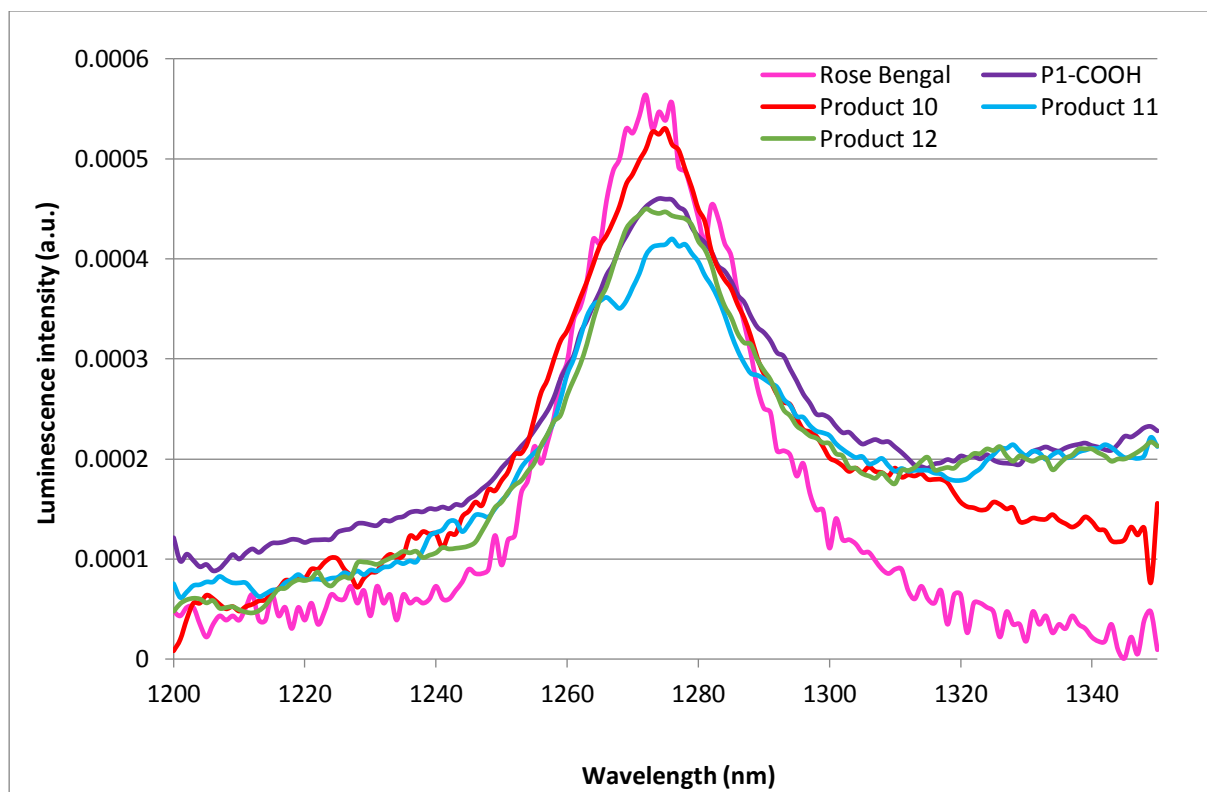


Figure 80: Singlet oxygen production spectra of P1-COOH ($\lambda_{exc} = 414$ nm) and different porphyrin-Zn blocks ($\lambda_{exc} = 421$ nm) in comparison to Rose Bengal as standard (in ethanol)

Figure 81 shows the singlet oxygen luminescence decay of P1-COOH and the porphyrin-Zn blocks. All the compounds showed monoexponential decay, with three phases: phase (i) shows an increase of luminescence, followed by a plateau in phase (ii), and phase (iii) is the decay of the singlet oxygen luminescence.

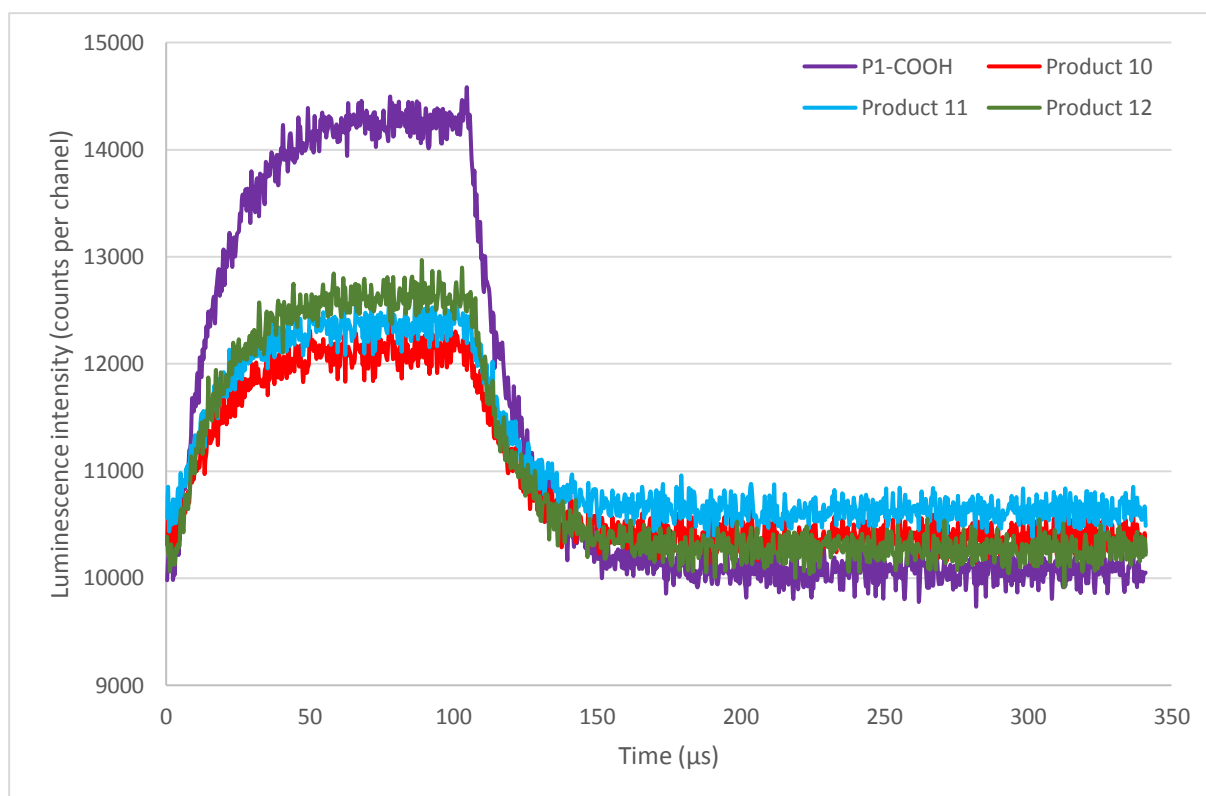


Figure 81: Singlet oxygen production lifetime of P1-COOH ($\lambda_{exc} = 414$ nm) and different porphyrin-Zn blocks ($\lambda_{exc} = 421$ nm) (in ethanol)

Table 21 summarized the photophysical properties of the porphyrin-Zn blocks. In general, it appears that the number of porphyrin does not influence significantly the photophysical properties. The absorption and fluorescence spectra of compounds **10**, **11** and **12** are very similar to each other. The molar extinction coefficient (ϵ), fluorescence quantum yield and singlet oxygen quantum yield also are not influenced significantly by the number of porphyrin units in the blocks.

Table 21: Fluorescence quantum yield, singlet oxygen quantum yield, fluorescence lifetime and singlet oxygen lifetime of the synthesized products, in ethanol (L/mol.cm)

Product	Φ_f^a	Φ_{Δ}^b	τ_f^c	τ_{Δ}^d
P1-COOH	0.08*	0.50	10.1	16
Product 10	0.08 [§]	0.54	1.9	18
Product 11	0.07 [§]	0.43	1.9	16
Product 12	0.06 [§]	0.46	2.2-10.6	16

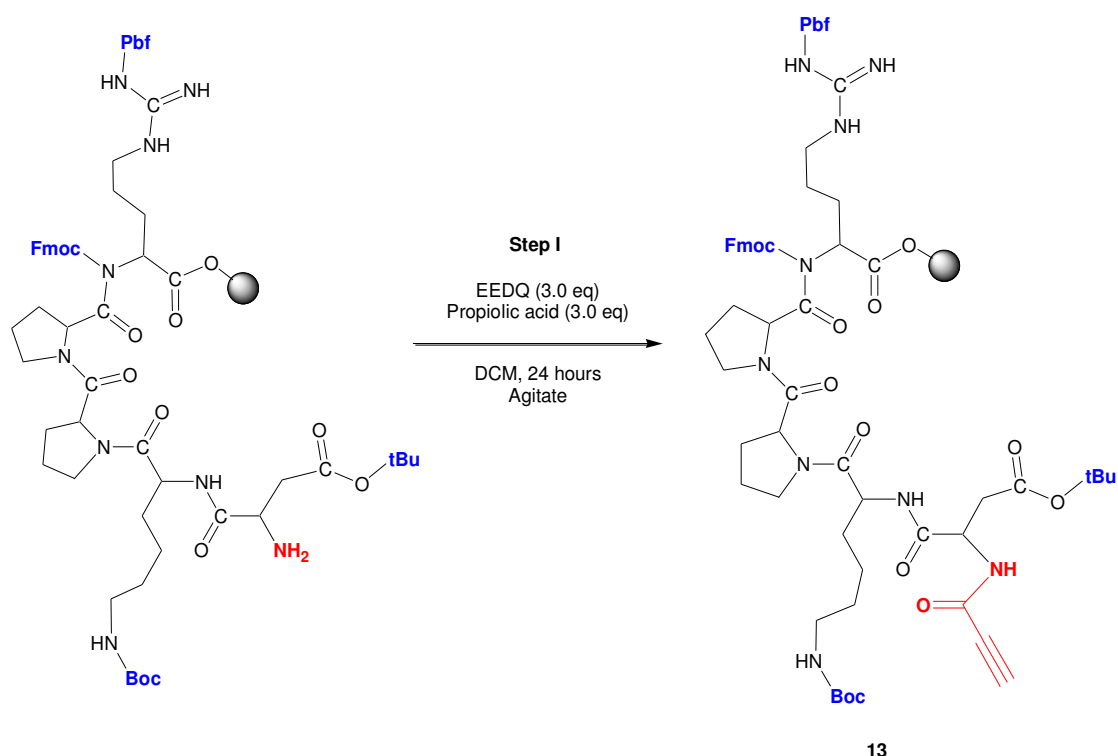
^a Fluorescence quantum yield relative to fluorescence of TPP as a standard (* $\lambda_{exc} = 414$ nm, [§] $\lambda_{exc} = 421$ nm); ^b Singlet oxygen production quantum yield relative to Rose Bengal as standard; ^c Fluorescence lifetime (ns); ^d Singlet oxygen lifetime (μ s).

4.2.4 Building DKPPR blocks through click chemistry

In the third part of the synthesis approach, the DKPPR peptide was synthesized through solid-phase synthesis technique. The synthesis was done using either Wang resin or 2-chlorotrityl resin, depending on whether the subsequent reactions will be conducted on solid or liquid phase:

- For subsequent reaction on solid phase, the peptide is conserved on the resin and hence Wang resin is used,
- For subsequent reaction on liquid phase synthesis, the peptide needs to be removed from the resin, whilst maintaining the protection groups on the side chain of amino acids. 2-chlorotrityl resin is used because it is more acid labile and could be removed under mild acidic condition without affecting the side chains protections.

The DKPPR peptide in its protected form has a single unprotected amino group on the aspartic acid, D for controlled introduction of alkyne functional group necessary for further click reaction. The modification of the amine group to contain an alkyne was completed without difficulties on both solid and liquid phase (Scheme 11).



Scheme 11: Introduction of alkyne functional group on the NH_2 -terminal of aspartic acid. The example here is conducted on solid phase (black circle represent Wang resin)

After the synthesis of DKPPR with an alkyne functional group, click reaction was conducted between DKPPR-alkyne and the building blocks **4'**, **5'** and **6'**. Three different experimental approaches were carried out: two on solid phase and one on liquid phase (Figure 82).

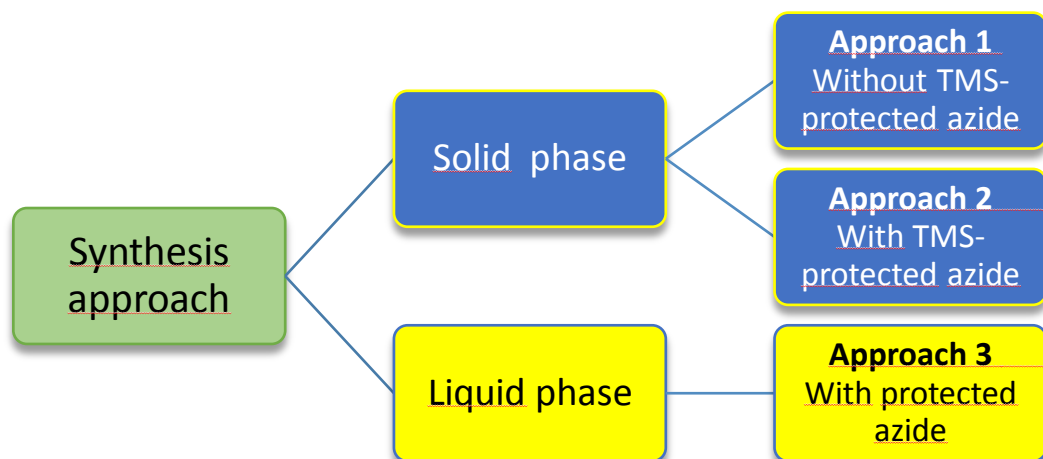
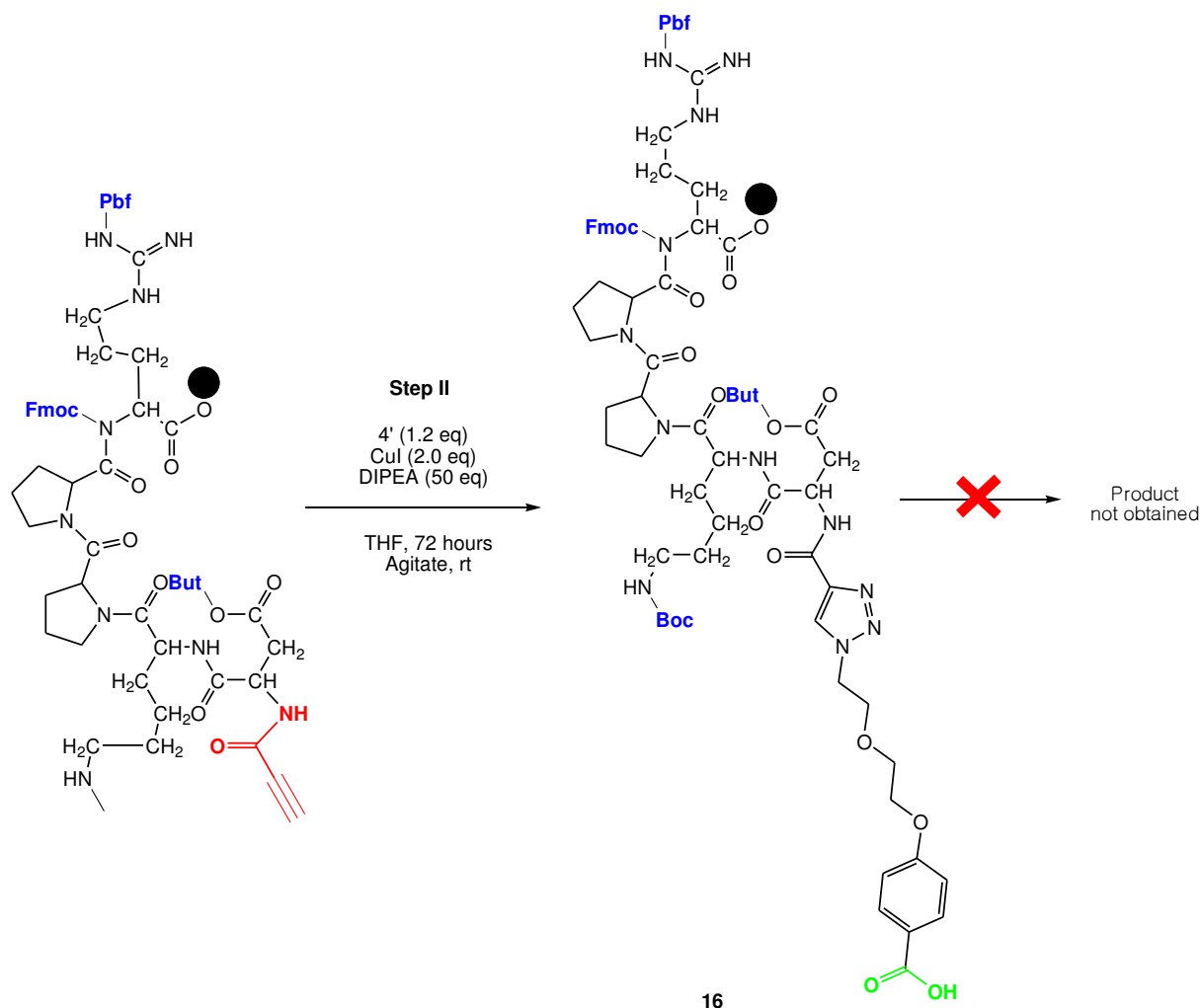


Figure 82: The synthesis approaches to synthesize DKPPR-building blocks

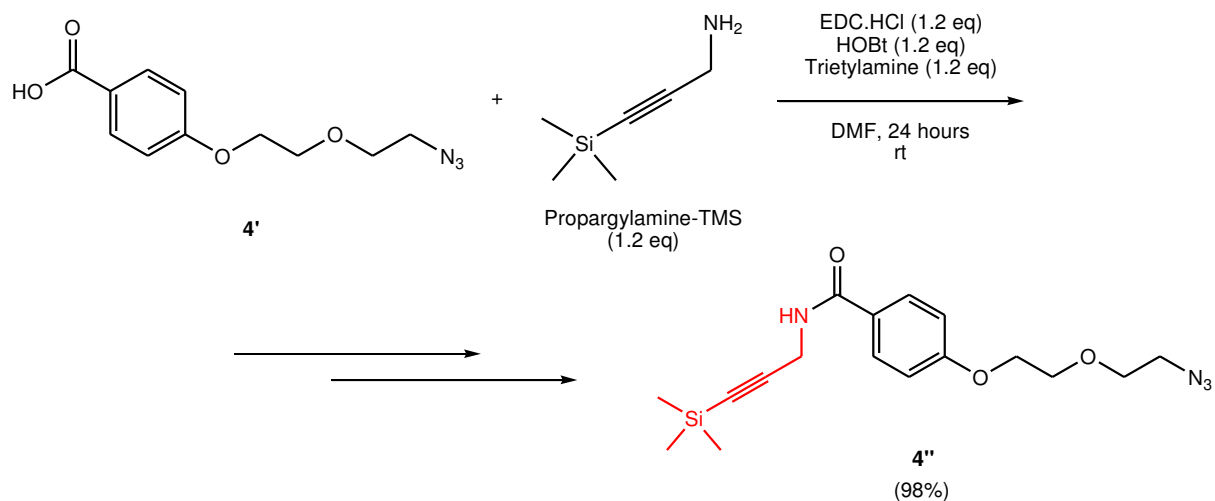
The synthesis **Approach 1** through solid phase synthesis was first attempted with building block of one-arm, compound **4'**, as illustrated in Scheme 12 (**Step II**). Protected DKPPR on Wang resin was clicked with **4'** in the presence of CuI and DIPEA and the reaction was allowed to stir at room temperature for 72 hours. The reaction was then continued to introduce a second alkyne group on the carboxylic group present on **4'** (green).



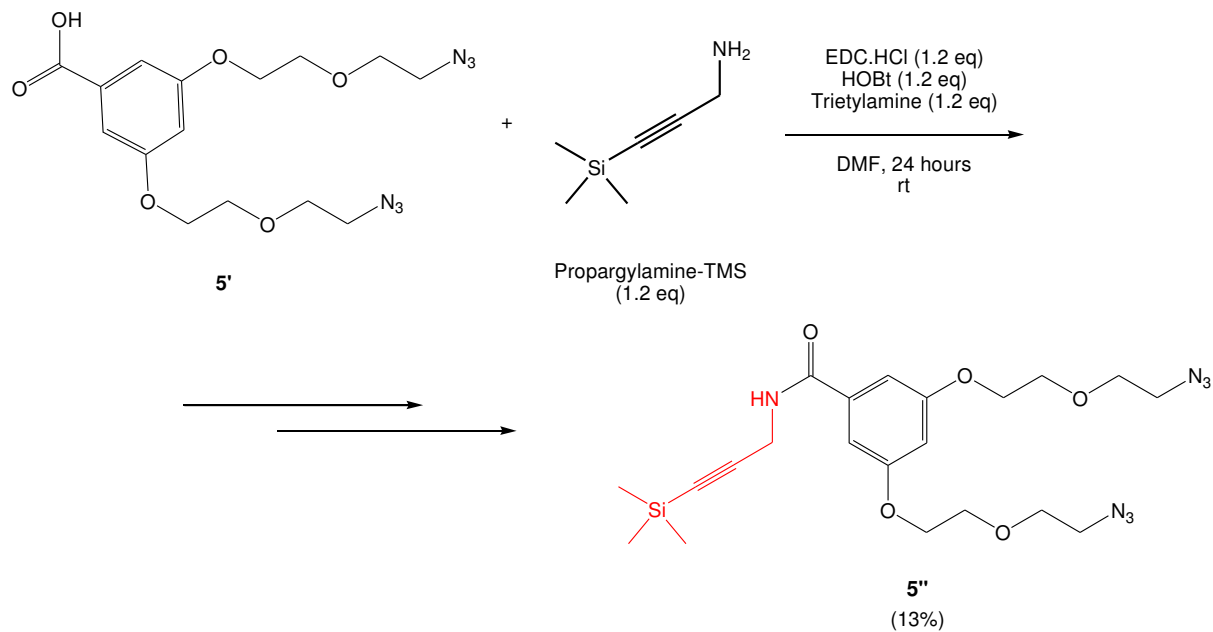
Scheme 12: Click reaction of DKPPR-alkyne and 4'

However, multiple attempts made were unsuccessful, despite changing different coupling agents (i. carbonyldiimidazole, CDI, ii. EDC.HCl/HOBt) and prolonging reaction time (up to five days). Upon cleavage from the solid support and purification by HPLC, compound **16** was isolated as the major product, based on mass analysis (m/z : 914.42, found: $M[+]$ 915.45, $M[2+]$: 458.45). This failure to substitute the carboxyl group (coloured in green) into alkyne group could be due to steric hindrance of this molecule which is still attached on solid support resin, which may prevent the insertion of alkyne at the end of the block.

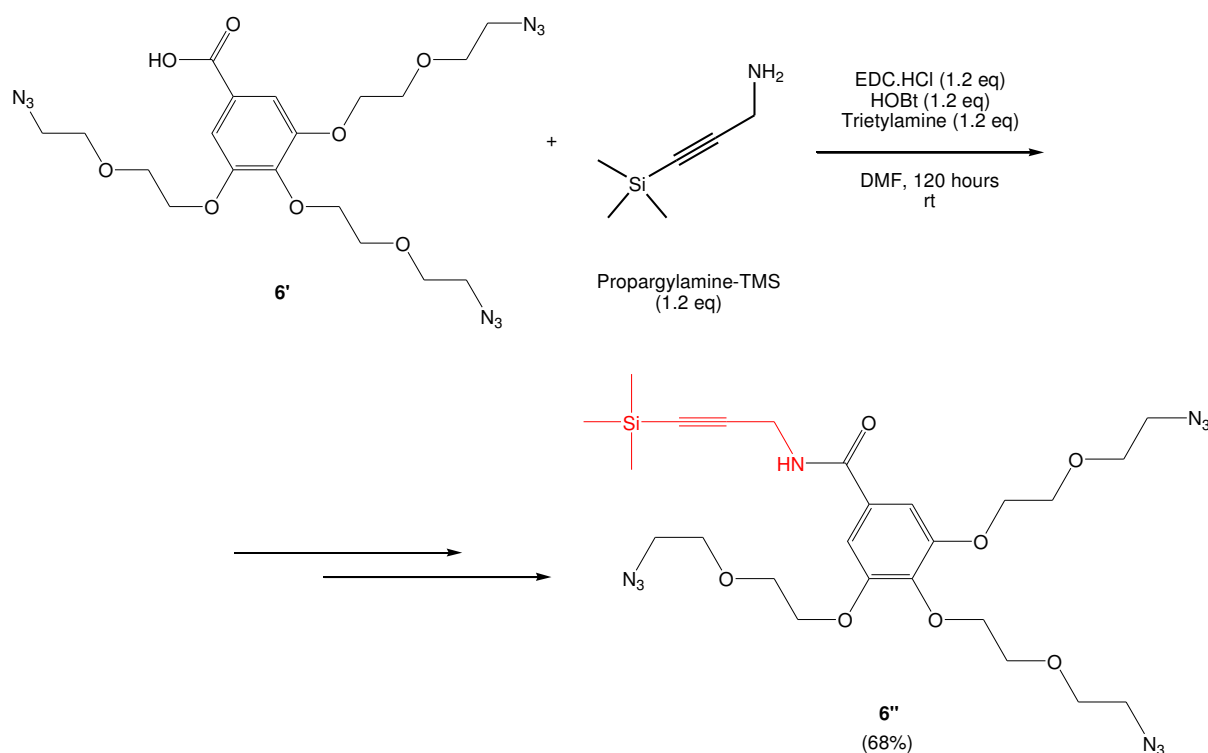
The synthesis approach was then changed. In **Approach 2**, the building blocks **4'**, **5'** and **6'** were modified with the introduction of TMS-protected alkyne on the carboxylic group of the building blocks, leading to the formation of one- (**4''**), two- (**5''**) and three-arm (**6''**) building blocks (Schemes 13, 14 and 15 respectively).



Scheme 13: Synthesis of modified building block 4''



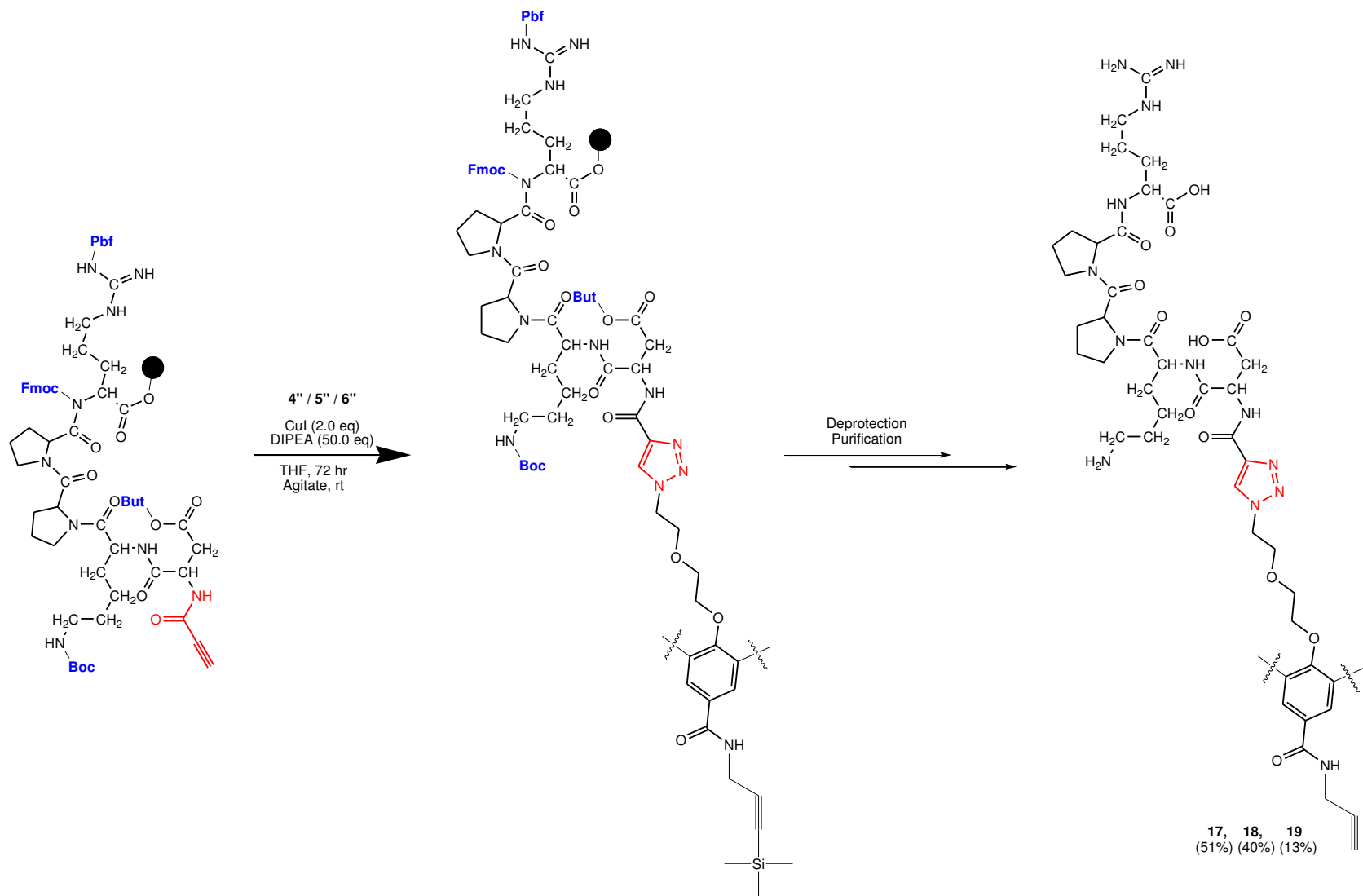
Scheme 14: Synthesis of modified building block 5''



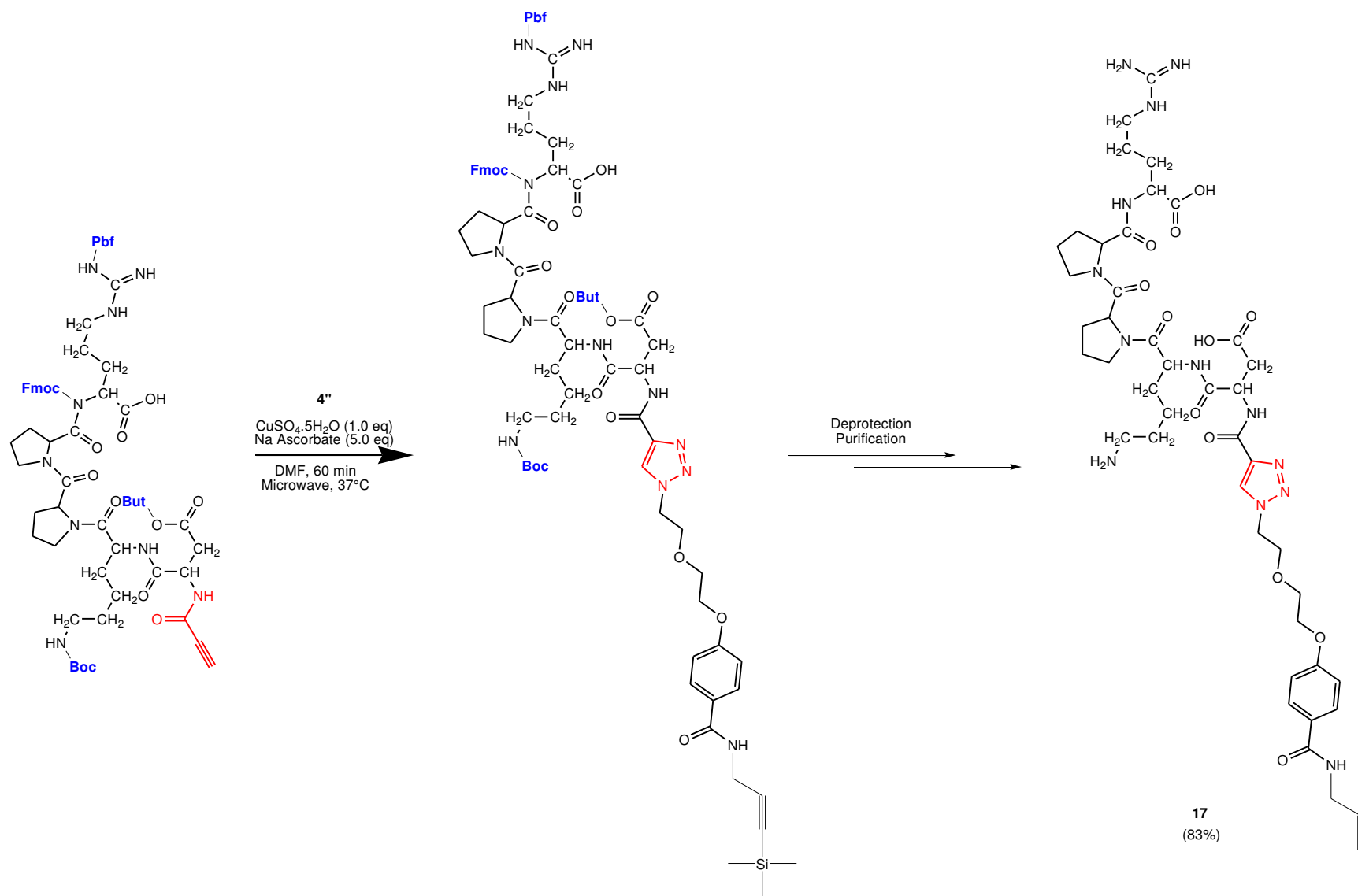
Scheme 15: Synthesis of modified building block **6''**

DKPPR-arm-alkyne products were successfully obtained following deprotection with a mixture of TFA/TIPS/water (95%:2.5%:2.5%) and purification by RP-HPLC, giving one-arm DKPPR block (**17**), two-arms DKPPR block (**18**) and three-arms DKPPR block (**19**) (Scheme 16). Yields of the one- and two-arm products obtained were satisfactory (51% (product **17**), 40% (product **18**)), but for the three-arm block, improvement on the synthesis method may be necessary (13% (product **19**)).

The last synthesis technique, Approach 3 was conducted on liquid phase. Protected DKPPR-alkyne was reacted with modified one-arm block (**4''**) and the reaction was pursued by using microwave-assisted technique. As described earlier, microwave-assisted technique can be useful in conducting click-reaction involving peptides and some studies have already proven the capability of microwave in this area. Interestingly, the product was obtained in 83% yield after 60 minutes reaction time (Scheme 17).



Scheme 16: Synthesis of DKPPR-building blocks on solid phase (Approach 2)



Scheme 17: Synthesis of one-arm DKPPR block on liquid phase (Approach 3)

Table 22 summarizes the different synthesis approaches that were investigated in this study. **Approach 1** failed to produce DKPPR-block with alkyne group at the end of the block (in Step III). Synthesis **Approach 2** has managed to produce the DKPPR-building blocks. Synthesis **Approach 3** has shown good capability in producing DKPPR-one arm block through microwave-assisted technique.

Table 22: List of different trials for the synthesis of DKPPR-blocks

Approach	Step I and II	Product	Step III	Product
1	Solid phase Wang resin-Protected DKPPR-alkyne <i>clicked</i> N ₃ -One-arm- OH	Protected DKPPR-one- arm-OH Successfully obtained	Coupling of alkyne functional group, followed by deprotection	DKPPR-one-arm- alkyne Not obtained
2	Solid phase Wang resin-Protected DKPPR-alkyne <i>clicked</i> N ₃ -One-arm- alkyne-TMS	Protected DKPPR-one- arm-alkyne-TMS Successfully obtained	Deprotection	DKPPR-building blocks-alkyne Successfully obtained
3	Liquid phase Protected DKPPR- alkyne <i>clicked</i> N ₃ -One-arm-alkyne- TMS	Protected DKPPR-one- arm-alkyne-TMS Successfully obtained	Deprotection	DKPPR-one-arm- alkyne Successfully obtained

4.2.5 Building the Porphyrin-DKPPR platform through click chemistry

A final click between one-arm porphyrin-azide block and one-arm DKPPR-alkyne block was conducted in liquid phase, in the presence of $\text{CuSO}_4 \cdot 5\text{H}_2\text{O}$ and sodium ascorbate as the catalyst in THF/water (4:1) mixture and the reaction was left at room temperature for 24 hours. Following its purification, four fractions were obtained as detected at 423 nm; at (1) 17.07 minutes, (2) 17.61 minutes, (3) 21.81 minutes and (4) 25.26 minutes (Figure 83). All these fractions contained porphyrin molecules. By comparing the absorbance at 214 nm which corresponded to the absorbance by peptide bond, it was observed that among the four peaks, peak (1) showed the most intense absorbance at both wavelengths.

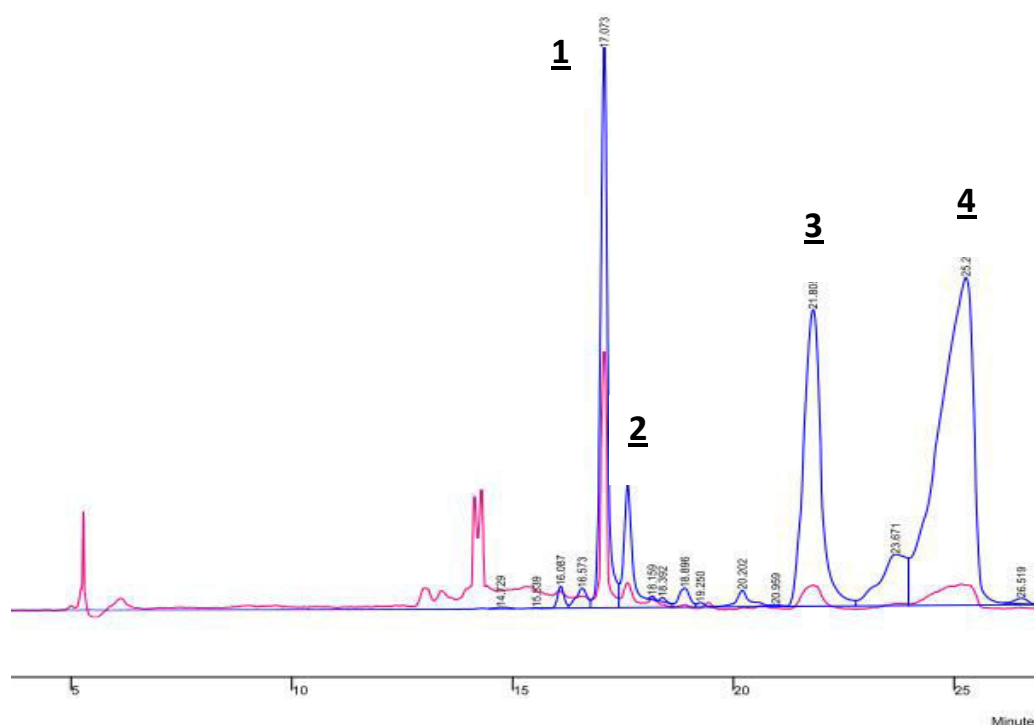


Figure 83: The RP-HPLC chromatogram of P1-DKPPR purification. (BLUE: peaks detected at 423 nm, RED: peaks detected at 214 nm)

Sample from peak (1) was then sent for mass analysis, showing a mass of 2080.83 (M^{+1}) which corresponds to the mass of porphyrin-DKPPR platform but with the presence of potassium ions. This phenomenon could happen due to the presence of potassium in the medium used during mass analysis ([Appendix 6, Product 20](#)).

4.2.6 ELISA Competitive Assay

A preliminary ELISA competitive study was performed with the platform and results are presented in Figure 84. The porphyrin-DKPPR complex retained its ability to target NRP-1 receptor although with a reduced ability as compared to DKPPR alone (EC_{50} : 150 μ M as compared to 18.3 μ M for DKPPR).

As described earlier in this chapter, there are reports on the possibility of triazole ring to reduce the activity of conjugated molecules. This phenomenon might happen with DKPPR-porphyrin conjugate. Nevertheless, the experiment will need to be repeated in order to confirm the result. This however could serve as a starting idea that the ability of conjugated DKPPR to replace VEGF- A_{165} binding did not completely diminished, but is reduced, following its conjugation with porphyrin through click chemistry technique.

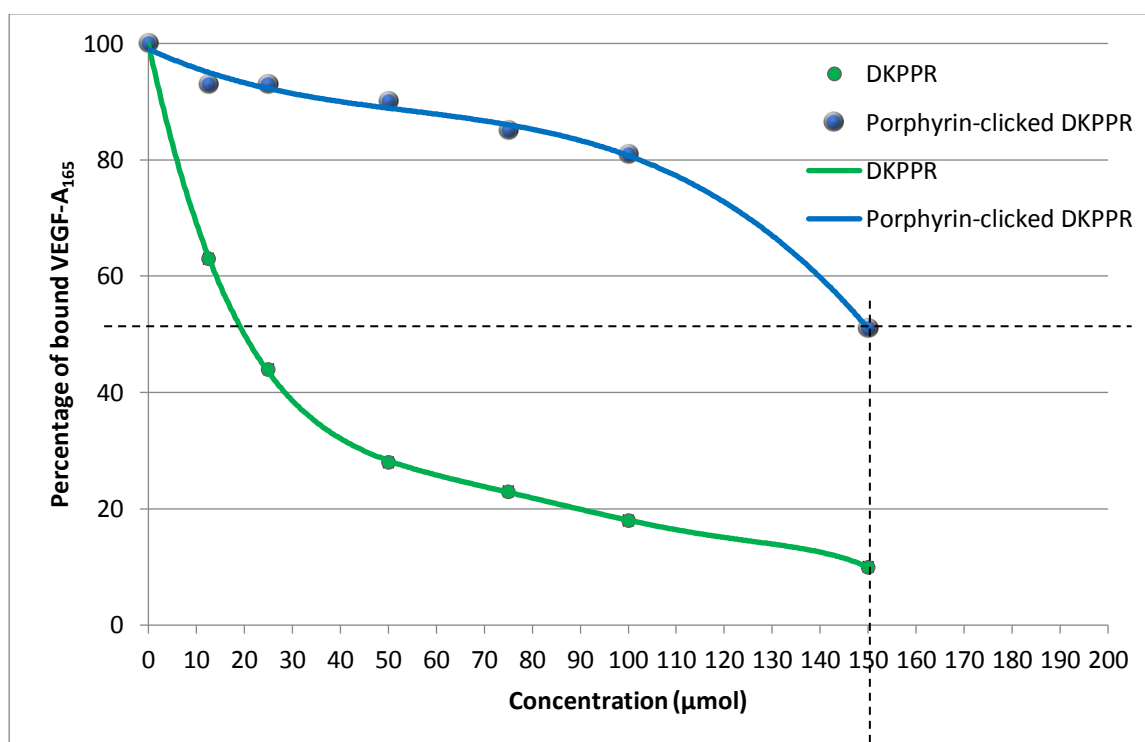


Figure 84: Percentage of bound VEGF $_{165}$ after introduction of DKPPR (green) and porphyrin-DKPPR platform (blue) respectively

4.3 CONCLUSION AND FUTURE PERSPECTIVE

Click chemistry was successfully used to prepare the blocks of porphyrins and DKPPR. Six blocks were synthesized and characterized, and one of the final platforms were managed to be synthesized and tested through ELISA competitive assay. The synthesis of porphyrin platforms were tested under different reaction conditions to see the effect of different synthesis conditions on their percentage of yield. In general, microwave-based reactions give good yield under shorter reaction time as compared to the conventional stirring method for one-arm porphyrin block, with the best yield of 97%, but for two-arm block, a longer period of time is necessary to obtain a good synthetic yield. Two-arm porphyrin block was obtained with 80% yield. With regards to three-arm block, a much longer time is needed and in this study, leaving the reaction for 5 days gave 77% of product.

The synthesis of DKPPR blocks were conducted in both solid and liquid phases. All three blocks were successfully synthesized through solid phase, and one-arm DKPPR block was synthesized through liquid phase as an example of liquid phase synthesis. One-arm DKPPR block and one-arm porphyrin block were then 'clicked' together to give the platform of porphyrin-DKPPR. ELISA assay has shown that the platform sustained the NRP-1 targeting ability, although a little lower as compared to the free DKPPR; 50% VEGF-A₁₆₅ displacement as compared to 80% by free DKPPR.

It is of highest interest to continue the study by performing the necessary click reactions between the different porphyrin blocks and DKPPR peptide blocks to obtain the nine different platforms. ELISA assays will then be conducted on the platforms in order to investigate their targeting capability on NRP-1 receptor and also to subsequently to evaluate their photodynamic activity on cancerous cells.

Conclusion

In the PDT field, although there are efficient PS agents available in the clinics, these agents are usually not specific in term of accumulation at the tumours or neo-vessels. This called for the development of targeted PS to improve its delivery especially since the untargeted PS could accumulate in any body tissues following *in vivo* administration and reduce the amount that is needed in diseased tissues for effective PDT.

This thesis was hence prepared in the attempts to have a better understanding on the necessary design to have good targeted PS. The work presented was conducted under one main goal: to investigate the capability to improve the delivery of PS for PDT applications. Two different targeting approaches were studied: active, indirect targeting by using peptide to target NRP-1 receptor and active, direct targeting by using FA to directly target FR on the surface of cancerous cells. The two approaches have their own capability in reducing cell viability and many data available in the literature show that these receptors are good targets in anti-cancer therapy. There were three objectives outlined at the beginning of this thesis:

- i. To evaluate the stability of folic acid (FA) molecule as a targeting agent and a novel photosensitizer-folic acid (PS-FA) conjugate intended for the treatment of ovarian cancer through the Design of Experiment (DoE) approach.
- ii. Design of platforms with porphyrin(s) and peptide(s) as a targeting agent towards NRP-1 receptor.
 - ii.a Improvement of DKPPR peptide through development of KDKPPR peptide as a way to improve the specificity of NRP-1 towards human glioblastoma multiforme tissues, and the evaluation of the importance of each amino acid in KDKPPR sequence.
 - ii.b Synthesis of different platforms of PS and DKPPR peptide through click chemistry technique to investigate the influence of different number of PS and peptide molecules in one platform on the efficacy and targeting capability of the platform towards human glioblastoma multiforme tissues for PDT application.

The first part of the thesis (Chapter 2) was dedicated to the evaluation of FA stability under different environmental conditions, in the form of single molecule and as conjugate with a PS. The uniqueness of this study lies on the evaluation of multiple environmental factors at one time, with the aim of determining the most important factors of all through the DoE approach. To the best of our knowledge, there is no such studies ever been reported before in the literature. Instead, there are only studies evaluating the stability of FA under the influence of one, or maximum two environmental conditions, and they provide limited data

without correlation with other possible factors. Hence this study was designed to provide the missing correlation which was achieved by the DoE approach.

In general, the results showed that the stability of FA was improved tremendously through conjugation with PS. This is a very positive result as it means that a PS-FA has the needed stability to be used as a targeting conjugate for PDT. From the experimental data, a binary Fisher's tree was developed and it was found that light is the most discriminating factor on the degradation of FA or PS-FA, which means that the presence or absence of light is the factor that has the most influence on the molecules' stability. This is followed by oxygen, temperature and type of molecule. Light alone is destructive on the stability of PS-FA, but not on FA. FA will be degraded in the presence of light and other factors, such as oxygen or medium pH. This finding could be further strengthened by conducting a detailed study with more inclusion factors such as longer storage time and more diversified media. The PS-FA conjugate is indeed of interest to our PDTeam and more research is on the way to further evaluate its ability in PDT applications. In addition, molecular modelling studies could also be conducted to get ideas on the dynamic interaction of the conjugate on the FR, hence helping to develop a suitable conjugate for FR targeting.

The second part of this thesis (Chapter 3) revolves around the evaluation of a peptide KDKPPR through a technique called alanine-scanning. This study was conducted to investigate the importance of each amino acid in the sequence on their NRP-1 binding capability. All the analogues of the native peptides were evaluated *in vitro* through ELISA study, which showed that the most important amino acid to be conserved is the C-terminal arginine R₆. The substitution of N-terminal lysine, Lys₁ and aspartic acid, Asp₂ with alanine showed the least effect on the binding affinity. The importance of the amino acids could be summarized as Arg₆>Pro₄=Pro₅>Lys₃>Asp₂=Lys₁.

The two prolines at sequence four (Pro₄) and five (Pro₅) have some importance on the binding and is also believed to have contribution on the overall conformation of the peptide. The dynamic confirmation of the peptide either in the form of linear or pseudocycle may have certain effect on the hydrophilicity of the peptide. This has not been investigated and may be of interest to be determined in the future as a way to better understand the behaviour of the peptides under dynamic conditions. The retro and retro-inverso peptides however did not show satisfactory ability to bind on NRP-1. However, since they may offer an advantage of being more stable as compared to the L-peptides, there are still potential of their application in the future, subjected to further research and evaluations.

In the interest of using this peptide in conjugation with a PS, the most possible peptide to be used in the place of KDKPPR will be KAKPPR. Although ADKPPR also showed similar affinity on the NRP-1 receptor, the presence of Lys₁ on the peptide sequence is needed (because of the free NH₂ function) to form conjugation between the peptide and PS.

Chapter 4 explored the possibility of synthesizing multiple PS-peptide conjugate through click chemistry technique. The one-, two- and three-arms building blocks of PS (porphyrin) and one-, two- and three-arms building blocks of peptide was synthesized separately through this technique. Different experimental conditions were evaluated to determine the best reaction. One-arm porphyrin was successfully synthesized with 97% yield, two-arm with 80% yield and three-arms with 77% yield. The photophysical properties of the different porphyrin building blocks did not differ significantly between each other. The building blocks of peptide were synthesized through solid and liquid phase approaches, with the best yield of 83%, 40% and 13% for one-, two- and three-arms peptide respectively.

The different building blocks of porphyrin and peptides will be clicked together in future works that will follow. This will produce platforms with different numbers of PS and peptide. This will be useful to evaluate the possibility of increasing the targeting capability of conjugates with multiple numbers of peptide molecules. In term of having multiple PS in one platform, the initial photophysical properties analyses showed that the presence of more porphyrin molecules in one building block did not have significant improvement as compared to having single porphyrin molecule. This gives some ideas that perhaps more porphyrin molecules in one platform are not useful to increase PDT effect. Nevertheless, it is necessary to conduct further studies to confirm this hypothesis.

With the finding presented in this thesis, it is now known that:

- i. The stability of FA is significantly improved by the formation of PS-FA conjugate. The most important factors in determining the degradation of PS-FA is light whilst the degradation of FA is influenced by light in combination with other factors such as unsuitable media. Light alone usually will not cause huge degradation of FA.

The PS-FA intended for PDT application is found to have good stability against degradation, albeit a little degradation still has to be expected. Handling of the conjugate will hence be much easier and could ensure that the conjugated PS can be effectively delivered to the targeted ovarian cancer cells.

- ii. The good binding capability of KDKPPR peptide on NRP-1 receptor ($EC_{50}=6.0 \mu\text{M}$) lies on the presence of the last four amino acids: -KPPR. The C-terminal Arg₆ is the most important. The first two amino acids: KD- is of lesser importance and could be substituted with alanine without much effect on the peptide's binding ability. KAKPPR showed the lowest EC_{50} value among all of the analogues tested.

Substituting Lys₃ with arginine (KDRPPR) did not show detrimental effect on the binding. The *retro* and *retro-inverso* peptides however are not useful in improving NRP-1 binding. For future application in NRP-1 targeting, KDKPPR could be replaced by KAKPPR and similar targeting capability could be expected.

- iii. The synthesis of porphyrin and peptide building blocks is possible by using click chemistry technique. The reaction rate is slower with increasing number of clickable arms. The photophysical properties of the porphyrin building blocks showed no significant difference among each other. A sample of 1-to-1 porphyrin-peptide clicked platform which was tested through ELISA showed that the targeting capability was maintained, albeit with a lower EC_{50} .

The three main objectives outlined at the beginning of this thesis are among the active studies currently conducted by our PDT team in order to develop third-generation PS with specific aim for the treatment of ovarian cancer and glioblastoma. These two cancers are known to be difficult to treat with currently available anti-cancer therapy and hence PDT may have a role in improving the available treatment. It is hoped that the finding presented in this thesis will be useful as guidance in producing effective PS in the future, and can help to further improve the application of PDT in broader area of cancer treatment.

Materials and Experimental Section

CHAPTER II: The evaluation of folic acid stability: As free molecule and as conjugate for PDT application

MATERIALS

This project was divided into two parts; (1) the stability evaluation of FA and (2) the stability evaluation of PS-FA.

FA was purchased from Sigma-Aldrich and used as received. The buffered solution pH 4, pH 7 and pH 10 and DMSO were obtained from Sigma-Aldrich and used as received. Methanol for HPLC (CHROMASOLV 99.9% purity) was also obtained from Sigma-Aldrich. Purified water milli-Q was used as necessaries during purification. Formic acid was obtained from Carlo Erba Reagents with 99% purity. PS-FA was synthesized in the LRGP laboratory by a PhD student, Aurélie Stallivieri under the supervision of Dr Céline Frochot and Dr Régis Vanderesse (details are outlined in her thesis).

EXPERIMENTAL SECTION

A. Stability testing condition

Label	Solvent	Temperature	Time	Light	Oxygen	Molecule
A	DMSO	RT	1 hour	No	No	FA
B	DMSO	4°C	1 week	No	Yes	PS-FA
C	DMSO	-20°C	1 day	No	No	PS-FA
D	DMSO	40°C	15 minutes	Yes	Yes	FA
E	Methanol	RT	15 minutes	Yes	No	FA
F	Methanol	4°C	1 day	No	Yes	FA
G	Methanol	-20°C	1 week	No	Yes	PS-FA
H	Methanol	40°C	1 hour	No	No	PS-FA
I	Buffer pH 4	RT	1 day	No	Yes	FA
J	Buffer pH 4	RT	1 week	Yes	No	PS-FA
K	Buffer pH 4	4°C	1 hour	No	Yes	FA
L	Buffer pH 4	-20°C	1 hour	No	No	FA
M	Buffer pH 4	40°C	15 minutes	No	No	PS-FA
N	Buffer pH 7	RT	1 day	Yes	No	FA
O	Buffer pH 7	RT	1 week	No	Yes	FA
P	Buffer pH 7	4°C	1 day	No	No	PS-FA
Q	Buffer pH 7	-20°C	15 minutes	No	Yes	FA
R	Buffer pH 7	40°C	1 hour	Yes	Yes	PS-FA
S	Buffer pH 10	RT	15 minutes	No	Yes	PS-FA
T	Buffer pH 10	4°C	1 hour	No	No	PS-FA
U	Buffer pH 10	-20°C	1 week	No	No	FA
V	Buffer pH 10	40°C	1 day	Yes	Yes	FA
W	Powder	RT	1 hour	Yes	Yes	PS-FA
X	Powder	4°C	15 minutes	No	No	FA
Y	Powder	-20°C	1 day	No	Yes	PS-FA
Z	Powder	40°C	1 week	No	No	FA

Each experiment was repeated three times. All the samples were prepared in standard techniques and conditions to minimize the variable that may affect the outcome of the experiments.

A small clear glass bottle with a volume of 8.5 mL was used in all experiments. The cover is made from polyethylene and was further secured with *Parafilm M* when necessary. The fact that the bottle is clear enables the presence of light on the sample and in the experiment where light is to be obscured, the bottle was covered with aluminium paper. All bottles, covered and without aluminium covers were placed at the same setting, allowing same temperature and amount of light fluctuations. In term of evaluating different temperatures, the samples were placed in an oven set at the specific temperature for 40°C, in the fridge at 4°C and freezer at -20°C. As for the samples kept at room temperatures, the samples were let to experience the different temperatures that might fluctuate during the course of the experiment.

The oxygen present in the glass bottle was removed by displacement with nitrogen gas. Nitrogen was allowed to flow into the solution prepared and subsequently the glass bottle was secured with *Parafilm M* and kept accordingly.

RP-HPLC analysis was conducted with an elution program as detailed in the chapter. The samples were diluted five times with methanol. 40 μ L from the diluted samples were injected into RP-HPLC for the analysis.

B. Statistical analysis – Design of experiments

From the study conducted, six factors were taken into consideration for the statistical analysis:

- light (with; without);
- oxygen (with; without);
- molecule (FA; PS-FA);
- time (15minutes; 1hour; 1day; 1 week);
- temperature (-20;4; RT; 40°C);
- medium (DMSO, methanol; buffer pH 4; buffer pH7; buffer pH 10; powder).

The measured response variable Y corresponds to the degradation level of the molecules investigated and is represented by only two values (binary response): 0 for low-degradation (<45% degradation) and 1 for high degradation (>45% degradation).

Table B1 presents the first part of the experimental data that were used in the **<Model Identification>** part, with 19 experimental conditions in triplicates. The second part **<Model Validation>** is presented in Table B2, with 11 conditions in triplicates.

Table B1 : 56 experiments used in model identification step

Exp No	Light	Oxygen	Molecule	Time	Temp	Medium	Degradation
1	No	No	FA	1 hr	RT	DMSO	0
2	No	No	FA	1 hr	RT	DMSO	0
3	No	No	FA	1 hr	RT	DMSO	0
4	No	Yes	PS-FA	1 week	4°C	DMSO	0
5	No	Yes	PS-FA	1 week	4°C	DMSO	0
6	No	Yes	PS-FA	1 week	4°C	DMSO	0
7	Yes	Yes	FA	15 min	40°C	DMSO	0
8	Yes	Yes	FA	15 min	40°C	DMSO	0
9	Yes	Yes	FA	15 min	40°C	DMSO	0
10	No	No	PS-FA	1 h	40°C	MeOH	0
11	No	No	PS-FA	1 h	40°C	MeOH	0
12	No	No	PS-FA	1 h	40°C	MeOH	0
13	No	Yes	FA	24 hr	RT	Buff pH 4	1
14	No	Yes	FA	24 hr	RT	Buff pH 4	1
15	No	Yes	FA	24 hr	RT	Buff pH 4	1
16	Yes	No	PS-FA	1 week	RT	Buff pH 4	1
17	Yes	No	PS-FA	1 week	RT	Buff pH 4	1
18	Yes	No	PS-FA	1 week	RT	Buff pH 4	1
19	No	No	FA	1 hr	-20°C	Buff pH 4	0
20	No	No	FA	1 hr	-20°C	Buff pH 4	0
21	No	No	FA	1 hr	-20°C	Buff pH 4	0
22	No	Yes	FA	1 week	RT	Buff pH 7	0
23	No	Yes	FA	1 week	RT	Buff pH 7	0
24	No	Yes	FA	1 week	RT	Buff pH 7	0
25	No	No	PS-FA	24 hr	4°C	Buff pH 7	0
26	No	No	PS-FA	24 hr	4°C	Buff pH 7	0
27	No	No	PS-FA	24 hr	4C	Buff pH 7	0
28	No	Yes	FA	15 min	-20°C	Buff pH 7	0
29	No	Yes	FA	15 min	-20°C	Buff pH 7	0
30	No	Yes	FA	15 min	-20°C	Buff pH 7	0
31	Yes	Yes	PS-FA	1 hr	40°C	Buff pH 7	0
32	Yes	Yes	PS-FA	1 hr	40°C	Buff pH 7	0
33	Yes	Yes	PS-FA	1 hr	40°C	Buff pH 7	0
34	No	Yes	PS-FA	15 min	RT	Buff pH 10	0
35	No	Yes	PS-FA	15 min	RT	Buff pH 10	0
36	No	Yes	PS-FA	15 min	RT	Buff pH 10	0
37	No	No	PS-FA	1 hr	4°C	Buff pH 10	0
38	No	No	PS-FA	1 hr	4°C	Buff pH 10	0
39	No	No	PS-FA	1 hr	4°C	Buff pH 10	0
40	No	Yes	PS-FA	24 hr	-20°C	Powder	0
41	No	Yes	PS-FA	24 hr	-20°C	Powder	0
42	No	Yes	PS-FA	24 hr	-20°C	Powder	0
43	No	No	FA	1 week	40°C	Powder	0
44	No	No	FA	1 week	40°C	Powder	0
45	No	No	FA	1 week	40°C	Powder	0
46	Yes	Yes	PS-FA	15 min	4°C	DMSO	0
47	Yes	Yes	PS-FA	15 min	4°C	DMSO	0
48	Yes	No	FA	24 hr	-20°C	DMSO	0
49	Yes	No	FA	24 hr	-20°C	DMSO	0
50	Yes	No	FA	24 hr	-20°C	DMSO	0
51	Yes	Yes	FA	1 hr	-20°C	MeOH	1
52	Yes	Yes	FA	1 hr	-20°C	MeOH	1
53	Yes	Yes	FA	1 hr	-20°C	MeOH	1
54	No	No	PS-FA	24 hr	40°C	MeOH	0
55	No	No	PS-FA	24 hr	40°C	MeOH	0
56	No	No	PS-FA	24 hr	40°C	MeOH	0

Table B2: 33 experiments in model validation step

Exp No	Light	Oxygen	Molecule	Time	Temp	Medium	Degradation
57	No	No	PS-FA	24 hr	-20°C	DMSO	0
58	No	No	PS-FA	24 hr	-20°C	DMSO	0
59	No	No	PS-FA	24 hr	-20°C	DMSO	0
60	Yes	No	FA	15 min	RT	MeOH	0
61	Yes	No	FA	15 min	RT	MeOH	0
62	Yes	No	FA	15 min	RT	MeOH	0
63	No	Yes	FA	24 hr	4°C	MeOH	0
64	No	Yes	FA	24 hr	4°C	MeOH	0
65	No	Yes	FA	24 hr	4°C	MeOH	0
66	No	Yes	PS-FA	1 week	-20°C	MeOH	0
67	No	Yes	PS-FA	1 week	-20°C	MeOH	0
68	No	Yes	PS-FA	1 week	-20°C	MeOH	0
69	No	Yes	FA	1 hr	4°C	Buff pH 4	1
70	No	Yes	FA	1 hr	4°C	Buff pH 4	1
71	No	Yes	FA	1 hr	4°C	Buff pH 4	1
72	No	No	PS-FA	15 min	40°C	Buff pH 4	0
73	No	No	PS-FA	15 min	40°C	Buff pH 4	0
74	No	No	PS-FA	15 min	40°C	Buff pH 4	0
75	Yes	No	FA	24 hr	RT	Buff pH 7	1
76	Yes	No	FA	24 hr	RT	Buff pH 7	1
77	Yes	No	FA	24 hr	RT	Buff pH 7	1
78	No	No	FA	1 week	-20°C	Buff pH 10	0
79	No	No	FA	1 week	-20°C	Buff pH 10	0
80	No	No	FA	1 week	-20°C	Buff pH 10	0
81	Yes	Yes	FA	24 hr	40°C	Buff pH 10	0
82	Yes	Yes	FA	24 hr	40°C	Buff pH 10	0
83	Yes	Yes	FA	24 hr	40°C	Buff pH 10	0
84	Yes	Yes	PS-FA	1 hr	RT	Powder	0
85	Yes	Yes	PS-FA	1 hr	RT	Powder	0
86	Yes	Yes	PS-FA	1 hr	RT	Powder	0
87	No	No	FA	15 min	4°C	Powder	0
88	No	No	FA	15 min	4°C	Powder	0
89	No	No	FA	15 min	4°C	Powder	0

Re-classification of the conditions <time>, <temperature> and <medium> were made into two levels to further simplify the analysis, as described earlier in Figure 51. Following this classification, the data in Table B1 and B2 were revised into Table B3 and B4.

Table 23: Modified design of experiments for the 56 experiments – Model Identification

Exp No	Light	Oxygen	Molecule	Time	Temp	Medium	Degradation
1	No	No	FA	ST	T2	M1	0
2	No	No	FA	ST	T2	M1	0
3	No	No	FA	ST	T2	M1	0
4	No	Yes	PS-FA	LT	T1	M1	0
5	No	Yes	PS-FA	LT	T1	M1	0
6	No	Yes	PS-FA	LT	T1	M1	0
7	Yes	Yes	FA	ST	T2	M1	0
8	Yes	Yes	FA	ST	T2	M1	0
9	Yes	Yes	FA	ST	T2	M1	0
10	No	No	PS-FA	ST	T2	M1	0
11	No	No	PS-FA	ST	T2	M1	0
12	No	No	PS-FA	ST	T2	M1	0
13	No	Yes	FA	LT	T2	M2	1
14	No	Yes	FA	LT	T2	M2	1
15	No	Yes	FA	LT	T2	M2	1
16	Yes	No	PS-FA	LT	T2	M2	1
17	Yes	No	PS-FA	LT	T2	M2	1
18	Yes	No	PS-FA	LT	T2	M2	1
19	No	No	FA	ST	T1	M2	0
20	No	No	FA	ST	T1	M2	0
21	No	No	FA	ST	T1	M2	0
22	No	Yes	FA	LT	T2	M2	0
23	No	Yes	FA	LT	T2	M2	0
24	No	Yes	FA	LT	T2	M2	0
25	No	No	PS-FA	LT	T1	M2	0
26	No	No	PS-FA	LT	T1	M2	0
27	No	No	PS-FA	LT	T1	M2	0
28	No	Yes	FA	ST	T1	M2	0
29	No	Yes	FA	ST	T1	M2	0
30	No	Yes	FA	ST	T1	M2	0
31	Yes	Yes	PS-FA	ST	T2	M2	0
32	Yes	Yes	PS-FA	ST	T2	M2	0
33	Yes	Yes	PS-FA	ST	T2	M2	0
34	No	Yes	PS-FA	ST	T2	M2	0
35	No	Yes	PS-FA	ST	T2	M2	0
36	No	Yes	PS-FA	ST	T2	M2	0
37	No	No	PS-FA	ST	T1	M2	0
38	No	No	PS-FA	ST	T1	M2	0
39	No	No	PS-FA	ST	T1	M2	0
40	No	Yes	PS-FA	LT	T1	M1	0
41	No	Yes	PS-FA	LT	T1	M1	0
42	No	Yes	PS-FA	LT	T1	M1	0
43	No	No	FA	LT	T2	M1	0
44	No	No	FA	LT	T2	M1	0
45	No	No	FA	LT	T2	M1	0
46	Yes	Yes	PS-FA	ST	T1	M1	0
47	Yes	Yes	PS-FA	ST	T1	M1	0
48	Yes	No	FA	LT	T1	M1	0
49	Yes	No	FA	LT	T1	M1	0
50	Yes	No	FA	LT	T1	M1	0
51	Yes	Yes	FA	ST	T1	M1	1
52	Yes	Yes	FA	ST	T1	M1	1
53	Yes	Yes	FA	ST	T1	M1	1
54	No	No	PS-FA	LT	T2	M1	0
55	No	No	PS-FA	LT	T2	M1	0
56	No	No	PS-FA	LT	T2	M1	0

Table 24: Modified design of experiments for the 33 experiments – Model Validation

Exp No	Light	Oxygen	Molecule	Time	Temp	Medium	Degradation
57	No	No	PS-FA	LT	T1	M1	0
58	No	No	PS-FA	LT	T1	M1	0
59	No	No	PS-FA	LT	T1	M1	0
60	Yes	No	FA	ST	T2	M1	0
61	Yes	No	FA	ST	T2	M1	0
62	Yes	No	FA	ST	T2	M1	0
63	No	Yes	FA	LT	T1	M1	0
64	No	Yes	FA	LT	T1	M1	0
65	No	Yes	FA	LT	T1	M1	0
66	No	Yes	PS-FA	LT	T1	M1	0
67	No	Yes	PS-FA	LT	T1	M1	0
68	No	Yes	PS-FA	LT	T1	M1	0
69	No	Yes	FA	ST	T1	M2	1
70	No	Yes	FA	ST	T1	M2	1
71	No	Yes	FA	ST	T1	M2	1
72	No	No	PS-FA	ST	T2	M2	0
73	No	No	PS-FA	ST	T2	M2	0
74	No	No	PS-FA	ST	T2	M2	0
75	Yes	No	FA	LT	T2	M2	1
76	Yes	No	FA	LT	T2	M2	1
77	Yes	No	FA	LT	T2	M2	1
78	No	No	FA	LT	T1	M2	0
79	No	No	FA	LT	T1	M2	0
80	No	No	FA	LT	T1	M2	0
81	Yes	Yes	FA	LT	T2	M2	0
82	Yes	Yes	FA	LT	T2	M2	0
83	Yes	Yes	FA	LT	T2	M2	0
84	Yes	Yes	PS-FA	ST	T2	M1	0
85	Yes	Yes	PS-FA	ST	T2	M1	0
86	Yes	Yes	PS-FA	ST	T2	M1	0
87	No	No	FA	ST	T1	M1	0
88	No	No	FA	ST	T1	M1	0
89	No	No	FA	ST	T1	M1	0

CHAPTER III: Modification of KDKPPR peptide to investigate the effect on its binding on NRP-1 receptor

MATERIALS

Reagents were obtained from the following sources and used as received without further purification. The amino acids were obtained from different resources; Fmoc-(L)-Lysine(Boc)-OH, Fmoc-(L)-Arginine(Pbf)-OH, Fmoc-(D)-Aspartic acid(tBu)-OH and Fmoc-(D)-Arginine(Pbf)-OH were obtained from Iris Biotech GmbH (Germany); Fmoc-(L)-Alanine-OH and Fmoc-(D)-Proline-OH were from Fluka, Sigma-Aldrich Chemie GmbH (Germany); Fmoc-(L)-Proline-OH, Fmoc-(D)-Lysine(Boc)-OH, and Fmoc-(D)-Alanine-OH were purchased from Novabiochem (Germany) and Fmoc-(L)-Aspartic acid(OtBu)-OH was from Senn Chemicals AG (Switzerland).

The resins used were already with embedded amino acid and it is the last amino acid in the sequence. Fmoc-(L)-Arginine(Pbf)-Wang resin (100-200 mesh), Fmoc-(L)-Lysine(Boc)-Wang resin (100-200 mesh) and Fmoc-(L)-Alanine-Wang resin (100-200 mesh) were obtained from Novabiochem (Germany), whilst the Fmoc-(D)-Lysine(Boc)-Wang resin (100-200 mesh) was obtained from Iris Biotech GmbH (Germany).

The other reagents were used as received from the suppliers, exception was for DMF for solubilising the reagents which were kept in activated molecular-sieve to ensure the absence of water in the reactant solution. Piperidine was from Sigma-Aldrich (Germany), HBTU was from Iris Biotech GmbH (Germany), N-methylmorpholine (NMM) from Alfa-Aesar GmbH (Germany), N-methylpyrrolidone (NMP) was from PROLABO (Rhone-Poulenc) and acetic anhydride was from Riedel de Haen, Sigma-Aldrich GmbH (Germany). DMF, DCM and ethanol used during the synthesis were from Sigma-Aldrich and of high purity.

The cleavage mixture was a combination of trifluoroacetic acid (TFA), triisopropylsilane (TIPS) and water. TFA was obtained from Acros Organic (Belgium) whilst TIPS was from Aldrich Chemistry, Sigma-Aldrich GmbH (Germany). Acetonitrile for purification of crude peptides by RP-HPLC was obtained from Sigma-Aldrich GmbH, (Germany). Purified Milli-Q water was used whenever necessary (PURITE, Select Analyst HP 25, England). RP-HPLC analysis and purification was performed on Waters® HPLC with a UV/Visible detector, by using Macherey-Nagel (MN) C₁₈ column (refer Table 3 for complete protocol).

Deuterated dimethylsulfoxide, DMSO-d₆ used for NMR spectroscopy was purchased from Euriso-Top (France). NMR spectra (Proton NMR, COSY and TOCSY) were recorded on Avance 300 MHz NMR spectrometer (Bruker) by Dr Olivier Fabre. Two different mass analysis were performed; high resolution mass analysis was by Dr Fabian Lachaud in Faculté de Science, Université de Lorraine, Vandœuvre-Lès-Nancy, Nancy and low resolution mass

analysis by Mme Mathilde Achard in LCPM, with LC-MS spectrometer 2020 (Shimadzu, Japan) through electron-spray ionization (ESI) technique.

The materials used for ELISA assays were as follows: a 96-well plate, receptor rrNPN-1/Fc chimera recombinant from rat (reference number 566-N1-025 R&D Systems, kept at -20°C); Biotinylated VEGF 0.5 µg/mL (Human VEGF Biotinylated Fluorokine Flow Cytometry Kit, R&D Systems) Tween-20 solution (0.05% in phosphate-buffered saline pH 7.4 as the washing buffer; bovine serum albumin, BSA solution (0.5% in phosphate-buffered saline pH 7.4) as the blocking buffer; Streptavidine-HRP (reference number DY998 R&D Systems) as the enzyme-linked ligand to help in detection of positive reaction; colour reagent A (hydrogen peroxidase) and colour reagent B (tetramethylbenzidin) (reference number DY999 R&D Systems) and Sulphuric acid 2N solution (reference number DY994 R&D Systems) as the stop solution.

EXPERIMENTAL SECTION

A. Peptide synthesis, purification and characterization

The native KDKPPR and all the analogues were synthesized on a Wang resin-based solid phase peptide synthesizer (ResPep XL, Intavis AG Bioanalytical Instruments, Germany) at 100 μ mol synthesis scale by using a standard protocol ([Appendix 2](#)). Acid-labile protecting groups (Boc, tert-butyl and Pbf) were present where necessary on the side-chain of individual amino acids. Deprotection of Fmoc-group from the amino acids was successfully achieved by using 20% piperidine solution in DMF. The activations of incoming amino acids were performed with HBTU in the presence of NMM, in DMF and the unreacted amino acids were eventually capped with acetic anhydride at the end of each coupling phase.

Trifluoroacetic acid (TFA) cleavage was conducted on the synthesized peptides following a standard protocol with triisopropylsilane (TIPS) as the scavenger (95% TFA: 2.5% TIPS: 2.5% Water) at room temperature for two hours. The cleaved peptides were then precipitated in cold diethyl ether and lyophilized before purification through a reversed-phase C₁₈ HPLC (RP-HPLC) (see details in Table 22). The fractions recovered after purification was lyophilized and white-coloured powders were obtained. They were further characterized *via* mass spectrometry and NMR analysis to confirm the presence of the desired peptides. The synthesized peptides were then stored at -20°C until required for biological assays.

Table A1: Purification protocol used for all peptides

Column	Machery-Nagel VP 150/20 Nucleosil 100-5 C ₁₈		
Solvent	Water/Acetonitrile/0.1% Trifluoroacetic acid		
Gradient	Time (min)	Water (% conc.)	Acetonitrile (% conc.)
	0	95	5
	25	0	100
	30	0	100
	35	95	5
Flow rate	12 mL/min		
Detector	UV/Visible		
Wavelength	UV/Visible (nm)	214	

B. ELISA competitive binding assay

ELISA assays were conducted by biologists from *Centre de Recherche en Automatique de Nancy*, CRAN (UMR 7039), *Université de Lorraine*, CNRS, Dr Cédric Boura and Thibaut Peterlini. The ELISA assays were done in triplicates. Streptavidin-linked HRP (Horseradish Peroxidase) is used as the enzyme-linked antibody in the form of Streptavidin HRP-VEGF₁₆₅, in competition with the tested peptides on the targeted receptor. It binds on the surface of the bonded peptide, and the quantity of HRP-VEGF₁₆₅-bonded NRP-1 was measured, giving blue colour and upon introduction of its colour substrate (hydrogen peroxide/tetramethylbenzidin), colour change occurs from blue to yellow.

The competitive ELISA assays were conducted based on a standard protocol developed in CRAN for NRP-1 based study. The NRP-1 receptor was reconstituted in 125 µL of phosphate-buffered saline, PBS at a concentration of 200 µg/mL and was further diluted in PBS to obtain a final concentration of 2 µg/mL. 100 µL of this solution was deposited in each well of the 96-well plate and incubated overnight at room temperature. The wells were then emptied, washed three times with 200 µL of the washing buffer and dabbed to soak up any remaining fluid.

The remaining non-specific binding sites present in the wells were subsequently blocked by using the blocking buffer. 300 µL of this buffer was added into the wells and incubated for one hour at 37°C. The wells were emptied without rinsing and carefully dabbed to remove any excess fluid present.

VEGF-A₁₆₅ (0.5 µg/mL) and the peptides to be tested were then introduced into the wells along with heparin (50 µg/mL), with the total volume of 400 µL for each well. In order to have a wider observation on concentration-dependent effect, the peptide solutions were prepared at different concentrations with a starting concentration of 200 µM. Table 23 described the amount of each buffer and sample which were added into the 96-well plate. Each test was conducted in triplicate.

Table B1: The amount of peptide, VEGF-A₁₆₅, heparin and blocking buffer added into each well with specific concentration of the tested peptides

Test/Concentration	Peptide (μL)	VEGF-A ₁₆₅ (μL)	Heparin (μL)	Blocking buffer (μL)
Blank	-	-	16	384
Negative control	-	4	16	380
Peptide: 150 μM	300	4	16	80
Peptide: 100 μM	200	4	16	180
Peptide: 75 μM	150	4	16	230
Peptide: 50 μM	100	4	16	280
Peptide: 25 μM	50	4	16	330
Peptide: 12.5 μM	25	4	16	355
Peptide: 6.5 μM	13	4	16	367
Peptide: 0 μM	-	4	16	380

Following the introduction of the test solutions into the wells, they were incubated at room temperature for two hours and subsequently washed with washing buffer and dabbed to remove any remaining liquid.

Streptavidin-HRP was then prepared as diluted solution in blocking buffer (1 in 200). 100 μL of this Streptavidin-HRP solution was added into the wells and the plate was left to incubate for 20 minutes at room temperature with limited light exposure by covering with aluminium foil. The wells were then washed three times with the washing buffer and carefully dabbed to remove any excess liquid present.

100 μL of substrate for Streptavidin-HRP was then added into the wells, which consisted of a 1:1 mixture of hydrogen peroxide, H₂O₂ and tetramethylbenzidin, TMB. The plate was then incubated at room temperature for 30 minutes protected from light, and the development of blue colour was checked every 10 minutes during the process. 50 μL of stop solution was then added, changing the blue colour into yellow. The amount of bonded peptide was determined by measuring the absorbance at 450 nm for blue and 540 nm for yellow.

Absorbance at two wavelengths is then conducted at 450 nm and 540 nm which correspond to blue and yellow. TMB is very sensitive and may produce significant background signal if excessive protein or antibody is used. Hence, for a safer practice, the reading at 450 nm is usually being subtracted with the reading at 540 nm as a way for correcting the reading because absorbance at 450 nm alone will usually give a much higher and less accurate reading. This step will ensure that corrections are made for any optical imperfection occurred from the plate [350].

CHAPTER IV: Synthesis of Porphyrin (P1-COOH) and DKPPR Peptide Platform through Click Chemistry

MATERIALS

Chemicals and solvents were purchased and used without further modifications. The chemicals used in the synthesis of building blocks were as follows: diethylene glycol (99%, Sigma-Aldrich, Germany), triethylamine (99%, Riedel-de Haën, Germany), methanesulfonyl chloride (98%, Alfa Aesar, Germany), sodium azide (99%, Acros Organic, Belgium), 3-chloropropylamine HCl (98%, Alfa Aesar, Germany), methyl 4-hydroxybenzoate (99%, Acros Organics, Belgium), methyl 3,5-dihydroxybenzoate (98%, Alfa Aesar, Germany), methyl 3,4,5-trihydroxybenzoate (98%, Alfa Aesar, Germany), potassium carbonate anhydrous, K₂CO₃ (99%, Acros Organics, Belgium), potassium hydroxide, KOH (Riedel-de Haën, Czech Republic) and Amberlite IR-120 (Fluka, Germany).

The synthesis of porphyrin and porphyrin platforms required the following chemicals: pyrrole (99%, Acros Organics, Belgium), benzaldehyde (99%, Aldrich, Germany), 4-carboxybenzaldehyde (Aldrich, Germany), boron trifluoride diethyl etherate (Avocado Research Chemicals Ltd., UK), *p*-chloranil (99%, Aldrich, Austria), dicyclohexylcarbodiimide, DCC (99%, Aldrich, Germany), *N*-hydroxysuccinimide, NHS (98%, Alfa-Aesar, Germany), propargylamine (99%, Acros Organics, Belgium), zinc acetate dihydrate (98%, Sigma-Aldrich, Germany), copper (II) sulphate pentahydrate, CuSO₄·5H₂O (Prolabo, Paris) and L-ascorbic acid, sodium salt (99%, Alfa Aesar, Germany). All light sensitive products and corresponding reactions were conducted in the dark, under protection from light by aluminium foil.

The synthesis of DKPPR peptide and the corresponding platforms utilized reagents which include: piperidine (Sigma-Aldrich, Germany), HBTU (Iris Biotech GmbH, Germany), NMP (PROLABO, Rhone-Poulenc), NMM (Alfa-Aesar GmbH, Germany) and acetic anhydride (Riedel-de Haen, Sigma-Aldrich GmbH, Germany), and as for the amino acids: Fmoc-L-Proline-OH from Novabiochem, Germany; Fmoc-L-Lysine(Boc)-OH from Iris Biotech GmbH, Germany; Fmoc-L-Aspartic acid(tBu)-OH from Benn Chemicals AG (Switzerland) and Fmoc-L-Arginine(Pbf)-Wang resin (100-200 mesh) was obtained from Novabiochem (Germany). Other reagents used include propiolic acid (98% Alfa-Aesar, Germany), 2-ethoxy-1-ethoxycarbonyl-1,2-dihydroquinoline, EEDQ (99%, Aldrich, Germany), copper (I) iodide (98%, Alfa Aesar, Germany), DIPEA (98%, Acros Organics, Belgium), EDC.HCl (Iris Biotech, Germany), HOBT (Propeptide, France) and propargylamine-TMS. Solvents used are obtained from Sigma-Aldrich and were used as received: DCM, DMF, petroleum ether, ethyl acetate, acetonitrile, tetrahydrofuran and methanol.

Different equipments were also used in the synthesis and purification of the synthesized compounds. The main ones include: microwave oven (Discover System, CEM, USA), two high-performance liquid chromatography (HPLC) systems: Waters™ (Waters™ 600 Controller with Waters™ 486 Tunable Absorbance Detector) and Varian®, rotary evaporator (Rotavapor R-215 with Vacuum Pump V-700 and Distillation chiller B-741, Büchi, Switzerland) and lyophilizator (Labconco, USA).

NMR (Proton NMR, COSY and TOCSY) were recorded on Avance 300 MHz NMR spectrometer (Bruker) by Dr Olivier Fabre. Chemical shifts were reported as part per million (ppm). Two different mass analysis were performed; high resolution mass analysis was by Dr Fabian Lachaud in Faculté de Science, Université de Lorraine, Vandœuvre-Les-Nancy, Nancy and the low resolution mass analysis was performed by Mme Mathilde Achard in LCPM, by LC-MS spectrometer 2020 (Shimadzu, Japan) through electron-spray ionization (ESI) technique.

EXPERIMENTAL SECTION

A. SYNTHESIS OF SPACERS

A1. Synthesis of MsO-DEG-MSO, 1

Diethylene glycol (1.0 equiv, 100 mmol) and triethylamine (3.2 equiv, 320 mmol) were solubilised in DCM (600 mL) and cooled down to -10°C before methanesulfonyl chloride (4.0 equiv, 400 mmol - diluted in 100 mL DCM) was added drop wise in 1 hour. Upon completion, they were left to agitate at room temperature for 24 hours under nitrogen. The crude compound was purified through crystallization in hot methanol and dried under vacuum.

Product **1**: [Yield: 70%. ¹H NMR (CDCl₃): δ (ppm) 3.06 (s, 6H, CH₃), 3.79 (ddd, 4H, CH₂-O), 4.37 (ddd, 4H, CH₂-O-MsO), TLC (DCM/MeOH: 95/5) Rf: 0.67 – visualization by phosphomolybdic acid (PMA) stain]

A2. Synthesis of MsO-DEG-N₃, 2

Compound **1** (1.0 equiv, 20 mmol) was solubilised in acetonitrile (50 mL) in the presence of sodium azide (1 equiv, 20 mmol) and left to agitate at 70°C for 40 hours under nitrogen, affording compound **2** after column purification with petroleum ether and ethyl acetate (65:35).

Product **2**: [Yield: 76%, ¹H NMR (CDCl₃) : δ (ppm) 3.04 (s, 3H, CH₃), 3.38 (t, 2H, CH₂-N₃), 3.68 (t, 2H, CH₂-O), 3.76 (t, 2H, CH₂-O), 4.35 (t, 2H, CH₂-O-MsO), TLC (PE/EtOAc: 65/35) Rf: 0.69 – visualization by 10% triphenylphosphine (PPh₃) followed by dipping in ninhydrin stain]

A3. Synthesis of 3-azidopropan-1-amine, 3

3-chloropropylamine.HCl (1.0 equiv, 15 mmol) was solubilised in water (50 mL) with sodium azide (3.0 equiv, 45 mmol) and left to agitate at 80°C for 24 hours. Two-third of the water was then removed under reduced pressure (90 mbar, 45°C) and the remaining solution was cooled with ice-bath. Diethyl ether (20 mL) was added followed by potassium hydroxide (2.3 equiv, 34.5 mmol – dissolved in 2 mL water) in drop wise in order to ensure that the temperature maintained below 10°C. The organic and aqueous phase was then separated. The aqueous phase was extracted with more diethyl ether (20 mL for multiple times) and combined organic phase was dried under reduced pressure, giving product **3** as yellowish oil.

Product **3**: [Yield: 56%, ¹H NMR (CDCl₃): δ (ppm) 1.59 (m, 2H, CH₂), 2.58 (t, 2H, CH₂-N₃), 3.37 (t, 2H, CH₂-NH₂)]

A4. Synthesis of Methyl 4-(2-(2-azidoethoxy)ethoxy)benzoic acid, **4'**

4-hydroxybenzoate (1.0 equiv, 3.3 mmol) was reacted with **2** (1.33 equiv, 4.4 mmol) in DMF (25 mL), in the presence of potassium carbonate (3.33 equiv, 11 mmol) at 80°C overnight. The crude was then washed and purified through column chromatography with petroleum ether and ethyl acetate (50:50) giving compound **4** as light-yellowish oil. Compound **4** (1.0 equiv, 2.3 mmol) was then saponified in ethanol (20 mL) in the presence of potassium hydroxide (2.0 equiv, 4.6 mmol) at 80°C for 24 hours. After the reaction was completed, the crude was neutralized with Amberlite IR-120, washed and extracted with cold diethyl ether (50 mL for 3 times) to give product **4'** as light-yellowish powder.

Product **4**: [Yield: 70%, ¹H NMR (CDCl₃) : δ (ppm) 3.32(t, 2H, CH₂-N₃), 3.66 (t, 2H, CH₂-O), 3.81 (t, 2H, CH₂-O), 4.01 (s, 3H, COOCH₃), 4.11 (t, 2H, CH₂-O-Ar), 6.86 (d, 2H, Ar), 7.90 (d, 2H, Ar), TLC (PE/EtOAc: 60/40) Rf: 0.71]

Product **4'**: [Yield: 97%, ¹H NMR (CDCl₃): δ (ppm) 3.41 (t, 2H, CH₂-N₃), 3.76 (t, 2H, CH₂-O), 3.88 (t, 2H, CH₂-O), 4.22 (t, 2H, CH₂-O-Ar), 6.95 (d, 2H, Ar), 8.00 (d, 2H, Ar). TLC (PE/EtOAc: 60/40) Rf: 0.46]

A5. Synthesis of 1,3-bis-(2-(2-azidoethoxy)ethoxy)phenyl)-ethenol, **5**

3,5-dihydroxybenzoate (1.0 equiv, 3.0 mmol) was reacted with **2** (2.2 equiv, 6.6 mmol) in DMF (30 mL), in the presence of potassium carbonate (6.66 equiv, 20 mmol) at 80°C overnight. The crude was then washed and purified through column chromatography with petroleum ether and ethyl acetate (50:50) giving compound **5** as light-yellowish oil. Compound **5** (1.0 equiv, 1 mmol) was then saponified in ethanol (20 mL) the presence of potassium hydroxide (2.0 equiv, 2 mmol) at 80°C for 24 hours. After the reaction was completed, the crude was neutralized with Amberlite IR-120, washed and extracted with cold diethyl ether (50 mL for 3 times) to give product **5'** as light-yellowish oil.

Product **5**: [Yield: 95%, ¹H NMR (CDCl₃) : δ (ppm) 3.37 (t, 4H, CH₂-N₃), 3.70 (t, 4H, CH₂-O), 3.82 (t, 4H, CH₂-O), 3.85 (s, 3H, COOCH₃), 4.13 (t, 4H, CH₂-O-Ar), 6.67 (t, 1H, Ar), 7.17 (d, 2H, Ar), TLC (PE/EtOAc: 60/40) Rf: 0.60]

Product **5'**: [Yield: 90%, ¹H NMR (CDCl₃) : δ (ppm) 3.42 (t, 4H, CH₂-N₃), 3.68 (t, 4H, CH₂-O), 3.78 (t, 4H, CH₂-O), 4.14 (t, 4H, CH₂-O-Ar), 6.77 (s, 1H, H₄ Ar), 7.06 (s, 2H, H₂ & H₆), 12.94 (s, 1H, COOH), TLC (PE/EtOAc: 60/40) Rf: 0.38]

A6. Synthesis of 1(3,4,5-tris-(2-(2-azidoethoxy)ethoxy)-phenyl)-ethenol, **6**

3,4,5-trihydroxybenzoate (1.0 equiv, 2.7 mmol) was reacted with **2** (3.3 equiv, 8.9 mmol) in DMF (40 mL), in the presence of potassium carbonate (10 eq.) at 80°C overnight. The crude was then washed and purified through column chromatography with petroleum ether and ethyl acetate (50:50) giving compound **6** as light-yellowish oil. Compound **6** (1.0 equiv, 1 mmol) was then saponified in ethanol (20 mL) in the presence of potassium hydroxide (2.0 equiv, 2 mmol) at 80°C overnight. After the reaction was completed, the crude was neutralized with Amberlite IR-120, washed and extracted with cold diethyl ether (50 mL for 3 times) to give product **6'** as yellowish oil.

Product **6**: [Yield: 96%, $^1\text{H NMR (CDCl}_3)$: δ (ppm) 3.39 (t, 6H, $\text{CH}_2\text{-N}_3$), 3.74 (t, 6H, $\text{CH}_2\text{-O}$), 3.82 (t, 2H, $\text{CH}_2\text{-OAr}_{\text{para}}$), 3.87 (t, 4H, $\text{CH}_2\text{-OAr}_{\text{meta}}$), 3.88 (s, 3H, COOCH_3), 4.21 (t, 4H, $\text{CH}_2\text{-OAr}_{\text{para}}$), 4.24 (t, 2H, $\text{CH}_2\text{-OAr}_{\text{meta}}$), 7.30 (s, 2H, Ar.), TLC (PE/EtOAc: 60/40) Rf: 0.58]

Product **6'**: [Yield: 75%, $^1\text{H NMR (CDCl}_3)$: δ (ppm) 3.40 (m, 6H, $\text{CH}_2\text{-N}_3$), 3.75 (t, 6H, $\text{CH}_2\text{-O}$), 3.85 (t, 2H, $\text{CH}_2\text{-OAr}_{\text{para}}$), 3.90 (t, 4H, $\text{CH}_2\text{-OAr}_{\text{meta}}$), 4.24 (t, 4H, $\text{CH}_2\text{-OAr}_{\text{meta}}$), 4.29 (t, 2H, $\text{CH}_2\text{-OAr}_{\text{para}}$), 7.39 (s, 2H, Ar.), TLC (PE/EtOAc: 60/40) Rf: 0.32]

B. PREPARATION OF PORPHYRIN (P1-COOH) AND CLICK REACTION

B1. Synthesis of porphyrin P1-COOH (5-(4-carboxyphenyl)-10,15,20-triphenyl porphyrin), **7**

Porphyrin P1-COOH was synthesized by the Lindsey method [80] as previously described in Chapter 1. The reaction condition used was mild with dry DCM as the solvent and under the flow of nitrogen. Pyrrole and benzaldehyde were distilled before-hand in order to ensure highest percentage of pure compound is used in the reaction. During the reaction, pyrrole (4.0 equiv), benzaldehyde (3.0 equiv) and 4-carboxybenzaldehyde (1.0 equiv) were added into DCM and left to stir at room temperatures. After 15 minutes, boron trifluoroetherate ($\text{BF}_3\cdot\text{OEt}_2$) was added and it was left to stir at room temperature for 2 hours. The intermediate porphyrinogene formed was then oxidized to form porphyrin by the addition of *para*-chloranil, an oxidizing agent and left to stir at 60°C for 2 hours.

The crude porphyrin mixture was then purified through two-steps purifications; (1) filtration through silica to eliminate tar and other unwanted polymers that formed together during the synthesis. The filtration was done by using a fritted Buchner filter funnel loaded with silica. The first elution step was by using DCM as the eluent and during this process, tetraphenylporphyrin will be eluted out. In the second step, DCM and ethanol mixture was used in order to elute porphyrin P1-COOH out of the silica. However, through filtration alone pure porphyrin is very difficult to obtain and hence, a second purification step is needed.

The semi-purified porphyrin was then subjected to (2) column purification by using silica (63-200 μm) with DCM and ethanol (97:3) as the eluent. By this method, porphyrin P1-COOH could be separated from other impurities more effectively. The eluted fraction which contained porphyrin P1-COOH was combined together and dried, giving the pure porphyrin P1-COOH as purple powder.

Product **7**: [Yield: 15%, $^1\text{H NMR (CDCl}_3)$: δ (ppm) -2.75 (s, 2H, $\text{NH}_{\text{inner ring}}$), 7.78 (d, 9H, $\text{CH}_{\text{pyrrole}}$), 8.22 (d, 6H, Ar), 8.37 (d, 2H, Ar_{COOH}), 8.53 (d, 2H, Ar_{COOH}), 8.82 (d, 8H, Ar). TLC (DCM/EtOH: 97/3) Rf: 0.48].

B2. Synthesis of Porphyrin P₁-CO-NH-propargyl, **8**

Compound **8** was prepared from porphyrin P₁-COOH (**7**) in a one-pot synthesis. Porphyrin P₁-COOH (1.0 equiv, 0.15 mmol) was dissolved in DCM (20 mL) and dicyclohexyl carbodiimide (DCC) (1.0 equiv, 0.15 mmol) and *N*-hydroxysuccinimide (NHS) (2.0 equiv, 0.3 mmol) were added into the solution. After specified time length (as detailed out in Table 1), propargylamine (in excess, 100 μ L) was added and the reaction was allowed to continue under the time length experimented to obtain compound **8**.

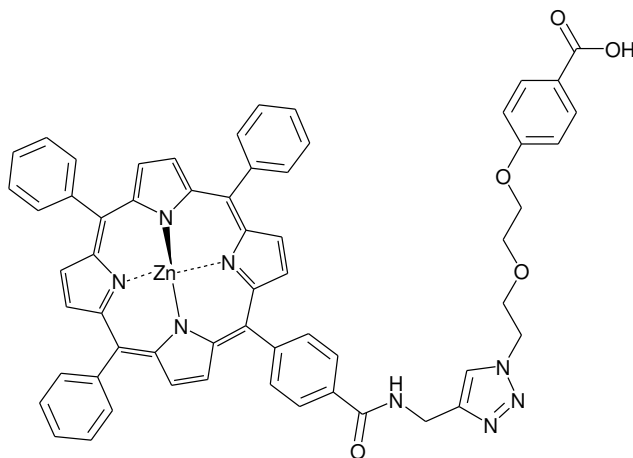
Product **8**: [Yield: 95%, ¹H NMR (CDCl₃) : δ (ppm) -2.89 (s, 2H, NH_{inner ring}), 3.33 (s, 1H, CH_{propargyl}), 4.24 (s, 2H, CH₂-propargyl), 7.81 (d, 9H, CH_{pyrrole}), 8.20 (d, 6H, Ar), 8.31 (d, 4H, Ar_{CONH}), 8.83 (d, 8H, Ar), 9.31 (t, 1H, NH-CH₂), TLC (DCM/EtOH: 97/3) Rf: 0.72].

B3. Synthesis of Porphyrin P₁-CO-NH-propargyl-Zn, **9**

Porphyrin P₁-CO-NH-alkyne (1.0 equiv, 0.1 mmol) was dissolved in THF (10 mL) and zinc acetate dihydrate (3.6 equiv, 0.36 mmol) was added. The mixture was then heated to 67°C and left to agitate under reflux for 2 hours. This reaction was monitored by UV/Visible spectrometer to confirm the insertion of zinc in the middle of the porphyrin ring. A sample from the reaction mixture was subjected to UV/Visible scanning from 200 nm to 800 nm to observe the change of Q-bands and complete metallation was indicated by the collapse of original four Q-bands into two (557 and 597 nm), and the shifting of Soret band from around 415 nm to 423 nm. At the end of the reaction, THF was removed under reduced pressure and the product was re-dissolved in DCM, washed with water (50 mL for five times) to remove the remaining zinc acetate. The product was then dried under reduced pressure to give compound **8** as bright purple crystalline solid.

Product **9**: [Yield: 99%, ¹H NMR (CDCl₃): δ (ppm) 4.56 (s, 1H, CH_{propargyl}), 4.84 (s, 2H, CH₂-propargyl), 7.80 (d, 9H, CH_{pyrrole}), 8.18 (d, 6H, Ar), 8.33 (d, 4H, Ar_{CONH}), 8.77 (d, 8H, Ar), TLC (DCM/EtOH: 97/3) Rf: 0.81]

B4. Click reaction between Porphyrin P₁-CO-NH-propargyl-Zn, 9 and 4'

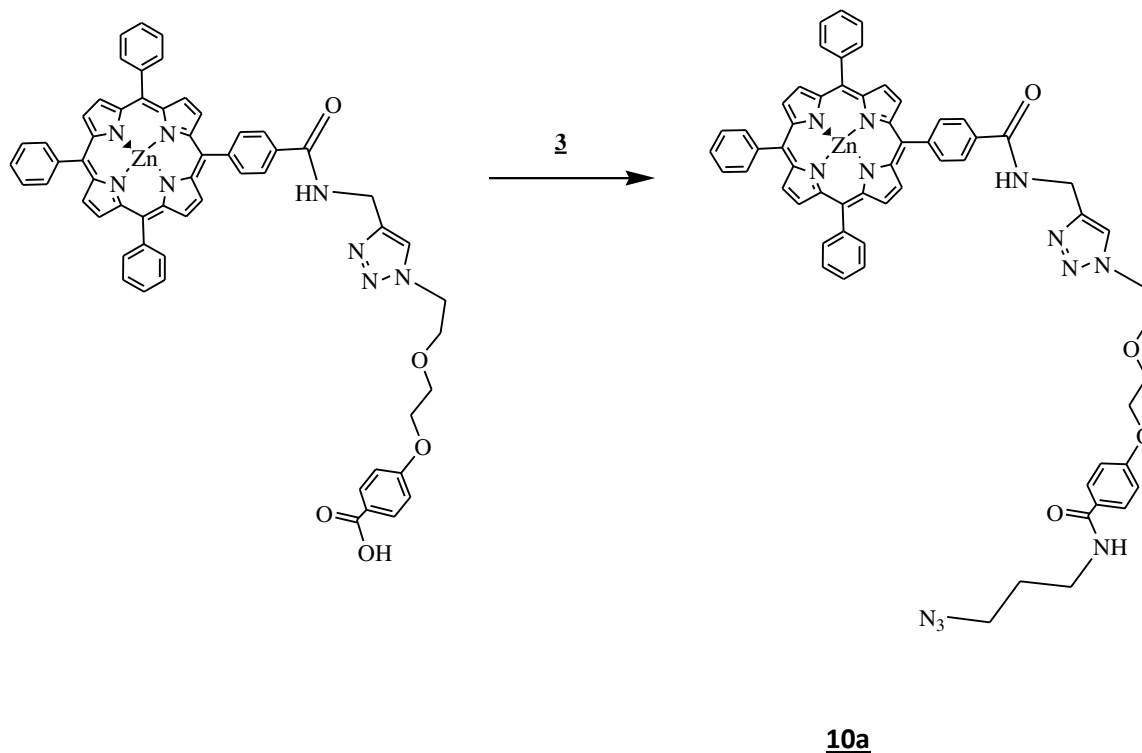


10

Click reaction between compound **4'** (1.0 equiv, 0.017 mmol) and **9** (1.0 equiv, 0.017 mmol) was conducted in the presence of CuSO₄·5H₂O (0.1 equiv, 0.002 mmol) and sodium ascorbate (0.5 equiv, 0.01 mmol). At the end of the synthesis, the crude product was washed with water (20 mL for three times) to eliminate the remaining catalyst and purified through column chromatography with a gradient of DCM and methanol from 98% DCM until 90% DCM to fully elute compound **10** from the column. The fraction containing compound **10** was combined and dried to give product **10** as dark purplish powder.

Product 10: [Yield: 97%, ¹H NMR (DMSO-d₆) : δ (ppm) 3.79 (t, 2H, CH₂-triazole ring), 3.94 (t, 2H, CH₂-O), 4.18 (t, 2H, CH₂-O), 4.58 (t, 2H, CH₂-O-Ar), 4.67 (d, 2H, CH₂-NH), 7.05 (d, 2H, H₃ & H₅ Ar), 7.80 (d, 9H, CH_{pyrrole}), 7.89 (d, 2H, H₄ & H₆ Ar), 8.17 (d, 7H, Ar & CH_{triazole}), 8.26 (dd, 4H, ArCONH), 8.75 (d, 8H, Ar), 9.40 (t, 1H, NH-CH₂), 12.47 (s, 1H, COOH-Ar). TLC (DCM/MeOH: 95/5) R_f: 0.40, Mass: Expected M^[+1]: 1009.27, M^[+2]: 505.14, M^[+3]: 337.09. Seen M^[+1]: 1009.30, M^[+2]: 505.30, M^[+3]: 337.10. Retention time on HPLC: 27.34 minutes

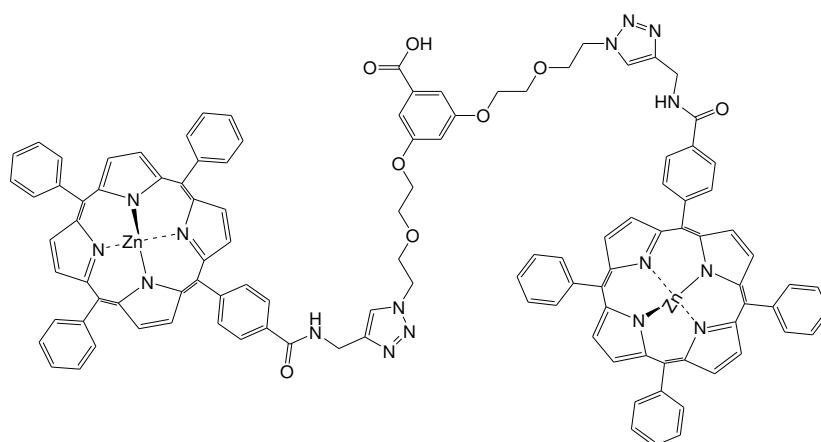
B5. Conjugation of azide group on 10



Compound **10** (1.0 equiv, 0.1 mmol), EDC.HCl (2.0 equiv, 0.2 mmol) and NHS (4.0 equiv, 0.4 mmol) were dissolved in 5mL DCM/methanol (4:1) and microwaved at 300 W, 40°C, 100 minutes. The coupling agents were added in extra, in the middle of the reactions (2 times supplementary addition). The reaction was monitored by TLC [Rf: 0.65 in DCM/methanol (93/7) for P₁-clicked-NHS] and subsequently compound **3** was added into the reaction vessel and the coupling was also conducted in microwave (300 W, 60°C, 120 minutes). The crude product was washed with HCl (1M), saturated NaHCO₃ and water. Purification was conducted through silica column purification (DCM/methanol (95:5), giving product **11** as purple solid.

Product 10a: [Yield: 72%, ¹H NMR (DMSO-d₆) : δ (ppm) 1.68 (m, 2H, N₃-CH₂-CH₂-CH₂-NH-), 2.93 (m, 2H, N₃-CH₂-CH₂-CH₂-NH-), 3.18 (q, 2H, N₃-CH₂-CH₂-CH₂-NH-), 3.80 (t, 2H, CH₂-triazole ring), 3.94 (t, 2H, CH₂-O), 4.17 (t, 2H, CH₂-O), 4.59 (t, 2H, CH₂-O-Ar), 4.68 (d, 2H, CH₂-NH), 7.03 (d, 2H, H₃ & H₅ Ar), 7.80 (d, 9H, CH_{pyrrole}), 7.79-8.77 (m, 29 H, CH_{porphyrin ring} & H₄ & H₆ Ar), 9.37 (t, 1H, NH-CH₂). TLC (DCM/MeOH: 95/5) Rf: 0.56, Mass: Expected M^[+1]: 1091.34, M^[+2]: 546.17, M^[+3]: 364.45. Seen M^[+1]: 1092.34

B6. Click reaction between Porphyrin P₁-CO-NH-propargyl-Zn, 9 and 5'

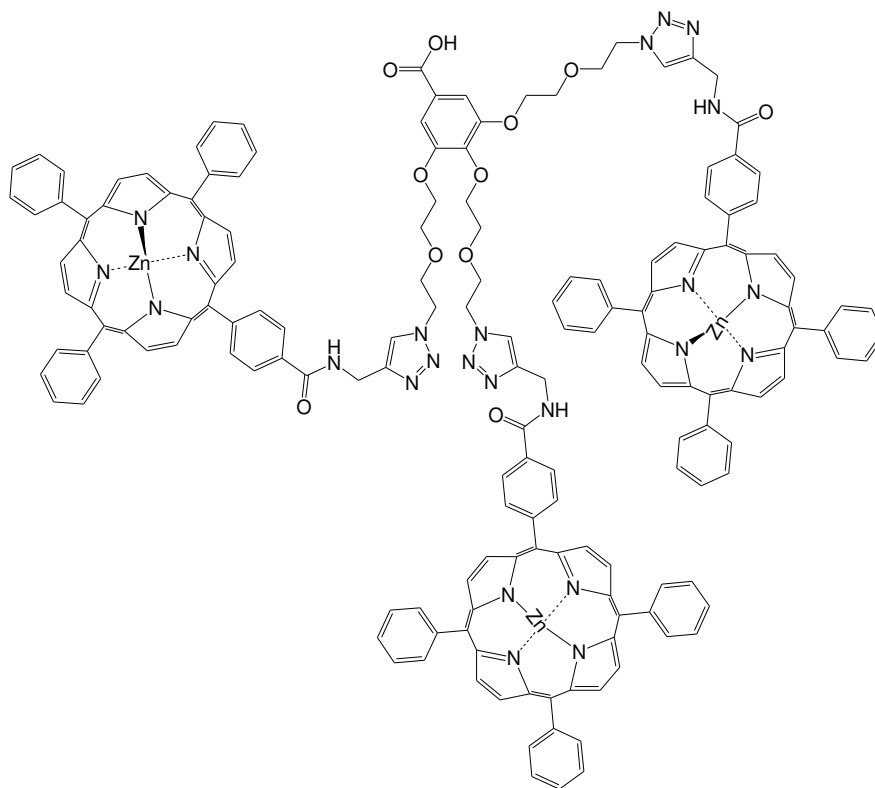


11

Product **11** was synthesized through the method as listed in Table 3. At the end of the reaction, the crude was washed with water to eliminate the $\text{CuSO}_4 \cdot 5\text{H}_2\text{O}$ and sodium ascorbate. It was then purified through silica column purification with a gradient of DCM and methanol from 98% DCM until 90% DCM followed by RP-HPLC to give product **11** as purple powder.

Product 11: [Yield: 80%, $^1\text{H NMR}$ (DMSO-d_6) δ (ppm) 3.79 (t, 4H, CH_2 -triazole ring), 3.87 (t, 4H, CH_2 -O), 4.09 (t, 4H, CH_2 -O), 4.53 (t, 4H, CH_2 -O-Ar), 4.65 (d, 2H, CH_2 -NH), 6.72 (s, 1H, H_3 Ar), 7.08 (s, 2H, H_2 & H_6 Ar), 7.76-8.76 (m, 54H, $\text{CH}_{\text{porphyrin ring}}$), 9.41 (t, 2H, NH-CH_2). **TLC** (DCM/MeOH : 95/5) Rf: 0.29, **Mass: Expected** $\text{M}^{[+1]}$: 1895.51, $\text{M}^{[+2]}$: 948.26, $\text{M}^{[+3]}$: 632.50, $\text{M}^{[+4]}$: 474.63, $\text{M}^{[+5]}$: 379.90, $\text{M}^{[+6]}$: 316.75, $\text{M}^{[+7]}$: 271.64, $\text{M}^{[+8]}$: 237.81. **Seen** $\text{M}^{[+4]}$: 473.35, $\text{M}^{[+6]}$: 314.30, $\text{M}^{[+8]}$: 235.25. **Retention time on HPLC:** 31.31 minutes

B7. Click reaction between Porphyrin P1-CO-NH-propargyl-Zn, 9 and 6'



12

The reaction was evaluated through conditions listed in Table 4 and one of the reactions, B6 was left to continue stirring at room temperature for 5 days. The reaction was monitored each day by TLC to observe the formation of product **12**. The crude was washed and purified by silica column purification (DCM/MeOH [95:5]) followed by RP-HPLC to give the expected product with 76.8% yield as confirmed by mass analysis and NMR spectroscopy.

Product 12: [Yield: 77%, $^1\text{H NMR}$ (DMSO-d_6): δ (ppm) 3.80 (t, 6H, CH_2 -triazole ring), 3.94 (t, 6H, CH_2 -O), 4.17 (t, 6H, CH_2 -O), 4.59 (t, 6H, CH_2 -O-Ar), 7.80 (d, 27H, $\text{CH}_{\text{pyrrole}}$), 7.89 (d, 2H, $\text{CH}_{\text{aromatic-COOH}}$), 8.17 (d, 27H, Ar & $\text{CH}_{\text{triazole}}$), 8.26 (dd, 12H, Ar_{CONH}), 8.75 (d, 24H, Ar), 9.40 (t, 3H, NH-CH_2), 12.47 (s, 1H, COOH-Ar] **TLC** (DCM/MeOH : 95/5) Rf: 0.21]. **Mass:** **Expected** $\text{M}^{[+1]}$: 2781.74, $\text{M}^{[+2]}$: 1391.37, $\text{M}^{[+3]}$: 927.91, $\text{M}^{[+4]}$: 696.19, $\text{M}^{[+5]}$: 557.15, $\text{M}^{[+6]}$: 464.46, $\text{M}^{[+3]}$: 398.25. **Seen** $\text{M}^{[+4]}$ + 4 Na^+ : 719.37. **Retention time on HPLC:** 32.12 minutes

C. DETERMINATION OF PHOTOPHYSICAL PROPERTIES OF THE PORPHYRIN-SPACERS

Photophysical properties of the three building blocks were determined through measurements of UV absorbance, singlet oxygen and fluorescence emission. The UV/visible absorbance were recorded on a UV-3600 Shimadzu spectrophotometer. Singlet oxygen production was measured by the IR detector through a SPEX double grating monochromator (600 grating/mm blazed 1 μm). Fluorescence emission spectra were recorded on a SPEX Fluorolog-3 spectrofluorimeter (Jobin Yvon, Longjumeau, France) with a thermo-stated cell compartment (25°C) by using a 450 watt Xenon lamp. All spectra were recorded by using four optical faces quartz cells.

The determination of singlet oxygen quantum yield [φ_{Δ} ($^1\text{O}_2$)] was estimated based on singlet oxygen luminescence at 1270 nm in ethanol as solvent and Rose Bengal as standard reference. Excitation was done with a Xe-arc and the light was separated in a SPEX 1680, 0.22 μm double monochromator. The detection at 1270 nm was carried out through a PTI S/N 1565 monochromator, with an emission monitoring by a liquid nitrogen-cooled Ge-detector model (EO-817L, North Coast Scientific Co, OH, USA).

The absorbance value at the excitation wavelength (423 nm) of the reference (Rose Bengal) and the sample solutions were set to be approximately 0.2 by dilutions.

Rose Bengal was chosen as the reference for singlet oxygen production due to its high singlet oxygen quantum yield in ethanol ($\varphi_{\Delta}= 0.68$). A 100% efficiency of singlet oxygen production will be equal to 1, but in general $\varphi_{\Delta} < 1$ since it is an estimated value based on a standard. The singlet oxygen quantum yield φ_{Δ} was then calculated by using the following formula:

$$\varphi_{\Delta} = \frac{\varphi_{\Delta o}}{D} \times D_o \times \frac{I}{I_o}$$

Where;

$\varphi_{\Delta o}$ = Singlet oxgen quantum yield of the standard (Rose Bengal)

D = Absorbance of sample at 423 nm

D_o = Absorbance of standard (Rose Bengal) at 423 nm

I = Intensity of luminescence of sample at 1270 nm

I_o = Intensity of luminescence of standard (Rose Bengal) at 1270 nm

Fluorescence production was observed with a solution of tetraphenyl porphyrin (TPP) in toluene as the standard reference. In order to produce fluorescence emission, the sample which was solubilised in ethanol was subjected to excitation at 423 nm which is the *lambda maxima* for the sample and during this process, fluorescence emission was set to be detected between 550 nm and 750 nm. The absorbance value at the excitation wavelength (423 nm) of both the TPP as reference and the sample solutions were set to be approximately 0.2 by dilutions. The recorded fluorescence intensity was then used to calculate the fluorescence quantum yield by using the following formula:

$$\varphi\phi_f = \varphi_{fo} \times \frac{D_o}{D} \times \frac{I}{I_o}$$

Where;

$\varphi\phi_{fo}$ = Fluorescence quantum yield of the standard (P1-COOH in toluene)

D = Absorbance of sample at 423 nm

D_o = Absorbance of standard (TPP) at 423 nm

I = Area under the curve of the fluorescence emission produced by the sample

I_o = Area under the curve of the fluorescence emission produced by the standard (TPP)

D. PREPARATION OF PEPTIDE (DKPPR) AND CLICK REACTION

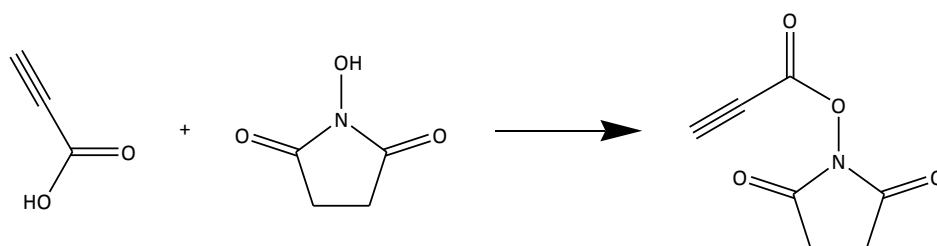
Peptide synthesis was conducted at 0.1 mmol synthesis scale, as elaborated in Chapter 3 and hence will not be described here-in. The synthesis method could be referred to in [Appendix 2](#) at the end of this thesis.

D1. Synthesis of protected DKPPR-alkyne on solid phase, **13**

EEDQ (2-ethoxy-1-ethoxycarbonyl-1,2-dihydroquinoline) (3.0 equiv, 0.3 mmol) and propiolic acid (3.0 equiv, 0.3 mmol) were dissolved in DCM (3 mL) and transferred into the reactor containing protected peptide on resin. This mixture was allowed to agitate at room temperature for 24 hours, and the mixture solution was red-orange at the end of the reaction. At the end of the reaction time, the mixture was washed three times with DCM (5 mL) and was used directly in the next synthesis step (See D3).

D2. Synthesis of protected DKPPR-alkyne on liquid phase

The synthesis was started by the synthesis of succinimidyl-3-propiolate, in which the propiolic acid that will be used for the introduction of alkyne group on free amine on aspartic acid is pre-activated by NHS.



14

Propiolic acid (1.0 equiv, 10 mmol) and NHS (1.0 equiv, 10 mmol) were dissolved in ethyl acetate (30 mL) in a tricol and cooled down to 0°C under continuous stirring and nitrogen flow. Separately, DCC (1.0 equiv, 10 mmol) was dissolved in ethyl acetate (10 mL) and added into the mixture of propiolic acid and NHS, dropwise in approximately one hour. The reaction was left to stir at room temperature for 6 hours at 0-4°C and the precipitated by-product, dicyclohexyl urea was removed by filtration by using Celite-545[®]. The filtrate was concentrated through evaporation and washed with saturated sodium chloride, dried with magnesium sulphate and further concentrated to approximately 1 mL. The concentrated solution was cooled to -5°C and 20 mL of heptanes was added before it was further cooled down to -20°C. A recirculating chiller system with ethanol as the cooling liquid was used to achieve very low temperature necessary for the reaction. The solid precipitated presence was left at -20°C for 2 hours, filtered and dried under vacuum to give product **14** as light brownish powder.

To synthesize the protected DKPPR-alkyne on liquid phase, product **14** (5.0 equiv, 0.5 mmol) and the protected DKPPR peptide powder were dissolved in DCM (10 mL). The reaction was left to pursue at room temperature for 6 days and purified by RP-HPLC (Table 31) to give the pure product **15** as white powder.

Table 25: The purification condition for product **15**

Purification of 15			
Column (Analytical)	Machery-Nagel Nucleosil 100-5 VP 150/21		
Column (Preparative)	Machery-Nagel Nucleosil 100-5 VP 150/21		
Solvent	Water/Acetonitrile/0.1% TFA		
Gradient	Time (min)	Water (% conc.)	Acetonitrile (% conc.)
	0	95	5
	10	60	40
	25	25	75
	35	95	5
Flow rate	12 ml/min (Preparative)		
Detector	UV/Visible at 214 nm		

Product **14**: [Yield: 56%, ¹H NMR (CDCl₃): δ (ppm) 2.86 (d, 4H, CH₂-succinimide), 3.29 (t, 1H, CH_{propargyl}), TLC (DCM/Ethanol: 97/3) Rf: 0.75]

Product **15**: [Yield: 48%. Mass: Expected M^[+1]: 1072.53, M^[+2]: 536.77, M^[+3]: 358.18. Seen M^[+1]: 1072.65, M^[+2]: 357.25. Retention time on HPLC: 23.33 minutes.

D3. Approach 1: Click reaction between protected DKPPR-alkyne on solid support, 13 and 4', and addition of second alkyne group on carboxylic group of 4'

Protected DKPPR-alkyne on solid phase was dissolved in THF (3 mL) and compound 4' (1.2 equiv, 0.12 mmol), CuI (2.0 equiv, 0.2 mmol) and diisopropylethylamine (50 equiv, 5 mmol) were added in THF. The mixture was dark green upon mixing. It was allowed to agitate at room temperature for 72 hours. This phase produced DKPPR-one arm block.

The addition of second alkyne group was conducted by adding propargylamine (in excess, 100 μ L) with carbodiimidazol (2.0 equiv) in THF (3 mL). However this reaction did not work.

D4. Approach 2: Click reaction between protected DKPPR-alkyne on solid support, 13 and modified building blocks 4'', 5'' and 6''

Synthesis of modified building blocks 4'', 5'' and 6''

Building block (1.0 equiv, 0.2 mmol) was dissolved in DMF (10 mL) with EDC.HCl (1.2 equiv, 0.24 mmol) and HoBT (1.2 equiv, 0.24 mmol). Separately, triethylamine (1.2 equiv, 0.24 mmol) was mixed with propargylamine-TMS (1.2 equiv, 0.12 mmol). The two solutions were then combined and let to stir at room temperature for 24 hours (for 4'', 5'') and 120 hours (for 6''). The crude was washed with HCl 1M, saturated NaHCO₃ and water and subsequently purified through column chromatography with petroleum ether and ethyl acetate as the eluent (70:30 to 60:40), giving the purified compound as yellowish oil.

Product 4'': [Yield: 98%, ¹H NMR (DMSO-d₆): δ (ppm) 0.10 (s, 9H, Si-CH₃), 3.40 (t, 2H, CH₂-N₃), 3.66 (t, 2H, CH₂-O), 3.78 (t, 2H, CH₂-O), 4.06 (d, 2H, CH₂-NH), 4.15 (t, 2H, CH₂-O-Ar), 6.98 (d, 2H, H₃ & H₅ Ar), 7.79 (d, 2H, H₂ & H₆), 8.73 (t, 1H, NH-CH₂). TLC (PE/EtOAc: 70/30) Rf: 0.34]

Product 5'': [Yield: 13%, ¹H NMR (DMSO-d₆) : δ (ppm) 0.15 (s, 9H, Si-CH₃), 3.40 (t, 4H, CH₂-N₃), 3.65 (t, 4H, CH₂-O), 3.79 (t, 4H, CH₂-O), 4.09 (d, 2H, CH₂-NH), 4.14 (t, 4H, CH₂-O-Ar), 7.03 (s, 2H, H₂ & H₆), 7.49 (1H, H₄ Ar), 8.00 (t, 1H, NH-CH₂), TLC (PE/EtOAc : 60/40) Rf: 0.37]

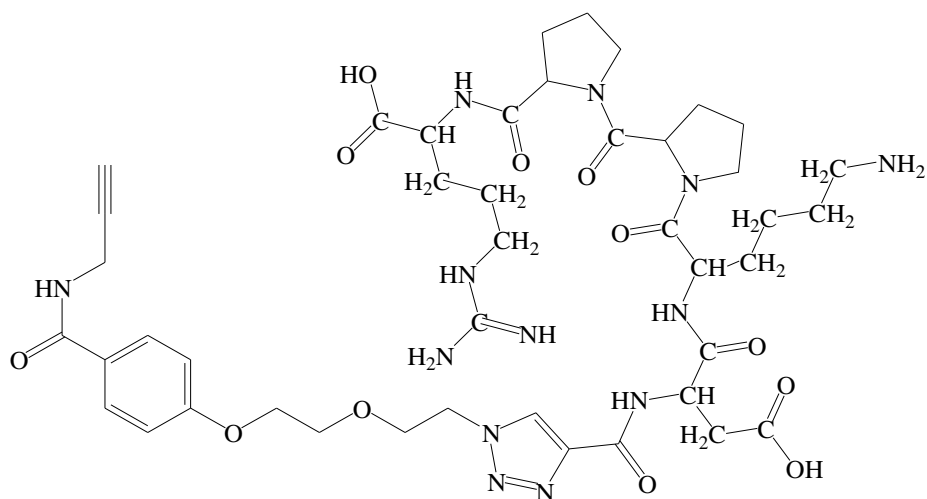
Product 6'': [Yield: 68%, ¹H NMR (CDCl₃): δ (ppm) 0.07 (s, 9H, Si-CH₃), 3.41 (t, 6H, CH₂-N₃), 3.74 (t, 6H, CH₂-O), 3.85 (t, 6H, CH₂-O), 4.18-4.26 (m, 8H, CH₂-NH & CH₂-O-Ar), 6.98 (s, 2H, H₂ & H₆ Ar). TLC (PE/EtOAc: 70/30) Rf: 0.13]

Click reaction between protected DKPPR on Wang resin and building blocks 4'', 5'' and 6''

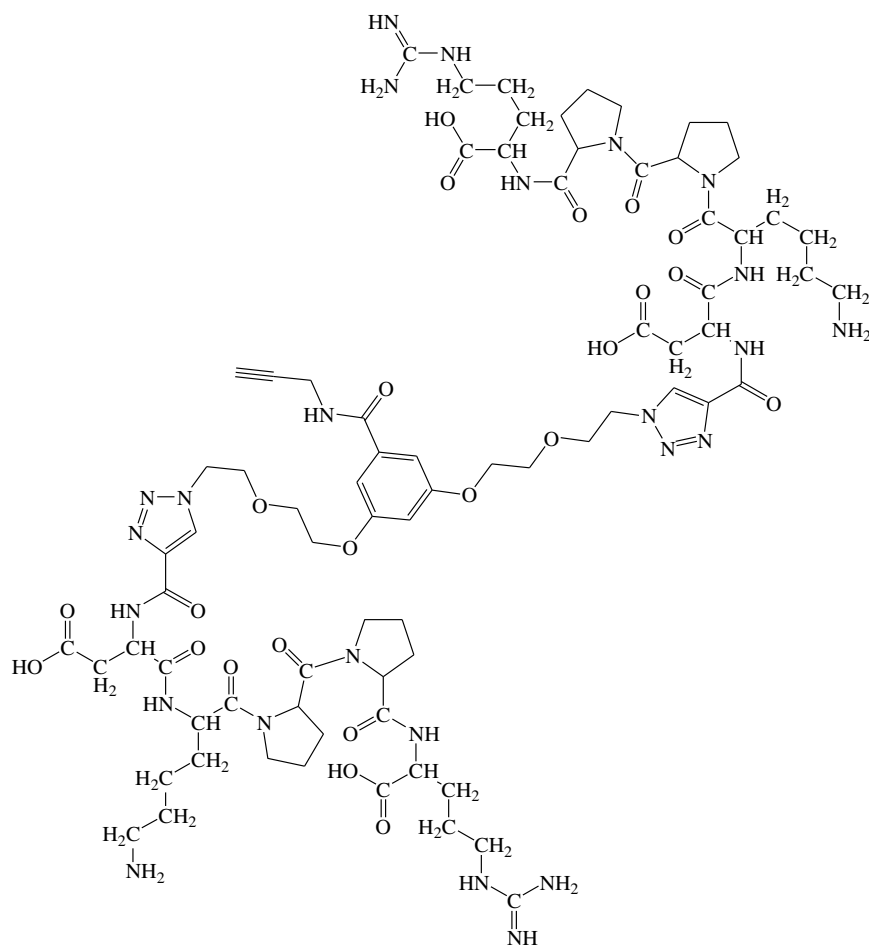
Product **14** was clicked with **4''** (1.0 equiv), **5''** (0.33 equiv) or **6''** (0.20 equiv) in the presence of CuI (2.0 equiv, 0.2 mmol) and DIPEA (50 equiv, 5 mmol). The reactions were left to agitate for 72 hours before the protecting groups were cleaved by using a mixture of trifluoroacetic acid (TFA), triisopropylsilane (TIPS) and water (95 TFA:2.5 TIPS:2.5 water). The crude mixture was then lyophilized and purified by RP-HPLC, giving the clicked peptide product **17**, **18** and **19**. Table 32 below simplified the RP-HPLC condition for the purification of the three products.

Table 26: The purification condition for products **17**, **18** and **19**

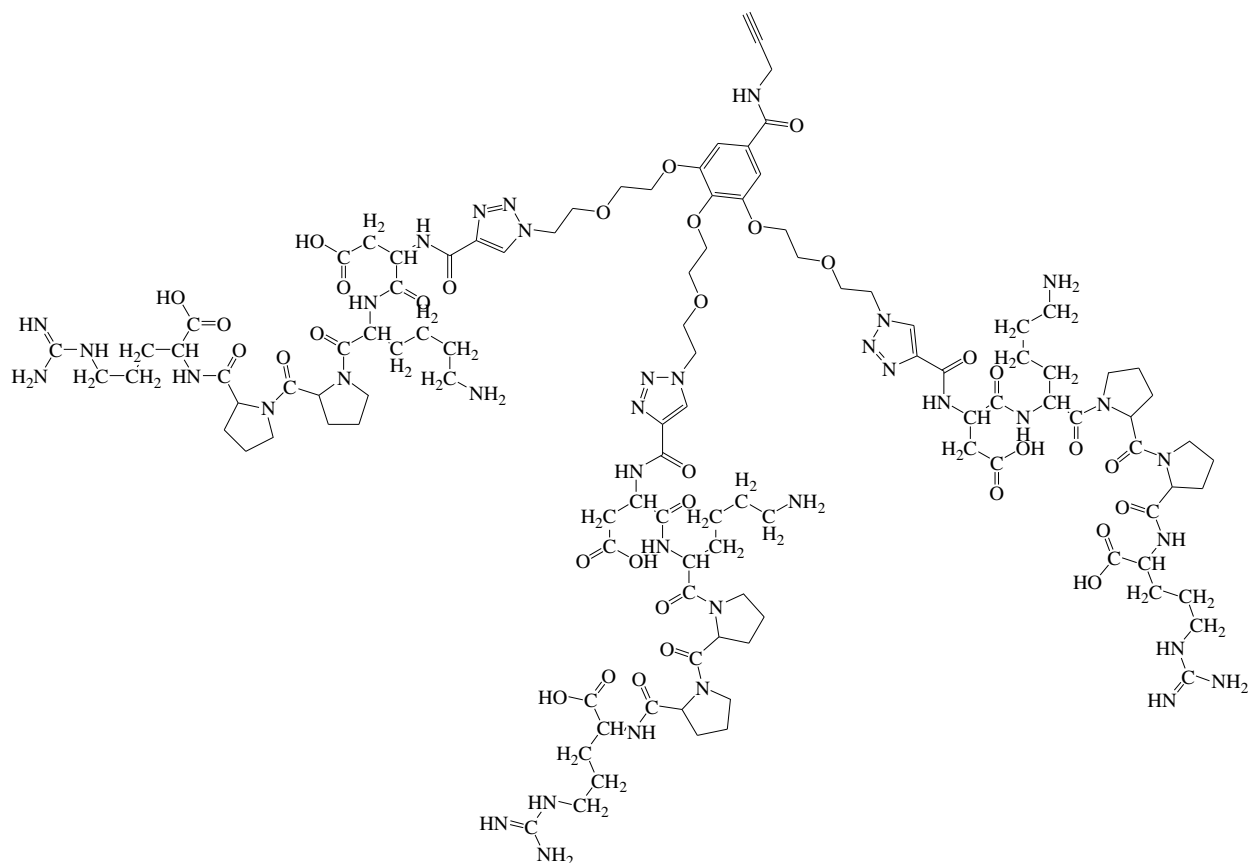
	Purification of 17 , 18 and 19		
Column (Analytical)	Agilent Pursuit 5 C18 150 x 4.6 mm		
Column (Preparative)	Agilent Pursuit 5 C18 150 x 21.2 mm		
Solvent	Water/Acetonitrile/0.1% TFA		
Gradient	Time (min)	Water (% conc.)	Acetonitrile (% conc.)
	0	90	10
	5	90	10
	20	0	100
	30	0	100
33	90	10	
Flow rate	1 ml/min (analytical) 12 ml/min (preparative)		
Detector	UV/Visible at 214 nm		



Product **17**: [Yield: 51%. $^1\text{H NMR}$ (DMSO-d_6): δ (ppm) 1.32-1.62 (5H, $\gamma\text{-CH}_2$, $\delta\text{-CH}_2$, $\beta\text{-H}$, Lys_2), 1.49-1.72 (4H, $\gamma\text{-CH}_2$, 2 $\beta\text{-H}$, Arg_5), 1.78-2.13 (8H, 2 $\gamma\text{-CH}_2$, 4 $\beta\text{-H}$, Pro_3 & Pro_4), 2.71 (2H, 2 $\beta\text{-H}$, Asp_1), 2.73 (2H, $\epsilon\text{-CH}_2$, Lys_2), 3.10 (2H, $\delta\text{-CH}_2$, Arg_5), 3.35 (s, 1H, $\text{CH}_{\text{propargyl}}$), 3.46-3.64 (4H, 4 $\delta\text{-H}$, Pro_3 & Pro_4), 4.02 (t, 2H, $\text{CH}_2\text{-N}_3$), 4.04 (d, 2H, $\text{CH}_2\text{-NH}$), 4.12 (1H, $\alpha\text{-H}$, Arg_5), 4.15 (t, 2H, $\text{CH}_2\text{-O}$), 4.20 (t, 2H, $\text{CH}_2\text{-O}$), 4.30 (t, 2H, $\text{CH}_2\text{-O-Ar}$), 4.35 (1H, $\alpha\text{-H}$, Pro_3), 4.52 (1H, $\alpha\text{-H}$, Lys_2), 4.55 (1H, $\alpha\text{-H}$, Pro_4), 4.77 (1H, $\alpha\text{-H}$, Asp_1), 7.03 (d, 2H, H_3 & H_5 Ar), 7.17 (d, 2H, H_2 & H_6), 7.62 (1H, $\epsilon\text{-NH}$, Arg_5), 7.99 (1H, $\epsilon\text{-NH}$, Lys_2), 8.04 (1H, $\epsilon\text{-NH}$, Asp_1), 8.64 (t, 1H, NH-CH_2). **Mass**: Expected $\text{M}^{[+1]}$: 970.46, $\text{M}^{[+2]}$: 485.73, $\text{M}^{[+3]}$: 324.95. **Seen**: 970.40, $\text{M}^{[+2]}$: 486.00, $\text{M}^{[+3]}$: 323.95. **Retention time on HPLC**: 11.33 minutes.]



Product **18**: [Yield: 40%, $^1\text{H NMR}$ (DMSO-d_6): δ (ppm) 1.35-1.65 (10H, 2 γ - CH_2 , 2 δ - CH_2 , 2 β -H, Lys₂), 1.49-1.72 (8H, 2 γ - CH_2 , 4 β -H, Arg₅), 1.80-2.10 (16H, 4 γ - CH_2 , 8 β -H, Pro₃ & Pro₄), 2.71 (4H, 4 β -H, Asp₁), 2.75 (4H, 2 ϵ - CH_2 , Lys₂), 3.10 (4H, 2 δ - CH_2 , Arg₅), 3.33 (s, 1H, $\text{CH}_{\text{propargyl}}$), 3.49-3.69 (8H, 8 δ -H, Pro₃ & Pro₄), 3.80 (t, 4H, $\text{CH}_2\text{-N}_3$), 4.04 (d, 4H, $\text{CH}_2\text{-NH}$), 4.14 (2H, 2 α -H, Arg₅), 4.13 (t, 4H, $\text{CH}_2\text{-O}$), 4.19 (t, 4H, $\text{CH}_2\text{-O}$), 4.28 (t, 4H, $\text{CH}_2\text{-O-Ar}$), 4.35 (2H, 2 α -H, Pro₃), 4.55 (2H, 2 α -H, Lys₂), 4.62 (2H, 2 α -H, Pro₄), 4.76 (2H, 2 α -H, Asp₁), 7.40 (2H, 2 ϵ -NH, Arg₅), 7.57 (d, 2H, H₂ & H₆ Ar), 7.80 (d, 2H, H₄ Ar), 8.05 (2H, 2 ϵ -NH, Lys₂), 8.35 (2H, 2 ϵ -NH, Asp₁), 8.65 (t, 1H, NH-CH_2). **Mass: Expected** $M^{[+1]}$: 1744.84, $M^{[+2]}$: 872.92, $M^{[+3]}$: 582,28, $M^{[+4]}$: 436.96. **Seen** $M^{[+2]}$: 873.10 $M^{[+3]}$: 583.55. **Retention time on HPLC**: 12.91 minutes.]



Product **19**: [Yield: 13%. $^1\text{H NMR (DMSO-}d_6)$: δ (ppm) 1.39-1.71 (15H, 3 γ -CH₂, 3 δ -CH₂, 3 β -H, Lys₂), 1.48-1.72 (12H, 3 γ -CH₂, 6 β -H, Arg₅), 1.82-2.13 (24H, 6 γ -CH₂, 12 β -H, Pro₃ & Pro₄), 2.73 (6H, 6 β -H, Asp₁), 2.75 (6H, 3 ϵ -CH₂, Lys₂), 3.11 (6H, 3 δ -CH₂, Arg₅), 3.32 (s, 1H, CH_{propargyl}), 3.52-3.75 (12H, 12 δ -H, Pro₃ & Pro₄), 3.83 (t, 6H, CH₂-N₃), 4.02 (d, 6H, CH₂-NH), 4.11 (t, 6H, CH₂-O), 4.16 (3H, 3 α -H, Arg₅), 4.18 (t, 6H, CH₂-O), 4.26 (t, 2H, CH₂-O-Ar), 4.35 (3H, 3 α -H, Pro₃), 4.57 (3H, 3 α -H, Pro₄), 4.71 (3H, 3 α -H, Lys₂), 4.77 (3H, 3 α -H, Asp₁), 7.58 (3H, 3 ϵ -NH, Arg₅), 7.69 (d, 2H, H₂ & H₆ Ar), 8.19 (3H, 3 ϵ -NH, Lys₂), 8.61 (3H, 3 ϵ -NH, Asp₁), 8.68 (t, 1H, NH-CH₂). **Mass: Expected** M^[+1]: 2553.23, M^[+2]: 1277.62, M^[+3]: 852.08, M^[+4]: 639.31, M^[+5]: 511.65. **Seen** M^[+3]: 852.76, M^[+4]: 639.82, M^[+5]: 512.06. **Retention time on HPLC**: 16.51 minutes.]

[The mass of the products seen after purification are in the presence of one water molecule. This is not surprising due to the hydrophilic characteristics of DKPPR peptide]

References

1. Delehanty, J.B., et al., *Peptides for specific intracellular delivery and targeting of nanoparticles : implications for developing nanoparticles-mediated drug delivery*. Therapeutic Delivery, 2010. **1**(3): p. 411-433.
2. Sharman, W.M., J.E. van Lier, and C.M. Allen, *Targeted photodynamic therapy via receptor mediated delivery systems*. Advanced Drug Delivery Reviews, 2004. **56**: p. 53-76.
3. Ormond, A.B. and H.S. Freeman, *Dye sensitizers for photodynamic therapy*. Materials, 2013. **6**: p. 817-840.
4. Boyle, R.W.J., Leanne B, *Unique diagnostic and therapeutic roles of porphyrins and phthalocyanines in photodynamic therapy, imaging and theranostics*. Theranostics, 2012. **2**(9): p. 916-966.
5. Kamarulzaman, E.E., et al., *Molecular modelling, synthesis and biological evaluation of peptide inhibitors as anti-angiogenic agent targeting Neuropilin-1 for anticancer application*. J Biomol Struct Dyn, 2016. **14**: p. 1-49.
6. Kamarulzaman, E.E., et al., *New Peptide-Conjugated Chlorin-Type Photosensitizer Targeting Neuropilin-1 for Anti-Vascular Targeted Photodynamic Therapy*. Int J Mol Sci, 2015. **16**(10): p. 24059-80.
7. Michor, F., Y. Iwasa, and M.A. Nowak, *Dynamic of cancer progression*. Nature Reviews Cancer, 2004. **4**: p. 197-206.
8. Bryan, G., *Randomised controlled trials of interventions to prevent oral mucositis in patients undergoing treatment for cancer*, in Faculty of Medical and Human Sciences 2010, University of Manchester: Manchester. p. 276.
9. Prevention, C.f.D.C.a. *Global Cancer Statistics*. 2015.
10. WHO, W.H.O. *Cancer*. February 2014 - 28 August 2014]; Available from: <http://www.who.int/mediacentre/factsheets/fs297/en/>.
11. Collins, I. and P. Workman, *New approaches to molecular cancer therapeutics*. Nature Chemical Biology, 2006. **2**(12): p. 689-700.
12. Greaves, M., *Evolutionary determinants of cancer*. Cancer Discovery, 2015. **5**: p. 806-820.
13. Schroeder, A., et al., *Treating metastatic cancer with nanotechnology*. Nature Reviews Cancer, 2012. **12**: p. 39-50.
14. Kinzler, K.W. and B. Vogelstein, *Gatekeepers and caretakers*. Nature, 1997. **386**(6627).
15. Srivastava, S. and W.E. Grizzle, *Biomarkers and the genetics of early neoplastic lesions*. Cancer biomarkers : section A of Disease markers, 2010. **9**(1-6): p. 41-64.
16. Srivastava, S., M. Verma, and D.E. Henson, *Biomarkers for early detection of colon cancer*. Clinical Cancer Research, 2001. **7**: p. 1118-1126.
17. Olsson, A.-K., et al., *VEGF receptor signalling - in control of vascular function*. Nature Reviews Molecular Cell Biology, 2006. **7**: p. 359-371.
18. Hoeben, A., et al., *Vascular endothelial growth factor and angiogenesis*. Pharmacological Reviews, 2004. **56**(4): p. 549-580.
19. Kerbel, R.S., *Tumor angiogenesis: Past, present and the near future*. Carcinogenesis, 2000. **21**(3): p. 505-515.
20. Ferrara, N., *VEGF and the quest for tumour angiogenesis factors*. Nature Reviews Cancer, 2002. **2**(10): p. 795-803.
21. Weis, S.M. and D.A. Cheresh, *Tumor angiogenesis : molecular pathways and therapeutic targets*. Nature Medicine, 2011. **17**(11): p. 1359-1370.
22. Mikkelsen, T. and D. Reardon *Antiangiogenic therapy for glioblastoma: New directions*. Targeting Tumor Angiogenesis, 2010. **Spring 2010**, 1-5.

23. Matthies, A.M., et al., *Neuropilin-1 participates in wound angiogenesis*. The American Journal of Pathology, 2002. **160**(1): p. 289-296.
24. Duffy, A.M., D.J. Bouchier-Hayes, and J.H. Harmey, *Vascular endothelial growth factor (VEGF) and its role in non-endothelial cells : Autocrine signalling by VEGF*, in *Madame Curie Bioscience Database (Internet)2000*, Landes Bioscience: Austin, Texas.
25. Ashikari-Hada, S., et al., *Heparin regulates vascular endothelial growth factor165-dependent mitogenic activity, tube formation, and its receptor phosphorylation of human endothelial cells. Comparison of the effects of heparin and modified heparins*. The Journal of Biological Chemistry, 2005. **280**(36): p. 31508-31515.
26. Chaudhary, B., et al., *Neuropilin 1 : Function and therapeutic potential in cancer*. Cancer Immunology, Immunotherapy, 2014. **63**(2): p. 81-99.
27. Glinka, Y., et al., *Neuropilin-1 exerts co-receptor function for TGF-beta-1 on the membrane of cancer cells and enhances responses to both latent and active TGF-beta*. Carcinogenesis, 2011. **32**(4): p. 613-621.
28. Chaudhary, B., et al., *Neuropilin 1: function and therapeutic potential in cancer*. Cancer Immunol Immunother, 2014. **63**(2): p. 81-99.
29. Whitaker, G.B., B.J. Limberg, and J.S. Rosenbaum, *Vascular endothelial growth factor receptor-2 and neuropilin-1 form a receptor complex that is responsible for the differential signaling potency of VEGF(165) and VEGF(121)*. J Biol Chem, 2001. **276**(27): p. 25520-25531.
30. Geretti, E. and M. Klagsbrun, *Neuropilins : Novel targets for anti-angiogenesis therapies*. Cell Adh Migr, 2007. **1**(2): p. 56-61.
31. Pavelock, K., et al., *Differential expression and regulation of the vascular endothelial growth factor receptors neuropilin-1 and neuropilin-2 in rat uterus*. Endocrinology, 2001. **142**(2): p. 613-622.
32. Latil, A., et al., *VEGF overexpression in clinically localized prostate tumors and neuropilin-1 overexpression in metastatic forms*. Int J Cancer, 2000. **89**(2): p. 167-171.
33. Fakhari, M., et al., *Selective upregulation of vascular endothelial growth factor receptors Neuropilin-1 and -2 in human neuroblastoma*. Cancer, 2002. **94**(1): p. 258-263.
34. Berge, M., et al., *Neuropilin-1 is upregulated in hepatocellular carcinoma and contributes to tumour growth and vascular remodelling*. J Hepatol, 2011. **55**(4): p. 866-75.
35. Ellis, L.M., *The role of neuropilins in cancer*. Mol Cancer Ther, 2006. **5**(5): p. 1099-1107.
36. Zhao, X., H. Li, and R.J. Lee, *Targeted drug delivery via folate receptor*. Expert Opinion on Drug Delivery, 2008. **5**(3): p. 309-319.
37. Chen, C., et al., *Structural basis for molecular recognition of folic acid by folate receptors*. Nature, 2013. **500**(7463): p. 486-489.
38. Marchetti, C., et al., *Targeted drug delivery via folate receptors in recurrent ovarian cancer: A review*. OncoTargets and Therapy, 2014. **7**: p. 1223-1236.
39. Kalli, K.R., et al., *Folate receptor alpha as a tumor target in epithelial ovarian cancer*. Gynecol Oncol, 2008. **108**(3): p. 619-26.
40. Parker, N., et al., *Folate receptor expression in carcinomas and normal tissues determined by a quantitative radioligand binding assay*. Analytical Biochemistry, 2005. **338**(2): p. 284-293.
41. Bhattacharya, R., et al., *Attaching folic acid on gold nanoparticle using noncovalent interaction via different polyethylene glycol*. Nanomedicine: Nanotechnology, Biology, and Medicine, 2007. **3**(3): p. 224-238.
42. WorldHealthOrganization, *National cancer control programmes, in Policies and managerial guidelines2002*, World Health Organization: Geneva.
43. AmericanCancerSociety, *Cancer treatment & survivorship Facts & Figures 2014-2015*, 2014, American Cancer Society.
44. Bosch, F.I. and L. Rosich, *The Contributions of Paul Ehrlich to Pharmacology: A Tribute on the Occasion of the Centenary of His Nobel Prize*. Pharmacology, 2008. **82**(3): p. 171-179.
45. Mandal, A. *History of chemotherapy*. News Medical, 2014.

46. Parasuraman, S., *Basic principles of chemotherapy: Timeline history of chemotherapy development*, 2013.
47. Society, A.C., *Cancer immunotherapy*, 2015, American Cancer Society.
48. Vasudev, N.S. and A.R. Reynolds, *Anti-angiogenic therapy for cancer: current progress, unresolved questions and future directions*. *Angiogenesis*, 2014. **17**(3): p. 471-494.
49. Dougherty, T.J., et al., *Photoradiation therapy. II. Cure of animal tumors with hematoporphyrin and light*. *J Natl Cancer Inst*, 1975. **55**(1): p. 115-21.
50. Dolmans, D.E.J.G.J., D. Fukumura, and R.K. Jain, *Photodynamic therapy for cancer*. *Nature Reviews Cancer* 2003. **3**: p. 380-387.
51. Agostinis, P., et al., *Photodynamic Therapy of Cancer : An Update*. *CA : A Cancer Journal for Clinicians*, 2011. **61**(4): p. 250-281.
52. Hargus, J.A., *Naturally-derived porphyrin and chlorin photosensitizers for photodynamic therapy*, in *The Department of Chemistry* 2005, Louisiana State University: Louisiana.
53. Dai, T., et al., *Concepts and principles of photodynamic therapy as an alternative antifungal discovery platform*. *Front Microbiol.*, 2012. **3**(120): p. 1-16.
54. Agostinis, P., et al., *Photodynamic therapy of cancer*. *CA-Cancer J Clin*, 2011. **61**(4): p. 250-281.
55. Luksiene, Z., A. Kalvelyte, and R. Supino, *On the combination of photodynamic therapy with ionizing radiation*. *J Photochem Photobiol B*, 1999. **52**(1-3): p. 35-42.
56. Colasanti, A., et al., *Combined effects of radiotherapy and photodynamic therapy on an in vitro human prostate model*. *Acta Biochim Pol*, 2004. **51**(4): p. 1039-1046.
57. Zhu, T.C. and J.C. Finlay, *The role of photodynamic therapy (PDT) physics*. *Medical Physics*, 2008. **35**(7): p. 3127-3136.
58. Figge, F.H., G.S. Weiland, and L.O. Manganiello, *Studies on cancer detection and therapy; the affinity of neoplastic, embryonic, and traumatized tissue for porphyrins, metalloporphyrins, and radioactive zinc hematoporphyrin*. *Anat Rec*, 1948. **101**(4): p. 657.
59. Denis, T.G. and M.R. Hamblin, *Synthesis, bioanalysis and biodistribution of photosensitizer conjugates for photodynamic therapy*. *Bioanalysis*, 2013. **5**(9): p. 1099-1114.
60. Bhuvaneswari, R., et al., *Photodynamic therapy in combination with antiangiogenic approaches improve tumor inhibition*, in *Current cancer treatment - Novel beyond conventional approaches*, P.O. Ozdemir, Editor 2011, InTech.
61. Moor, A., B. Ortel, and T. Hasan, *Mechanisms of photodynamic therapy*. *Photodynamic therapy*, ed. T. Patrice, D.-P. Hader, and G. Jori 2003, Cambridge, UK: The Royal Society of Chemistry.
62. Yoon, I., J.Z. Li, and Y.K. Shim, *Advance in photosensitizers and light delivery for photodynamic therapy*. *Clinical Endoscopy*, 2013. **46**: p. 7-23.
63. Classen, M. and G.N.J. Tytgat, *Gastroenterological Endoscopy* 2011: Thieme. 852.
64. van den Bergh, H., *On the evolution of some endoscopic light delivery systems for photodynamic therapy*. *Endoscopy*, 1998. **30**(4): p. 392-407.
65. Cochrane, C., et al., *New design of textile light diffusers for photodynamic therapy*. *Materials Science and Engineering C: Materials for Biological Applications*, 2013. **33**(3): p. 1170-1175.
66. Wiegell, S.R., et al., *Daylight photodynamic therapy for actinic keratosis: An international consensus: International Society for Photodynamic Therapy in Dermatology*. *Journal of the European Academy of Dermatology and Venereology*, 2012. **26**(6): p. 673-9.
67. Staicu, A., et al., *Studies about phthalocyanine photosensitizers to be used in photodynamic therapy*. *Romanian Reports in Physics*, 2013. **65**(3): p. 1032-1051.
68. Sharman, W.M., C.M. Allen, and J.E. van Lier, *Photodynamic therapeutics: basic principles and clinical applications*. *Drug Discovery Today*, 1999. **4**(11): p. 507-517.
69. Holt, J.J. and S.U.o.N.Y.a.B. Chemistry, *Synthesis, Photophysical Properties, and Biological Activity of Tetramethylrosamine Analogs* 2008: State University of New York at Buffalo.
70. Gomer, C.J. and T.J. Dougherty, *Determination of [³H]- and [¹⁴C] Hematoporphyrin derivatives distribution in malignant and normal tissue*. *Cancer Research*, 1979. **39**: p. 146-151.

71. Bonnett, R., *Photosensitizers of the porphyrin and phthalocyanine series for photodynamic therapy*. Chemical Society Reviews, 1995. **24**: p. 19-33.
72. Brown, J., S. Brown, and D. Vernon, *Photodynamic therapy - new light on cancer treatment*. JSDC, 1999. **115**: p. 249-253.
73. Capella, M.A. and L.S. Capella, *A light in multidrug resistance: Photodynamic treatment of multidrug-resistant tumors*. Journal of Biomedical Science, 2003. **10**(4): p. 361-366.
74. Kamarulzaman, E.E., et al., *Vascular-targeted photodynamic therapy*. Advances in Cancer Therapy, ed. H. Gali-Muhtasib 2011: InTech.
75. Ethirajan, M., et al., *Photosensitizers for Photodynamic Therapy and Imaging*. Advances in Photodynamic Therapy : Basic, Translational and Clinical, ed. M.R. Hamblin and P. Mroz 2008, Norwood: Artech House.
76. Lucky, S.S., K.C. Soo, and Y. Zhang, *Nanoparticles in Photodynamic Therapy*. Chemical Reviews, 2015. **115**(4): p. 1990-2042.
77. Novakova, V., et al., *A phthalocyanine-mestranol conjugate for photodynamic therapy prepared via click chemistry*. Tetrahedron Letters, 2010. **51**(7): p. 1016-1018.
78. Clement, S., et al., *X-ray induced singlet oxygen generation by nanoparticle-photosensitizer conjugates for photodynamic therapy: determination of singlet oxygen quantum yield*. Scientific Reports, 2016. **6**(19954): p. 1-9.
79. Gianotti, E., et al., *Verteporfin based silica nanoplatfom for photodynamic therapy*. Chemistry Select, 2016. **2**: p. 127-131.
80. Lindsey, J.S., et al., *Rothemund and Adler-Longo reactions revisited: Synthesis of tetraphenylporphyrins under equilibrium conditions*. The Journal of Organic Chemistry, 1987. **52**(5): p. 827-836.
81. Zhi-Cheng, S., et al., *Synthesis, characterization and spectral properties of substituted tetraphenylporphyrin iron chloride complexes*. Molecules, 2011. **16**: p. 2960-2970.
82. Leznoff, C. and P. Svirskaya, *The Synthesis of Unsymmetrical Tetraarylporphyrins on Solid Phases*. Angewandte Chemie International Edition in English, 1978. **17**(12): p. 947-947.
83. Chouikrat, R., et al., *Microwave-assisted synthesis of zinc 5-(4-carboxyphenyl)-10,15,20-triphenylporphyrin and zinc 5-(4-carboxyphenyl)-10,15,20-triphenylchlorin*. Journal of Porphyrins and Phthalocyanines, 2015. **19**(04): p. 595-600.
84. Jain, N., A. Kumar, and S.M.S. Chauhan, *Synthesis of transition metal porphyrins from free-base 5,10,15,20-tetraarylporphyrins under microwave irradiation in ionic liquids*. Synthetic Communications: An International Journal for Rapid Communication of Synthetic Organic Chemistry, 2005. **35**(9): p. 1223-1230.
85. Petit, A., et al., *Microwave irradiation in dry media: A new and easy method for synthesis of tetrapyrrolic compounds*. Synthetic Communications, 1992. **22**(8): p. 1137-1142.
86. Lucas, R., et al., *A facile and rapid iodine-catalyzed meso-tetraphenylporphyrin synthesis using microwave activation*. Tetrahedron Letters, 2008. **49**: p. 5537-5539.
87. Arsenault, G.P., E. Bullock, and S.F. MacDonald, *Pyromethanes and Porphyrins Therefrom*. Journal of the American Chemical Society, 1960. **82**(16): p. 4384-4389.
88. Woodward, R.B., et al., *The total synthesis of Chlorophyll A*. Tetrahedron, 1990. **46**(22): p. 7599-7659.
89. Boudif, A. and M. Momenteau, *Synthesis of a Porphyrin-2,3-diacrylic acid using a new '3+1' type procedure*. Journal of the Chemical Society, Chemical Communications 1994: p. 2069-2070.
90. Boudif, A. and M. Momenteau, *A new convergent method for porphyrin synthesis based on a '3+1' condensation*. Journal of the Chemical Society, Perkins Transactions 1, 1996. **1**: p. 1235-1242.
91. Rothemund, P., *A new porphyrin synthesis. The synthesis of porphin*. Journal of the American Chemical Society, 1936. **58**(4): p. 625-627.
92. Lindsey, J.S., *The synthesis of meso-substituted porphyrins*, in *Metalloporphyrins Catalyzed Oxidations* F. Montanari and L. Casella, Editors. 1994, Kluwer Academic Publishers. p. 49-86.

93. Rothmund, P., *Porphyrim Studies. III.¹ The Structure of the Porphine² Ring System*. Journal of the American Chemical Society, 1939. **61**(10): p. 2912-2915.
94. Rothmund, P., *A New Porphyrin Synthesis. The Synthesis of Porphin1*. Journal of the American Chemical Society, 1936. **58**(4): p. 625-627.
95. Adler, A.D., F.R. Longo, and W. Shergalis, *Mechanistic Investigations of Porphyrin Syntheses. I. Preliminary Studies on ms-Tetraphenylporphin*. Journal of the American Chemical Society, 1964. **86**(15): p. 3145-3149.
96. Adler, A.D., et al., *A simplified synthesis for meso-tetraphenylporphine*. The Journal of Organic Chemistry, 1967. **32**(2): p. 476-476.
97. Vicente, M. and K.M. Smith, *Syntheses and functionalizations of porphyrin macrocycles*. Current Organic Synthesis, 2014. **11**(1): p. 3-28.
98. Lash, T.D., *Porphyrim synthesis by the "3+1" approach: New applications for an old methodology*. Chemistry A European Journal, 1996. **2**: p. 1197-1200.
99. Arsenault, G.P., E. Bullock, and S.F. MacDonald, *Pyromethanes and Porphyrins Therefrom1*. Journal of the American Chemical Society, 1960. **82**(16): p. 4384-4389.
100. Boudif, A. and M. Momenteau, *Synthesis of a porphyrin-2,3-diacrylic acid using a new '3 + 1' type procedure*. Journal of the Chemical Society, Chemical Communications, 1994(18): p. 2069-2070.
101. Giovannetti, R., *The Use of Spectrophotometry UV-Vis for the Study of Porphyrins, Macro to Nano Spectroscopy*. June 29, 2012 ed, ed. J. Uddin2012: CC BY 3.0.
102. Che, C.-M., et al., *Gold(III) porphyrins as a new class of anticancer drugs: cytotoxicity, DNA binding and induction of apoptosis in human cervix epitheloid cancer cells*. Chemical Communications, 2003(14): p. 1718-1719.
103. Lamberti, M.J., N.B.R. Vittar, and V.A. Rivarola, *Breast cancer as photodynamic therapy target: Enhanced therapeutic efficiency by overview of tumor complexity*. World Journal of Clinical Oncology, 2014. **5**(5): p. 901-907.
104. Golstein, P. and G. Kroemer, *Cell death by necrosis: Towards a molecular definition*. Trends in Biochemical Sciences, 2006. **32**(1): p. 37-43.
105. Oleinick, N.L., R.L. Morris, and I. Belichenko, *The role of apoptosis in response to photodynamic therapy: What, where, why, and how*. Photochem Photobiol Sci, 2002. **1**(1): p. 1-21.
106. Bamrungsap, S., et al., *A focus on nanoparticles as a drug delivery system*. Nanomedicine: Nanotechnology in Therapeutics, 2012. **7**(8): p. 1253-1271.
107. Lembo, D. and R. Cavalli, *Nanoparticulate delivery systems for antiviral drugs*. Antivir Chem Chemother, 2010. **21**(2): p. 53-70.
108. Zwicke, G.L., G.A. Mansoori, and C.J. Jeffery, *Utilizing the folate receptor for active targeting of cancer nanotherapeutics*. Nano Reviews, 2012. **3**: p. 18496.
109. Stallivieri, A., et al., *The Interest of Folic Acid in Targeted Photodynamic Therapy*. Curr Med Chem, 2015. **22**(27): p. 3185-3207.
110. Chatterjee, D.K., L.S. Fong, and Y. Zhang, *Nanoparticles in photodynamic therapy: An emerging paradigm*. Advanced Drug Delivery Reviews, 2008. **60**(15): p. 1627-1637.
111. Savellano, M.D. and T. Hasan, *Targeting cells that overexpress the epidermal growth factor receptor with polyethylene glycolated BPD verteporfin photosensitizer immunoconjugates*. Photochem Photobiol, 2003. **77**(4): p. 431-439.
112. Soukos, N.S., et al., *Epidermal growth factor receptor-targeted immunophotodiagnosis and photoimmunotherapy of oral precancer in vivo*. Cancer Res, 2001. **61**(11): p. 4490-4496.
113. Cavanaugh, P.G., *Synthesis of chlorin e6-transferrin and demonstration of its light-dependent in vitro breast cancer cell killing ability*. Breast Cancer Res Treat, 2002. **72**(2): p. 117-130.
114. Daniels, T.R., et al., *The transferrin receptor part I: Biology and targeting with cytotoxic antibodies for the treatment of cancer*. Clin Immunol, 2006. **121**(2): p. 144-58.
115. Derycke, A.S., et al., *Transferrin-conjugated liposome targeting of photosensitizer ALPcS4 to rat bladder carcinoma cells*. J Natl Cancer Inst, 2004. **96**(21): p. 1620-1630.

116. Schneider, R., et al., *Design, synthesis, and biological evaluation of folic acid targeted tetraphenylporphyrin as novel photosensitizers for selective photodynamic therapy*. Bioorg Med Chem, 2005. **13**(8): p. 2799-808.
117. Gravier, J., et al., *Improvement of meta-tetra(hydroxyphenyl)chlorin-like photosensitizer selectivity with folate-based targeted delivery. synthesis and in vivo delivery studies*. J Med Chem, 2008. **51**(13): p. 3867-77.
118. Akhlynina, T.V., et al., *Insulin-mediated intracellular targeting enhances the photodynamic activity of chlorin-e6*. Cancer Res, 1995. **55**(5): p. 1014-9.
119. Tirand, L., et al., *A peptide competing with VEGF₁₆₅ binding on Neuropilin-1 mediates targeting of a chlorin-type photosensitizer and potentiates its photodynamic activity in human endothelial cells*. J Control Release, 2006. **111**(1-2): p. 153-164.
120. Thomas, N., et al., *Tissue distribution and pharmacokinetics of an ATWLPPR-conjugated chlorin-type photosensitizer targeting Neuropilin-1 in glioma-bearing nude mice*. Photochem Photobiol Sci, 2008. **7**(4): p. 433-441.
121. Thomas, N., et al., *Peptide-conjugated chlorin-type photosensitizer binds Neuropilin-1 in vitro and in vivo*. J Photochem Photobiol B, 2009. **96**(2): p. 101-108.
122. Thomas, N., et al., *Photodynamic therapy targeting Neuropilin-1: Interest of pseudopeptides with improved stability properties*. Biochem Pharmacol, 2010. **80**(2): p. 226-35.
123. Wang, H.M., et al., *Porphyrin with amino acid moieties: A tumor photosensitizer*. Chemo-Biological Interactions, 2008. **172**(2): p. 154-158.
124. Vivès, E., J. Schmidt, and A. Pèlerin, *Cell-penetrating and cell-targeting peptides in drug delivery*. Biochimica et Biophysica Acta (BBA) - Reviews on Cancer, 2008. **1786**(2): p. 126-138.
125. Teesalu, T., et al., *C-end rule peptides mediate Neuropilin-1-dependent cell, vascular, and tissue penetration*. Proceedings of the National Academy of Sciences, 2009. **106**(38): p. 16157-16162.
126. Zanuy, D., et al., *Sequence dependence of C-end rule peptides in binding and activation of neuropilin-1 receptor*. Journal of Structural Biology, 2013. **182**(2): p. 78-86.
127. Keyt, B.A., et al., *The carboxyl-terminal domain (115/165) of vascular endothelial growth factor is critical for its mitogenic potency*. The Journal of Biological Chemistry, 1996. **271**: p. 7788-7795.
128. Elpek, G.Ö., *Neuropilins and liver*. World J Gastroenterol, 2015. **21**(23): p. 7065-7073.
129. Kamarulzaman, E.E., et al., *New peptide-conjugated chlorin-type photosensitizer targeting Neuropilin-1 for anti-vascular targeted photodynamic therapy*. International Journal of Molecular Sciences, 2015. **16**: p. 24059-24080.
130. Hu, B., et al., *Neuropilin-1 promotes human glioma progression through potentiating the activity of the HGF/SF autocrine pathway*. Oncogene, 2007. **26**(38): p. 5577-5586.
131. Bechet, D., et al., *Innovations of photodynamic therapy for brain tumors; Potential of multifunctional nanoparticles*. Journal of Carcinogenesis & Mutagenesis, 2012. **S8**: p. 1-7.
132. Dhas, N.L., P.P. Ige, and R.R. Kudarha, *Design, optimization and in-vitro study of folic acid conjugated-chitosan functionalized PLGA nanoparticle for delivery of bicalutamide in prostate cancer*. Powder Technology, 2015. **283**: p. 234-245.
133. Feng, X., et al., *A novel folic acid-conjugated TiO₂-SiO₂ photosensitizer for cancer targeting in photodynamic therapy*. Colloids and Surfaces B: Biointerfaces, 2015. **125**: p. 197-205.
134. Leamon, C.P., et al., *Folate-vinca alkaloid conjugates for cancer therapy: A structure-activity relationship*. Bioconjugate Chemistry, 2014. **25**: p. 560-568.
135. Azais, H., et al., *[FRalpha: a target for prophylactic photodynamic therapy of ovarian peritoneal metastasis?]*. Bull Cancer, 2014. **101**(12): p. 1109-1113.
136. Qualls, M.M. and D.H. Thompson, *Chloroaluminum phthalocyanine tetrasulfonate delivered via acid-labile diplasmenylcholine-folate liposomes: Intracellular localization and synergistic phototoxicity*. International Journal of Cancer, 2001. **93**(3): p. 384-392.
137. Kim, Y.I., *Folate and colorectal cancer: an evidence-based critical review*. Mol Nutr Food Res, 2007. **51**(3): p. 267-92.

138. Pfiffner, J.J., et al., *Isolation of an antianemia factor (vitamin Bc conjugate) in crystalline form from yeast*. Science, 1945. **102**(2644): p. 228-230.
139. Biamonte, A.R. and G.H. Schneller, *A study of folic acid stability in solutions of the B-complex vitamins*. Journal of the American Pharmaceutical Association, 1951. **40**(7): p. 313-320.
140. Scheindlin, S., A. Lee, and I. Griffith, *The action of riboflavin on folic acid*. Journal of Pharmaceutical Sciences, 1952. **41**(8): p. 420-427.
141. Akhtar, M.J., M.A. Khan, and I. Ahmad, *Identification of photoproducts of folic acid and its degradation pathways in aqueous solution*. Journal of Pharmaceutical and Biomedical Analysis, 2003. **31**(3): p. 579-588.
142. Araújo, M.M., et al., *Mechanism of folic acid radiolysis in aqueous solution*. Lwt-Food Sci. Technol., 2015. **63**(1): p. 599-603.
143. Jones, M.L. and P.F. Nixon, *Tetrahydrofolates are greatly stabilized by binding to bovine milk folate-binding protein*. The Journal of Nutrition, 2002. **132**(9): p. 2690-2694.
144. Farber, S., et al., *The action of pteroylglutamic conjugates on man*. Science, 1947. **106**: p. 619-621.
145. Farber, S. and L.K. Diamond, *Temporary remissions in acute leukemia in children produced by folic acid antagonist, 4-aminopteroyl-glutamic acid*. N Engl J Med, 1948. **238**(23): p. 787-93.
146. Kim, Y.I., *Folic acid supplementation and cancer risk: Point*. Cancer Epidemiology, Biomarkers & Prevention, 2008. **17**(9): p. 2220-2225.
147. Shea, B., et al., *Folic acid and folinic acid for reducing side effects in patients receiving methotrexate for rheumatoid arthritis*. Cochrane Database Syst Rev, 2013(5).
148. Maurer, A.H., et al., *Imaging the folate receptor on cancer cells with ^{99m}Tc-Etarfolatide: Properties, clinical use and future potential of folate receptor imaging*. The Journal of Nuclear Medicine, 2014. **55**(5): p. 701-704.
149. Schneider, R., et al., *Design, synthesis, and biological evaluation of folic acid targeted tetraphenylporphyrin as novel photosensitizers for selective photodynamic therapy*. Bioorganic & Medicinal Chemistry, 2005. **13**(8): p. 2799-2808.
150. Fisher, R.A., *The Design of Experiments* 1971, New York, USA: Hafner Publishing Company.
151. Kim, D.W., et al., *Application of Design of Experiment Method for Thrust Force Minimization in Step-feed Micro Drilling*. Sensors, 2008. **8**(1): p. 211.
152. Bastogne, T., et al. *Contribution of experiment designs in photodynamic therapy: Photosensitizer design, treatment analysis and optimization*. in *13th World Congress of the International Photodynamic Association, IPA 2011*. 2011. Innsbruck, Austria.
153. Bevilacqua, A., M.R. Corbo, and M. Sinigaglia, *Design of experiments: A powerful tool in food microbiology*. Current Research, Technology and Education Topics in Applied Microbiology and Microbial Biotechnology, 2010: p. 1419-1429.
154. Lewis, G.A., D. Mathieu, and Phan-Tan-Luu, *Pharmaceutical Experimental Design*, ed. D. Mathieu. Vol. 92. 2005: Taylor & Francis.
155. Rathore, A.S., R. Branning, and D. Cecchini, *Quality: Design space for biotech products*. BioPharm International, 2007. **20**(4).
156. Azais, H., et al., *FR α : a target for prophylactic photodynamic therapy of ovarian peritoneal metastasis?* Bulletin Du Cancer, 2014. **101**(12): p. 1109-1113.
157. Azais, H., et al., *Fischer 344 Rat A Preclinical Model for Epithelial Ovarian Cancer Folate-Targeted Therapy*. International Journal of Gynecological Cancer, 2015. **25**(7): p. 1194-1200.
158. Azais, H., et al., *Assessment of the specificity of a new folate-targeted photosensitizer for peritoneal metastasis of epithelial ovarian cancer to enable intraperitoneal photodynamic therapy. A preclinical study*. Photodiagnosis Photodyn Ther, 2015. **13**: p. 130-138.
159. Teng, I.T., et al., *Phospholipid-functionalized mesoporous silica nanocarriers for selective photodynamic therapy of cancer*. Biomaterials, 2013. **34**(30): p. 7462-7470.
160. Younis, I.R., et al., *Influence of pH on the dissolution of folic acid supplements*. International Journal of Pharmaceutics, 2009. **367**(1-2): p. 97-102.

161. Araújo, M.M., et al., *LC/MS/MS identification of some folic acid degradation products after E-beam irradiation*. Radiation Physics and Chemistry, 2012. **81**(8): p. 1166-1169.
162. Liang, X.S., F.Q. Zhao, and L.X. Hao, *Research on stability of synthetic folic acid*. Advanced Materials Research, 2013. **781-784**: p. 1215-1218.
163. Dick, M.I.B., I.T. Harrison, and K.T.H. Farrer, *The thermal stability of folic (pteroylglutamic) acid*. Aust J Exp Biol Med, 1948. **26**(3): p. 239-244.
164. O'Broin, J.D., et al., *Nutritional stability of various naturally occurring monoglutamate derivatives of folic acid*. Am J Clin Nutr, 1975. **28**(5): p. 438-44.
165. Fosgerau, K. and T. Hoffmann, *Peptide therapeutics: current status and future directions*. Drug Discovery Today, 2015. **20**(1): p. 122-128.
166. Made, V., S. Els-Heindl, and A. G. Beck-Sickinger, *Automated solid-phase peptide synthesis to obtain therapeutic peptides*. Beilstein J. Org. Chem., 2014. **10**: p. 1197-1212.
167. Russell, P.J., *iGenetics: A molecular approach (3rd Edition)* 2014, Edinburgh Gate, England: Pearson Education Limited.
168. Kreil, G., *D-amino acids in animal peptides*. Annu Rev Biochem, 1997. **66**: p. 337-45.
169. Bai, L., S. Sheeley, and J.V. Sweedler, *Analysis of Endogenous D-Amino Acid-Containing Peptides in Metazoa*. Bioanal Rev, 2009. **1**(1): p. 7-24.
170. Li, H., R. Aneja, and I. Chaiken, *Click chemistry in peptide-based drug design*. Molecules 2013. **18**: p. 9797-9817.
171. Merrifield, R.B., *Solid Phase Peptide Synthesis. I. The Synthesis of a Tetrapeptide*. Journal of the American Chemical Society, 1963. **85**(14): p. 2149-2154.
172. Merrifield, R.B., *Solid Phase Peptide Synthesis. II. The Synthesis of Bradykinin*. Journal of the American Chemical Society, 1964. **86**(2): p. 304-305.
173. Merrifield, R.B., *Solid-Phase Peptide Synthesis. III. An Improved Synthesis of Bradykinin**. Biochemistry, 1964. **3**(9): p. 1385-1390.
174. Gutte, B. and R.B. Merrifield, *The Synthesis of Ribonuclease A*. Journal of Biological Chemistry, 1971. **246**(6): p. 1922-1941.
175. Marglin, B. and R.B. Merrifield, *The Synthesis of Bovine Insulin by the Solid Phase Method1*. Journal of the American Chemical Society, 1966. **88**(21): p. 5051-5052.
176. Sakakibara, S., et al., *Use of Anhydrous Hydrogen Fluoride in Peptide Synthesis. I. Behavior of Various Protective Groups in Anhydrous Hydrogen Fluoride*. Bulletin of the Chemical Society of Japan, 1967. **40**(9): p. 2164-2167.
177. Pietta, P.G. and G.R. Marshall, *Amide protection and amide supports in solid-phase peptide synthesis*. Journal of the Chemical Society D: Chemical Communications, 1970(11): p. 650-651.
178. Carpino, L.A. and G.Y. Han, *9-Fluorenylmethoxycarbonyl function, a new base-sensitive amino-protecting group*. Journal of the American Chemical Society, 1970. **92**(19): p. 5748-5749.
179. Wang, S.S., *p-alkoxybenzyl alcohol resin and p-alkoxybenzyloxycarbonylhydrazide resin for solid phase synthesis of protected peptide fragments*. J Am Chem Soc, 1973. **95**(4): p. 1328-33.
180. Chang, C.D. and J. Meienhofer, *Solid-phase peptide synthesis using mild base cleavage of N alpha-fluorenylmethyloxycarbonylamino acids, exemplified by a synthesis of dihydrosomatostatin*. Int J Pept Protein Res, 1978. **11**(3): p. 246-9.
181. Barlos, K., et al., *Synthesis of Protected Peptide-Fragments Using Substituted Triphenylmethyl Resins*. Tetrahedron Letters, 1989. **30**(30): p. 3943-3946.
182. Barlos, K., et al., *Application of 2-chlorotriptyl resin in solid phase synthesis of (Leu15)-gastrin I and unsulfated cholecystokinin octapeptide*. International Journal of Peptide and Protein Research, 1991. **38**(6): p. 555-561.
183. Mergler, M., et al., *Peptide synthesis by a combination of solid-phase and solution methods I: A new very acid-labile anchor group for the solid phase synthesis of fully protected fragments*. Tetrahedron Letters, 1988. **29**(32): p. 4005-4008.

184. Mergler, M., et al., *Peptide synthesis by a combination of solid-phase and solution methods II synthesis of fully protected peptide fragments on 2-methoxy-4-alkoxy-benzyl alcohol resin*. Tetrahedron Letters, 1988. **29**(32): p. 4009-4012.
185. Sieber, P., *A new acid-labile anchor group for the solid-phase synthesis of C-terminal peptide amides by the Fmoc method*. Tetrahedron Letters, 1987. **28**(19): p. 2107-2110.
186. Aapptec, L. *Practical synthesis guide to solid phase peptide chemistry*.
187. Uhlig, T., et al., *The emergence of peptides in the pharmaceutical business: From exploration to exploitation*. EuPA Open Proteomics, 2014. **4**: p. 58-69.
188. Peterson, G. *Recent advances in the Design and Synthesis of peptidomimetics*. 2001.
189. Tugyi, R., et al., *Partial D-amino acid substitution: Improved enzymatic stability and preserved Ab recognition of a MUC2 epitope peptide*. PNAS, 2005. **102**(2): p. 413-418.
190. Webb, A.I., et al., *T cell determinants incorporating beta-amino acid residues are protease resistant and remain immunogenic in vivo*. The Journal of Immunology, 2005. **175**: p. 3810-3818.
191. Li, H., R. Aneja, and I. Chaiken, *Click chemistry in peptide-based drug design*. Molecules (Basel, Switzerland), 2013. **18**(8): p. 9797-9817.
192. Hamzeh-Mivehroud, M., et al., *Phage display as a technology delivering on the promise of peptide drug discovery*. Drug Discovery Today, 2013. **18**(23/24): p. 1144-1157.
193. Okarvi, S.M., *Peptide-based radiopharmaceuticals and cytotoxic conjugates: Potential tools against cancer*. Cancer Treatment Reviews, 2008. **34**(1): p. 13-26.
194. Tam, J.P., et al., *Alanine scan of endothelin: Importance of aromatic residues*. Peptides, 1994. **15**(4): p. 703-708.
195. Cong, Y., et al., *Identification of the critical amino acid residues of immunoglobulin E and immunoglobulin G epitopes on alpha_{s1}-casein by alanine scanning analysis*. Journal of Dairy Science, 2013. **96**(11): p. 6870-6876.
196. Hobson, D. and O.C. Uhlenbeck, *Alanine Scanning of MS2 Coat Protein Reveals Protein-Phosphate Contacts Involved in Thermodynamic Hot Spots*. Journal of Molecular Biology, 2006. **356**(3): p. 613-624.
197. Scott, W.N., et al., *Development of laminin receptor agonists: Identification of important functional residues by alanine scanning*. Biochimica et Biophysica Acta (BBA) - Protein Structure and Molecular Enzymology, 2000. **1481**(1): p. 25-36.
198. Montigiani, S., et al., *Alanine Substitutions in Calmodulin-binding Peptides Result in Unexpected Affinity Enhancement*. Journal of Molecular Biology, 1996. **258**(1): p. 6-13.
199. Betts, M.J. and R.B. Russell, *Amino acid properties and consequences of substitutions*. Bioinformatics for Geneticists, ed. M.R. Barnes and I.C. Gray 2003: Wiley.
200. Giannis, A. and T. Kolter, *Peptidomimetics for Receptor Ligands Discovery, Development, and Medical Perspectives*. Angewandte Chemie, International Edition in English, 1993. **32**(9): p. 1244-1267.
201. Ahn, J.M., et al., *Peptidomimetics and peptide backbone modifications*. Mini-Reviews in Medicinal Chemistry, 2002. **2**(5): p. 463-473.
202. Cudic, P. and M. Stawikowski, *Pseudopeptide synthesis via Fmoc solid-phase synthetic methodology*. Mini-Reviews in Organic Chemistry, 2007. **4**(4): p. 268-280.
203. Dutta, A.S. and T. Bernard, *Design and therapeutic potential of peptides*. Advances in Drug Research. Vol. Volume 21. 1991: Academic Press. 145-286.
204. Gentilucci, L., R. De Marco, and L. Cerisoli, *Chemical modifications designed to improve peptide stability: Incorporation of non-natural amino acids, pseudo-peptide bonds and cyclization* Current Pharmaceutical Design, 2010. **16**(28): p. 3185-3203.
205. Sewald, N. and H.D. Jakubke, *Peptide and protein design, pseudopeptides and peptidomimetics*, in *Peptides: Chemistry and Biology* 2009, Wiley-VCH Verlag GmbH & Co. KGaA. p. 411-455.
206. Wiley, R.A. and D.H. Rich, *Peptidomimetics derived from natural products*. Medicinal Research Reviews, 1993. **13**(3): p. 327-384.

207. Spatola, A.F., *Chemistry and Biochemistry of amino-acids, Peptides and Proteins*, ed. B. Weinstein. Vol. VII. 1983, New York, U.S.A: M. Dekker.
208. Goodman, M., *Methods of organic chemistry (Houben-Weyl)*. Synthesis of peptides and peptidomimetics. Vol. E 22. 2004.
209. Guichard, G., et al., *Antigenic mimicry of natural L-peptides with retro-inverso peptidomimetics*. Proc. Natl. Acad. Sci. U. S. A., 1994. **91**(21): p. 9765-9769.
210. Chorev, M. and M. Goodman, *A dozen years of retro-inverso peptidomimetics*. Accounts of Chemical Research, 1993. **26**(5): p. 266-273.
211. Chorev, M. and M. Goodman, *Recent developments in retro peptides and proteins - An ongoing topochemical exploration*. Trends in Biotechnology, 1995. **13**(10): p. 438-445.
212. Goodman, M. and M. Chorev, *Concept of linear modified retro-peptide structures*. Accounts of Chemical Research, 1979. **12**(1): p. 1-7.
213. Bhattacharyya, J. and K.K. Sharma, *Conformational specificity of mini-alphaA-crystallin as a molecular chaperone*. J Pept Res, 2001. **57**(5): p. 428-34.
214. Wermuth, J., et al., *Stereoisomerism and biological activity of the selective and superactive $\alpha_v\beta_3$ integrin inhibitor cyclo(-RGDfV-) and its retro-inverso peptide*. Journal of the American Chemical Society, 1997. **119**(6): p. 1328-1335.
215. Sakurai, K., H.S. Chung, and D. Kahne, *Use of a retroinverso p53 peptide as an inhibitor of MDM2*. Journal of the American Chemical Society, 2004. **126**(50): p. 16288-16289.
216. Atzori, A., et al., *Effect of sequence and stereochemistry reversal on p53 peptide mimicry*. Plos One, 2013. **8**(7).
217. Bednarek, M.A., et al., *Structure-function studies on the cyclic peptide MT-II, lactam derivative of alpha-melanotropin*. Peptides, 1999. **20**(3): p. 401-409.
218. Nitsche, C., et al., *Retro peptide-hybrids as selective inhibitors of the Dengue virus NS2B-NS3 protease*. Antiviral Res., 2012. **94**(1): p. 72-79.
219. Van Regenmortel, M. and S. Muller, *D-peptides as immunogens and diagnostic reagents*. Current Opinion in Biotechnology, 1998. **9**(4): p. 377-382.
220. Li, C., et al., *Limitations of peptide retro-inverso isomerization in molecular mimicry*. The Journal of Biological Chemistry, 2010. **285**(25): p. 19572-19581.
221. Van Regenmortel, M.H., et al., *The potential of retro-inverso peptides as synthetic vaccines*. Developments in Biological Standardization, 1998. **92**: p. 139-143.
222. Brady, L. and G. Dodson, *Reflections on a peptide*. Nature, 1994. **368**(6473): p. 692-693.
223. O'mahony, D.J., *Retro-inversion peptides that target gastro-intestinal tract transport receptors and use thereof*, 1999.
224. Li, C., et al., *Functional consequences of retro-inverso isomerization of a miniature protein inhibitor of the p53-MDM2 interaction*. Bioorganic & Medicinal Chemistry, 2013. **21**(14): p. 4045-4050.
225. Skriner, K., K. Adolph, and J. Hollidt, *hnRNP A3-related citrullinated peptides and use thereof for diagnosis of rheumatoid arthritis*, 2013. p. 24pp.
226. Sørensen, B., et al., *Human immunodeficiency virus vaccine*, 2013, (Bionor Immuno AS, Norway): WO 2013182660 A1 20131212. p. 106.
227. Kem, D.C., *Compositions comprising D-amino acid peptides binding to autoantibodies against a G-protein coupled receptor and therapeutic use thereof*, 2014, (University of Oklahoma, USA): WO 2014144095 A2 20140918. p. 55.
228. Raucher, D. and G. Bidwell, III, *Thermally targeted delivery of compositions comprising cell penetrating peptides, elastin-like peptides and therapeutic peptides for treatment of tumors*, 2014, (University of Mississippi Medical Center, USA): US 8841414 B1 20140923. p. 104, Cont -in-part of U S Ser No 162,283.
229. Vilcinskas, A., A.-K. Poeppel, and J. Wiesner, *Antifungal polypeptides LserFCP1-73 and LserFCP1-77 against plant pathogenic fungi*, 2014, (Fraunhofer-Gesellschaft zur Foerderung der Angewandten Forschung e.V., Germany): WO 2014124786 A1 20140821. p. 40.

230. Aloysius, H. and L. Hu, *Improving the specificity of the prostate-specific antigen substrate Glutaryl-Hyp-Ala-Ser-Chg-Gln as a promoiety*. Chem. Biol. Drug Des., 2015. **86**(4): p. 837-848.
231. Davis, E.M., et al., *Peptide-mediated PEGylation of polysulfone reduces protein adsorption and leukocyte activation*. ASAIO J FIELD, 2015. **61**(6): p. 710-717.
232. Gaudriault, G., et al., *Retro-inverso analogs of spadin display increased antidepressant effects*, 2015, (Medincell, Fr.; Centre National de la Recherche Scientifique): WO 2015110915 A2 20150730. p. 71.
233. Li, X., et al., *D-SP5 peptide-modified highly branched polyethylenimine for gene therapy of gastric adenocarcinoma*. Bioconjugate Chem., 2015. **26**(8): p. 1494-1503.
234. Prades, R., et al., *Applying the retro-enantio approach to obtain a peptide capable of overcoming the blood-brain barrier*. Angewandte Chemie, 2015. **127**(13): p. 4039-4044.
235. Wei, X., et al., *A D-Peptide ligand of nicotine acetylcholine receptors for brain-targeted drug delivery*. Angewandte Chemie, International Edition, 2015. **54**(10): p. 3023-3027.
236. Dattoli, S., et al., *Synthesis and assay of retro- $\alpha_4\beta_1$ integrin-targeting motifs*. Eur J Med Chem, 2014. **73**: p. 225-232.
237. Xu, J., et al., *Mitochondrial JNK activation triggers autophagy and apoptosis and aggravates myocardial injury following ischemia/reperfusion*. Biochim. Biophys. Acta - Molecular Basis of Disease, 2015. **1852**(2): p. 262-270.
238. Wei, X., et al., *Retro-Inverso Isomer of Angiopep-2: A Stable D-Peptide Ligand Inspires Brain-Targeted Drug Delivery*. Mol. Pharmaceutics, 2015. **11**(10): p. 3261-3268.
239. Wang, Y.X. and P. Yu, *Peptide compounds that bind to human immunodeficiency virus Rev response element*, 2015, (United States Dept. of Health & Human Services, USA). WO 2015061573 A1 20150430. p. 85.
240. Veyssiere, J., et al., *Retroinverso analogs of spadin display increased antidepressant effects*. Psychopharmacology, 2015. **232**(3): p. 561-574.
241. Liu, Y., et al., *Integrin $\alpha_v\beta_3$ targeting activity study of different retro-inverso sequences of RGD and their potentiality in the designing of tumor targeting peptides*. Amino Acids, 2015. **47**(12): p. 2533-2539.
242. Li, H.L., et al., *Novel retro-inverso peptide inhibitor reverses angiotensin receptor autoantibody-induced hypertension in the rabbit*. Hypertension, 2015. **65**(4): p. 793-799.
243. Lee, Y.S., et al., *Modification of amphipathic non-opioid Dynorphin A analogues for rat brain bradykinin receptors*. Bioorganic & Medicinal Chemistry Letters, 2015. **25**(1): p. 30-33.
244. Khachatoorian, R., et al., *Structural characterization of the HSP70 interaction domain of the hepatitis C viral protein NS5A*. Virology, 2015. **475**: p. 46-55.
245. Jakova, E. and J.S. Lee, *Superposition of an AC field improves the discrimination between peptides in nanopore analysis*. Analyst, 2015. **140**(14): p. 4813-4819.
246. Diamond, B.A., *Complement C1q-derived peptides in the treatment of autoimmune disease*, 2015, (The Feinstein Institute for Medical Research, USA): US 20150104472 A1 20150416. p. 65.
247. De la Fuente-Nunez, C., et al., *D-enantiomeric peptides that eradicate wild-type and multidrug-resistant biofilms and protect against lethal Pseudomonas aeruginosa infections*. Chemistry & Biology, 2015. **22**(2): p. 196-205.
248. Colletti, S.L., et al., *Conjugates of peptides with targeting moieties for the simultaneous delivery of therapeutic oligonucleotides to target cells*, 2015, (Merck Sharp & Dohme Corp., USA): WO 2015069587 A2 20150514. p. 137.
249. Alves, F.L., M.L.V. Oliva, and A. Miranda, *Conformational and biological properties of Bauhinia bauhinioides kallikrein inhibitor fragments with bradykinin-like activities*. Journal of Peptide Science, 2015. **21**(6): p. 495-500.
250. Zhang, H., et al., *Peptide-based peroxidase inhibitors and methods of using same*, 2014, (The Medical College of Wisconsin, Inc., USA): US 20140194342 A1 20140710. p. 46, Cont -in-part of U S Ser No 500,040.

251. Yamamoto, T., et al., *Mastoparan peptide causes mitochondrial permeability transition not by interacting with specific membrane proteins but by interacting with the phospholipid phase*. *Febs Journal*, 2014. **281**(17): p. 3933-3944.
252. Wang, J., et al., *Retro-inverso CendR peptide-mediated polyethyleneimine for intracranial glioblastoma-targeting gene therapy*. *Bioconjugate Chemistry*, 2014. **25**(2): p. 414-423.
253. Turley, E.A., S.B. Bahrami, and M.J. Bissell, *Peptides that stimulate subcutaneous adipogenesis*, 2014, (University of California, USA): WO 2014082042 A2 20140530. p. 119pp.
254. Takayama, K., *Development of an oligoarginine peptide displaying rapid cell penetration for improved intestinal absorption*. *Yakugaku Zasshi-Journal of the Pharmaceutical Society of Japan*, 2014. **134**(1): p. 55-61.
255. Quebatte, G., E. Kitas, and J. Seelig, *riDOM, a cell-penetrating peptide. Interaction with DNA and heparan sulfate*. *J. Phys. Chem. B*, 2013. **117**(37): p. 10807-10817.
256. Levine, B.C., et al., *Autophagy-inducing peptide analogs comprising Beclin 1 residues or D-retro-inverso sequence*, 2014, (University of Texas System, USA; Baylor College of Medicine): US 8802633 B1 20140812. p. 7.
257. Iorns, E., et al., *Replication attempt: "Effect of BMAP-28 antimicrobial peptides on leishmania major promastigote and amastigote growth: Role of leishmanolysin in parasite survival"*. *Plos One*, 2014. **9**(12).
258. Gonzalez, L.I., *Synthetic stereoisomer peptides in the retro-inverso and inverso configuration, and with cyclic and linear structure, their polymer conjugates, their encapsulation in polymer particles, and uses thereof*, 2013, (USA): US 20130156723 A1 20130620. p. 57, Cont -in-part of Appl No PCT/US2010/054583.
259. Deiber, J.A., M.V. Piaggio, and M.B. Peirotti, *Global chain properties of an all L- α -eicosapeptide with a secondary α -helix and its all retro d-inverso- α -eicosapeptide estimated through the modeling of their CZE-determined electrophoretic mobilities*. *Electrophoresis*, 2014. **35**(5): p. 755-761.
260. Combette, J.-M. and C. Deloche, *Cell-permeable peptide inhibitors of JNK signal transduction pathway in the treatment of JNK signaling-associated disease*, 2014, (Xigen Inflammation Ltd., Cyprus): WO 2014206427 A1 20141231. p. 208.
261. Awahara, C., et al., *Effect of prime-site sequence of retro-inverso-modified HTLV-1 protease inhibitor*. *Bioorganic & Medicinal Chemistry*, 2014. **22**(8): p. 2482-2488.
262. Acerra, N., et al., *Retro-inverso of intracellular selected β -amyloid-interacting peptides: implications for a novel Alzheimer's disease treatment*. *Biochemistry*, 2014. **53**(13): p. 2101-11.
263. Willbold, D., *Method for the removal of β -amyloid from donated blood, blood products and organs to prevent Alzheimer's disease*, 2013, (Forschungszentrum Juelich GmbH, Germany): WO 2013150126 A2 20131010. p. 45.
264. Verardo, G. and A. Gorassini, *Characterization of N-Boc/Fmoc/Z-N¹-formyl-gem-diaminoalkyl derivatives using electrospray ionization multi-stage mass spectrometry*. *Journal of Mass Spectrometry*, 2013. **48**(11): p. 1136-1149.
265. Tarasova, N.I., A.O. Perantoni, and S. Tanigawa, *Synthetic β -catenin peptide inhibitors of Wnt pathway influence β -catenin activity and degradation, for use in cancer therapy*, 2013, (The United States of America, As Represented by the Secretary, Department of Health and Human Services, USA). Application: US. p. 29.
266. Sokoll, K., *Anti-cancer peptides and uses thereof*, 2013, (PharmaGap Inc., Can): WO 2013026157 A1 20130228. p. 107.
267. Shukla, D. and V. Tiwari, *Anti-heparan sulfate peptides that block herpes simplex virus infection in vivo*, 2013, (University of Illinois, USA): US 20130189784 A1 20130725. p. 33, Cont -in-part of Appl No WO/US2011/052002.

268. Schneider, A., et al., *Peptides regulating protein kinase PKM ζ derived from KIBRA protein for use in improving memory and cognition*, 2013, (Sygnis Bioscience GmbH & Co. KG, Germany): WO 2013041239 A1 20130328. p. 87.
269. Ngoei, K., et al., *A novel retro-inverso peptide is a preferential JNK substrate-competitive inhibitor*. International Journal of Biochemistry & Cell Biology, 2013. **45**(8): p. 1939-1950.
270. Moss, R.L. and A. Fernandez, *Inhibition of Myosin Binding Protein C (MyBP-C) binding to myosin as a treatment for heart failure*, 2013, (Wisconsin Alumni Research Foundation, USA): US 20130345135 A1 20131226. p. 37.
271. Li, Y., et al., *Potent retro-inverso D-peptide for simultaneous targeting of angiogenic blood vasculature and tumor cells*. Bioconjugate Chemistry, 2013. **24**(1): p. 133-143.
272. Erba, P., *Platelet rich plasma and prominin-1 derived peptide stimulate lymphangiogenesis and use in treatment of lymphatic system disease*, 2013, (Centre Hospitalier Universitaire Vaudois (C.H.U.V.), Switz.): WO 2013065017 A2 20130510. p. 37.
273. Jung, J., *Inhibition of Mycobacterium tuberculosis immune evasion*, 2013, (USA): US 20130287792 A1 20131031. p. 17.
274. Franceschini, C., et al., *C-terminal trans,trans-muconic acid ethyl ester partial retro-inverso pseudopeptides as proteasome inhibitors*. Journal of Enzyme Inhibition and Medicinal Chemistry, 2013. **28**(5): p. 1034-1039.
275. Eccleston, M., S. Vainikka, and G.S. Morris, *Molecules that inhibit or prevent interaction between Src family kinase and androgen or estrogen receptor for treatment of gynecological disorders or cancer*, 2013, (ValiRx PLC, UK): WO 2013064830 A2 20130510. p. 53.
276. Davis, E.M., et al., *Evidence of extensive diversity in bacterial adherence mechanisms that exploit unanticipated stainless steel surface structural complexity for biofilm formation*. Acta Biomaterialia, 2013. **9**(4): p. 6236-6244.
277. Combette, J.-M. and C. Deloche, *Use of cell-permeable peptide inhibitors of the JNK signal transduction pathway for the treatment of dry eye syndrome*, 2013, (Xigen Inflammation Ltd., Cyprus): WO 2013079213 A1 20130606. p. 77.
278. Chorev, M., *From retro-inverso to a post-translational modification of a complement regulatory protein*. Biopolymers, 2013. **100**(3): p. 235-235.
279. Chen, X.Y., et al., *Retro-inverso carbohydrate mimetic peptides with Annexin1-binding selectivity, are stable in vivo, and target tumor vasculature*. Plos One, 2013. **8**(12).
280. Parthasarathy, V., et al., *A Novel Retro-Inverso Peptide Inhibitor Reduces Amyloid Deposition, Oxidation and Inflammation and Stimulates Neurogenesis in the APP^{swe}/PS1 Δ E9 Mouse Model of Alzheimer's Disease*. PLoS ONE, 2013. **8**(1): p. e54769.
281. Verdini, A.S., et al., *Immunostimulation by a Partially Modified Retro-Inverso-Tuftsins Analog Containing Thr¹ ψ [NHCO](R,S)Lys² Modification*. J. Med. Chem., 1991. **34**(12): p. 3372-3379.
282. Djordjevic, S. and P.C. Driscoll, *Targeting VEGF signalling via the neuropilin co-receptor*. Drug Discovery Today, 2013. **18**(9-10): p. 447-455.
283. Becherucci, C., et al., *Antiinflammatory effect of tuftsins and its retro-inverso analog in rat adjuvant arthritis*. Agents and Actions, 1992: p. C115-C117.
284. Paulesu, L., et al., *Effect of tuftsins and its retro-inverso analog on the release of interferon (IFN-gamma) and Tumor-Necrosis-Factor (TNF-alpha) by human-leukocytes*. Immunology Letters, 1992. **34**(1): p. 7-11.
285. Comley, J. *ELISA Assays: Recent innovations take analyte detection to new levels*. Drug Discovery World, 2012.
286. Anderson, G.L. and L.A. McNellis, *Enzyme-Linked Antibodies: A laboratory introduction to the ELISA assay*. Journal of Chemical Education, 1998. **75**(10): p. 1275.
287. Powers, J.L., et al., *A direct, competitive enzyme-linked immunosorbent assay (ELISA) as a quantitative technique for small molecules*. Journal of Chemical Education, 2012. **89**(12): p. 1587-1590.

288. Perrigo, B.J. and B.P. Joynt, *Use of ELISA for the detection of common drugs of abuse in forensic whole blood samples*. Canadian Society of Forensic Science Journal, 1995. **28**(4): p. 261-269.
289. Marin, S.J., et al., *Comparison of drugs of abuse detection in meconium by EMIT II and ELISA*. J Anal Toxicol, 2009. **33**(3): p. 148-154.
290. Marin, S.J., M. Merrell, and G.A. McMillin, *Drugs of Abuse detection in meconium: A comparison between ELISA and biochip microarray*. Journal of Analytical Toxicology, 2011. **35**: p. 40-45.
291. Nording, M., et al., *On the semi-quantification of polycyclic aromatic hydrocarbons in contaminated soil by an enzyme-linked immunosorbent assay kit*. Analytica Chimica Acta, 2006. **555**(1): p. 107-113.
292. Nording, M., et al., *Analysis of dioxins in contaminated soils with the calux and caflux bioassays, an immunoassay, and gas chromatography/high-resolution mass spectrometry*. Environmental toxicology and chemistry / SETAC, 2007. **26**(6): p. 1122-1129.
293. Booster. *ELISA principle*. [cited 2016 18 May 2016]; Available from: <https://www.bosterbio.com/protocol-and-troubleshooting/elisa-principle>.
294. Wilson, K.J., et al., *The behavior of peptides on reverse-phase supports during high-pressure liquid-chromatography*. Biochemical Journal, 1981. **199**(1): p. 31-41.
295. Meek, J.L., *Prediction of peptide retention times in high-pressure liquid chromatography on the basis of amino acid composition*. Proc Natl Acad Sci U S A, 1980. **77**(3): p. 1632-1636.
296. Schweizer, M., et al., *Prediction of short peptides composition by RP-HPLC coupled to ESI mass spectrometry*. Food Chemistry, 2007. **105**(4): p. 1606-1613.
297. Nishino, N., et al., *Design of Analogs of Trapoxin, Cyl-1, and Chlamydocin for MHC Class-I Molecule Up-Regulation*, in *Peptides: The Wave of the Future: Proceedings of the Second International and the Seventeenth American Peptide Symposium, June 9-14, 2001, San Diego, California, U.S.A.*, M. Lebl and R.A. Houghten, Editors. 2001, Springer Netherlands: Dordrecht. p. 528-529.
298. Lee, D.L., C.T. Mant, and R.S. Hodges, *A novel method to measure self-association of small amphipathic molecules - Temperature profiling in reversed-phase chromatography*. Journal of Biological Chemistry, 2003. **278**(25): p. 22918-22927.
299. Nath, S.A., Ashish, and V. Veena, *Molecular dynamics simulation of Tuftsin and its analogs in a receptor like environment*. The Pharma Innovation Journal, 2015. **3**(11): p. 55-67.
300. Pal, D. and P. Chakrabarti, *Cis peptide bonds in proteins: Residues involved, their conformations, interactions and locations*. Journal of Molecular Biology, 1999. **294**: p. 271-288.
301. Filira, F., et al., *Synthesis of O-glycosylated tuftsins by utilizing threonine derivatives containing an unprotected monosaccharide moiety*. International Journal of Peptide and Protein Research, 1990. **36**(1): p. 86-96.
302. Bai, K.B., et al., *Design, synthesis and in vitro activity of novel drug delivery systems containing tuftsins derivatives and methotrexate*. Bioconjugate Chemistry, 2008. **19**: p. 2260-2269.
303. Siemion, I.Z., et al., *¹³C Nuclear Magnetic Resonance and circular dichroism studies of the tuftsins conformation in water*. European Journal of Biochemistry, 1980. **112**: p. 339-343.
304. Patton, G.C., *Development and applications of click chemistry*, 2004.
305. Hein, C.D., X.-M. Liu, and D. Wang, *Click chemistry, a powerful tool for pharmaceutical sciences*. Pharmaceutical Research, 2008. **25**(10): p. 2216-2230.
306. Kolb, H.C., M.G. Finn, and K.B. Sharpless, *Click Chemistry: Diverse Chemical Function from a Few Good Reactions*. Angew Chem Int Ed Engl, 2001. **40**(11): p. 2004-2021.
307. Waqar, A., *Click chemistry for colloidal assembly*, in *Material Science and Engineering 2011*, University of Illinois: Urbana-Champaign. p. 82.
308. Ball, P. *The click concept*. Chemistry World, 2007. 46-51.

309. Liang, L. and D. Astruc, *The copper(I)-catalyzed alkyne-azide cycloaddition (CuAAC) click reaction and its applications. An overview*. Coordination Chemistry Reviews, 2011. **255**(23 & 24): p. 2933-2945.
310. Meldal, M. and C.W. Tornøe, *Cu-catalyzed azide-alkyne cycloaddition*. Chemical Reviews, 2008. **108**(8): p. 2952-3015.
311. Le Droumaguet, B. and K. Velonia, *Click chemistry : A powerful tool tool to create polymer-based macromolecular chimeras*. Macromolecular Rapid Communication, 2008. **29**: p. 1073-1089.
312. Moses, J.E. and A.D. Moorhouse, *The growing applications of click chemistry*. Chemical Society Reviews, 2007. **36**(8): p. 1249-1262.
313. Acherar, S., et al., *Synthesis of porphyrin, chlorin and phthalocyanine derivatives by azide-alkyne click chemistry*. Curr Med Chem, 2015. **22**: p. 3217-3254.
314. Kolb, H.C. and K.B. Sharpless, *The growing impact of click chemistry on drug discovery*. Drug Discov Today, 2003. **8**(24): p. 1128-37.
315. Kolb, H.C., M.G. Finn, and K.B. Sharpless, *Click chemistry : Diverse chemical function from a few good reactions*. Angewandte Chemie International Edition, 2001. **40**(11): p. 2004-2021.
316. Nwe, K. and M.W. Brechbiel, *Growing applications of "Click Chemistry" for bioconjugation in contemporary biomedical research*. Cancer Biotherapy & Radiopharmaceuticals, 2009. **24**(3): p. 289-302.
317. Akeroyd, N., *Click chemistry for the preparation of advanced macromolecular architectures*, in *Department of Chemistry and Polymer Science* 2010, Stellenbosch University: Stellenbosch.
318. Whiting, M., et al., *Inhibitors of HIV-1 protease by using in situ click chemistry*. Angew Chem Int Ed Engl, 2006. **45**(9): p. 1435-9.
319. Tron, G.C., et al., *Click chemistry reactions in medicinal chemistry: Applications of the 1,3-dipolar cycloaddition between azides and alkynes*. Medicinal Research Reviews, 2008. **28**(2): p. 278-308.
320. Lutz, J.F. and H.G. Börner, *Modern trends in polymer bioconjugates design*. Progress in Polymer Science, 2008. **33**(1): p. 1-39.
321. Rostovtsev, V.V., et al., *A stepwise Huisgen cycloaddition process: Copper(I)-catalyzed regioselective "ligation" of azides and terminal alkynes*. Angewandte Chemie International Edition, 2002. **41**(14): p. 2596-2599.
322. lehl, J., et al., *Click chemistry for the efficient preparation of functionalized [60]fullerene hexakis-adducts*. Chemical Communications, 2008(21): p. 2450-2452.
323. Megiatto, J.D., et al., *[2]Catenanes decorated with porphyrin and [60]Fullerene groups: Design, convergent synthesis, and photoinduced processes*. Journal of the American Chemical Society, 2010. **132**(11): p. 3847-3861.
324. Dumoulin, F. and V. Ahsen, *Click chemistry : The emerging role of the azide-alkyne Huisgen dipolar addition in the preparation of substituted tetrapyrrolic derivatives*. Journal of Porphyrins and Phthalocyanines, 2011. **15**: p. 481-504.
325. Avti, P.K., D. Maysinger, and A. Kakkar, *Alkyne-azide "click" chemistry in designing nanocarriers for applications in biology*. Molecules, 2013. **18**(8): p. 9531-9549.
326. Isele, U., et al., *Pharmacokinetics and body distribution of liposomal zinc phthalocyanine in tumor-bearing mice: Influence of aggregation state, particle size, and composition*. J Pharm Sci, 1995. **84**(2): p. 166-173.
327. Hao, E., T.J. Jensen, and M.G.a.H. Vicente, *Synthesis of porphyrin-carbohydrate conjugates using "click" chemistry and their preliminary evaluation in human HEP2 cells*. Journal of Porphyrins and Phthalocyanines, 2009. **13**(01): p. 51-59.
328. Kushwaha, D. and V.K. Tiwari, *Click chemistry inspired synthesis of glycoporphyrin dendrimers*. The Journal of Organic Chemistry, 2013. **78**(16): p. 8184-8190.
329. Bakleh, M.E., et al., *An efficient route to VEGF-like peptide porphyrin conjugates via microwave-assisted 'click-chemistry'*. Tetrahedron, 2009. **65**(36): p. 7385-7392.

330. Garcia, G., et al., *Microwave-mediated 'click-chemistry' synthesis of glycoporphyrin derivatives and in vitro phototoxicity for application in photodynamic therapy*. Tetrahedron, 2011. **67**: p. 4924-4932.
331. Grin, M.A., et al., *Synthesis of chlorin-carbohydrate conjugates by 'click chemistry'*. Mendeleev Communications, 2008. **18**(3): p. 135-137.
332. Daly, R., et al., *Synthesis and biological evaluation of a library of glycoporphyrin compounds*. Chemistry, 2012. **18**(46): p. 14671-14679.
333. Garcia, G., et al., *Microwave-mediated 'click-chemistry' synthesis of glycoporphyrin derivatives and in vitro phototoxicity for application in photodynamic therapy*. Tetrahedron, 2011. **67**(26): p. 4924-4932.
334. Lafont, D., et al., *Monoglycoconjugated phthalocyanines: Effect of sugar and linkage on photodynamic activity*. Photodiag Photodyn Ther, 2013. **10**(3): p. 252-259.
335. Gedye, R., et al., *The use of microwave ovens for rapid organic synthesis*. Tetrahedron Letters, 1986. **27**(3): p. 279-282.
336. Giguere, R.J., et al., *Application of commercial microwave ovens to organic synthesis*. Tetrahedron Letters, 1986. **27**(41): p. 4945-4948.
337. Surati, M.A., S. Jauhari, and K.R. Desai, *A brief review: Microwave assisted organic reaction*. Archives of Applied Science Research, 2012. **4**(1): p. 645-661.
338. Hayes, B.L., *Recent advances in microwave-assisted synthesis*. Aldrichimica ACTA, 2004. **37**(2): p. 66-76.
339. Krim, J., et al., *Microwave-assisted click-chemistry: synthesis of mono and bis-1,2,3-triazole acyclonucleoside analogues of Acyclovir via copper(I)-catalyzed cycloaddition*. ARKIVOC, 2009(xiii): p. 142-152.
340. Rijkers, D.T.S., et al., *Efficient microwave-assisted synthesis of multivalent dendrimeric peptides using cycloaddition reaction (click) chemistry*. Chemical Communications, 2005: p. 4581-4583.
341. Thundimadathil, J., *Click chemistry in peptide science: A mini-review. Synthesis of clickable peptides and applications*. Chemistry Today, 2013. **31**(2).
342. Castro, V., H. Rodraguez, and F. Albericio, *CuAAC: An efficient click chemistry reaction on solid phase*. ACS Combinatorial Science, 2016. **18**(1): p. 1-14.
343. Ahmad Fuaad, A.A.H., et al., *Peptide conjugation via CuAAC 'Click' Chemistry*. Molecules, 2013. **18**: p. 13148-13174.
344. Colombeau, L., et al., *Synthesis of zinc 5-(4-propargylamidocarboxyphenyl)-10,15,20-triphenylchlorin*. Trends in Organic Chemistry, 2011. **15**: p. 33-40.
345. Shen, D.-M., C. Liu, and Q.-Y. Chen, *Synthesis and Versatile Reactions of β -Azidotetraarylporphyrins*. European Journal of Organic Chemistry, 2007. **2007**(9): p. 1419-1422.
346. Santos, F.d.C., et al., *Synthesis of porphyrin-quinolone conjugates*. Tetrahedron Letters, 2008. **49**(51): p. 7268-7270.
347. Locos, O.B., et al., *Efficient Synthesis of Glycoporphyrins by Microwave-Mediated "Click" Reactions*. European Journal of Organic Chemistry, 2010. **2010**(6): p. 1026-1028.
348. Severac, M., et al., *Synthesis of new azido porphyrins and their reactivity in copper(I)-catalyzed Huisgen 1,3-dipolar cycloaddition reaction with alkynes*. Tetrahedron Letters, 2007. **48**(37): p. 6518-6522.
349. Chouikrat, R., *Nanoparticules multifonctionnelles excitables par les rayons X pour la thérapie photodynamique*, in *Laboratoire Reactions et Genie des Procédés 2015*, Université de Lorraine: Nancy.
350. R&D Systems, I. *ELISA Development Guide*.

Résumé

La thérapie photodynamique (PDT) est un type de traitement du cancer qui offre de nombreux avantages. Une stratégie pour améliorer l'efficacité de la PDT est l'élaboration de photosensibilisateurs (PSs) de troisième génération, composés d'une molécule photoactivable couplée à un agent de ciblage. Les travaux de recherche de cette thèse portent sur l'amélioration de la sélectivité du traitement PDT en concevant des PSs ciblés. La première partie de la thèse est consacrée à l'étude d'un PS couplé à de l'acide folique (PS-FA). L'acide folique est une unité bien connue de ciblage qui se lie de façon efficace au récepteur de l'acide folique sur-exprimé à la surface de nombreuses cellules cancéreuses. Nous avons particulièrement vérifié la stabilité de l'acide folique sous l'influence des facteurs environnementaux. La deuxième partie est consacrée à l'étude du peptide KDKPPR conçu pour cibler neuropiline-1, un récepteur surexprimé dans les néovaisseaux. Plusieurs modifications du peptide ont été faites et les analogues ont été testés par des analyses ELISA afin d'évaluer leur capacité de liaison à la suite des modifications. La troisième partie de la thèse a consisté en la synthèse de porphyrines couplées à des blocs porteurs de 1, 2 ou 3 peptides grâce à la technique de chimie click pour former de multiples conjugués avec des nombres différents de porphyrines et peptides attachés aux plateformes.

Mots-clés : thérapie photodynamique ; administration ciblée de drogues ; Acide folique; KDKPPR ; Chimie click

Abstract

Photodynamic therapy (PDT) is a type of cancer therapy that could offer many advantages. One possible way to improve the effectiveness of PDT is the elaboration of third generation photosensitizers (PSs) which consisted of PSs coupled with targeting agents. This thesis focuses on improving the selectivity of PS delivery through designing targeted PS agents. The first part of the thesis deals with the study of a PS-folic acid (PS-FA). FA is a well-known targeting unit which bonds with high efficiency to folic acid receptor over-expressed on the surface of many cancer cells. We particularly checked the stability of folic acid under the influence of environmental factors. The second part is devoted to the study of KDKPPR peptide designed to target neuropilin-1, a receptor over-expressed in neovessels. Several modifications of the peptide were made and the analogues were tested through ELISA assays to evaluate their binding capability following the modifications. The third part of the thesis is related to the synthesis of porphyrin and peptide building blocks through click chemistry technique to form multiple conjugates with different numbers of porphyrins and peptides attached to the platforms.

Keywords: Photodynamic therapy; Targeted-drug delivery; Folic acid; KDKPPR; Click chemistry